PhD degree in Molecular Medicine (curriculum in Molecular Oncology)

European School of Molecular Medicine (SEMM),

University of Milan

Settore disciplinare: Bio/11

Complete resolution of sister chromatid intertwines requires the Polo-like kinase Cdc5 and the phosphatase Cdc14 in budding yeast

Lucia Francesca Massari

European Institute of Oncology, Milan

Matricola n. R10719

Supervisor: Dr. Rosella Visintin

European Institute of Oncology, Milan

Anno accademico 2016-2017

Table of contents

Figures index

Introduction

Results

Discussion

Tables index

List of abbreviations

APC/C	Anaphase promoting complex or cyclosome
ATP	Adenosine triphosphate
bp	base pair
Cdk	Cyclin-dependent kinase
CEN	Centromere
CPC	Chromosomal passenger complex
CTD	Topo II C-terminal domain
DAPI	4',6-diamidino-2-phenylindole
DNA	Deoxyribonucleic acid
dsDNA	double stranded DNA
DSB	Double strand break
FEAR	Cdc14 early anaphase release
GFP	Green fluorescent protein
IF	Indirect Immunofluorescence
HJ	Holliday Junction
HU	Hydroxyurea
HR	Homologous recombination
KT	Kinetochore
MAP	Microtubules-associated protein
MCC	Mitotic checkpoint complex
MEN	Mitotic exit network
MT	Microtubule
rDNA	ribosomal DNA
SAC	Spindle assembly checkpoint
SCS	Sister chromatid separation
SCI	Sister chromatid intertwine
SCJ	Sister chromatid junction
SE	Spindle elongation
SMC	Structural maintenance of chromosomes
SPB	Spindle pole body
SPOC	Spindle position checkpoint
ssDNA	single stranded DNA
SUMO	Small ubiquitin-like modifier
TEL	Telomere
ts	thermosensitive

Abstract

During mitosis the newly replicated genetic material, organized in sister chromatids, is equally subdivided into the daughter cells through a fine-regulated process called chromosome segregation. Sister chromatids are held together and identified as sisters by cohesin. At the metaphase-to-anaphase transition, when all chromatids are correctly attached to the spindle, cohesin is cleaved and chromosome segregation initiates. Beside cohesin, all linkages between sister chromatids need to be removed to allow for their complete separation. Additional linkages include DNA linkages (or sister chromatid intertwines, SCIs), such as recombination intermediates and DNA catenanes.

In *Saccharomyces cerevisiae* a mutant that lacks the activities of the Polo-like kinase Cdc5 and the phosphatase Cdc14, two major mitotic regulators, has been identified that proved to be particularly suitable for studying SCIs that persist in mitosis. The *cdc5 cdc14* double mutant arrests with short and stable mitotic spindles and unseparated nuclei, despite having cleaved cohesin. In addition to having a spindle elongation defect, these cells are also impaired in the resolution of cohesin-independent linkages between chromatids.

We found that these linkages mostly consist of DNA catenanes, that persist in *cdc5 cdc14* cells at their terminal arrest and that are sufficient to counteract spindle elongation. Our results suggest that Cdc5 is required for their resolution.

This finding, together with the knowledge that Cdc5 promotes Cdc14 activation and that both proteins are essential for spindle elongation and mitotic exit, allows us to speculate that they coordinate different aspects of chromosome segregation to guarantee genome integrity throughout mitosis.

1. Introduction

1.1 Mitosis

1.1.1 Historical background

"Omnis cellula e cellula."

(Virchow, 1855)

"Omnis nucleus e nucleo."

(Flemming, 1882)

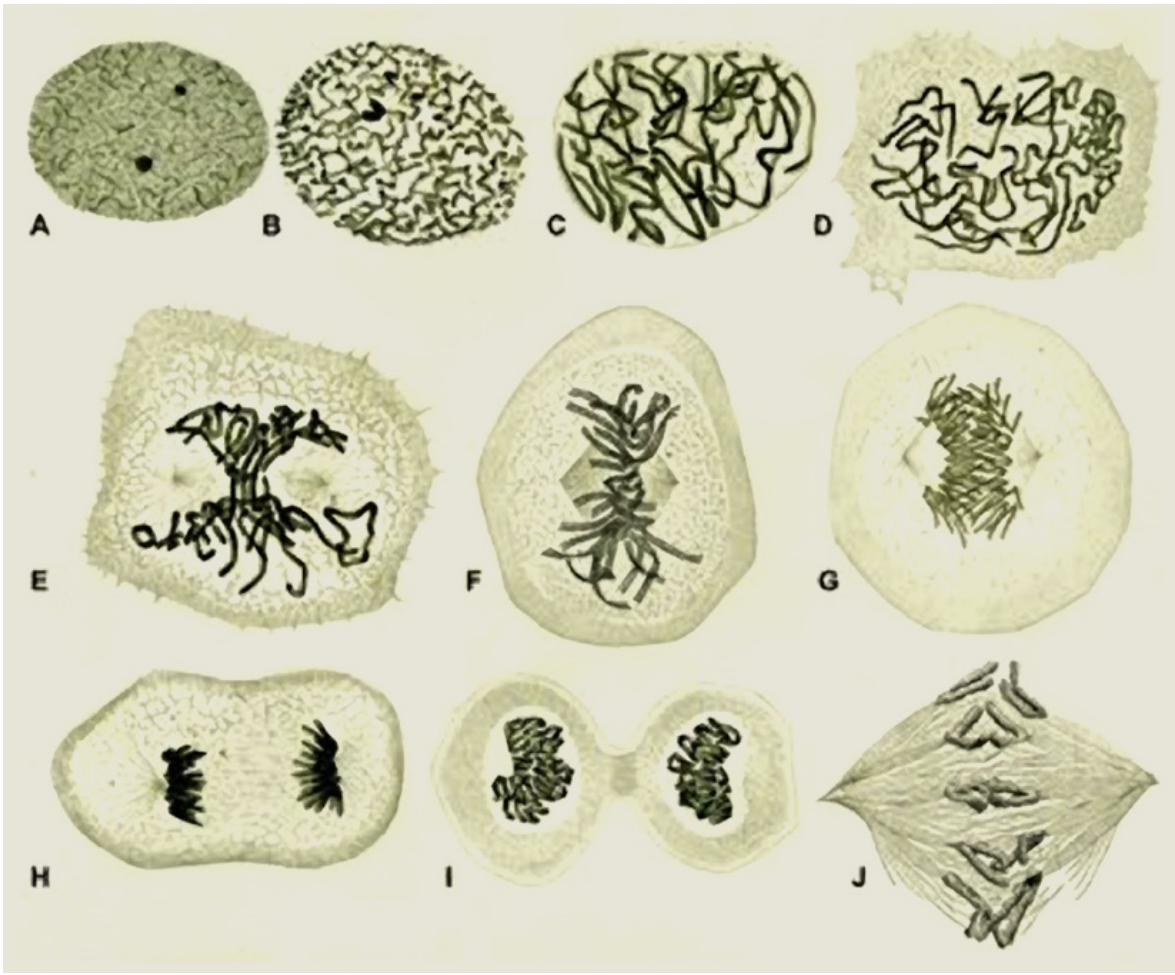

Figure 1. 1 Walther Flemming's observations of chromatin morphologies.
Hand drawn illustrations from Zellsubstanz, Kern und Zelltheilung (Flemming, 1882).

All organisms are made of cells and rely on cell division for their growth and reproduction. This concept has its roots in the 17th century, when the invention of the first microscopes allowed Robert Hooke and Antoni van Leeuwenhoek to observe that different organisms are made of units that Hooke named "*cellulae*". In the first half of the 19th century the improvements in microscopy allowed Theodor Schwann and Matthias Schleiden to formulate a "cell theory" affirming that all organisms are made of cells that are the basic units of life. However, Schwann and Schleiden believed that cells form *de novo* from a crystallization of organic substances outside of cells. In the next few years Barthelemy Dumortier, Robert Remak, Rudolf Virchow and other scientists showed that all cells originate from pre-existing cells through cell division. During division cells undergo dramatic rearrangements that were first described by Walther Flemming in the second half of the 19th century. Flemming illustrated his observations through series of detailed beautiful drawings. He noticed that the nuclear material (that he named "chromatin" for its ability to stain easily) had a variable morphology. In some cells, it appeared as an amorphous tangle, while in others it formed "threads" that he named "mitosen" from the Greek word for thread "μίτος". Flemming proposed that the amorphous chromatin transforms into the threads, thereby providing continuity to the nuclear material, though he did not have the instruments to prove it (Paweletz, 2001). Few years later these threads were renamed "chromosomes" (chromatin-bodies), while the term mitosis has come to indicate the process.

Two centuries later, the concept that the nuclear or "genetic" material is passed from mother to daughter cells has become common knowledge. However, the exact mechanisms through which cells divide and correctly inherit the genetic material are not fully understood and are still the object of extensive research.

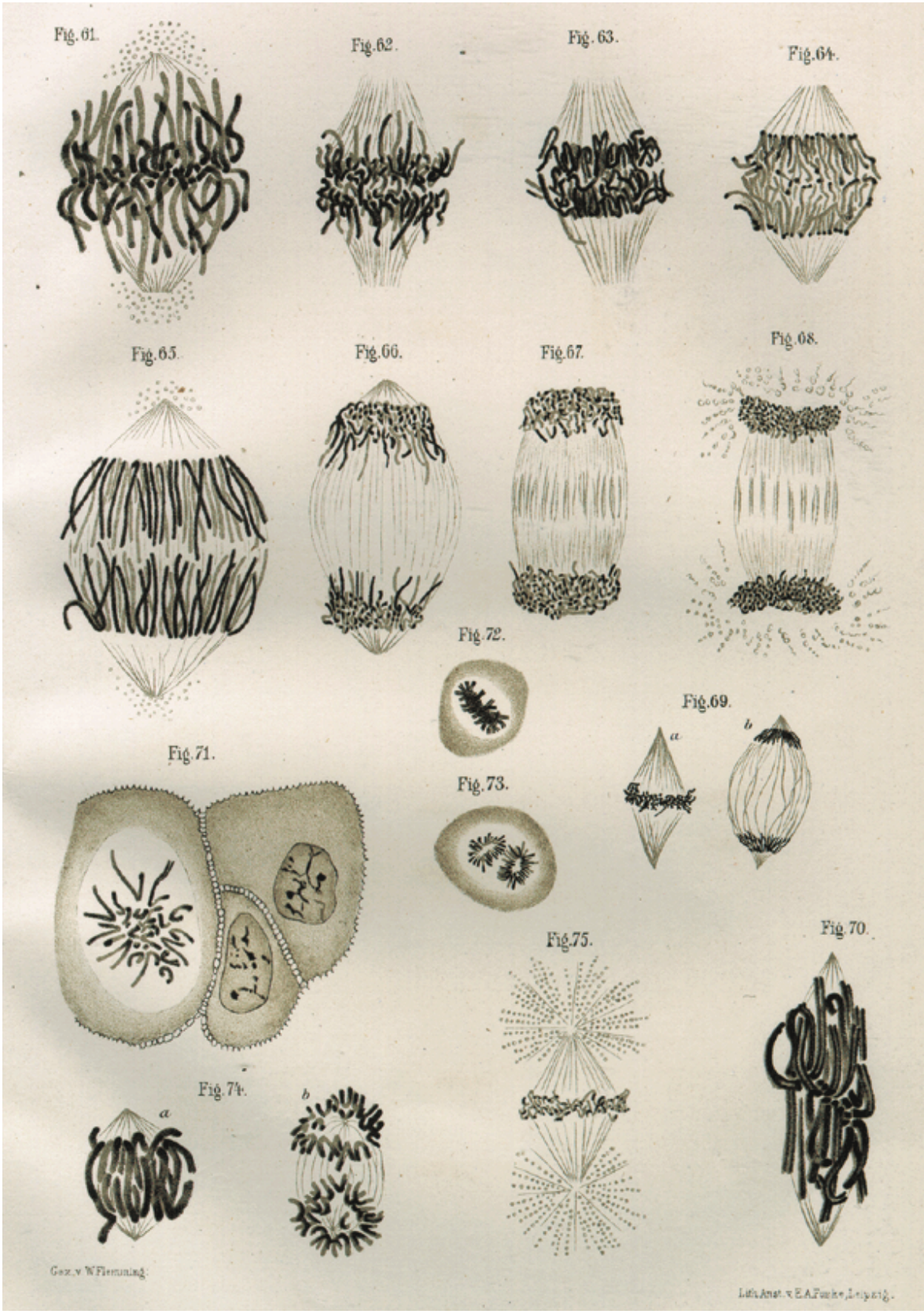

Figure 1. 2 Walther Flemming's observations of "*mitosen*".
Hand drawn illustrations from Zellsubstanz, Kern und Zelltheilung (Flemming, 1882).

1.1.1 Overview of mitotic processes

The central event of mitosis is the separation into the two daughter cells of the genetic material, duplicated in the previous S or "Synthesis" phase and then condensed into rod-shaped structures named sister chromatids. This process is known as chromosome segregation and relies on the combined action of the mitotic spindle and of cohesin. The mitotic spindle is a bipolar cytoskeletal structure composed by microtubules (MTs) that contacts sister chromatids and pulls them apart; cohesin is a protein complex that holds together sister chromatids since their replication, thereby identifying them as sisters and allowing their correct attachment and orientation on the spindle.

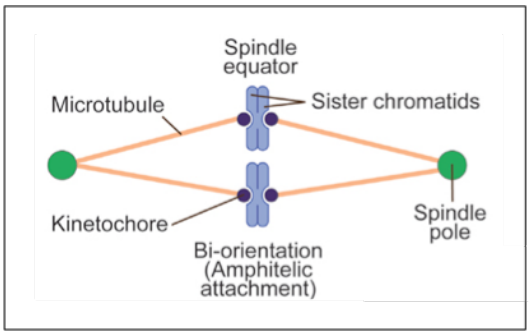

Figure 1. 3 Correct attachment of chromatids to the spindle.
Modified from (Krenn and Musacchio, 2015).

Although some features of mitosis vary among different organisms, the core steps are shared by all eukaryotes. All the steps preparatory for chromosome segregation are collectively known as mitotic entry, while chromosome segregation itself and the steps to reset the conditions for the new cell cycle are known as mitotic exit. Despite being a continuous process, mitosis is traditionally divided into serial phases: prophase, prometaphase (present only in vertebrates), metaphase, anaphase and telophase. During prophase, the genetic material is condensed into chromatids and centrosomes, organelles that function as microtubule organizing centers, move to opposite poles of the nucleus and start to assemble the spindle. Next, in vertebrate cells, the nuclear envelope breaks down (prometaphase) to allow the spindle microtubules to contact chromatids. In the budding

yeast *Saccharomyces cerevisiae*, the model organism used in this thesis, the nuclear envelope remains intact throughout mitosis and the spindle assembles inside the nucleus from Spindle Pole Bodies (SPBs, the yeast equivalent of centrosomes) that are embedded in the membrane. The attachment between microtubules and chromatids takes place on a multiprotein complex named kinetochore (KT) that assembles on a specialized region on each chromatid named centromere. In order to correctly separate, each sister must bind to microtubules emanating from SPBs at the opposite poles of the cell, achieving the so-called "bi-polar orientation". When all chromatids are correctly attached to the spindle (metaphase), a signaling cascade is activated leading to the activation of a protease named separase that cleaves cohesin, allowing chromatids to separate (anaphase). Next, spindle elongation pulls chromatids further apart. In telophase the spindle is disassembled, the nuclear envelope is reassembled forming two separate nuclei and chromosomes decondense. After chromosome segregation is completed, mother and daughter cells separate through a process named cytokinesis that squeezes the cells on a pre-determined plane (in yeast on the "bud-neck") through the action of a contractile acto-myosin ring. For review see (Morgan, 2007; Dörter and Momany, 2016)

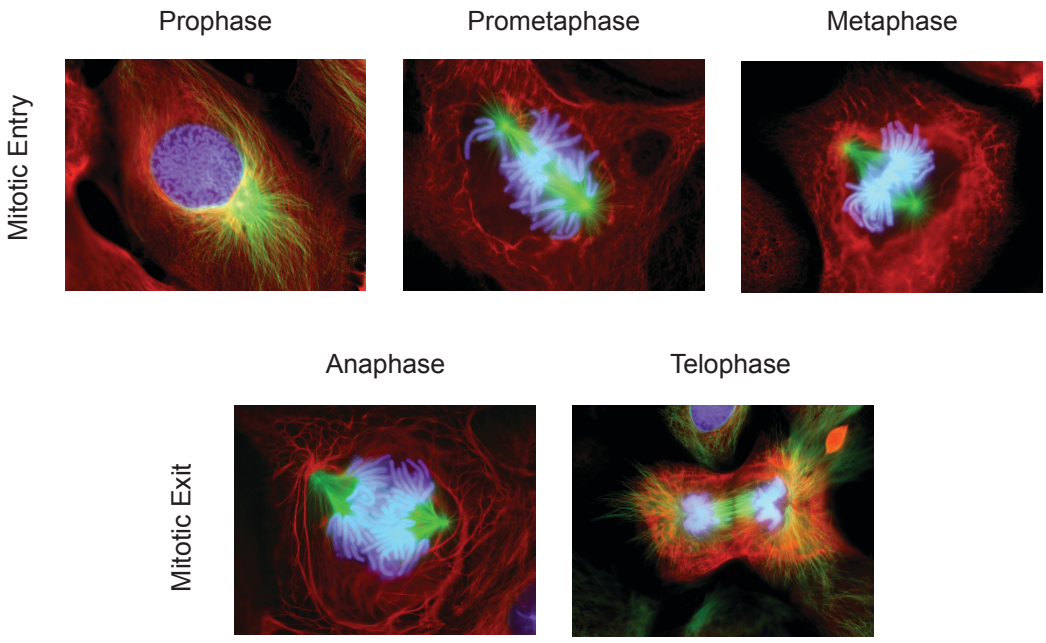

Figure 1. 4 The phases of mitosis.
Images of Newt lung cells stained with fluorescent dyes undergoing mitosis. Courtesy of Prof. Conly Rieder.

1.1.2 Regulation of mitosis

For a correct execution of mitosis, it is fundamental that all mitotic events are executed in the right order. This is achieved by the monitoring activity of the cell cycle control system, whose main mitotic players are the cyclin-dependent kinases (Cdks), B-type cyclins and the Anaphase Promoting Complex or Cyclosome (APC/C).

Cdks are a class of kinases whose activity is determined by the interaction with different subunits named cyclins. While higher eukaryotes have several Cdks, budding yeast has only one, Cdc28. Different types of cyclins, expressed in different cell cycle stages, confer Cdks a different substrate specificity (Peeper *et al.*, 1993). By phosphorylating different substrates in distinct cell cycle stages, Cdks and cyclins ensure the correct sequence of events to proceed through the cell cycle. In mitosis, Cdks bound to mitotic B-type cyclins promote early mitotic events such as chromosome condensation, nuclear envelope breakdown and spindle assembly. Budding yeast has four mitotic cyclins, Clb1,2,3,4, among which Clb2 plays the major role (Bloom and Cross, 2007). In addition, also the S-phase cyclin Clb5 promotes early mitotic events.

Mitotic Cdks regulate mitosis up to metaphase. Next, progression through anaphase and mitotic exit are characterized by a decrease in mitotic-Cdk activity and by its inactivation (Sullivan and Morgan, 2007). Lowering kinase activity at anaphase onset is required to promote chromosome segregation (for example, for spindle stabilization and elongation). Inactivating mitotic-Cdk allows its phosphorylations to be reverted, which is necessary to exit from mitosis and to reset the conditions for the new cell cycle. Low kinase activity is achieved by inactivating Cdks through degradation of cyclins. Cyclins are targeted for degradation by the APC/C, a large multi-protein complex that ligates ubiquitin, a small regulatory protein, onto substrates (Sudakin *et al.*, 1995). Poly-ubiquitilated substrates are recognized and degraded by the proteasome. The APC/C is activated at the metaphase to anaphase transition by binding with its regulatory subunit Cdc20. Active APC/C^{Cdc20} targets S and M cyclins for degradation. The other major target

of the APC/C^{Cdc20} is securin, a protein that binds to separase keeping it inactive (Visintin, 1997). Thus, APC/C^{Cdc20} coordinates cohesin cleavage and chromosome segregation with mitotic-Cdks inactivation. Later in anaphase, APC/C detaches from Cdc20 and binds to its other activator Cdh1. APC/C^{Cdh1} completely degrades M cyclins and keeps Cdks inactive up to the next G1 (Schwab, Lutum and Seufert, 1997; Visintin, 1997; Zachariae, 1998). In addition to mitotic-Cdks inactivation, mitotic exit requires the active dephosphorylation of Cdks substrates (De Wulf, Montani and Visintin, 2009). In budding yeast this is carried out by the phosphatase Cdc14. This phosphatase plays a major role in anaphase in budding yeast because, in addition to dephosphorylating Cdks substrates, it also promotes some early-anaphase events and contributes to mitotic-Cdks inactivation by activating the APC/C^{Cdh1} and promoting the accumulation of the mitotic-Cdks inhibitor Sic1 (Visintin *et al.*, 1998).

Beside Cdks, two other classes of kinases contribute to mitotic events, the Polo-like kinases (Sunkel and Glover, 1988) and the Aurora kinases. Budding yeast has only one of each, Cdc5 (Kitada *et al.*, 1993) and Ipl1 (Chan and Botstein, 1993; Francisco, Wang and Chan, 1994), respectively. Cdc5 promotes entry into mitosis (Park *et al.*, 2003), chromatid condensation (St-Pierre *et al.*, 2009) and separation (Alexandru *et al.*, 2001), Cdc14 activation in mitotic exit (Stegmeier and Amon, 2004) and finally cytokinesis (Yoshida *et al.*, 2006). Ipl1 contributes to chromosome condensation (Lavoie, Hogan and Koshland, 2004) and is required for establishing the bipolar orientation of chromatids on the spindle (Krenn and Musacchio, 2015) and for spindle disassembly (Buvelot *et al.*, 2003). Similarly, beside Cdc14 other phosphatases work in mitosis, namely protein phosphatase type 2A (PP2A) and protein phosphatase type 1 (PP1). Both PP2A and PP1 counteract Aurora B once bipolar orientation is achieved (Espert *et al.*, 2014); PP2A also regulates Cdk activation in mitotic entry and is required to prevent precocious Cdc14 activation (Queralt *et al.*, 2006; Queralt and Uhlmann, 2008).

1.1.3 Mitotic checkpoints

Beside Cdks and APC/C, that control cell cycle progression by dictating the correct series of events, the cell cycle is also regulated by checkpoints that allow passing to a subsequent step of the cell cycle only if the previous ones have been correctly completed. Checkpoints get activated in the presence of errors and halt the cell cycle to provide the cell with additional time to correct them (Hartwell and Weinert, 1989).

The main checkpoint in mitosis is the highly conserved Spindle Assembly Checkpoint (SAC), also known as mitotic checkpoint. The SAC acts at the metaphase to anaphase transition and controls that all chromatids are attached to the spindle and that are attached with the correct, bipolar orientation (Musacchio and Salmon, 2007; Corbett, 2017). Central to SAC activity is the Mitotic Checkpoint Complex (MCC), that comprises Mad2, Cdc20 and BubR1 and is formed at unattached KTs (Rieder *et al.*, 1995). Indeed, unattached KTs act as catalysts for the conversion of Mad2 from an open (O-Mad2) to a closed (C-Mad2) conformation (De Antoni *et al.*, 2005; Nezi *et al.*, 2006; Mapelli and Musacchio, 2007). C-Mad2 closes around Cdc20 thereby sequestering it, preventing APC/C activation. BubR1 binds to Mad2-Cdc20 stabilizing the complex (Sczaniecka *et al.*, 2008; Faesen *et al.*, 2017). It has been recently found that the MCC complex can also directly bind to the APC/C, further inhibiting it (Izawa and Pines, 2015; Alfieri *et al.*, 2016). Fundamental to recruit Mad2 at unattached KTs is the kinase Mps1 (Yamagishi *et al.*, 2012; London and Biggins, 2014); when the KT binds to microtubules, Mps1 activity is lost and it stops producing MCC. In addition, also the kinase Aurora B, which phosphorylates several KT components when the KT is not attached, is inhibited (Krenn and Musacchio, 2015). This allows the phosphatases PP2A and PP1 to revert Mps1 and Aurora B phosphorylations (Liu *et al.*, 2010; London *et al.*, 2012; Espert *et al.*, 2014). Overall, this results in a shift in the kinase-phosphatase balance in favor of phosphatases that inhibits the recruitment of SAC components to the kinetochore, thereby silencing the SAC (Espert *et al.*, 2014).

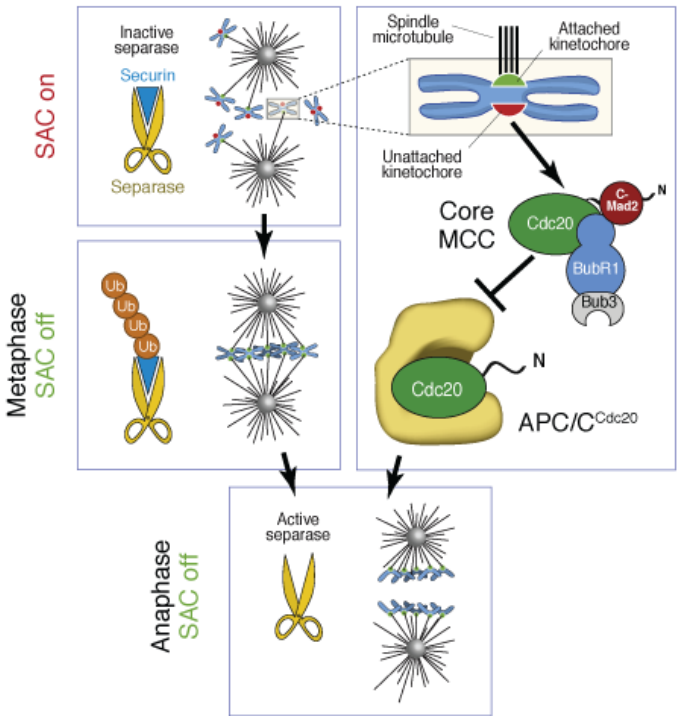

Figure 1. 5 The spindle assembly checkpoint.
Modified from (Musacchio, 2015).

In addition to this control system that halts the cell cycle if KTs are not attached, also other mechanisms exist that control that the attachment is bipolar. First, the geometry of kinetochores itself facilitates their attachment from opposite spindle poles (Indjeian and Murray, 2007). Second, an "error correction" mechanism exists that senses the presence of tension between kinetochores, that is established only when chromatids are attached to distinct spindle poles. Upon a low-tension signal, Aurora B promotes the detachment of MTs, generating unattached KTs that activate the SAC (Krenn and Musacchio, 2015). When tension is achieved, Aurora B is displaced from KTs and phosphatases prevail.

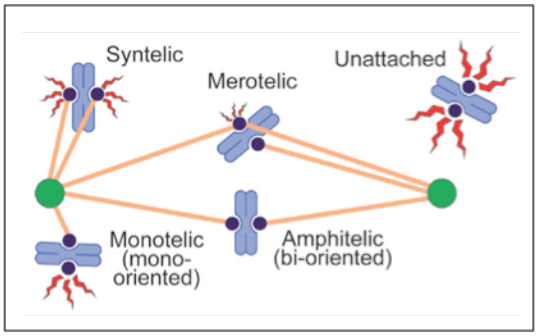

Figure 1. 6 Types of kinetochore-microtubule attachments.
Modified from (Krenn and Musacchio, 2015).

Beside the SAC, yeast has two other checkpoints monitoring mitotic events, the Spindle Positioning Checkpoint (SPOC) (Piatti *et al.*, 2006), that monitors that the spindle is correctly positioned toward the bud-neck before allowing mitotic exit, and the NoCut checkpoint, that delays cytokinesis if chromatids have not fully separated (Norden *et al.*, 2006).

1.1.2 Consequences of faulty mitosis

The majority of human cancers is characterized by an abnormal karyotype both with additional or missing chromosomes, and with chromosomes carrying structural rearrangements, such as translocations. This condition is known as aneuploidy and arises in consequence of chromosome instability. It is intuitive that aneuploidy can arise in mitosis because of errors in chromosome segregation. Indeed, mitosis is a highly complex process in which the genetic material has to undergo several structural rearrangements in order to be properly segregated and defects in the mitotic machinery can lead to the missegregation of one or more chromosomes. For example, chromosome missegregation can arise when chromatid cohesion is compromised, when chromatids are not compacted or when are not correctly attached to the spindle. Indeed, errors in sister chromatids

cohesion and condensation, in spindle functions and in SAC activity, can all lead to aneuploidy (Ganem and Pellman, 2012; Bakhoum *et al.*, 2014; Bastians, 2015).

In addition, chromosome instability can arise in mitosis also as a consequence of "problems" originated in S phase that are not resolved before chromosome segregation. These consist of different types of entanglements between sister chromatids. Some originate physiologically during replication, while others in consequence of replication stress or DNA damage (Mankouri, Huttner and Hickson, 2013; Baxter, 2015). The presence of entanglements between chromatids prevents their full separation. Undergoing mitosis and cytokinesis can lead to DNA breakage and to genome instability in the next cell cycle.

1.2 Chromatid identity and condensation

For a correct partition of the genetic material, it is important that the identity of sister chromatids is maintained up to chromosome segregation in order to separate them into the two daughter cells. This is achieved by holding sister chromatids together from their replication up to anaphase onset, through protein complexes named cohesin.

Another important feature of chromatids essential for a correct segregation is their compaction. Indeed, centimeters-long DNA molecules need to undergo extensive structural rearrangements to be shortened enough to be segregated into micrometers-long cells. The process by which chromatin is rearranged into forming short, rod-shaped chromosomes is known as chromosome condensation. Chromosome condensation serves several functions. Beside shortening chromatin (compaction), it drives the separation of entangled sister DNA molecules by folding each of them on itself (resolution) and confers to chromatin the proper physical properties to sustain the forces of the pulling mitotic spindle in anaphase. Essential players in chromosome condensation are the Structural Maintenance of Chromosomes (SMC) complexes, including condensin and the abovementioned cohesin.

SMC complexes are large, ring-shaped protein complexes that organize chromatin architecture by mediating interactions between different DNA segments. Beside SMC complexes, other factors are required for chromosome structural organization: type II topoisomerases, that provide the enzymatic activity necessary to disentangle DNA molecules, and histone modifications, that contribute to compaction.

1.2.1 SMC complexes

SMC complexes are ring-shaped multiprotein complexes that play pivotal roles in chromatin architecture and share the same core structure: they are composed by two

structural maintenance (SMC) proteins, a "kleisin" protein, and additional regulatory subunits. SMC proteins are characterized by the presence of two coiled-coil domains, separated by a hinge domain and flanked by two globular domains that contain Walker A (at the N-terminus) or Walker B (at the C-terminus) motifs. SMC molecules fold on themselves at the hinge domain forming an intramolecular coiled-coil structure. The N- and C-terminal Walker domains bind each other forming a functional ATPase domain of the ATP-binding cassette (ABC) family. Two different SMC proteins (Smc1 and Smc3 in cohesin, Smc2 and Smc4 in condensin) bind each other at the hinge domain. At the other end, the two heads bind each other dynamically in an ATP-dependent manner. The kleisin subunit (in yeast, Scc1 in cohesin, Brn1 in condensin) binds to the SMC heads stabilizing the interaction and closing the ring (Hirano, 2006; Uhlmann, 2016).

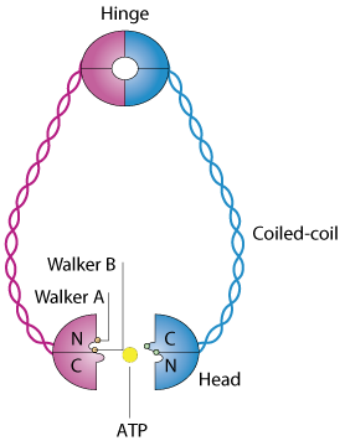

Figure 1. 7 General structure of the core of SMC complexes.
Modified from (Hirano, 2006).

Since it was discovered that the SMC complexes are ring-shaped, it was proposed a model for their activity in which they topologically embrace DNA and by embracing more than one DNA segment they structure chromatin architecture (Haering *et al.*, 2002). Several evidences have been now gathered supporting this model for all complexes (Gruber, Haering and Nasmyth, 2003; Ivanov and Nasmyth, 2005, 2007; Haering *et al.*, 2008; Cuylen, Metz and Haering, 2011; Kanno, Berta and Sjögren, 2015; Murayama and Uhlmann, 2015; Wilhelm *et al.*, 2015).

Cohesin main function is to keep sister chromatids together from replication to segregation, while condensin main function is in chromosome compaction and resolution. However, they also have additional, sometimes overlapping roles: cohesin collaborates in chromosome condensation (Guacci, Koshland and Strunnikov, 1997; Bhalla, 2002) and both cohesin and condensin participate to transcription regulation (Hadjur *et al.*, 2009) and to DNA repair (Sjögren and Nasmyth, 2001). In addition to cohesin and condensin, a third SMC complex exists, the Smc5/6 complex (Fousteri and Lehmann, 2000). This complex, differently from the other two, has its main function in DNA repair and recombination.

1.2.2 Cohesin: identifying chromatids as sisters

The cohesin ring is formed by the two SMC proteins Smc1 and Smc3 and the kleisin Scc1 (Guacci, Koshland and Strunnikov, 1997; Michaelis, Ciosk and Nasmyth, 1997; Losada, Hirano and Hirano, 1998). Three additional subunits bind to the cohesin core: Scc3 and Pds5 bind to Scc1, while Wpl1 interacts with Scc1, Scc3, Pds5 and Smc3. The pivotal role of cohesin is to hold sister chromatids together since their replication, to make sure that during chromosome segregation the duplicated chromosomes are correctly separated into the two daughter cells. For this purpose, cohesin is loaded onto DNA before its replication and then cleaved at the metaphase to anaphase transition only when all chromatids are correctly attached to the spindle.

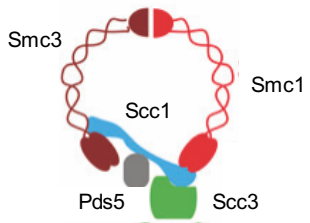

Figure 1. 8 The cohesin complex.
Budding yeast subunits are indicated. Modified from (Marston, 2014).

1.2.2.1 Cohesin loading

The establishment of cohesion between chromatids requires first that cohesin is loaded onto chromatin (Ciosk *et al.*, 2000), next that it is stabilized (Uhlmann and Nasmyth, 1998). In budding yeast, cohesin is loaded in late G1, when Scc1 is synthesized (Guacci, Koshland and Strunnikov, 1997; Michaelis, Ciosk and Nasmyth, 1997). Cohesin loading is mediated by the Scc2-Scc4 complex that tethers cohesin to DNA and promotes DNA entrapment into the cohesin ring (Ciosk *et al.*, 2000; Haering *et al.*, 2008; Murayama and Uhlmann, 2014). This reaction requires ATP hydrolysis by the Smc head domains (Arumugam *et al.*, 2003; Murayama and Uhlmann, 2014) and opening of the ring; whether this happens between the hinge domains or the head domains is still matter of debate (Gruber *et al.*, 2006; Murayama and Uhlmann, 2014, 2015; Uhlmann, 2016; Litwin and Wysocki, 2017).

After having embraced DNA, the cohesin ring is not stably bound and tends to detach from it. A mechanism for this has been recently proposed: two "sensor" lysine residues on the ATPase head of Smc3 interact with the DNA inducing ATP hydrolysis that destabilizes the Smc3-Smc1 interaction (Murayama and Uhlmann, 2015), promoting Wpl1-Pds5-Scc3-dependent dissociation of Scc1 from Smc3, thereby opening the ring (Rowland *et al.*, 2009; Chan *et al.*, 2012, 2013; Murayama and Uhlmann, 2015). Cohesin embracing of DNA is stabilized in S phase by the acetyltrasferase Eco1. Eco1 acetylates the two sensor lysine residues of Smc3 and this inhibits Wpl1 releasing activity (Tóth *et al.*, 1999; Rowland *et al.*, 2009). Next, cohesion is maintained by Scc3 and Pds5, that inhibits Smc3 deacetylation (Rowland *et al.*, 2009).

Cohesin loading takes place at specific sites that are marked by Scc2-Scc4. However, cohesin localization does not overlap with Scc2-Scc4 because the transcription machinery pushes cohesin away from transcribed regions to convergent transcription termination sites (Lengronne *et al.*, 2004; Ocampo-Hafalla *et al.*, 2016). Cohesin is enriched in a region surrounding the centromere, defining it as the pericentromere, and on

chromosome arms on not uniformly distributed regions (Blat and Kleckner, 1999; Megee *et al.*, 1999; Tanaka *et al.*, 1999). The enrichment at pericentromeres facilitates the bipolar attachment to the spindle by establishing a specific geometry of kinetochores (Tanaka *et al.*, 2000; Ng *et al.*, 2009). When kinetochores are bound to the spindle, this cohesin counteracts the pulling force of the spindle. The presence of the two opposing forces results in the establishment of tension and in centromeres being pulled-apart (for up to 10 kb, corresponding to 1μm) while chromosome arms remain associated (Goshima and Yanagida, 2000; He, Asthana and Sorger, 2000; Tanaka *et al.*, 2000).

1.2.2 Condensin: shaping chromosomes

Condensin is a highly conserved complex present in all eukaryotes; primitive condensin complexes have also been found in many prokaryotes and archaea. Higher eukaryotes have two condensin complexes, Condensin I and II, which differ for their non-SMC subunits. Budding yeast instead has only one, homologous to Condensin I, composed by the SMC proteins Smc2 and Smc4, the kleisin Brn1 and the HEAT (huntington, elongation factor 3, protein phosphatase 2A, Tor1 kinase) repeat proteins Ycs4 and Ycg1. The main role of condensin is to organize the three-dimensional structure of the genome. In mitosis, this means condensing chromatin into chromosomes.

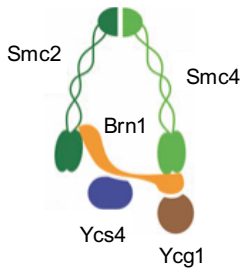

Figure 1. 9 The condensin complex.
Budding yeast subunits are indicated. Modified from (Marston, 2014).

Though the exact mechanism by which condensin achieve DNA condensation is still a matter of investigation, it is believed that condensin creates loops within the same DNA molecule. By analogy with cohesin it has been suggested that condensin achieves this by topologically embracing DNA (Haering *et al.*, 2008; Cuylen, Metz and Haering, 2011).

1.2.2.1 Condensin localization and loading

In budding yeast, condensin is enriched at specific chromosome loci, including centromeres, the rDNA array (the locus containing repeats of the rRNA genes), subtelomeric regions and RNA polymerase III (Pol III) transcribed genes (Wang *et al.*, 2005; D'Ambrosio, Schmidt, *et al.*, 2008). Condensin recruitment at different loci is mediated by different factors. For example, its recruitment at centromeres and at the rDNA requires the interaction with monopolin, a structural complex that organizes rDNA and centromeres architecture, that is enriched in these regions (Johzuka and Horiuchi, 2009). In addition, the recruitment of condensin at the rDNA locus necessitates also nucleolar proteins Fob1 and Tof2 (Johzuka and Horiuchi, 2009). Instead, recruitment at Pol III transcribed genes, such as the tRNA genes, involves the transcription factor complex of Pol III TFIIIC (D'Ambrosio, Schmidt, *et al.*, 2008).

Though in different organisms, including the fission yeast *Schizosaccharomyces pombe*, condensin localizes in proximity of highly transcribed Pol II genes, this was never assessed in *S. cerevisiae*. It was found instead that transcription counteracts condensin enrichment at the rDNA and at the subtelomeric Y' repeats (Clemente-Blanco *et al.*, 2009, 2011). Indeed, condensin enrichment at these regions requires anaphase-specific Cdc14-dependent transcription inhibition. It was also proposed that condensin localization is influenced by the presence of nucleosomes, that would act as a barrier for condensin association (Toselli-Mollereau *et al.*, 2016). In budding yeast this is supported by the

observation that condensin binding pattern negatively correlates with nucleosomes occupancy (Piazza *et al.*, 2014). Finally, condensin loading might also depend on DNA structure, as it has been shown to bind to ssDNA where it promotes its re-annealing (Sakai *et al.*, 2003)

The mechanisms by which condensin is loaded onto DNA are only now starting to be elucidated. Evidences have been collected for condensin topologically embracing DNA (Cuylen, Metz and Haering, 2011). However, it was found that condensin binds DNA also physically, and this finding can help explaining how they are able to create large, stable DNA loops (Piazza *et al.*, 2014). Two interaction surfaces have been identified: the hinge domain between Smc2 and Smc4 that can bind to ssDNA (but not dsDNA) promoting its reannealing (Sakai *et al.*, 2003) and a second interaction surface, that has just been characterized in yeast and humans, involving Brn1 and Ycg1 (Piazza, Haering and Rutkowska, 2013; Kschonsak *et al.*, 2017). This interaction is not sequence or structure specific, thus providing a general mechanism for condensin binding to the DNA throughout the genome. Intriguingly, it was found that the flexible Brn1 kleisin subunit acts as a "safety belt" that entraps DNA in a groove formed by Ycg1, thereby stably anchoring the condensin complex to the DNA. This finding suggests that being anchored to the DNA may promote subsequent DNA embracing (Kschonsak *et al.*, 2017).

1.2.2.2 Models of Condensin activity

To create a specific chromatin architecture, condensin complexes need to mediate interactions between distal DNA loci, creating loops. Currently, two models are taken into consideration for how condensin can achieve this (Uhlmann, 2016). (1) Condensin may crosslink stochastic pairwise chromatin interactions. This model is supported by Brownian dynamics simulation of a budding yeast chromosome (Cheng *et al.*, 2015) but has the limit that in this way condensin would promote both intra- and inter-molecular pairing. (2) The

second model is the loop extrusion mechanism that predicts that a chromatin loop is pushed through the condensin ring and next extended (Nasmyth, 2001). This model is supported by polymer dynamics simulations as well (Fudenberg *et al.*, 2016; Goloborodko *et al.*, 2016). A recent study showed that yeast condensin is able to translocate on DNA in an ATP-dependent manner, and "to move two DNA substrates relative to one another" (Terakawa *et al.*, 2017). This finding indicates that condensin has the motor activity that is necessary to create a loop by sliding on DNA, thus supporting this second model.

How condensin ability to create loops results in the global chromatin organization and how the latter changes from interphase to mitosis remain unclear. Recently, the development of chromosome conformation capture techniques provided a powerful tool to investigate these questions. Recent Hi-C (high-throughput sequencing based chromosome conformation capture) (Lieberman-Aiden *et al.*, 2009) studies from different species (Naumova *et al.*, 2013; Gibcus *et al.*, 2017; Kakui *et al.*, 2017; Lazar-Stefanita *et al.*, 2017; Schalbetter *et al.*, 2017) revealed a common pattern for chromatin interaction. It has been observed that in interphase chromatin local-range interactions are favored, while in mitotic chromosomes a relative decrease in local range interactions and a relative increase in long-range interactions are seen, suggesting that assembling chromosomes in mitosis requires an increase in chromatin interactions in a specific length range (Kakui and Uhlmann, 2017b). These changes in chromatin interactions are dependent on condensin and, in yeast, also on cohesin (Kakui *et al.*, 2017; Lazar-Stefanita *et al.*, 2017; Schalbetter *et al.*, 2017), consistent with its role in condensation (Guacci, Koshland and Strunnikov, 1997).

1.2.2.3 Condensin regulation

In yeast, condensin remains always associated with the DNA, but its localization changes throughout the cell cycle (Freeman, Aragon-Alcaide and Strunnikov, 2000). This supports the idea that chromosome formation in mitosis requires an activation of the condensin

complex. Indeed, different post-translational modifications have been found to influence condensin localization or activity in mitosis. First, Smc4 phosphorylation by mitotic Cdk in early mitosis is necessary to initiate chromosome condensation, likely by stabilizing condensin interaction with chromatin (Robellet *et al.*, 2015). Next, in early anaphase, condensin is further phosphorylated by Cdc5 on non-SMC subunits (St-Pierre *et al.*, 2009). This boosts condensin supercoiling activity *in vitro,* and prompts its enrichment at the rDNA, which is required for rDNA condensation (St-Pierre *et al.*, 2009). It was recently found that Cdc5 activity is also required for condensin delocalization from centromeres to chromosome arms in anaphase and it was suggested to promote its supercoiling activity *in vivo* (Leonard *et al.*, 2015). In addition, also the Aurora kinase Ipl1 has been shown to be required for Ycg1 phosphorylation in mitosis and for anaphase rDNA condensation (Lavoie, Hogan and Koshland, 2004).

Besides kinases, also phosphatases have been shown to impact on condensin localization and activity: in early anaphase, Cdc14 promotes condensin enrichment at the rDNA, though indirectly by inhibiting rDNA transcription and by promoting Ycs4 sumoylation (D'Amours, Stegmeier and Amon, 2004; Sullivan *et al.*, 2004; Wang, Yong-Gonzalez and Strunnikov, 2004; Tomson *et al.*, 2006; Clemente-Blanco *et al.*, 2009); in late anaphase, instead, Cdc14 activity delocalizes condensin from the rDNA, promoting its decondensation (Varela *et al.*, 2009)

1.2.3.4 Other factors contributing to chromosome compaction

In addition to condensin, other factors contribute to chromosome condensation, including type II topoisomerases and histone tails modifications. In mitosis, a change in histone tails modifications promotes interactions between consecutive nucleosomes. While in interphase this interaction is prevented by acetylation of histone H4 on K16, in mitosis two phosphorylation events on histone H3, first by the kinase Haspin on T3, then by Aurora B

on S10, are necessary to recruit the deacetylase Hst2 that reverting H4 acetylation allows chromatin compaction (Neurohr *et al.*, 2011; Wilkins *et al.*, 2014).

Though the classical model for chromosome formation (hierarchical folding) predicts sequential levels of coiling, in which nucleosomes play a central role in establishing the first levels of folding, recent studies assessing the relative contribution of condensin and nucleosomes seem to question this view (Shintomi, Takahashi and Hirano, 2015; Kakui and Uhlmann, 2017a; Shintomi *et al.*, 2017). These findings are based on a novel technique to follow chromosome formation *in vitro* (by treating *Xenopus* sperm chromatin with *Xenopus* eggs extracts or with purified factors) through which it was initially found that only six factors are required: the two condensin complexes, topoisomerase II, core histones and three histone chaperones, required for histone deposition (Shintomi, Takahashi and Hirano, 2015). When the same technique was next applied to mice sperm chromatin, which differently from Xenopus' is devoid of histones, the relative contribution of condensin and nucleosome to condensation could be analyzed. It was found that treatment with extracts depleted of Asf1, a histone chaperone, prevented histone deposition but still allowed the formation of structures similar to chromosomes, in which a DAPI-dense signal on the axis is surrounded by a blurred signal. Instead, condensin I and II depletion resulted in amorphous chromatin masses (Shintomi *et al.*, 2017).

1.3 Sister chromatid separation

Chromosome segregation requires that any linkage between sister chromatids that has been previously established is removed. As previously explained, chromatids are held together by proteinaceous linkages consisting of cohesin. In addition, chromatids are also connected by DNA linkages or intertwines that arise throughout replication as a consequence of the double helical structure of DNA. Both types of linkages need to be removed to allow chromosome segregation.

1.3.1 Protein linkages: cohesin

Establishment of cohesion between sister chromatids in S phase holds them together until anaphase onset. The presence of cohesin is fundamental to correctly orient chromatids on the spindle and to oppose resistance to the spindle pulling force, thereby promoting and stabilizing the bipolar attachment. At metaphase, when all kinetochores are correctly attached to the spindle, cohesin is cleaved, triggering chromosome segregation and marking entry into anaphase. Cohesin cleavage is the final step of a signaling cascade that starts with SAC silencing and culminates with the activation of a cysteine protease, named separase (Esp1 in budding yeast) that cleaves the Scc1 subunit of the cohesin complex (Uhlmann *et al.*, 2000). SAC inactivation is necessary as it renders Cdc20 available for the activation of the APC/C^{Cdc20} that targets for degradation the separase inhibitor, securin (Pds1 in yeast), that, before anaphase, binds and inhibits the separase (Cohen-Fix *et al.*, 1996; Ciosk *et al.*, 1998; Shirayama *et al.*, 1999; Uhlmann, Lottspelch and Nasmyth, 1999; Uhlmann *et al.*, 2000). The Pds1-Esp1 interaction has also the function to promote Esp1 accumulation in the nucleus, so that it can rapidly cleave cohesin upon Pds1 degradation.

In addition to Pds1 degradation, cohesin cleavage is also regulated by Scc1 phosphorylation. Indeed, Scc1 cleavage is promoted by Cdc5-dependent phosphorylation (Hornig *et al.*, 2002).

While cohesin cleavage is sufficient to start chromosome segregation in presence of a functional mitotic spindle (Uhlmann *et al.*, 2000), some complexes may still remain on chromatids. These are subsequently removed in anaphase by the combined action of the spindle and condensin that, by pulling chromatids apart, expose cohesin complexes to the action of the separase (Renshaw *et al.*, 2010).

1.3.1 DNA linkages:

> *"Since the two chains in our model are intertwined, it is essential for them to untwist if they are to separate. […] Although it is difficult at the moment to see how these processes occur without everything getting tangled, we do not feel that this objection will be insuperable."*
>
> (Watson and Crick, 1953)

Full chromosome segregation requires that the sisters are completely separated from each other and that any possible entanglement between the two DNA molecules is unraveled. The occurrence of such entanglements is not rare, but rather occurs physiologically as a consequence of the double helix structure of DNA, which poses a topological problem for all the processes that need to use its information. Accessing DNA requires opening of the helix, which results in alterations of its twisting and in the formation of supercoils. Overwinding of the helix causes the accumulation of positive supercoiling, while underwinding causes negative supercoiling. For example, during DNA replication opening of the origin and subsequent replication fork progression require the turns of the helix to be pushed ahead of the fork. This reaction depends on the activity of DNA helicases and

results in the accumulation of positive supercoils ahead and negative supercoils behind the helicase. In principle, topological stress could diffuse along the DNA and be relieved simply by its axial rotation. However, eukaryotic DNA molecules are extremely long and different types of barriers are present, such as replication machineries, stable DNA-protein complexes or complexes anchoring DNA to the nuclear membrane that prevent rotation inside the nucleus. Thus, resolving topological stress requires an enzymatic activity. The enzymes deputed to this function are called DNA topoisomerases.

Despite the action of topoisomerases, in some occasions linkages between sister chromatids can occur throughout replication deriving from the turns of the helix of parental DNA and can persist in mitosis. Such linkages either consist of fully replicated, intertwined chromatids, or unreplicated parental DNA or result from processes of DNA recombination. Collectively, these linkages are known as Sister Chromatid Intertwines.

1.4 Sister chromatid intertwines

1.4.1 DNA Topoisomerases

DNA Topoisomerases are enzymes that alter DNA topology by cleaving one or two DNA strands, allowing the other strand or another double-strand to pass through the break, and then ligating the cleaved strand(s). DNA cleavage always involves the formation of a phosphodiester bond between one end of the cleaved DNA and the enzyme, thereby minimizing the risks associated to the formation of DNA single or double strand breaks. Eukaryotic topoisomerases are divided in two groups, type I and type II topoisomerases, according to their reaction: type I cleave and reseal a single DNA strand, while type II cleave and reseal dsDNA (Wang, 2002; Nitiss, 2009).

1.4.1.1 Type I Topoisomerases

Eukaryotic type I topoisomerases are monomeric enzymes whose reaction does not require ATP hydrolysis. They are classified in Type IA (or Top3) and Type IB (or Top1) and they differ for their structure and mechanism of reaction.

Topo IA targets negatively supercoiled DNA, where its binding results in unpairing of the strands, or positively supercoiled DNA if patches of ssDNA are already present. Topo IA acts through an "enzyme bridging" mechanism, in which the enzyme connects both ends of the cleaved strand and moves them across the other strand. Topo IA collaborates with RecQ helicases (Sgs1 in yeast, BLM in metazoans) to resolve ssDNA entanglements that originate during DNA recombination and replication: the helicase activity unwinds the intertwining exposing ssDNA on which Topo IA can act resolving it. Sgs1 (or BLM) and Topo IA form a stable complex together with the ssDNA binding

protein Rmi1 named the STR (or BTR) complex (Harmon, DiGate and Kowalczykowski, 1999; Ira *et al.*, 2003; Suski and Marians, 2008; Xu *et al.*, 2008).

Topo IB binds to dsDNA and relaxes both positively and negatively supercoiled DNA, by employing a "DNA rotation" mechanism. Topo IB introduces a nick on the DNA and, remaining covalently bound to only one of the ends, allows the two cleaved ends to rotate away from each other around the uncleaved strand, thereby relaxing supercoiling. Topo IB works mainly in relaxing positive supercoiling that accumulate ahead of the fork. However, it is not essential in yeast as its action can be compensated by Topo II (Bermejo *et al.*, 2007) (see below).

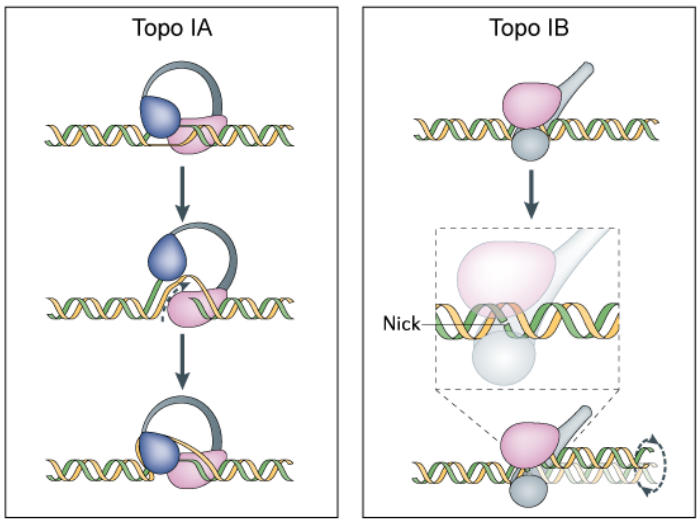

Figure 1. 10 Type I topoisomerases reaction mechanisms.
Modified from (Vos *et al*., 2011)

1.4.1.2 Type II Topoisomerases

Type II topoisomerases cleave dsDNA and can thereby resolve both supercoiling and intertwines formed between two dsDNA. The latter function is not shared with other topoisomerases and makes type II essential for genome stability and cell viability (DiNardo, Voelkel and Sternglanz, 1984; Holm *et al.*, 1985). While higher eukaryotes have two Topo II subtypes (Topo IIa and Topo IIb, where Topo IIa plays the main function), yeast has only one, Top2 (Goto and Wang, 1982, 1984), homolog to Topo IIa. Topo II are

homodimers organized in three domains: an N-terminal ATP-binding domain, a central, catalytic domain and a C-terminal regulatory domain (CTD). While the N-terminal and central domains are highly conserved, the C-terminal differs among species and isoforms (Nitiss, 2009). The large dimension of the dimer has made difficult to resolve its structure and early studies were able to determine the structure only of portions of the protein (Wigley *et al.*, 1991; Berger *et al.*, 1996; Classen, Olland and Berger, 2003; Dong and Berger, 2007; Nitiss, 2009). The structure of a fully functional construct containing the N-terminal and central domains (but not the unstructured C-terminal domain) in complex with a non-hydrolysable ATP-analogue and DNA was obtained for *S. cerevisiae* Top2 (Schmidt, Osheroff and Berger, 2012). Collectively, these studies showed that two subunits dimerize on three interfaces or "gates": on the N-terminal domain (N-gate), on the DNA cleavage site (DNA gate, between N-terminal and central domains) and on the C-terminal of the central domain (C-gate), while the central domain forms a cavity.

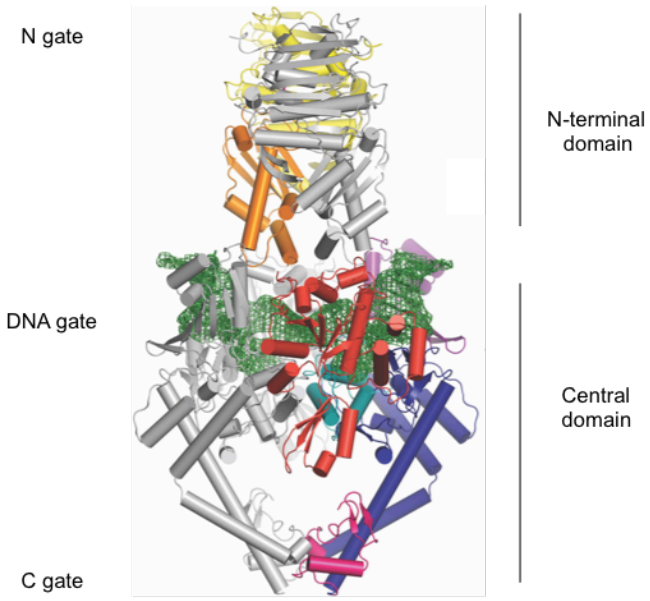

Figure 1. 11 Structure of *S. cerevisiae* Topo II (aa 1-1177) bound to DNA.
Modified from (Schmidt, Osheroff and Berger, 2012)

Topo II reaction involves binding of two dsDNA strands, cleavage of one of them (the G or gate segment), passage of the other (T segment) through the break and resealing of the break. First, the enzyme binds and bends the G segment; the binding of two ATPs at the N-terminal closes the N-gate, around the T segment; hydrolysis of one ATP promotes G segment cleavage through a reaction that results in the formation of a phospho-tyrosine bond between each strand and a tyrosine in each subunit; G segment cleavage allows the T segment to pass through the break and a conformational change prevents it to go back; next, the G segment is re-ligated, the second ATP hydrolyzed and the T segment released through the C-gate; finally, ADP release resets the enzyme for a new cycle (Roca and Wang, 1992, 1994; Berger *et al.*, 1996; Roca *et al.*, 1996; Nitiss, 2009; Schmidt, Osheroff and Berger, 2012).

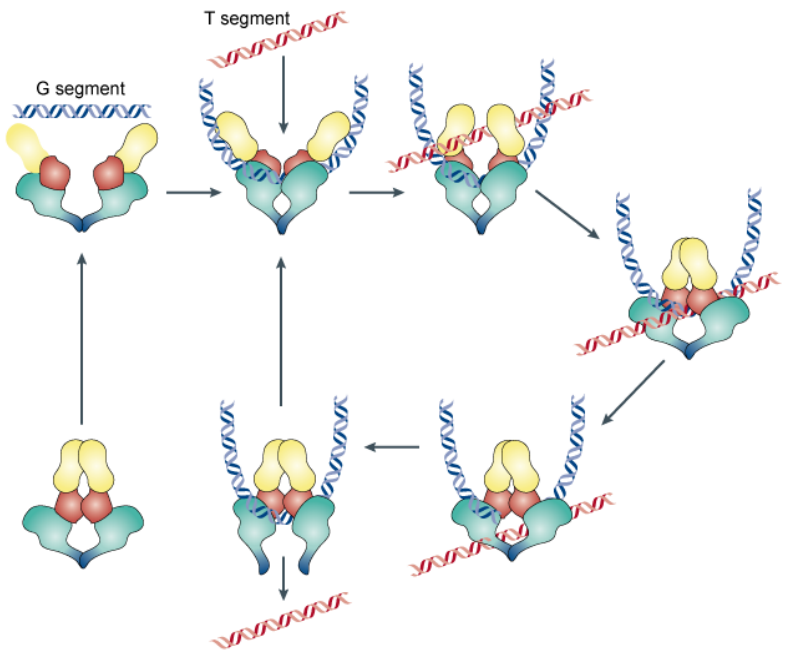

Figure 1. 12 Topo II reaction mechanism.
Modified from (Nitiss, 2009)

In all topoisomerase reactions the energy of the cleaved DNA bonds is preserved as each bond reforms. As DNA relaxation is energetically favorable, it can be carried out by ATP-independent enzymes, such as type I topoisomerases. Type II topoisomerases instead seem to be able to resolve intertwines below the expected thermodynamic equilibrium,

likely taking advantage of the energy generated by ATP hydrolysis (Rybenkov *et al.*, 1997). How Topo II achieves this *in vivo* is unclear, but it likely depends on Top2 preference for bent DNA substrates (Dong and Berger, 2007).

1.4.2 Sister chromatid intertwines

The presence of DNA linkages between sister chromatids can prevent their segregation in mitosis. Such linkages are often referred to as Sister Chromatid Intertwines (SCIs). Three types of SCIs exist, differing for their DNA structure and for the mechanisms that originate them. In two types, actual junctions between sister double helixes are present, and consist of regions of unreplicated parental DNA or of structures originated by homologous recombination. In the third type, DNA catenanes, the two double helixes are connected only by topological linkages.

Failure to complete replication results in sister chromatids in which patches of unreplicated and intertwined parental DNA are still present, keeping them joined. During chromosome segregation these intertwines, named hemicatenanes, can originate DNA bridges characterized by the presence of ssDNA. Although these structures do not normally occur during an unperturbed cell cycle, they can arise in conditions of replicative stress. Though the physiological relevance of this type of SCIs is unknown, their resolution is likely carried out by the STR complex (Suski and Marians, 2008).

The other two types of SCIs arise instead also in physiological conditions and persist in mitosis also in unperturbed cell cycles. Thus, the existence of mechanisms deputed to their resolution is fundamental for the execution of a faithful chromosome segregation.

1.4.3 Sister chromatid junctions

Homologous recombination (HR) is a conserved pathway deputed to the repair of DNA double strand breaks (DSBs) that exploits the information contained in one sister chromatid (or in the homologous chromosome) to repair the break in the other. This ensures that the lesion is repaired without altering the DNA sequence. HR requires that DNA broken ends are resected to a 3' overhang of ssDNA that can invade the homologous duplex DNA (forming the "displacement loop" or D-loop) to use it as a template for DNA synthesis. D-loops can either be quickly resolved by the action of helicases, or capture the second 3' overhang of the DSB, that will start DNA synthesis too. This, after sealing of the newly synthetized strands, leads to the formation of a stable four-way junction named double Holliday Junction (HJ). The stable connection between sister chromatids is often referred to as sister chromatid junction or SCJ. In addition to DSBs repair, SCJs can arise also during DNA replication when recombination mechanisms are used to allow replication in the presence of DNA lesions (DNA damage tolerance by template switching) by retrieving the information from the newly replicated sister chromatid and forming hemicatenane-like structures (Liberi *et al.*, 2005; Branzei *et al.*, 2006; Branzei, Vanoli and Foiani, 2008).

SCJs must be resolved to allow sister chromatid separation and segregation. This is achieved mainly through a process named "dissolution", that requires the activity of the (STR) complex. This complex can process both double HJs and hemicatenanes to non-crossover products (Harmon, DiGate and Kowalczykowski, 1999; Ira *et al.*, 2003; Liberi *et al.*, 2005; Branzei *et al.*, 2006), that is without exchanges between donor and recipient DNA sequences. SCJs can also be processed through "resolution" by the action of two structure-specific nucleases that can cleave HJs, Mus81-Mms4 and Yen1 (Matos and West, 2014; Talhaoui, Bernal and Mazón, 2016). As their activity is restricted to mitosis, they are thought to provide a back-up mechanism for the STR complex. Indeed, it has been proposed that they are required to process not fully ligated HJs, like nicked HJs, that

escape the STR complex (Talhaoui, Bernal and Mazón, 2016). Nucleolitic processing of HJs gives rise to a mixture of crossover and non-crossover products, depending on the orientation of the cleavage. In human cells, restricting nucleases activity is important to limit crossover events to prevent loss of heterozygosity and consequent loss of tumor suppressor genes. However, this concept is hardly applicable to yeast cells, hence limiting nucleases to mitosis might have other purposes. It has been proposed that, if active in S phase, they might cleave replication intermediates, thereby hindering DNA replication (Matos and West, 2014).

Mus81 and Mms4 are ERCC4 domain nucleases that work as a heterodimer in which Mus81 retains the catalytic activity, while Mms4 has regulatory functions. Although the Mus81-Mms4 complex can cleave fully ligated HJs, it was reported to be more efficient on 3' flaps, D-loops and nicked HJs; it cleaves HJs by introducing a nick and a counter-nick (Kaliraman *et al.*, 2001; Gallo-Fernández *et al.*, 2012; Schwartz *et al.*, 2012). Mus81-Mms4 is inactive in G1 and S phases and gets activated in G2/metaphase by the Cdk and Cdc5 kinases that collaborate to hyperphosphorylate Mms4, increasing its catalytic activity (Matos *et al.*, 2011; Gallo-Fernández *et al.*, 2012; Schwartz *et al.*, 2012; Matos, Blanco and West, 2013; Szakal and Branzei, 2013). The relative contribution of Cdk and Cdc5 is still to be determined. Mus81-Mms4 becomes inactive in anaphase concomitantly to Cdk and Cdc5 inactivation (Matos *et al.*, 2011).

Yen1 belongs to the XPG nucleases family and processes HJs as a homodimer by cleaving both sides of the HJ (Ip *et al.*, 2008). Yen1 is activated in early anaphase by the phosphatase Cdc14 that removes inhibitory phosphorylations mediated by Cdk. This inhibitory phosphorylation affects Yen1 both by inhibiting its catalytic activity and by preventing its nuclear entry (Matos *et al.*, 2011; Matos, Blanco and West, 2013; Blanco, Matos and West, 2014; Eissler *et al.*, 2014; García-Luis *et al.*, 2014).

The two consecutive waves of nucleases activity, in G2/metaphase by Mus81-Mms4 and in anaphase by Yen1, ensure that SCJs are actively resolved throughout mitosis,

allowing for proper chromosome segregation to take place. Although the requirement of these pathways for cell viability is evident after treatment with DNA damaging agents that induce HR, inactivation of redundant SCJs resolution pathways results in loss of viability and errors in chromosome segregation even in untreated cells. For example, deletion of both *SGS1* and *MMS4* results in synthetic lethality, while deletion of *MMS4* and *YEN1* increases the frequency of chromosome missegregation (Wagner and Crow, 2001; Blanco *et al.*, 2009; Matos, Blanco and West, 2013; García-Luis and Machín, 2014). This indicates that SCJs are formed in unchallenged cell cycles (likely as a consequence of endogenous replication stress) and that at least one mechanism of SCJs resolution must be active for a correct chromosome segregation.

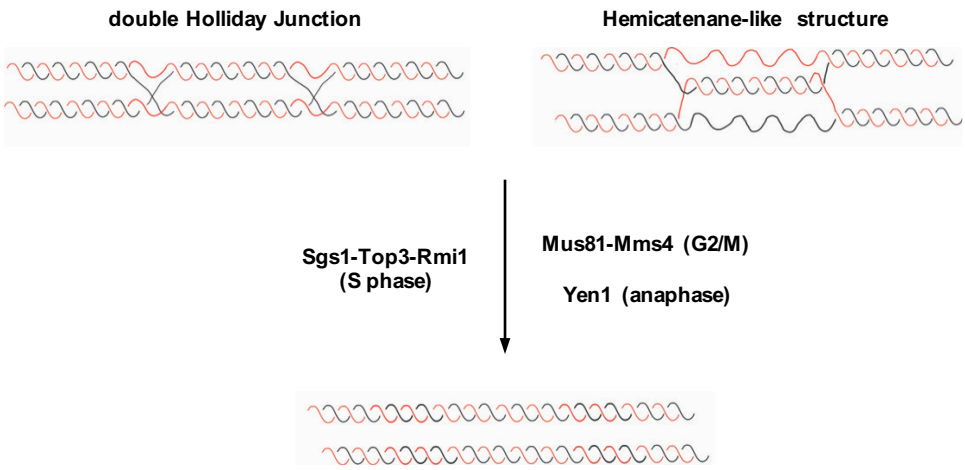

Figure 1. 13 SCJ structure and resolution.
Modified from (Baxter, 2015)

1.4.4 DNA catenanes

During DNA replication, progression of the replication forks requires the action of helicases that push the turns of the helix of parental DNA ahead of the fork. This generates topological tension that is relaxed by converting overtwisting of the helix into positive

supercoils. During replication elongation such supercoils are resolved by the action of topoisomerases to allow fork progression.

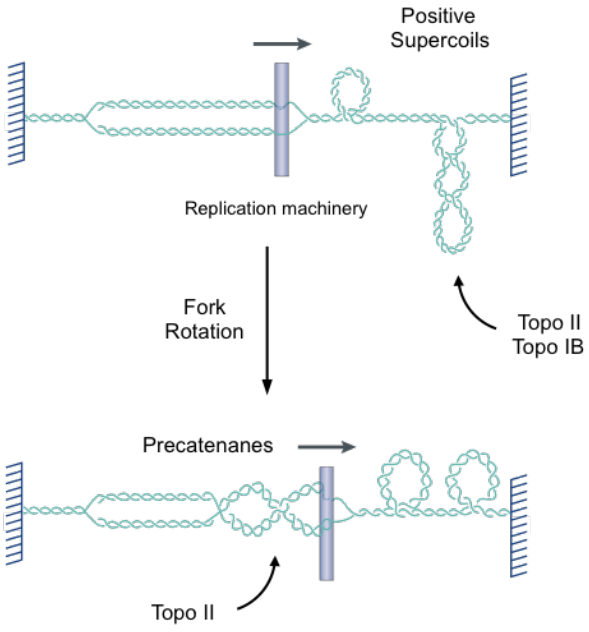

Figure 1. 14 Model for precatenane formation with fork rotation.
Modified from (Wang, 2002)

In addition to resolving supercoils ahead of the fork, cells employ a second mechanism to relax topological tension, that is fork rotation (Champoux and Been, 1980). Through fork rotation, the turns of the helix of parental DNA are converted into super-helixes between the newly replicated sister chromatids that are named "precatenanes" (converted into "catenanes" after completion of replication). The name catenane derives from initial studies performed on circular DNA, where this type of intertwining results in catenation of two circular molecules, but is now commonly used to indicate also intertwines between linear DNA. Though fork rotation does relax overwinding, and thereby assists fork progression, it leads to the entanglement of sister chromatids behind the fork and poses the problem of resolving them to allow segregation. Indeed, as soon as evidence was gathered for fork rotation, it was clear that only a small portion of parental helix turns are converted into catenanes, suggesting that fork rotation is restricted to specific regions or conditions. Early studies on Simian Virus SV40 DNA replication

revealed that catenation of sister chromatids is a physiological late replication intermediate that arises at replication termination, but also that, on average, only 10 out of the 500 intertwines of parental DNA form intertwines between the sisters (Sundin and Varshavsky, 1980, 1981). The low frequency of DNA catenanes and their occurrence mainly at replication termination was later confirmed also in yeast (Baxter and Diffley, 2008; Fachinetti *et al.*, 2010).

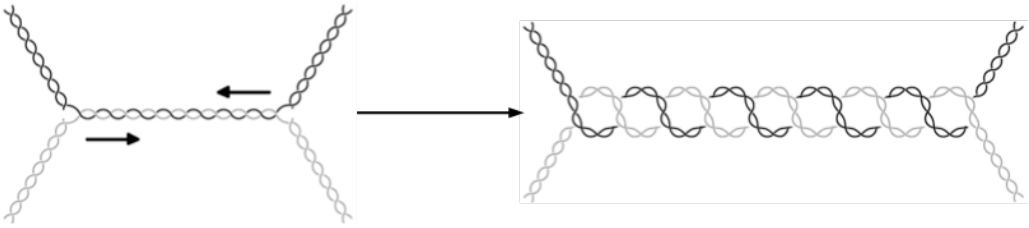

Figure 1. 15 Model for catenane formation at replication termination.
Modified from(Bush, Evans-Roberts and Maxwell, 2015)

In eukaryotes, two topoisomerases work to resolve DNA intertwines during replication, Topo I and Topo II. Being able to resolve positive supercoiling, both enzymes can resolve intertwines ahead of the fork and their action seems to be redundant in DNA replication (Bermejo *et al.*, 2007). Indeed, Topo II depletion or Topo I inactivation in yeast do not hinder fork progression and DNA replication; instead, when both proteins are inactive (or when Topo II is present but catalytically inactive, acting as a dominant negative) DNA replication stops (Bermejo *et al.*, 2007; Baxter and Diffley, 2008).

Topo II becomes essential at replication termination (DiNardo, Voelkel and Sternglanz, 1984; Baxter and Diffley, 2008; Fachinetti *et al.*, 2010), when fork rotation occurs and originates intertwines between sister chromatids that cannot be resolved by Topo I. The current explanation for why fork rotation occurs at replication termination is based on the concept of enzyme accessibility: the region of DNA available for topoisomerases action ahead of the fork progressively decreases as two forks converge, until the two large replisomes come in close proximity and prevent topoisomerases access

in between them. In this condition, supercoiling can only be relaxed by fork rotation. This model predicts that, in addition to replication termination, catenanes can arise at any region in which topoisomerases action ahead of the fork is prevented, for example at sites of stable protein-DNA structures. Evidence for this has been recently found: the presence of replication pausing sites (in particular tRNA genes and inactive replication origins) increases the number of catenanes in circular plasmids in yeast (Schalbetter *et al.*, 2015).

The rare occurrence of fork rotation implies that these events are restricted. This could be due to different mechanisms: the large size of the eukaryotic replisome creates an intrinsic resistance to rotation, while topoisomerases activity ahead of the fork might be sufficient to keep the topological tension below the level required to trigger fork rotation (Keszthelyi, Minchell and Baxter, 2016). Moreover, active mechanisms might exist that prevent fork rotation, as deletion of Tof1 or Csm3, subunits of a replication pausing complex, increases the number of catenanes on circular plasmid in yeast, through a yet unknown mechanism (Schalbetter *et al.*, 2015).

1.4.4.1 Complete catenane resolution in mitosis

A complete and error-free chromosome segregation requires that any linkage between sister chromatids is removed. The complete resolution of catenanes takes place in mitosis and specifically requires the enzymatic activity of Topo II. This function makes *TOP2* an essential gene while conditional *top2* mutants in yeast display in anaphase nuclei stretched through the bud-neck or DNA bridges and loose viability in mitosis (DiNardo, Voelkel and Sternglanz, 1984; Holm *et al.*, 1985; Uemura *et al.*, 1987).

The strand passage reaction catalyzed by Topo II implies that any segment of DNA can pass through any other segment of DNA. Therefore, Topo II can both catenate and decatenate DNA. As replicated sister chromatids are crowded inside the small nucleus and are held in close proximity by cohesin rings, the occurrence of catenation rather than

decatenation is not unlikely. Although it has been reported that Topo II enzymes have the ability to decatenate DNA *in vitro* below the expected thermodynamic equilibrium (Rybenkov *et al.*, 1997), this is not sufficient to explain how these enzymes are able to resolve every single intertwine *in vivo* (Stuchinskaya *et al.*, 2009). Thus, it has been suggested that other factors must intervene to drive Topo II reaction toward decatenation. Studies on prokaryotic genomes have shown that intra-chromosome compaction constrains each chromosome into its own separate volume and excludes any linkage with other chromosomes from this volume (Postow *et al.*, 2001), suggesting that chromosome compaction limits the presence of intertwines to specific regions, where Topo II decatenation reaction can prevail. Different studies, mostly from yeast, suggest that self-compaction promotes decatenation also in eukaryotes. Three factors have been involved in the process: cohesin cleavage, condensin and mitotic spindle.

Cohesin cleavage:

Studies in yeast have shown that the presence of cohesin prevents catenane resolution (Farcas *et al.*, 2011; Charbin, Bouchoux and Uhlmann, 2014). Though it has been suggested that the presence of the bulky cohesin complexes might block Topo II access to DNA, a most likely explanation is that cohesin, by keeping chromatids in close proximity, favors Topo II reaction to go toward catenation (Farcas *et al.*, 2011; Sen *et al.*, 2016). Indeed, it was shown that intertwines are retained between sister plasmids also when they are tethered by means different than cohesin (Sen *et al.*, 2016).

Condensin:

A collaboration between condensin and Topo II in shaping mitotic chromosomes has long been suspected, since they were both found to localize in what was defined as the chromosome “scaffold”, a proteinaceous structure that was hypothesized to form the axis of chromosomes (Paulson and Laemmli, 1977; Earnshaw *et al.*, 1985). Moreover, Topo II and condensin mutants were found to display similar defects in chromosome segregation

(DiNardo, Voelkel and Sternglanz, 1984; Holm *et al.*, 1985; Uemura *et al.*, 1987; Freeman, Aragon-Alcaide and Strunnikov, 2000; Bhalla, 2002). Next, studies on the highly repetitive, highly transcribed and late-segregating rDNA locus in yeast have shown that both Topo II and condensin are required for its segregation (D'Amours, Stegmeier and Amon, 2004; Sullivan *et al.*, 2004) and that Topo II overexpression-induced rDNA segregation requires condensin activity (D'Ambrosio, Kelly, *et al.*, 2008). Evidence for a role of condensin in decatenation has now been obtained, as condensin mutants fail to resolve catenanes in mitosis (Baxter *et al.*, 2011; Charbin, Bouchoux and Uhlmann, 2014). In particular, it was shown that, after bipolar attachment to the spindle, condensin is required to shift DNA conformation (as assayed on circular plasmid) to a more positively supercoiled status which biases Topo II activity toward decatenation (Baxter *et al.*, 2011; Sen *et al.*, 2016). It was also found that throughout anaphase condensin localizes along chromosome arms in a Cdc5-dependent manner; this re-localization correlates with an increase in its overwinding activity and results in recoiling chromatids stretched by the pulling action of the mitotic spindle (Renshaw *et al.*, 2010; Leonard *et al.*, 2015). As condensin-mediated chromatid recoiling guides the removal of leftover cohesin complexes (Renshaw *et al.*, 2010), by analogy it could guide resolution of leftover intertwines too. Recent data from *Drosophila* further support the model by which condensin promotes decatenation by biasing Topo II reaction: it was indeed shown that cleaving condensin on previously separated sister chromatids causes Topo II-dependent re-intertwining (Piskadlo, Tavares and Oliveira, 2017).

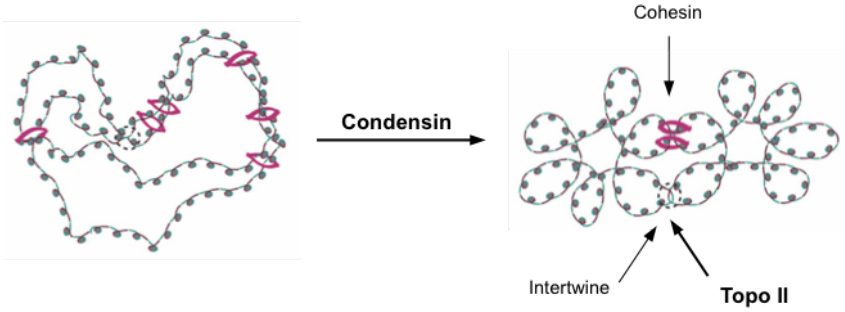

Figure 1. 16 Model for condensin-mediated decatenation.
Modified from (Baxter, 2015)

Although evidences indicate that condensin role in decatenation is mainly topological, it cannot be excluded that condensin contributes more directly in promoting Topo II activity. The prokaryotic SMC complex homologous to condensin has been found to physically interact with topoisomerase IV (the decatenating enzyme in prokaryotes) (Li *et al.*, 2010), but this interaction has never been found in eukaryotes. However, the finding that condensin localization along chromosome arms is required for Topo II localization on chromosome arms, too (Leonard *et al.*, 2015) suggests that condensin might have also a more direct role by promoting Topo II recruitment.

Mitotic spindle:

A role for the mitotic spindle in full catenane resolution has been proposed from the observation that cells arrested in metaphase become unable to separate dimeric plasmids when the spindle is disrupted (Baxter *et al.*, 2011; Charbin, Bouchoux and Uhlmann, 2014). This finding led to the hypothesis that the spindle, by pulling chromatids apart, exposes the last remaining intertwines to Topo II activity. Alternatively, as bipolar attachment to the spindle is required for condensin re-localization to chromosome arms, the action of the spindle in promoting decatenation might also be indirect through condensin activation (Leonard *et al.*, 2015).

1.4.5 NoCut Checkpoint

If DNA anaphase bridges are not resolved throughout mitosis, they pose a threat to genome stability when cells reach cytokinesis. It has been shown that cytokinesis can generate DSBs in *top2* and condensin mutants (Baxter and Diffley, 2008; Cuylen *et al.*, 2013), likely because constriction of the acto-myosin ring generates forces sufficient to break DNA.

The existence of a checkpoint system that delays the cell cycle to avoid DNA breakage at cytokinesis has been proposed in budding yeast (Norden *et al.*, 2006; Mendoza *et al.*, 2009). It is referred to as the "NoCut checkpoint" and relies on the activity of Aurora B. Indeed, it was shown that Aurora B delays abscission in the presence of bridges originated by replication stress, condensin or Topo II inhibition or dicentric chromosomes (Mendoza *et al.*, 2009; Amaral *et al.*, 2016). However, Aurora B is able to prevent DNA damage only in the first case (Baxter and Diffley, 2008; Cuylen *et al.*, 2013; Amaral *et al.*, 2016). Likely, this additional time is sufficient to resolve bridges that can actually be resolved, but not those originated from severely decondensed/catenated chromatids, as it is the case when Topo II and condensin are inactive. The mechanisms through which Aurora B recognizes anaphase bridges and delays abscission are still unclear. As Aurora B associates with the spindle midzone and this localization is required during cytokinesis to inhibit abscission in the presence of anaphase bridges, it has been proposed that Aurora B senses the chromatin status around the spindle midzone (Mendoza *et al.*, 2009). Supporting this is the finding that NoCut requires spindle stabilization and that spindle factors that are normally degraded in telophase persist in cells with anaphase bridges (Amaral *et al.*, 2016). A mechanism that delays abscission in response to chromatin bridges and depends on Aurora B has been found also in mammalian cells (Steigemann *et al.*, 2009).

1.5 The Mitotic Spindle

The mitotic spindle is a cytoskeletal structure responsible for pulling chromatids apart during segregation. It is composed of microtubules (MTs) that are tubular polymeric filaments formed by 13 protofilaments. Each protofilament is in turn formed by heterodimers of α- and β-tubulin aligned head-to-tail. This confers polarity to the MTs that have a highly dynamic, fast growing plus-end and a slow growing minus-end. MTs plus-ends are highly dynamic and alternate phases of rapid growth (rescue) and shortening (catastrophe), a phenomenon known as dynamic instability.

MTs need to be nucleated by apposite protein structures, named microtubule-organizing centers (MTOC), which contain a γ-tubulin complex that promotes their nucleation. MTs are nucleated at their minus-end, which remains connected to the MTOC, while the plus-end extends away. In budding yeast this function is carried out by the spindle pole bodies (SPBs). As yeast cells undergo a closed mitosis (the nuclear envelope does not break down), SPBs are embedded in the nuclear membrane and nucleate MTs both inside the nucleus, to form the mitotic spindle, and outside, to anchor the nucleus to the cell cortex. MTs extending outside the nucleus and contacting the cell cortex are named astral MTs (aMTs). MTs extending inside the nucleus are called kinetochore MTs (kMTs) if they contact kinetochores, or interpolar MTs (iMTs) if they contact MTs extending from the opposite SPB in a region named spindle midzone.

Spindle MT dynamics are regulated by two types of proteins: MT associated proteins (MAPs) and MT motor proteins. MAPs are proteins that share the ability to bind to MTs. They contribute to spindle functions in a wide variety of ways as they regulate kMT dynamics, spindle orientation and stability and the activity of spindle motors. MT motors are proteins that use ATP hydrolysis to generate mechanical energy to move along

MTs. Motors activity is employed in several spindle related processes, for example in sliding antiparallel MTs apart, in regulating chromosome position in metaphase and next in transporting chromosomes along the shortening kMTs in anaphase.

1.5.1 Spindle assembly and positioning

In G1, cells have only one SPB. In order to form a bipolar spindle, the SPB needs to be duplicated and next the two SPBs need to separate and migrate to the opposite sides of the nucleus. SPB separation requires the activity of Cdk and Kinesin 5 motor proteins Cin8 and Kip1 (Roof, Meluh and Rose, 1992; Saunders and Hoyt, 1992). Both Cin8 and Kip1 work by crosslinking the MTs emanating from the two SPBs inside the nucleus and, by moving to the plus-end, they slide them apart thereby generating forces that push the SPBs in opposite directions. Cin8 and Kip1 function in SPB separation and spindle formation is mediated by direct Cdk phosphorylation (Chee and Haase, 2010). Once the bipolar spindle is formed, a process of "search and capture" begins to allow kMTs interaction with chromosomes. This process is favored by the dynamic instability of MT plus-ends.

Next, to correctly segregate sister chromatids, the spindle must align perpendicularly to the bud-neck. This requires the interaction of aMTs with the cell cortex (Shaw *et al.*, 1997). Budding yeast employs two redundant pathways for positioning the spindle, one involving the plus-end binding protein Kar9 (Miller and Rose, 1998) and the other one involving the motor protein dynein (Dyn1) (Li *et al.*, 1993). The Kar9 pathway promotes migration of the nucleus to the bud-neck before anaphase entry by using actin as a cable to drag into the bud the aMTs emanating from one SPB (Beach *et al.*, 2000). Instead dynein, a large minus-end directed motor that localizes specifically on aMTs, after being actively transported to the aMT plus-end, drives aMT sliding along the cell cortex (Li *et al.*, 1993; Carvalho *et al.*, 2004; Moore, Li and Cooper, 2008).

1.5.2 Anaphase spindle elongation

Once the spindle is formed and correctly aligned to the bud-neck and once all kinetochores are bipolarly attached, cohesin is cleaved and the spindle starts elongating. This takes place in two consecutive steps, anaphase A and anaphase B. During anaphase A, separated sister chromatids are pulled to the SPB they are connected with through shortening of the kMTs. In this step, overall spindle length does not change. Next, during anaphase B, a progressive increase in length of the iMTs fully separates chromatids (Pearson *et al.*, 2001). Anaphase B can be further subdivided into a phase of fast spindle elongation when from the metaphase length of ~2μm it reaches 4-6μm, and a phase of slow elongation, when the spindle reaches a final length of 8-10μm (Straight, Sedat and Murray, 1998; Movshovich *et al.*, 2008).

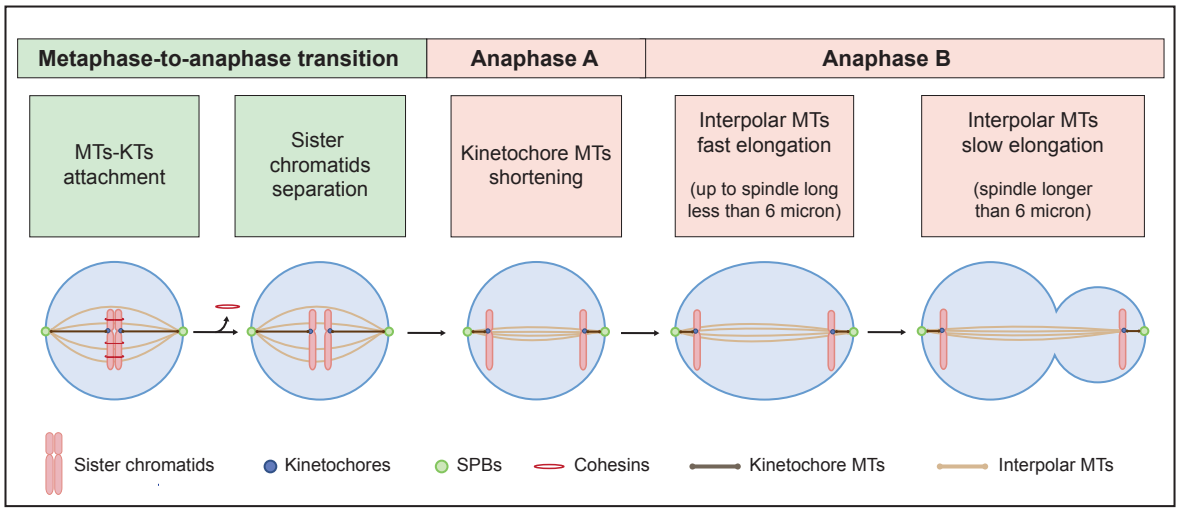

Figure 1. 17 Spindle elongation and chromosome segregation.
Modified from (Roccuzzo, 2013)

The forces that drive spindle elongation are generated at the spindle midzone, where iMTs from opposite poles interact with each other forming higher order geometrical arrays. Important for midzone functioning are MAPs and motors that both stabilize iMTs interactions, preventing the spindle to collapse, and slide them on each other, resulting in spindle elongation. Thus, regulation of MAPs and motor activity is essential for spindle

dynamics. This regulation is achieved mainly through phosphorylation and dephosphorylation events (Higuchi and Uhlmann, 2005).

Whilst high Cdk activity at mitotic entry contributes to increasing MT dynamics, a requisite for mitotic spindle assembly and MT-KT attachment, at anaphase onset, a first wave of Cdc14 activity (the phosphatase responsible for the reversal of Cdk phosphorylations) promotes stabilization of MT dynamics by dephosphorylating several MAPs and motor proteins (Higuchi and Uhlmann, 2005). Substrates of Cdc14 include the spindle-stabilizing protein Fin1 (Woodbury and Morgan, 2007), the kinetochore component Ask1 (Li and Elledge, 2003), the MAP Stu1 and the main midzone organizer, the MAP Ase1. Ase1 bundles antiparallel MTs at the midzone (Schuyler, Liu and Pellman, 2003). Before anaphase onset, Ase1 is phosphorylated by Cdks; only upon dephosphorylation by Cdc14 in early anaphase it can drive midzone assembly (Khmelinskii *et al.*, 2007) recruiting other midzone factors, including the Esp1-Slk19 complex, the chromosomal passenger complex (CPC) and motors proteins. The Esp1-Slk19 complex has been proposed to limit and define the midzone to the middle of the spindle (Jensen *et al.*, 2001). The CPC is formed by the Aurora B kinase Ipl1, Sli15, Bir1 and Nbl1 (Ruchaud, Carmena and Earnshaw, 2007). Earlier in mitosis Ipl1 localizes first to chromosomes and later to kinetochores where it plays a role in the MT-KT attachment error-correction system. Next, the dephosphorylation of Sli15 by Cdc14 localizes the complex to the spindle MTs where it promotes spindle midzone assembly (Pereira and Schiebel, 2003).

The major spindle motors involved in spindle elongation are the class-5 kinesins (BimC) Cin8 and Kip1 (Roof, Meluh and Rose, 1992; Saunders and Hoyt, 1992), that possess a plus-end directed motility. Cin8 was found to be able to move also toward the minus-end, though the significance of this activity remains unclear (Roostalu *et al.*, 2011; Shapira *et al.*, 2017). Cin8 and Kip1 are homotetrameric complexes (Hildebrandt *et al.*, 2006) that act by crosslinking and sliding apart anti-parallel MTs to generate an outwardly-

directed force (Roof, Meluh and Rose, 1992). Their action is at least in part redundant as cells can proliferate without either one of the two but not without both (Saunders *et al.*, 1995). During anaphase, they stabilize the spindle midzone (Fridman *et al.*, 2009) and regulate the switch from the fast to the slow phase of anaphase B spindle elongation (Straight, Sedat and Murray, 1998; Movshovich *et al.*, 2008; Gerson-Gurwitz *et al.*, 2009). The activity of Cin8 in anaphase is promoted by Cdc14. At anaphase onset, Cdc14 dephosphorylates Cin8 allowing its interaction with the spindle and promoting spindle fast elongation (Avunie-Masala *et al.*, 2011). Moreover, Cdc14-mediated Ase1 dephosphorylation is required for Cin8 recruitment to the midzone (Khmelinskii *et al.*, 2009). Later in anaphase, loss of Cdc14 activity causes a decrease in Cin8 activity, resulting in the slow spindle elongation phase (Avunie-Masala *et al.*, 2011).

1.5.3 Spindle disassembly

In telophase, after completion of chromosome segregation, the spindle disassembles. This requires dismantling of the spindle midzone, which results in the spindle splitting in half, and shortening of iMTs. Spindle midzone disassembly depends on the activation of the APC/C^{Cdh1} that targets for degradation several midzone stabilizing factors, including Ase1 (Juang *et al.*, 1997), Fin1 (Woodbury and Morgan, 2007) and Cin8 (Hildebrandt and Hoyt, 2001). iMT shortening is promoted by Ipl1 that phosphorylates the MT plus-end stabilizing protein Bim1, causing its detachment from MTs (Zimniak *et al.*, 2009; Woodruff, Drubin and Barnes, 2010). The depolymerizing activity of the kinesin Kip3 is also necessary for iMTs depolymerization (Straight, Sedat and Murray, 1998).

1.6 Mitotic Exit

Mitotic exit requires a decrease in Cdk activity, which implies both the inactivation of the Clb-Cdk complexes and the reversal of the Clb-Cdk phosphorylations that had promoted early mitotic events. In budding yeast both processes are driven by the essential phosphatase Cdc14 (Wan, Xu and Grunstein, 1992; Visintin *et al.*, 1998). Indeed, mutants lacking Cdc14 arrest in anaphase with high Clb-Cdk activity. Cdc14-mediated inhibition of Clb-Cdk is dual: on the one hand, it dephosphorylates the APC/C coactivator Cdh1 promoting its interaction with the APC/C (Visintin *et al.*, 1998; Jaspersen, Charles and Morgan, 1999), which then targets Clb cyclins for degradation (Schwab, Lutum and Seufert, 1997; Visintin, 1997; Zachariae, 1998); on the other hand, Cdc14 promotes the accumulation of the Cdk inhibitor Sic1, both by dephosphorylating and stabilizing Sic1 itself and by stimulating its transcription through dephosphorylation of its transcription factor Swi5 (Visintin *et al.*, 1998).

Cdc14 is regulated through changes in its cellular localization. From G1 until anaphase onset, Cdc14 is sequestered in the nucleolus by association with its inhibitor Cfi1 (also known as Net1). Dissociation from Cfi1 allows Cdc14 to be released from the nucleolus and to reach its substrates (Shou *et al.*, 1999; Visintin, Hwang and Amon, 1999; Traverso *et al.*, 2001). The association between Cdc14 and Cfi1 is regulated through phosphorylation. Their binding requires them to be un-phosphorylated while their dissociation, and thereby Cdc14 activation, is promoted by phosphorylation of both proteins (Visintin, Stegmeier and Amon, 2003; Azzam *et al.*, 2004; Manzoni *et al.*, 2010).

Cdc14 release takes place in two waves: first, at anaphase onset, the Cdc Fourteen Early Anaphase Release (FEAR) network promotes a transient release of the protein from the nucleolus to the nucleoplasm (Stegmeier, Visintin and Amon, 2002); next, later in

anaphase, the Mitotic Exit Network (MEN) promotes the complete release of Cdc14 that can now reach also the cytoplasm (Shou *et al.*, 1999). FEAR-mediated Cdc14 activation is not essential for mitotic exit, but promotes a series of early anaphase events required for chromosome segregation. Indeed, FEAR mutants are only slightly delayed in mitotic exit, but display defects in chromosome segregation. For example, FEAR-activated Cdc14 is required for spindle assembly and stabilization (Khmelinskii *et al.*, 2007, 2009), nuclear positioning (Ross and Cohen-Fix, 2004) and rDNA segregation (D'Amours, Stegmeier and Amon, 2004; Sullivan *et al.*, 2004; Torres-Rosell *et al.*, 2004; Wang, Yong-Gonzalez and Strunnikov, 2004). The MEN network instead is essential for mitotic exit and MEN mutants arrest in late mitosis, with high levels of Clb-Cdk activity (Jaspersen *et al.*, 1998). Among FEAR and MEN network components, the Polo-like kinase Cdc5 plays a pivotal role. It is the only one shared by both networks and is the only one that, when overexpressed, can induce Cdc14 release in cell cycle phases where the phosphatase is usually sequestered. Moreover, when inactive, the phosphatase is never released (Stegmeier, Visintin and Amon, 2002; Visintin, Stegmeier and Amon, 2003). The central function of Cdc5 and Cdc14 in promoting mitotic exit is underscored by the observation that both *cdc5* and *cdc14* single mutants arrest in anaphase with high levels of Cdk activity. However, it was recently discovered that the simultaneous inactivation of Cdc5 and Cdc14 results in a synthetic interaction, indicating that a pool of Cdc14 independent of Cdc5 also exists (Roccuzzo *et al.*, 2015).

1.6.1 The MEN network

The MEN network is a Ras-like GTPase signal transduction pathway that promotes exit from mitosis (Jaspersen *et al.*, 1998). It involves the GTPase Tem1, the GTPase activating protein (GAP) complex Bub2-Bfa1, the GDP-GTP exchanging factor (GEF) Lte1 and the kinases Cdc5, Cdc15 and Dbf2-Mob1.

Tem1 is activated by Lte1 and downregulated by Bub2-Bfa1, which is in turn activated by Cdc5 and inhibited by the kinase Kin4 (Hu *et al.*, 2001; D'Aquino *et al.*, 2005). The specific localization of these proteins determines Tem1 activation and also coordinates spindle positioning with mitotic exit, allowing mitotic exit to take place only if a spindle pole, with his set of chromosomes, has correctly moved into the daughter cell. Indeed, Tem1 is specifically located on the SPB that will enter the daughter cell, while its activator Lte1 is located on the bud cortex (Bardin, Visintin and Amon, 2000). In this way, Tem1 can be activated only if its SPB had entered the bud. Moreover, Kin4 is confined to the mother cell cortex (D'Aquino *et al.*, 2005) and Bub2-Bfa1 is located on the daughter SPB, too (Fraschini *et al.*, 2006). Thus, as long as the daughter SPB is located in the mother cell, an inhibitory signal keeps Tem1 inactive, but, as it transits into the bud, the inhibitory action of Kin4 is lost and the Lte1-mediated activation prevails. The pathway involving Kin4 and Bub2-Bfa1 senses a correct spindle alignment across the bud-neck, which results in the enrichment of Bub2-Bfa1 to the daughter SPB only if the spindle is correctly positioned (Piatti *et al.*, 2006). This pathway is known as the Spindle Positioning Checkpoint.

Tem1 activation leads to the activation of Cdc15, which phosphorylates and activates Dbf2 (Mah, Jang and Deshaies, 2001). Dbf2 in turn leads to Cdc14 activation, likely through direct phosphorylation of Cfi1 (Manzoni *et al.*, 2010). Dbf2 also phosphorylates Cdc14 to promote its translocation into the cytoplasm (Mohl *et al.*, 2009). Active Cdc14 further activates Cdc15, thereby enhancing its own release through a positive feedback loop (Bardin, Boselli and Amon, 2003). Cdc5 contributes to the MEN network in several ways as, in addition to inhibiting Bub2-Bfa1 (Hu *et al.*, 2001), it also regulates both Lte1 and Dbf2 and phosphorylates Cdc14. As a result, in *cdc5* mutants MEN signaling is completely abolished (Visintin, Stegmeier and Amon, 2003).

Cdc14 inactivation is next required to proceed into the next cell cycle. This is achieved through a negative feedback loop: the APC/C^{Cdh1}, activated by Cdc14, targets

Cdc5 for degradation that results in inactivation of the MEN network, in the absence of which Cdc14 is re-sequestered in the nucleolus (Visintin *et al.*, 2008; Lu and Cross, 2010; Manzoni *et al.*, 2010).

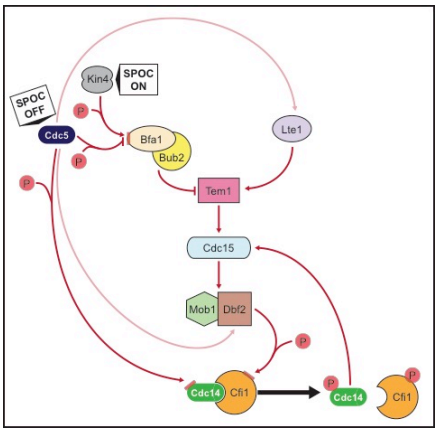

Figure 1. 18 The MEN network.
Modified from (Roccuzzo, 2013)

1.6.2 The FEAR network

The FEAR network is responsible for the early anaphase release of Cdc14. The first indications that such a pathway exists derived from the observations that Cdc14 has already diffused into the nucleoplasm before MEN is activated and that MEN mutants transiently release Cdc14 (Visintin and Amon, 2001; Stegmeier, Visintin and Amon, 2002). Subsequent studies identified several proteins as part of the FEAR network, in particular the separase Esp1 (Cohen-Fix and Koshland, 1999; Sullivan and Uhlmann, 2003), the kinases Cdc5 and Clb2-Cdk, the phosphatase PP2A in complex with its regulatory subunit Cdc55, the Cdc55 interacting proteins Zds1 and Zds2, the kinetochore protein Slk19 and the nucleolar proteins Spo12 (together with its paralog Bns1) and Fob1 (Stegmeier, Visintin and Amon, 2002; Rock and Amon, 2009).

FEAR is activated at anaphase onset when APC/C^{Ccd20}-mediated Pds1 degradation triggers Esp1 activation. Esp1 role in Cdc14 activation does not require its catalytic

activity but involves the kinetochore protein Slk19. The Esp1-Slk19 complex downregulates the phosphatase $PP2A^{Cdc55}$ (Queralt *et al.*, 2006; Wang and Ng, 2006; Yellman and Burke, 2006) through the Cdc55 interacting proteins Zds1 and Zds2 (Queralt and Uhlmann, 2008). $PP2A^{Cdc55}$ inhibition allows Clb2-Cdk to prevail and phosphorylate Cfi1 on six residues, mediating Cdc14 release (Azzam *et al.*, 2004). Esp1 also promotes Clb2-Cdk-mediated Spo12 activation. Spo12 contributes to Cdc14 activation by antagonizing Fob1, which stabilizes the Cdc14-Cfi1 interaction (Stegmeier *et al.*, 2004; Tomson *et al.*, 2009). Cdc5 promotes Cdc14 activation through direct phosphorylation (Shou *et al.*, 2002; Yoshida, Asakawa and Toh-e, 2002; Visintin, Stegmeier and Amon, 2003) and it might work either in parallel or downstream to Esp1. Indeed, though Cdc5 is active since S phase, its FEAR activity might require the parallel action of Clb2-Cdk acting downstream of Esp1; alternatively, Cdc5 might act downstream of Esp1, as suggested by the finding that it is able to interact with Esp1 and Slk19 (Rahal and Amon, 2008).

How the FEAR network is organized is still unclear, mostly because the double function of Cdc5 in Cdc14 release (as part of both FEAR and MEN networks) made epistatic analyses difficult to interpret (Stegmeier, Visintin and Amon, 2002; Visintin, Stegmeier and Amon, 2003). Moreover, it is still unclear whether also Spo12 works in parallel or downstream to Esp1. A recent study in which the FEAR network was studied analyzing the effect of inactivating its components on anaphase progression rather than on Cdc14 release, proposed a model in which Esp1, Cdc5 and Spo12/Bns1 are placed on parallel branches (Roccuzzo *et al.*, 2015). Indeed, their simultaneous inactivation results in a synthetic interaction which arrests cells after cohesin cleavage but before spindle elongation and chromosome segregation, while inactivating only one or two of them only slows down anaphase progression. This finding indicates that the FEAR network is essential for anaphase progression. It also suggests that Esp1, Cdc5 and Spo12 contribute to Cdc14 activation at least in part independently from each other, although it is also

possible that they have other functions, independent from Cdc14 activation, in promoting spindle elongation.

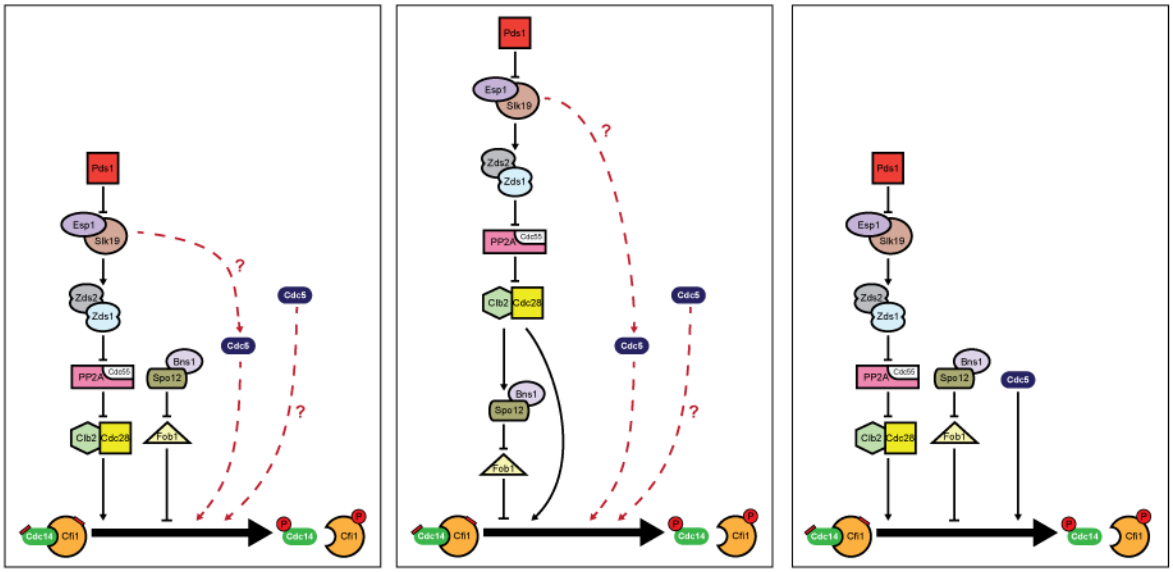

Figure 1. 19 Models for the FEAR network.
Modified from (Roccuzzo *et al*., 2015)

2. Materials and methods

2.1 Plasmids, primers and strains

2.1.1 Plasmids

Plasmids used in this study are listed in Table 2.1. Plasmids were amplified in TOP10 *Escherichia coli* cells (F- mcrA Δ(mrr-hsdRMS-mcrBC) φ80lacZΔM15 ΔlacX74 nupG recA1 araD139 Δ(ara-leu)7697 galE15 galK16 rpsL(StrR) endA1 λ). Cells were provided chemically competent for transformation.

2.1.2 Primers

Primers used in this study are listed in Table 2.2.

2.1.3 Yeast strains

All the *Saccharomyces cerevisiae* strains used in this study are isogenic to the W303 background (*ade2-1, can1-100, trp1-1 leu2-3,112, his3-11,15, ura3*) except for the mating type tester strains Ry72 and Ry73. Strains were generated either by transformation of circular or linearized plasmids or PCR-generated deletion cassettes, or by dissecting sporulated heterozygous diploid strains obtained by crossing haploid strains of opposite mating type (see section 2.3.4 and 2.5.1 for procedures). The relevant genotypes of the yeast strains used in this study are listed in Table 2.3.

2.2 Media and growth conditions

2.2.1 Media for *Escherichia coli*

Bacterial cells were grown in LB medium.

LB: 1% Bacto Tryptone (DIFCO)
0.5% yeast extract (DIFCO)
1% NaCl
pH 7.25

LB was supplemented with 50μg/ml ampicillin (LB + amp). For solid media 2% agar (DIFCO) was added to the medium. All strains were grown at 37°C.

2.2.2 Media for *Saccharomyces cerevisiae*

Yeast cells were grown in rich medium (YP) or synthetic minimal medium (SC).

YP: 1% yeast extract
2% Bacto Peptone
0.015% L-tryptophan
pH 5.4

YP was supplemented with 300μM adenine and either 2% glucose (YPD) or 2% raffinose (YPR) or 2% raffinose and 2% galactose (YPRG) as carbon sources. For solid media 2% agar (DIFCO) was added.

SC: 0.15% yeast nitrogen base (YNB, DIFCO) without aminoacids and ammonium sulfate.
0.5% ammonium sulfate
200nM inositol

SC was supplemented with either 2% glucose (SCD), or 2% raffinose (SCR) or 2% raffinose and 2% galactose (SCRG) as carbon sources and amino acids as required. For solid media 2% agar (DIFCO) was added.

All strains were grown at 23°C unless otherwise stated. Growth conditions for individual experiments are described in the corresponding figure legend.

2.3 DNA-based procedures

2.3.1 *Escherichia coli* transformation

Aliquots of 50µl of fresh chemically competent TOP10 cells were thawed on ice for approximately 10 min prior to the addition of plasmid DNA or the ligation mixture. Cells were incubated with DNA on ice for 30 min and then subjected to a heat shock for 30-45 sec at 42°C. After the heat shock, cells were returned to ice for 2 min. Finally, 950µl of LB medium were added and the cell suspension was incubated on a shaker at 37°C for 45 min before being plated onto LB + amp plates. Plates were incubated overnight (ON) at 37°C.

2.3.2 Plasmid DNA isolation from *Escherichia coli* (miniprep)

Clones picked from individual colonies were inoculated in 5ml LB + amp and grown ON at 37°C. Bacterial cells were transferred to micro-centrifuge tubes and pelleted for 1 min at 13,000 rpm. Minipreps were performed with the NucleoSpin Plasmid kit (Macherey-Nagel) following the manufacturer's instructions. Plasmids were eluted in 50µl of sterile double-distilled water (ddH_2O).

2.3.3 Plasmid DNA isolation from *Escherichia coli* (midiprep)

Plasmid-containing cells were inoculated in 200ml LB + amp and grown ON at 37°C. Cells were then pelleted by centrifuging 10 min at 5000 rpm with a Beckman Coulter centrifuge. Midipreps were performed with the NucleoBond Xtra Midi kit (Macherey-Nagel) following the manufacturer's instructions. Plasmids were eluted in ddH_2O up to a concentration of 1µg/µl.

2.3.4 High efficiency LiAc-based yeast transformation

Yeast cells were grown ON in 50ml of the appropriate medium. Next morning the cell culture was diluted to OD_{600} = 0.2 and allowed to grow until it had reached an OD_{600} of 0.4-0.7. Cells were then harvested at 3000 rpm for 3 min and washed with 50ml of ddH_2O. The pellet was then transferred to an eppendorf tube with 1ml of ddH_2O, washed with 1ml of 1X TE/LiAc solution and then resuspended in 250µl of 1X TE/LiAc solution. 50µl aliquots of competent cells were used for each transformation reaction with 300µl of 1X PEG/TE/LiAc solution, 5µl of 10mg/ml single-stranded salmon sperm denatured DNA and "x" µl (max 10µl) of DNA. After gentle mixing, the transformation reaction was incubated on a rotating wheel for 30 min at room temperature (RT). Cells were heat-shocked at 42°C for 15 min and then centrifuged for 3 min at 3000 rpm. In case of auxotrophic selection, the pellet was resuspended in 200µl of 1X TE and then plated on the appropriate selective medium. In case of selection for resistance to antibiotics G418 and hygromycin, the pellet was resuspended in 1ml YPD and incubated ON at RT on a rotating wheel to allow cells to recover after the heat-shock before exposure to antibiotic. Next morning cells were centrifuged, resuspended in 100µl ddH_2O and plated on a YEPD plate containing 220µg/ml of G418 or 300µg/ml of hygromycin B.

10X TE:	0.1mM Tris, bring to pH 8.0 with HCl 10mM EDTA pH 8
10X LiAc:	1M LiAc, bring to pH 7.0 with acetic acid
1X TE/LiAc:	1X TE 1X LiAc
1X PEG/TE/LiAc:	1X TE 1X LiAc 40% PEG 4000

2.3.5 Smash and Grab yeast genomic DNA isolation

Cells picked from individual yeast colonies were suspended in 200µl of Lysis buffer. Next, 200µl of phenol/chloroform/isoamyl alcohol 25:24:1 (SIGMA) and 1 volume of glass beads were added. Cells were shaken 10 min on a Vxr Ika-Vibrax shaker at 4°C and then centrifuged 5 min at 13000 rpm. The upper aqueous layer was transferred to new tubes to which 1ml 100% ethanol -20°C was added to precipitate DNA. After gently mixing, samples were incubated at -20°C for approximately 20 min and then centrifuged 4 min at 13000 rpm. Supernatants were removed, pellets were air-dried and resuspended in 50µl of ddH_2O.

Lysis buffer: 2% Triton X-100
1% SDS
100mM NaCl
10mM Tris, pH 8.0
1mM EDTA pH 8.0

2.3.6 Yeast genomic DNA extraction

Yeast cells of the desired strain were grown ON in 5-10ml of the appropriate medium to stationary phase. Cells were collected by centrifuging 3 min at 3000 rpm and washed with 1ml of ddH_2O. Pellets were then resuspended in 200µl of SCE solution added with 1.5mg/ml Zymolyase 100T (AMS Biotechnology) and 8µl β-mercaptoethanol and then incubated at 37°C until complete spheroplast formation (30 min-60 min). Digestion was checked under an optical microscope by looking for burst spheroplasts when mixed with an equal volume of 1% SDS. Next, 200µl of SDS solution were added and samples were incubated at 65°C for 5 min. 200µl of 5M KAc were then added. Samples were mixed and left on ice for 20 min. Samples were then centrifuged 10 min at 13000 rpm and the supernatant was carefully transferred to new tubes. DNA was then precipitated with 200µl of 5M NH_4Ac and 1ml of isopropanol, collected by centrifuging 15-30 sec at 3000 rpm

and resuspended in 180µl of 1X TE. The precipitation step was then repeated two more times with decreasing amounts of NH_4Ac and isopropanol (20µl NH_4Ac 5M and 400µl isopropanol; 10µl NH_4Ac 5M and 200µl isopropanol) and the DNA was finally resuspended in 30µl 1X TE.

SCE Solution: 0.1M sorbitol
60mM EDTA
0.1M NaCitrate
pH to 7.0

SDS solution: 50mM EDTA pH 8.0
0.1M Tris pH 9.0
2% SDS

2.3.7 DNA amplification through polymerase chain reaction (PCR)

PCR was performed using genomic yeast DNA or plasmid DNA as template, ExTaq (TaKaRa) DNA polymerase, 0.2mM dNTPs, 0.2µM forward and reverse primers (listed in Table 2.2), and with Veriti Thermal Cycler (Applied Biosystems). DNA amplified for transformation into yeast or for Southern probe preparation was purified with the Wizard SV Gel and PCR Clean-Up System (Promega) kits following manufacturer's instructions. PCR-mediated gene deletion and tagging were performed as described in (Longtine *et al.*, 1998).

2.3.8 Enzymatic restriction of DNA

For diagnostic DNA restriction, 0.5-2µg of plasmid DNA were digested for 1 hr at 37°C with 1-10 units of the appropriate restriction enzyme (New England Biolabs, NEB). The reaction volume (20-50µl, depending on DNA concentration) was made up with the appropriate buffer and ddH_2O. For preparative DNA restriction 5-10µg of plasmid DNA or

genomic DNA were incubated for 3 hrs at 37°C with 1-10 units of restriction enzyme. Enzymes were inactivated following manufacturer's instructions.

In the case of linearized integrative plasmids to be transformed into yeast, DNA was precipitated adding 1/10 volume 3M NaAc and 3 volumes 100% isopropanol and pelleted at 13000 rpm for 15 min. The pellet was washed with 200µl of 70% ethanol and finally resuspended in 10µl ddH_2O. In the case of DNA fragments cleaved for ligation reactions, DNA was directly loaded onto agarose gel.

2.3.9 Agarose gel electrophoresis

Following the addition of 1/5 volume of bromophenol blue (BPB) solution 6X, DNA samples were loaded on 0.5% - 1% agarose gels along with DNA markers. Gels were made in 1X Tris-Acetate-EDTA (TAE) buffer containing 1X SybrSafe (Invitrogen) and run at 80-120V until the desired separation was achieved. DNA bands were visualized with the GelDoc EZ Imager (Biorad).

6X BPB solution:	0.2% BFB
	50% glycerol
10X TAE buffer:	0.4M Tris acetate
	0.01M EDTA

2.3.10 Purification of DNA from agarose gel

Cut DNA was loaded into a 0.8% agarose gel to separate DNA fragments by electrophoresis. The DNA fragment of interest was then excised from the agarose gel with a sharp scalpel and extracted with the QIAquick Gel Extraction Kit (Quiagen) following the manufacturer's instructions. DNA fragments were eluted in 30-50µl of elution buffer.

2.3.11 DNA ligation

Vector DNA (50ng) was ligated with a 3- and 6-fold molar excess of insert DNA in the following conditions: 1X Quick DNA ligase buffer, 1µl Quick DNA ligase (New England Biolabs, NEB) and ddH_2O up to 10-20µl (depending on DNA concentration). Reactions were incubated 5 min RT and then transformed into *E. coli* cells.

2.3.12 Constructs for Cin8, Top2 and cv-Topo II overexpression

To create constructs for Cin8 and Top2 overexpression, *CIN8* and *TOP2* were cloned under the control of the *PGAL1/10* promoter in integrative vectors (*YIplac204* and *YIplac211*, respectively). *CIN8* was ordered as a synthetic gene from GenScript, flanked by the BamHI and SalI restriction sites. *TOP2* was amplified through PCR from genomic DNA with addition of the BamHI and XbaI restriction sites. After being cloned, *TOP2* was sequenced to check for the absence of mutations. Plasmid Rc74 (*YIplac211-PGAL-NLS-NLS-cvTopoII-PK3*) was a gift from Dr. F. Uhlmann. Plasmids Rc74 and Rc75 (*YIplac211-PGAL1/10-TOP2*) were linearized with StuI and plasmid Rc104 (*YIplac204-PGAL1/10-CIN8*) with Bsu36I, before being transformed into wild type yeasts.

2.3.13 Minichromosome purification

Samples of 15-30ml of synchronized cells were collected, resuspended in ice cold SE solution added with 0.02% NaN_3, and kept on ice until the end of the time-course. Cells were then resuspended in 0.5ml of SE added with 5µl of 10mg/ml Zymolyase 100T and incubated at 37°C with mild agitation up to spheroplast formation (40 min - 60 min, checked as in 2.3.6). Spheroplasts were collected by centrifugation for 10 min at 13000 rpm, supernatants removed by aspiration and pellets resuspended in 0.5ml of Tris-EDTA. SDS was added to a final concentration of 1% and samples were incubated at 65°C for 15 min. Then, 200µl of 5M KAc were added and samples were placed on ice for 1 hr. The

precipitates were removed by centrifugation for 5 min at 13000 rpm and the supernatants collected. The centrifugation step was repeated until the supernatant fractions were clear of any debris. Next, 2 volumes of 100% ethanol were added, samples were incubated for 5 min and DNA was collected by centrifugation for 1 min at 13000 rpm. The supernatants were aspirated and the DNA pellets allowed to air dry. Once dry, pellets were carefully resuspended in 0.3ml of 1X TE pH 7.4 added with 50µg/ml RNase A (Sigma) and incubated for 30 min at 37°C. Next, proteinase K (Sigma-Aldrich) was added to a final concentration of 100µg/ml and samples were incubated for further 30 min. DNA was precipitated by addition of 12.6µl of 5M NaCl and 0.63ml of 100% ethanol. Samples were centrifuged again, supernatants aspirated and the pellets air-dried. Pellets were finally resuspended in 70µl 1X TE pH 7.4.

SE Solution: 1M sorbitol
0.1M EDTA pH 7.5

Tris-EDTA: 20mM EDTA
50mM Tris-HCl pH 7.4

2.3.14 DNA quantification

Purified DNA was quantified either with the NanoDrop ND-1000 (EuroClone) at 220nm or stained with the Quant-iT PicoGreen dsDNA Assay (Life Technologies) and quantified with the Glomax Explorer System (Promega) at 475 nm, following the manufacturers' instructions.

2.3.15 Minichromosome electrophoresis

Equal amounts of purified mini-chromosome samples were added with BPB buffer and loaded into 0.5% agarose/TAE gels (without DNA dyes) and resolved at 35V for 24 hrs at

RT with a buffer recycling apparatus.

2.3.16 Southern blotting

Southern blot analysis was employed to assess the number of *pGAL-CIN8* constructs integrated in the genome after transformation and to detect the different topological isoforms of the pS14-8 mini-chromosome. For assessing copy number, DNA was extracted from cells as described in 2.3.6, digested with SalI and resolved on 0.8% agarose gels. For detecting pS14-8 mini-chromosome isoforms, DNA was purified, quantified and resolved as described in 2.3.13, 2.3.14, and 2.3.15.

Agarose gels were stained by incubation in TAE 1X added with 1X SybrSafe for 30 min to check the electrophoretic run. Gels were then sequentially incubated for 30 min in a depurination solution, 20 min in a denaturing solution twice, and 20 min in a neutralizing solution twice. After each incubation gels were rinsed with ddH_2O. DNA fragments were then transferred ON to positively charged nylon membranes (Amersham Hybond-N+, GE Healthcare) using capillary blotting in 20X SSC buffer. DNA was fixed to the membranes by UV crosslinking with the Stratalinker UV crosslinker.

To detect the *pGAL-CIN8* construct, a probe specific for *CIN8* was used and to detect the pS14-8 mini-chromosome a probe specific for the AmpR gene. Probes were first prepared by PCR, next ^{32}P-labeled with Prime-a-Gene labeling system (Promega) following the manufacturer's instructions and finally purified with the illustra ProbeQuant G-50 Micro Columns (GE Healthcare).

Membranes were first incubated in 50ml of pre-warmed PerfectHyb Plus Hybridization Buffer (Sigma) for 60 min at 65°C (pre-hybridization), next ON at 65°C in 25ml of new, pre-warmed PerfectHyb Plus Hybridization Buffer containing the ^{32}P-labeled probe (hybridization). Membranes were then washed twice in 50ml of pre-warmed washing solution I for 30 min at 65°C and twice in 50ml of pre-warmed washing solution

II for 30 min at 65°C. Membranes were then dried, placed in a cassette, and exposed to Amersham Hyperfilm ECL.

20X SSC:	3M NaCl 0.3M Na citrate pH7.5
Depurination Solution:	0.25N HCl
Denaturing Solution:	0.5M NaOH 1.5M NaCl
Neutralizing Solution:	1.5M NaCl 1M Tris-HCl pH 7.4
Washing Solution I:	2X SSC 1% SDS
Washing Solution II:	0.2X SSC 1% SDS

2.4 Protein-based procedures

2.4.1 Yeast protein extraction

Samples of 10ml of a cell culture at OD_{600} = 0.2-1 were collected and centrifuged for 2 min at maximum speed. The resulting pellets were washed with 1ml of cold 10mM Tris-HCl pH 7.5, transferred to 2ml Sarstedt tubes and frozen in liquid nitrogen. Pellets were then resuspended in 100µl of lysis buffer supplemented with complete protease inhibitor cocktail (Roche). An equal volume of acid-washed glass beads (Sigma) was added and the tubes were subjected to 4-7 rounds of Fast Prep (speed 6.5 for 45 sec) at 4°C in order to break the cells. Cell breakage was checked under the optical microscope. Lysed cells were transferred to new tubes. In order to quantify the protein content, 10µl were taken from each lysate, diluted 1:3 in cold 50mM Tris-HCl pH 7.5 / 0.3M NaCl and 3µl were used in the Biorad protein quantification assay. The absorbance was read at λ = 595 nm. Samples were added with 50µl of 3X SDS blue loading buffer, boiled at 95°C for 5 min and then centrifuged at 13000 rpm for 3 min. The supernatant, containing the protein extract, was collected in a new microcentrifuge tube. Extracts were stored at -20°C.

Lysis buffer:	50mM Tris-HCl pH 7.5 1mM EDTA pH 8 50mM DTT
3X SDS blue loading buffer:	9% SDS 30% glycerol 0.05% Bromophenol blue 6% β-mercaptoethanol 0.1875M Tris-HCl pH 6.8

2.4.2 SDS polyacrylamide gel elettrophoresis

Aliquots of 50μg of total protein extracts were separated based on their molecular weight on 7.5% polyacrylamide precasted gels (BioRad) in 1X running buffer.

10X Running buffer: 2M glycine
0.25M Tris-HCl
0.02M SDS
pH 8.3

2.4.3 Western blot hybridization

Proteins were transferred with the Trans-Blot Turbo Blotting System (BioRad) with the protocol for high molecular weight proteins. Ponceau S staining was used to roughly reveal the amount of proteins transferred onto the filters. Membranes were blocked for 1h at RT in 1X PBS-T added with 3% milk and then incubated in primary antibody (1:1000 anti-HA; 1:1000 anti-FLAG; 1:5000 anti-Pgk1) diluted in 1% milk 1% BSA 1X PBS-T for 2 hrs at RT or ON at 4°C. Membranes were next washed 3 x 10 min in 1X PBS-T and incubated with horseradish-peroxidase-conjugated anti-Mouse secondary antibody diluited 1:10000 in 3% milk 1X PBS-T. The antibody was then removed by washing the membrane 3 x 10 min in 1X PBS-T. Membranes were then incubated with Clarity Western ECL (BioRad) and imaged with ChemiDoc System (BioRad).

10X PBS buffer: 1.37M NaCl
27mM KCl
14.7mM KH_2PO_4
80mM Na_2HPO_4

10X TBS buffer: 25mM Tris base
150mM NaCl
2mM KCl

1X PBS-T buffer: 0.1% Tween
1X PBS

1X TBS-T buffer: 0.1% Tween
1X TBS

2.4.4 Precipitation of condensin subunits Brn1 and Ycg1

Cells carrying plasmids Rc193 and Rc194 were grown in SCR medium lacking uracil and tryptophan, condensin subunits overexpression was induced by addition of 2% galactose and 50ml of cells were collected 3 hrs after induction. Protein were extracted in lysis buffer supplemented with complete protease inhibitor cocktail (Roche) and quantified as described in 2.4.1. To precipitate Brn1-3HA-12His and Ycg1-3FLAG-9His, extracts were incubated with Ni-NTA agarose resin for 30 min, washed with lysis buffer 5 times and then added with SDS blue loading buffer and boiled at 95°C for 5 min. Samples were then spinned and loaded on 4-15% gradient polyacrylamide precasted gels (BioRad) and stained with coomassie.

Lysis buffer: 50mM NaH_2PO_4
10mM Tris-HCl
0.7% Triton X-100
10% glycerol
500mM NaCl
pH 8

2.5 Cell biology procedures

2.5.1 Tetrad dissection and analysis

MATa and *MATα* strains were mixed with a drop of water on a solid medium appropriate for the growth of both the haploids and incubated ON at permissive conditions. Cells were then streaked to single colonies on medium and temperature conditions selective for diploid cells. Single colonies of diploids were next amplified on rich media for 1 day and next patched onto sporulation plates to induce sporulation by starvation. Sporulation was checked after 3-5 days. To allow dissection of the individual spores inside the tetrads, the ascus was removed by digestion with 200µl of 0.1mg/ml Zymolyase 100T in ddH_2O at 37°C for 3 min. Approximately 20µl were then dripped in a line onto the appropriate agar plate. Individual tetrads were dissected using the Nikon dissection microscope. Spores were left to grow at 23°C for 3-5 days. Colonies were replica plated onto selective media to define their genotype.

Sporulation plates: 30g K-Acetate
60g Agar (DIFCO)
all amino acids at 1/4 of the normal concentration
up to 3l with ddH_2O

2.5.2 Activation/inactivation of conditional mutants

2.5.2.1 Regulation of gene expression

To regulate the expression of specific proteins, yeast strains in which the encoding genes were cloned under the control of inducible promoters were used. The *PGAL1/10* promoter induces the expression at high levels of a downstream gene after the addition of galactose, while it shuts it off after addition of glucose. To overexpress a gene of interest, 2% galactose was added at a specific time to cells growing in a media containing a poor carbon

source as raffinose. To express the URL-Cdc5 protein at almost physiological levels, cells were grown in a media containing 2% raffinose and 0.5% galactose.

2.5.2.2 Protein degradation

Degron systems can be used to induce the degradation of a specific protein in a time-regulated manner. In this thesis, the AID degron, induced by auxin (Nishimura *et al.*, 2009) was used. To degrade proteins through the AID system, 0.5mM of indole-3-acetic acid (IAA, a natural auxin; Sigma) were added to the medium at a specific time.

2.5.2.3 Inactivation of temperature sensitive alleles

Temperature sensitive alleles were inactivated by shifting cells from permissive (23°C) to restrictive temperature (usually 37°C).

2.5.2.4 Inactivation of kinases with ATP-analogues

The *cdc5-as1* ATP-analogue sensitive allele was inactivated by addition to the media of 5μM CMK inhibitor (Accenda Tech; dissolved in DMSO).

2.5.3 Synchronization experiments

2.5.3.1 G1 phase arrest and release

Cells were grown ON in the appropriate medium at 23°C. Cells were diluted to OD_{600} = 0.2 in fresh medium and left to grow for 1-2 hrs. Cells were then diluted again to OD_{600} = 0.2 and added with 5μg/ml α-mating factor synthetic peptide (Primm) dissolved in ddH_2O. After 90 min, 2.5μg/ml α-factor was re-added to the culture. The G1 arrest was considered complete when more than 90% of the cells showed the shmoo (after 2.30-3.30 hrs depending on strain, medium and temperature). After the arrest was complete, cells were released from the G1 block by filtrating them and washing out α-factor with 10 volumes of medium without the pheromone. Cells were next released into the appropriate medium in the absence of the pheromone.

2.5.3.2 S phase arrest

Cells were grown ON in the appropriate medium at 23°C. Cells were diluted to OD_{600} = 0.2 in fresh medium and left to grow for 1-2 hrs. Cells were then diluted again to OD_{600} = 0.2 and added with 10mg/ml hydroxyurea (HU, Sigma) (powder added directly to the medium).

2.5.3.3 Cdc20 depletion-mediated metaphase arrest

Cdc20 depletion leads cells to arrest in metaphase. In this thesis, it was achieved by inducing Cdc20 degradation with the AID degron. Cells were first arrested in G1 as previously described, and next released in a medium containing 0.5mM IAA (Sigma).

2.5.4 Indirect immunofluorescence (IF)

Samples of 1ml of cell culture at OD_{600} = 0.2 - 0.4 were collected by centrifugation for 1 min at 13000 rpm at RT and incubated ON at 4°C in 1ml of fixative solution. Cells were then pelleted and washed 3 times with 1ml of 0.1M KPi pH 6.4 and once with 1ml of sorbitol-citrate solution. Cells were then resuspended in 200µl of digestion solution and incubated at 35°C for 20-30 min to enzymatically digest the cell wall, creating spheroplasts. Digestion was checked as in 2.3.6. Spheroplasts were pelleted at 2000 rpm for 2 min and washed with 1ml of sorbitol-citrate solution. Pellets were then resuspended in an appropriate volume of sorbitol-citrate solution (20-200µl, depending on pellet size). 5µl of the resuspended spheroplasts were then loaded on a 30-well slide (ThermoScientific) previously treated for 10 min with 0.1% polylysine (Sigma). To fix cells onto the slide, the slide was incubated in ice cold methanol for 3 min and in ice cold acetone for 10 sec. Cells were then incubated for 60-90 min in a humid dark incubation chamber with a primary antibody diluted in PBS-BSA, washed 5 times with PBS-BSA and incubated with the secondary antibody diluted in PBS-BSA for further 60-90 min. Cells

were then washed 5 times with PBS-BSA and covered with a DAPI mount solution. The slide was covered with a coverslip and sealed with nail polish.

0.1 M KPi buffer pH 6.4:	27.8ml 1 M K_2HPO_4
	72.2ml 1 M KH_2PO_4
	900ml ddH_2O
Fixative solution:	3.7% formaldehyde
	0.1M KPi pH 6.4
1.2 M Sorbitol-citrate:	17.4g Anhydrous KH_2PO_4
	7g Citric acid
	218.64g Sorbitol
	up to 1l with ddH_2O
Digestion solution:	1.2M sorbitol-citrate
	10% glusulase (Perkin-Elmer)
	0.1mg/ml Zymolyase 100T
PBS-BSA:	1% crude BSA (Sigma)
	0.04M K_2HPO_4
	0.01M KH_2PO_4
	0.15M NaCl
	0.1% NaN_3
DAPI mount solution:	0.04M K_2HPO_4
	0.01M KH_2PO_4
	0.15M NaCl
	0.1% NaN_3
	0.05μg/ml DAPI
	0.1% p-phenylenediamine
	90% glycerol

Primary antibodies:	1:100 rat anti-tubulin (MCA78G, AbD Serotec) 1:500 mouse anti-Nop1 (MCA-28F2, EnCore Biotechnology)
Secondary antibodies:	1:100 FITC-conjugated anti-rat 1:500 CY3-conjugated anti-mouse

2.5.5 Nuclei staining (DAPI staining)

About 1ml of a cell culture at OD_{600} = 0.2 - 0.4 was collected by centrifugation and incubated 10 min at RT in 1ml of 70% ethanol. Cells were pelleted and then resuspended in 20µl of DAPI 0.001mg/ml.

2.5.7 Analysis of immunofluorescence samples

2.5.7.1 Cell cycle progression

IF slides were visualized with a Leica DMR HC BIOMED fluorescence microscope using a 100X oil immersion objective. Cell cycle progression was scored by subdividing cells into three categories (interphase, metaphase and anaphase) based on nuclear and spindle morphologies. 100 cells were analyzed for each sample.

2.5.7.2 Spindle length and nuclear morphology

For spindles length measurements and nuclear morphology analysis (Figures 3.2, 3.11, 3.15, 3.18, 3.20, 3.26) images were acquired with an upright AX70 Olympus Provis microscope carrying a 100X/1.40 oil UPlanSApo ∞/0.17/FN 26.5 Olympus objective and a Photometrics CoolSnap Black & White 12 bit camera, using MetaMorph software. Fiji software was used to analyze the images. 100 cells were analyzed for each sample.

2.5.7.3 DNA anaphase bridges

For nuclear, nucleolar and spindle morphology analyses in Figures 3.5, 3.13, 3.14, 3.16, 3.19, images were acquired with a DeltaVision Elite deconvolution microscope (Applied

Precision) equipped with an Olympus IX71 inverted microscope and a CoolSnap HQ2 (Photometrics) CCD camera and driven by SoftWoRx software. Images were acquired with an UPlanSApo 100X oil immersion objective (NA 1.4) as 12 z-stacks (0.5µm step) with FITC, TRITC and DAPI filters. Stacks were deconvoluted by Delta Vision SoftWoRx program (Applied Precision) and converted into a projection of sum of intensity (DAPI and TRITC filter in Figures 3.13, 3.14, 3.16, 3.19) or of maximum intensity (FITC filter in all and DAPI and TRITC in Figure 3.5) using Fiji software. At least 200 cells were analyzed for each sample.

2.5.8 Live imaging

Cells were grown in SCD medium added with 2% adenine to decrease autofluorescence, arrested in G1 as described in 2.5.3.1 and released from the G1 arrest directly into the microfluidic plates Y04C (CellASIC). Imaging was performed with a DeltaVision microscope setup as described in 2.5.7.3. For Figure 3.3, 8 z-stacks (0.6µm step) were acquired every 3 min with FITC and Cherry filters with a 100X oil immersion objective; for Figure 3.6, 8 z-stacks (0.6µm step) were acquired every 3 min with FITC and Cherry filters with a 60X oil immersion objective; for Figures 3.7, 3.8, 3.9, 15 z-stacks (0.4µm step) were acquired every 3 min with FITC filter with a 100X oil immersion objective. Reference images were acquired in DIC. Images were deconvoluted with SoftWoRx software. Measurements of spindle length and chromosome loci distances were performed on x,y,z with the Fiji software with a specifically developed plug-in (Spindle Z manual tracker). Representative images shown are projection to maximum intensity.

2.5.9 Flow cytometry

Samples of 1ml of cell culture at OD_{600} = 0.2 - 0.4 were collected by centrifugation for 1 min at 13000 rpm at RT and incubated ON at 4°C in 70% ethanol. Cells were then washed

with 1ml of 50mM Tris-HCl pH 7.4 and incubated ON at 37°C in 0.5ml of the same buffer containing 1mg/ml RNase A. Next, cells were collected by centrifugation, resuspended in 55mM HCl containing 5mg/ml of pepsin (Sigma) and incubated at 37°C. After 30 min cells were collected, resuspended in 50mM Tris-HCl pH 7.4 and sonicated 10 sec 3 times with 30 sec interval with Bioruptor UCD-300 (Diagenode) water-bath sonicator set on "low". Just before FACS reading, 100µl of cell suspension were added to 1ml of Sytox Green staining solution. Samples were acquired with FACSCalibur system (Becton Dickinson) operated via the CellQuest software. Data were analyzed with FlowJo Analysis 8.8.6 software.

Sytox green stock solution	1mM Sytox green (Invitrogen) DMSO
Sytox green staining solution:	1µl/ml 5 mM Sytox green 50mM Tris-HCl pH 7.4

Table 2. 1 Plasmids used in this study.

Name	Genotype	Origin
Rp27	*YIplac204-PGAL1/10*	Visintin lab
Rp177	*YIplac211-PGAL1/10*	Visintin lab
Rc74	*YIplac211-PGAL-NLS-NLS-cvTopoII-PK3*	D'Ambrosio et al., 2008
Rc75	*YIplac211-PGAL1/10-TOP2*	This thesis
Rc104	*YIplac204-PGAL1/10-CIN8*	This thesis
Rc193	*2μ URA3 leu2-d PGAL7-SMC4-3StrepTagII, PGAL10-SMC2 PGAL1-BRN1-3HA-12HIS*	St.-Pierre et al, 2009
Rc194	*2μ TRP1 leu2-d PGAL10-YCS4 PGAL1-YCG1-3FLAG-9HIS*	St.-Pierre et al, 2009
pS14-8	*YCp70-RAD5::LEU2*	Charbin et al, 2014

Table 2. 2 Primers used in this study.

Name	Sequence (5' -3')	Purpose
T1	GTCAACTGAACCGGTAAGCG	*TOP2* sequencing (3FW)
T2	CTCTTTCATTCCGAATCTGG	*TOP2* sequencing (630 RV)
T3	GGGTCCATCATATACAAAGG	*TOP2* sequencing (570 FW)
T4	CGCATTTTCTTCATTTGCGTCG	*TOP2* sequencing (1233RV)
T5	GCAACTGACAACAAGAGTC	*TOP2* sequencing (1104 FW)
T6	CCATTCTTTACGGTCATCTGCC	*TOP2* sequencing (1959 RV)
T7	GGAGAGAGGAAGAATCGCAC	*TOP2* sequencing (1760 FW)
T8	GGTAAATACCACTCTGGCTCC	*TOP2* sequencing (2459 RV)
T9	GGGTCCAACAATATTTACTTGC	*TOP2* sequencing (2260 FW)
T10	CCTTATTAAATCTGGGGAACCC	*TOP2* sequencing (3187 RV)

T11	GCGAATTTTACTACGTCAAG	*TOP2* sequencing (2984 FW)
T12	CAGCTGTTTTTTTAGCGG	*TOP2* sequencing (4000 RV)
T13	GAGGGCGAACTGAGTAAG	*TOP2* sequencing (3847 FW)
LM23	CTCACCAGTCACAGAAAAGC	Probe AmpR-2 (RV)
LM24	CAGGCATCGTGGTGTCACGC	Probe AmpR-3 (FW)
LM25	CCGTGTCGCCCTTATTCCC	Probes AmpR-3, AmpR-1 (RV)
LM26	GCTTAATCAGTGAGGCACC	Probes AmpR-2, AmpR-1 (FW)
748_F	GCTGCTCTATTAAGAAAAAGG	CIN8 probe (FW)
1759_R	CTAGTTGTGCCCTTAAATGATC	CIN8 probe (RV)

Table 2. 3 Yeast strains used in this study.

Name	**Genotype**	**Origin**
Ry1	*MATa, ade2-1, leu2-3, ura3, trp1-1, his3-11,15, can1-100, GAL, psi+*	Visintin lab
Ry72	*MATa* (mating type tester)	Fink lab
Ry73	*MATα* (mating type tester)	Fink lab
Ry1574	*MATa, cdc14-1*	Visintin lab
Ry1602	*MATa, cdc14-1, cdc5-as1(L158G)*	Visintin lab
Ry1029	*MATa, cdc14-1, cdc5::GAL-URL-3HA-CDC5::kanMX*	Visintin lab
Ry2446	*MATa, cdc5-as1(L158G)*	Visintin lab
Ry2774	*MATa, cdc14-3, cdc5-2 (msd2-1::URA3)*	Visintin lab
Ry2776	*MATa, cdc14-3, cdc5L158G*	Visintin lab
Ry2875	*MATa, cdc14-3, cdc5-1*	Visintin lab
Ry2882	*MATa, cdc14-1, cdc5-1*	Visintin lab
Ry2134	*MATa, cdc14-1, cdc5-as1(L158G), mad1::URA3*	Visintin lab

Ry2758	*MATa, cdc14-1, cdc5-as1(L158G), mad1::URA3, mcd1-1*	Visintin lab
Ry4326	*MATa, smc2-8*	Visintin lab
Ry4655	*MATa, cdc5-as1(L158G), smc2-8*	Visintin lab
Ry4931	*MATa, scc1::HIS3, SCC1-TEV268-HA::LEU2, pGAL-NLS-9MYC-TEV Protease-NLS::TRP1 (10 integrants), ura3::pADH1-OsTIR1-9MYC::URA3, CDC20-aid::KanMX*	This thesis
Ry5126	*MATa, ura3::pGAL-NLS-NLS-cvTOPII-Pk3::URA3 (+)*	This thesis
Ry5127	*MATa, ura3::pGAL-NLS-NLS-cvTOPII-Pk3::URA3 (-)*	This thesis
Ry5128	*MATa, ura3::pGAL-TOP2::URA3 (+)*	This thesis
Ry5129	*MATa, ura3::pGAL-TOP2::URA3 (-)*	This thesis
Ry5156	*MATa, cdc14-1, cdc5-as1(L158G), ura3::pGAL-NLS-NLS-cvTOPII-Pk3::URA3 (+)*	This thesis
Ry5164	*MATa, cdc14-1, cdc5-as1(L158G), ura3::pGAL-NLS-NLS-cvTOPII-Pk3::URA3 (-)*	This thesis
Ry5172	*MATa, cdc14-1, cdc5-as1(L158G), ura3::pGAL-TOP2::URA3 (+)*	This thesis
Ry5179	*MATa, cdc14-1, cdc5-as1(L158G), ura3::pGAL-TOP2::URA3 (-)*	This thesis
Ry5272	*MATa, cdc14-1, cdc5-as1(L158G), YEN1^{ON}-myc18::URA3*	This thesis
Ry5321	*MATa, cdc14-1, cdc5-as1(L158G), YEN1-myc18::URA3*	This thesis
Ry5597	*MATa, YCp70-RAD5::LEU2 (pS14-8)*	Charbin et al, 2014
Ry5648	*MATa, cdc14-1, cdc5-as1(L158G), YCp70-RAD5::LEU2 (pS14-8)*	This thesis
Ry5651	*MATa, cdc14-1, YCp70-RAD5::LEU2 (pS14-8)*	This thesis
Ry5654	*MATa, cdc5-as1(L158G), YCp70-RAD5::LEU2 (pS14-8)*	This thesis
Ry5815	*MATa, cdc14-1, cdc5-as1(L158G), LEU2::TetR-GFP, ChrXV326bp::tetO112::KanMX*	This thesis
Ry5824	*MATa, cdc14-1, cdc5-as1(L158G), LEU2::TetR-GFP, ChrXVhis3::tetO112::HIS3*	This thesis
Ry5956	*MATa, cdc14-1, cdc5-as1(L158G), trp1::PGAL-CIN8::TRP1 (x1)*	This thesis
Ry5966	*MATa, cdc14-1, cdc5-as1(L158G), trp1::PGAL-CIN8::TRP1 (x2)*	This thesis
Ry5992	*MATa, cdc14-1, cdc5-as1(L158G), trp1::PGAL-CIN8::TRP1 (x1), ura3::pGAL-NLS-NLS-ChVTOP2-Pk3::URA3,*	This thesis
Ry6067	*MATa, cdc14-1, cdc5-as1(L158G), smc2-8*	This thesis
Ry6070	*MATa, cdc14-1, smc2-8*	This thesis

Ry6099	*MATa, cdc14-1, cdc5-as1(L158G), HTB2-Cherry::HIS3, cfi1::CFI1-GFP::KanMX6*	This thesis
Ry6575	*MATa, cdc15-2, YCp70-RAD5::LEU2 (pS14-8)*	This thesis
Ry6589	*MATa, cdc14-1, cdc5-as1(L158G), ndc10-1, HTB2-Cherry::HIS3, ura3::pAFS125-TUB1p-GFPTUB1::URA3*	This thesis
Ry6591	*MATa, cdc14-1, cdc5-as1(L158G), HTB2-Cherry::HIS3, ura3::pAFS125-TUB1p GFPTUB1::URA3*	This thesis
Ry7037	*MATa, cdc14-1, smc2-8, cdc5-as1(L158G), ura3::pGAL-NLS-NLS-ChVTOP2-Pk3::URA3*	This thesis
Ry7098	*MATa, cdc14-1, cdc5-as1(L158G), LEU2::TetR-GFP, ChrXV1070K::tetO112::Hph, ura3::pRS306-mCherry-TUB1::URA3*	This thesis
Ry7220	*MATa, cdc14-1, cdc5-as1(L158G), YEN1^{ON}-myc9::KanMX4 PGAL-CIN8::TRP1 (x1)*	This thesis
Ry7287	*MATa, dyn1::URA3, cin8-3, kip1::HIS3*	This thesis
Ry7411	*MATa, ChrXV his3::tetO112::HIS3, LEU2::TetR-GFP, ura3::pADH1-OsTIR1-9MYC::URA3, CDC20-aid::KanMX*	This thesis
Ry7481	*MATa, LEU2::TetR-GFP, ChrXV 1070K::tetO112::Hph ura3::pADH1-OsTIR1-9MYC::URA3, CDC20-aid::KanMX*	This thesis
Ry7519	*MATa, LEU2::TetR-GFP, ChrXV 326K::tetO112::KanMX, ura3::pADH1-OsTIR1-9MYC::URA3, CDC20-aid::KanMX*	This thesis
Ry7522	*MATa, dyn1::URA3, cin8-3, kip1::HIS3, CDC20-aid::KanMX, ura3::pADH1-OsTIR1-9MYC::URA3,*	This thesis
Ry7538	*MATa, cdc14-1, cdc5-2 (msd2-1::URA3)*	This thesis
Ry7822	*MATa, cdc14-1, cdc5-as1(L158G), 2µ TRP1 leu2-d PGAL10-YCS4 PGAL1-YCG1-3FLAG-9HIS 2µ URA3 leu2-d PGAL7-SMC4-3StrepTagII, PGAL10-SMC2 PGAL1-BRN1-3HA-12HIS*	This thesis
Ry7824	*MATa, cdc14-1, cdc5-as1(L158G), 2µ TRP1 leu2-d PGAL10-YCS4 PGAL1-YCG1-3FLAG-9HIS 2µ URA3 leu2-d PGAL7-SMC4-3StrepTagII, PGAL10-SMC2 PGAL1-BRN1-3HA-12HIS*	This thesis

3. Results

The simultaneous inactivation of the phosphatase Cdc14 and the Polo-like kinase Cdc5 leads to cells arresting immediately after cohesin cleavage, with short and stable bipolar spindles and undivided nuclei, a phenotype that was defined as “mini-anaphase”. This synthetic interaction indicates that Cdc5 and Cdc14 redundantly control an essential process in early anaphase. Previous studies identified this process as spindle elongation (SE). However, it was observed that uncoupling SE from sister chromatid separation (SCS) in the *cdc5 cdc14* double mutant results in cells arresting in mini-anaphase with spindles transiently and slightly longer, more fragile and unstable. This suggested that these cells, beside being unable to elongate their spindles, may also retain some cohesin-independent residual cohesion between sister chromatids sufficient to counteract a defective spindle (Roccuzzo *et al.*, 2015).

Aim of this work is to identify the nature of this cohesion between sister chromatids and to understand the mechanisms underlying the SCS defect of the *cdc5 cdc14* double mutant, with the ultimate goal of providing new insights on how linkages are removed from chromatids in mitosis.

3.1 Characterization of the *cdc5 cdc14* double mutant phenotype

3.1.1 Characterization of the phenotype of different combinations of *cdc5* and *cdc14* mutant alleles

The original observation that *cdc5 cdc14* cells are defective in SCS derives from experiments performed with cells carrying the ATP-analogue sensitive allele *cdc5-as1* (Zhang *et al.*, 2005) and the temperature sensitive (*ts*) allele *cdc14-1* (Culotti and Hartwell, 1971). Other *CDC5* and *CDC14* allelic combinations, tested for the SE defect, were never characterized for the SCS defect (Roccuzzo *et al.*, 2015). To understand whether the latter is specific for the *cdc5-as1 cdc14-1* allelic combination or it is indicative of a general defect of *cdc5 cdc14* double mutants, we started our analysis by investigating the spindle and nuclear morphology phenotypes of all the available *cdc5* and *cdc14* mutant combinations. To this aim, we combined two *ts* alleles of *CDC14* (*cdc14-1* and *cdc14-3*) with two *ts* (*cdc5-1* and *cdc5-2*) (Hartwell *et al.*, 1973), an ATP-analogue sensitive (*cdc5-as1*) and a degron (*PGAL-URL-CDC5*) (Visintin *et al.*, 2008) alleles of *CDC5*. Mutant proteins were inactivated at the restrictive temperature of 37°C (*ts* alleles), by addition of the CMK inhibitor (*cdc5-as1*) (Snead *et al.*, 2007) or by addition of glucose (*PGAL-URL-CDC5*) (Visintin *et al.*, 2008). *cdc5-as1 cdc14-1*, *cdc5-as1 cdc14-3*, *cdc5-2 cdc14-1*, *cdc5-2 cdc14-3*, *cdc5-1 cdc14-1* and *cdc5-1 cdc14-3* cells were grown overnight and arrested in G1 by addition of α-factor at 23°C (permissive temperature for the *ts* mutants) in YPD, and then synchronously released into the next cell cycle at the non-permissive conditions characteristic of the allelic combination examined (Figure 3.2A). Instead, *PGAL-URL-CDC5 cdc14-1* cells were grown and arrested in G1 in YPR medium added with 0.5% galactose (YPRG 0.5%) at 23°C to achieve almost physiological levels of Cdc5 expression (Visintin *et al.*, 2008). In this construct, Cdc5 levels are determined by a balance between

Cdc5 expression driven by the galactose inducible promoter *PGAL* (West *et al.*, 1987), and Cdc5 degradation guided by the *URL* sequence fused to *CDC5* N-terminal end that causes the protein to be degraded *via* the N-end rule pathway (Bachmair, Finley and Varshavsky, 1986). G1 arrested cells were synchronously released into the next cell cycle in YPD at 37°C to deplete Cdc5 and inactivate Cdc14 respectively. *cdc5-as1 cdc14-1* cells were analyzed as control in this experimental set up as a different carbon source may impact on spindle elongation and morphology (Figure 3.2B). In both experiments, samples were collected every 30 min for 4 hrs and analyzed through indirect immunofluorescence (IF) and DAPI staining to visualize the spindle (anti-Tub1 antibody) and the nucleus, respectively. We monitored cell cycle progression by means of nuclear and spindle morphology to discriminate between interphase, metaphase and anaphase cells (Figure 3.1). Interphase cells have a single nucleus and 3-5 cytoplasmic microtubules emanating from one SPB, metaphase cells have an undivided nucleus and a short and thick bipolar spindle, whilst anaphase cells are characterized by a separating nucleus or two fully separated nuclear masses and an elongated spindle.

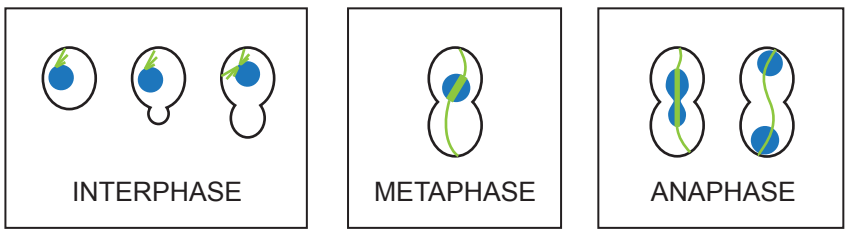

Figure 3. 1 Yeast cells morphology in interphase, metaphase and anaphase.
Blue: nucleus; green: spindle.

In agreement with previous results, we found that all the tested mutants arrested in a stage that morphologically resembles metaphase, with the exception of those carrying the *cdc5-1* allele that displayed a higher percentage of anaphase cells (up to 40% in *cdc5-1 cdc14-1* cells or to 20% in *cdc5-1 cdc14-3* cells) (Figure 3.2A,B). To characterize the SCS defect we next performed a more detailed analysis of spindle length and nuclear

morphology exclusively in cells with a bipolar spindle. With respect to spindle length, we arbitrarily classified cells into 5 groups (cells with spindles of <2µm, 2-3µm, 3-4µm, 4-6µm, >6µm) that reflect the different steps of mitosis: metaphase arrested cells have spindles of ~2µm, early anaphase cells of 4-6µm, and late anaphase of more than 6µm (Straight, Sedat and Murray, 1998; Movshovich *et al.*, 2008). As *cdc5-as1 cdc14-1* cells were previously reported to arrest with spindles of 2-4µm, we decided to further subdivide this category in two (2-3µm and 3-4µm spindles) to be able to detect for small differences in spindle length. In the same cells in which we measured the spindle, we tracked nuclear morphology and classified cells into three categories: with a single, unseparated nuclear mass; with a separating nuclear mass; or with two fully separated nuclear masses. The second category includes nuclear morphologies that are all representative of chromosome segregation taking place. As expected, *cdc5-as1 cdc14-1* cells arrested with short, very stable, metaphase-like spindles (<4µm, with a mode at 2-3µm); their nuclei remained undivided for the entire time-course, although a small percentage (~20%) of separating nuclei was observed around 120-150 min after the release (Figure 3.2A). The same behavior was observed in *cdc5-as1 cdc14-3*, *cdc5-2 cdc14-1*, *cdc5-2 cdc14-3* and *PGAL-URL-CDC5 cdc14-1* cells with only small differences in spindle length and nuclear separation (Figure 3.2A,B). Of note, *cdc5-as1 cdc14-1* cells grown in a raffinose (a poor carbon source) containing medium displayed slightly shorter spindles, likely a consequence of a smaller cell size (Jorgensen *et al.*, 2007). In *cdc5-1 cdc14-1* and *cdc5-1 cdc14-3* strains about 10-20% of cells elongated their spindles and a higher percentage of cells displayed separating nuclei, up to 60% in the *cdc5-1 cdc14-1* strain. In this strain the distinction between separating and fully separated nuclei could not be done because a mass of mitochondria, also stained by DAPI, aggregates at the bud-neck between separating nuclear masses. Despite being interesting, we did not investigate this phenotype as it goes beyond the aim of our work.

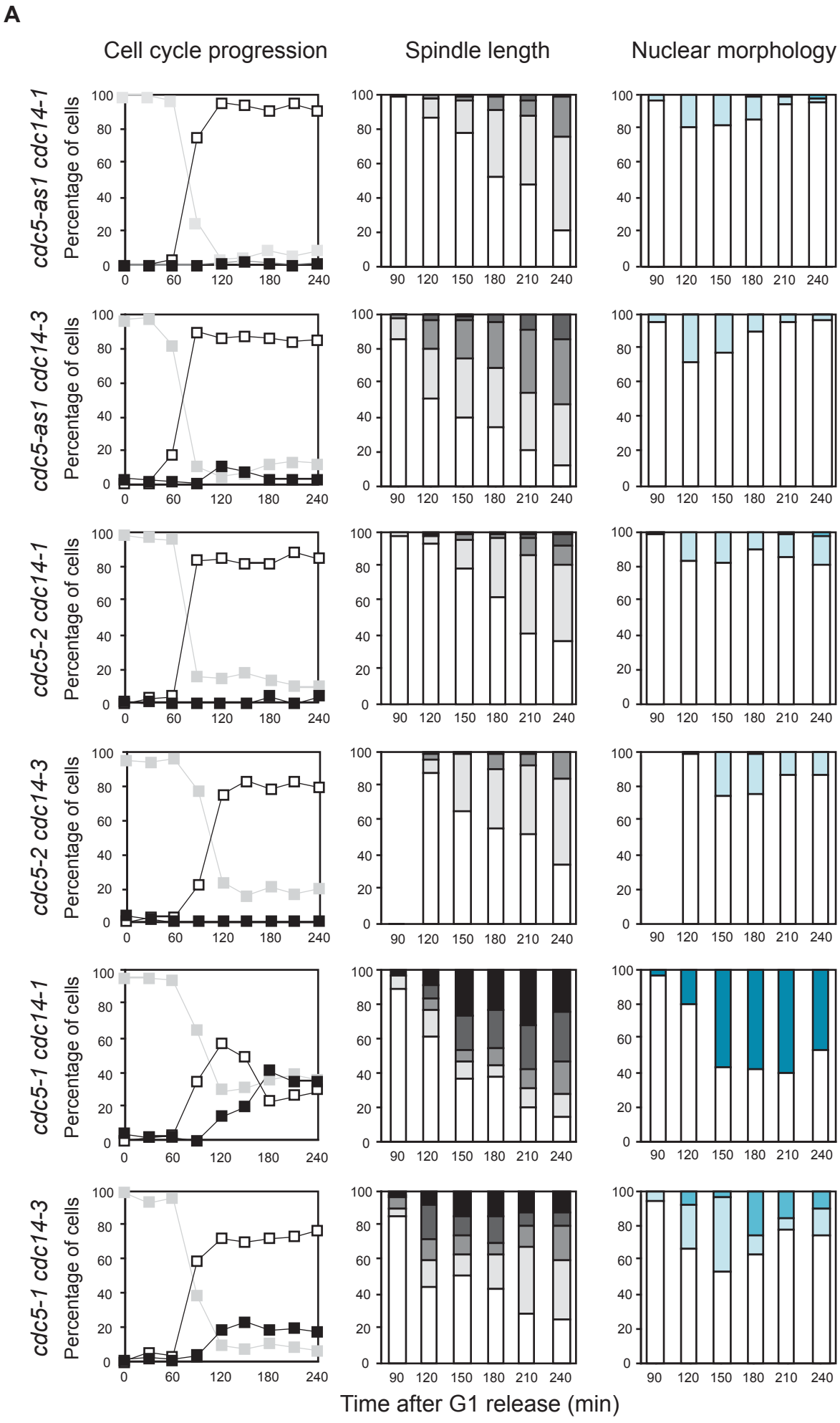
A
Cell cycle progression
Spindle length
Nuclear morphology
cdc5-as1 cdc14-1
cdc5-as1 cdc14-3
cdc5-2 cdc14-1
cdc5-2 cdc14-3
cdc5-1 cdc14-1
cdc5-1 cdc14-3
Percentage of cells
0
20
40
60
80
100
0
60
120
180
240
90
120
150
180
210
240
Time after G1 release (min)

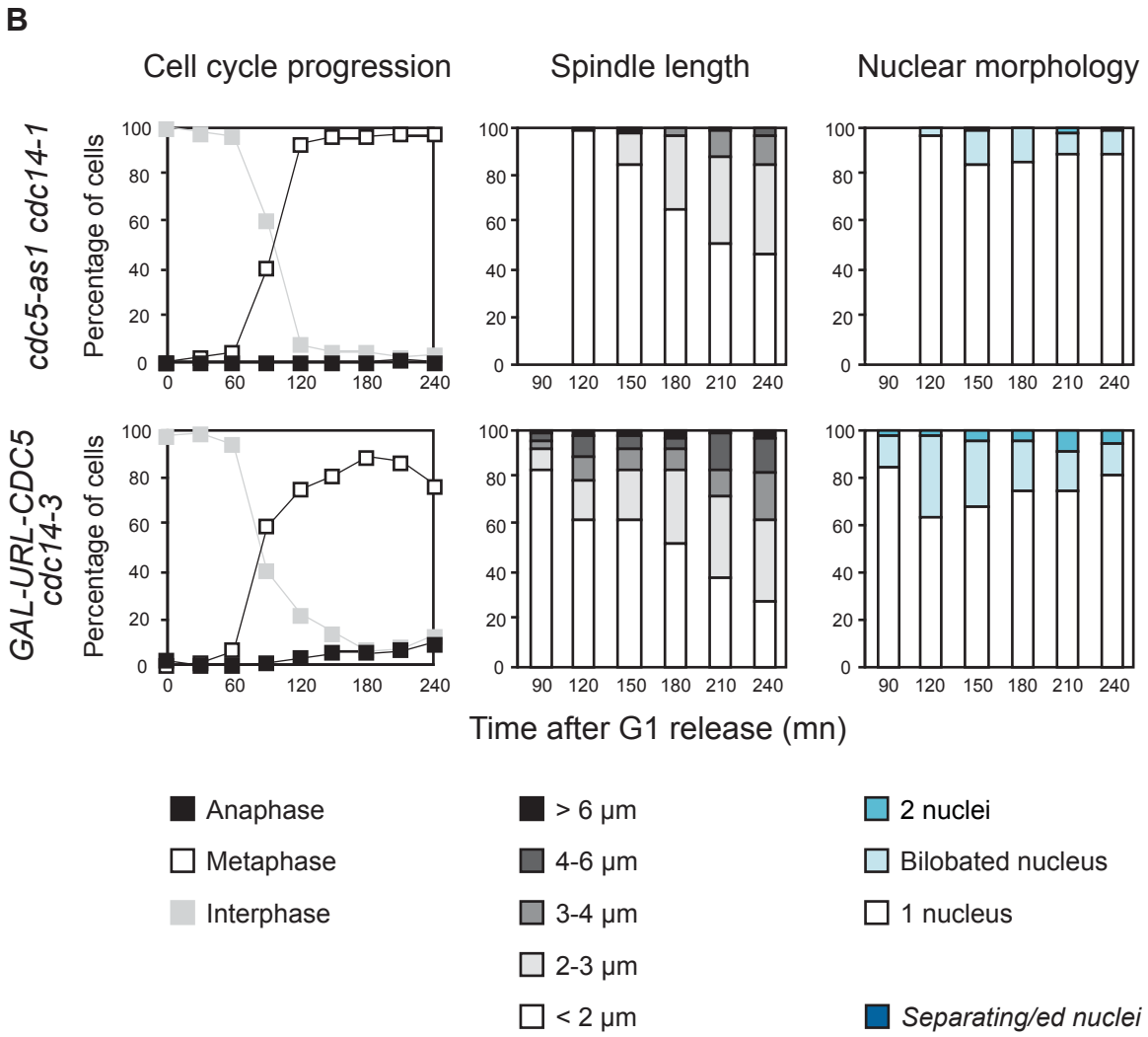

Figure 3. 2 Comparison between different allelic combinations of *cdc5 cdc14*.
A. *cdc5-as1 cdc14-1*, *cdc5-as1 cdc14-3*, *cdc5-2 cdc14-1*, *cdc5-2 cdc14-3*, *cdc5-1 cdc14-1* and *cdc5-1 cdc14-3* cells were arrested in G1 by addition of α-factor in YPD at 23°C and then synchronously released into the next cell cycle in new, prewarmed YPD medium supplemented with the CMK inhibitor to inactivate *cdc5-as1* at the non-permissive temperature for the *ts* mutants (37°C). **B.** *cdc5-as1 cdc14-1* and *PGAL-URL-CDC5 cdc14-1* cells were arrested in G1 by addition of α-factor at 23°C in YPR-G 0.5% to allow *CDC5* expression and then synchronously released into the next cell cycle in prewarmed YPD medium (to shut off *CDC5* expression) supplemented with the CMK inhibitor (to inactivate *cdc5-as1*) at 37°C (to inactivate *cdc14-1*). Samples were collected every 30 min for 240 min and analyzed through IF (anti-Tub1, DAPI). The percentage of interphase, metaphase and anaphase cells was evaluated throughout the time-course (left); starting from 90 min, when bipolar spindle formed, spindles were measured (center) and nuclei morphology was analyzed (right) (n=100).

Altogether, this analysis indicates that all the combinations of the *cdc5* and *cdc14* mutant alleles tested share the same phenotype, with the exception of the ones carrying the *cdc5-1* allele. As the spindles elongate more in *cdc5-1 cdc14-1* and *cdc5-1 cdc14-3* cells,

we hypothesize that the *cdc5-1* allele is less stringent in the SE defect. A lower stringency of this allele has already been suggested in regard to its ability to inhibit rDNA condensation (Walters *et al.*, 2014). As a consequence of having a more functional spindle, these strains managed to partially separate their nuclei. Having found that the *cdc5-as1 cdc14-1* strain exhibits the strongest SCS phenotype and the most stable cell cycle arrest, we decided to perform all our subsequent analyses with this mutant.

3.1.2 *cdc5 cdc14* cells retain residual cohesion between sister chromatids

Our hypothesis that *cdc5 cdc14* cells are defective in SCS was based on the difference in spindle length and stability that was observed in *cdc5 cdc14* cells in which SE was uncoupled from SCS. Indeed, it was noticed that when spindles are detached from chromatids by disrupting the kinetochores or when cells undergo mitosis with sister-less chromatids, spindles become slightly and transiently longer and more fragile (Roccuzzo *et al.*, 2015). The technique employed for the analysis was IF on fixed samples collected with a 30 min interval. To probe in more details a dynamic process such as SE, we decided to repeat this analysis with time-lapse experiments on living cells. Indeed, while IF provides a snapshot of a population at a given time, time-lapse experiments on living cells allow to follow individual cells continuously in time. We thus compared in live imaging *cdc5-as1 cdc14-1* cells with *cdc5-as1 cdc14-1 ndc10-1* cells in which the kinetochore is disrupted through inactivation of the inner kinetochore protein Ndc10 (Goh and Kilmartin, 1993). To monitor nuclear and spindle morphologies we inserted in our strains of interest a Cherry tagged version of the histone Htb2 (Htb2-Cherry) and a GFP tagged version of tubulin (Tub1-GFP). Cells were synchronized in G1 and released into the next cell cycle in the restrictive conditions. To avoid UV light induced DNA damage checkpoint activation, imaging was started when spindle morphology and nuclear positioning indicated that cells had reached metaphase. Cells were imaged every 3 min for 3 hrs. After measuring spindle

length on x, y, z throughout the time-lapse, we confirmed that in *cdc5-as1 cdc14-1* cells the spindles remain stable and short (between 1-4µm with a mode at 2-3µm) throughout the course of the experiment (Figure 3.3A). In contrast, and in agreement with what was already reported, the spindles of *cdc5-as1 cdc14-1 ndc10-1* cells became longer (up to 4-6µm), more fragile and soon collapsed; in few cases spindles reassembled after collapsing (Figure 3.3B). This result further supported the observation that residual cohesion persists between sister chromatids in *cdc5 cdc14* cells. It also explained the only partial phenotype visualized on fixed samples where only a small percentage of cells had longer spindles.

A

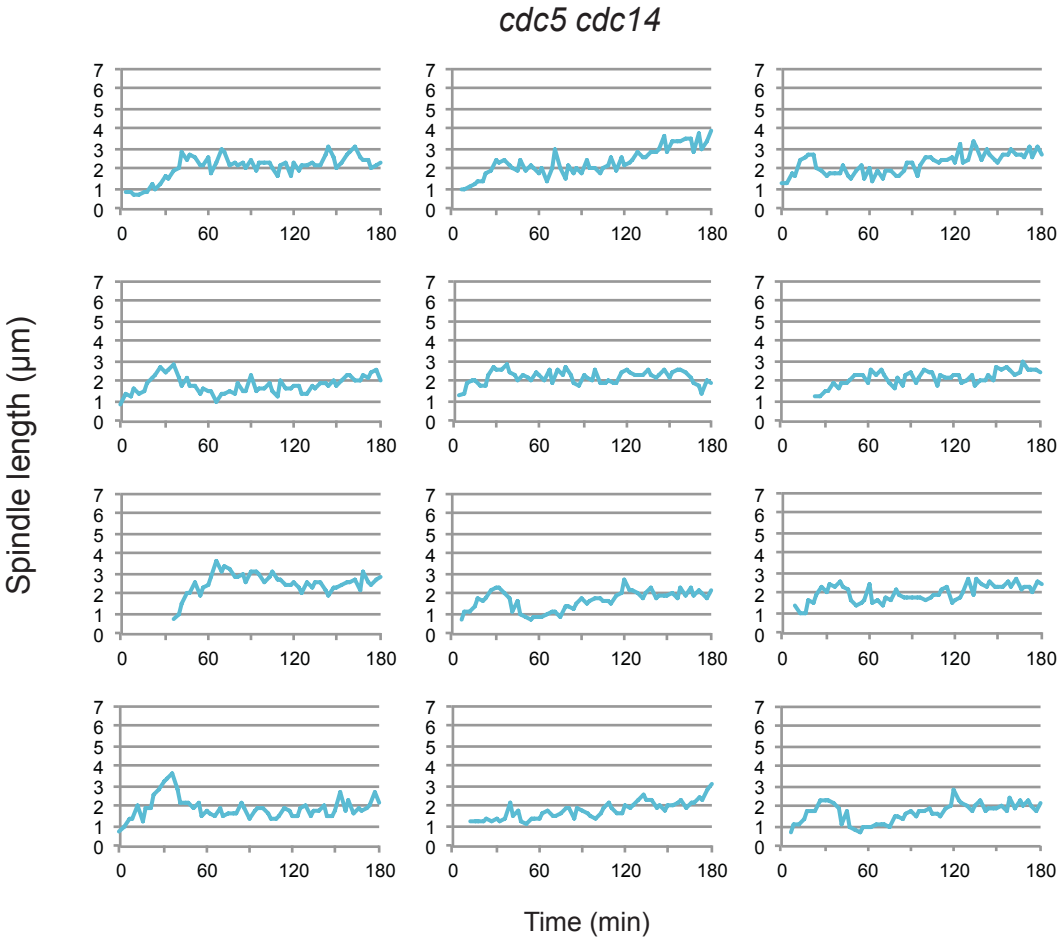

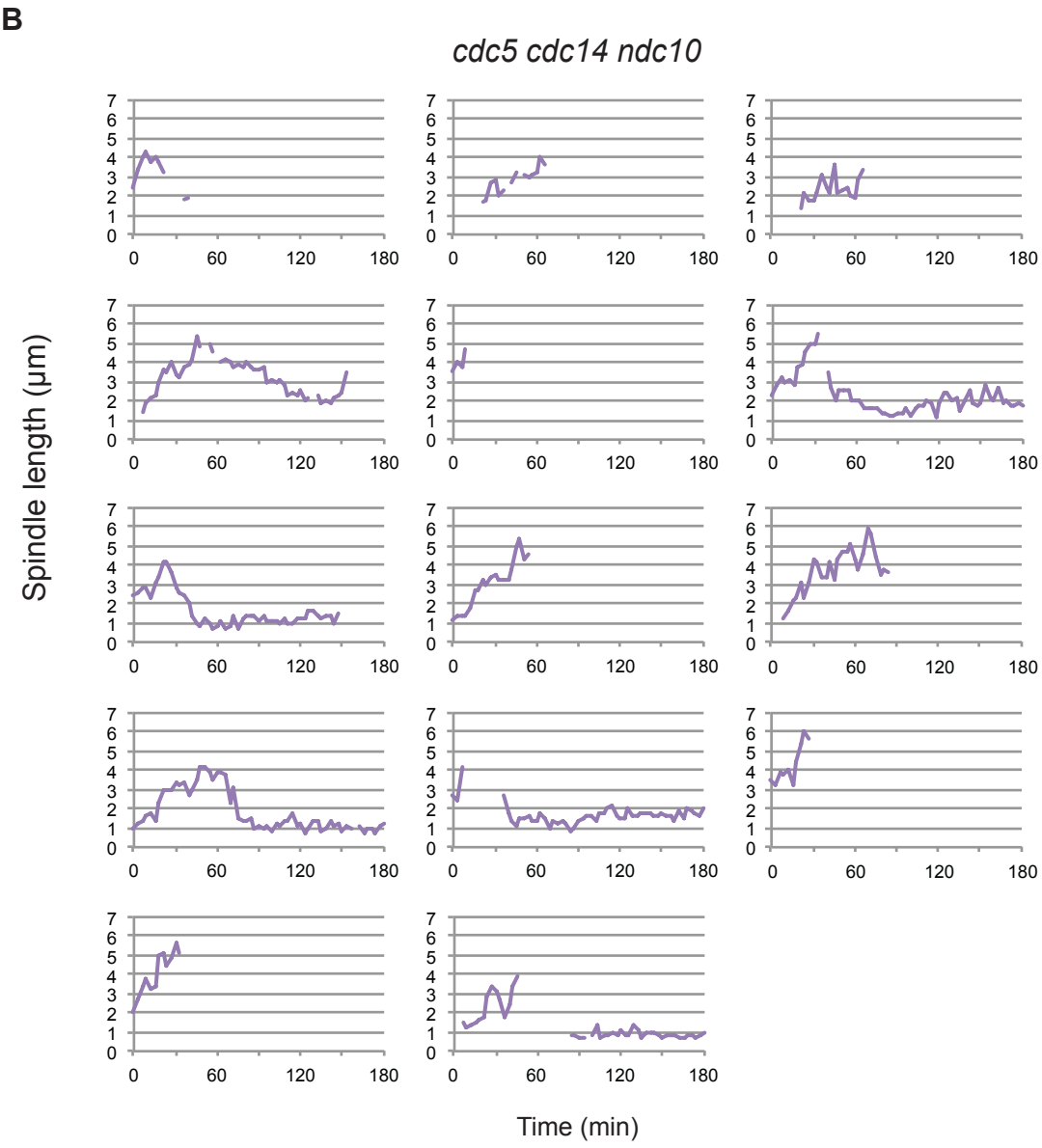

Figure 3. 3 *cdc5 cdc14* cells retain residual cohesion between sister chromatids.
cdc5-as1 cdc14-1 HTB2-Cherry GFP-TUB1 and *cdc5-as1 cdc14-1 ndc10-1 HTB2-Cherry GFP-TUB1* cells were arrested in G1 with α-factor in SCD medium at 23°C, loaded in the microfluidic plate and then released in SCD medium supplemented with CMK inhibitor at 37°C to inactivate *cdc5-as1* and *cdc14-1*, respectively. Cells were imaged starting from metaphase with a 3 min interval for 3 hours. Spindle length was measured throughout the time-lapse on x,y,z. **A**. Spindle length in *cdc5-as1 cdc14-1 HTB2-Cherry GFP-TUB1* cells. **B**. Spindle length in *cdc5-as1 cdc14-1 ndc10-1 HTB2-Cherry GFP-TUB1 cells*.

Together with spindle length, we monitored nuclear morphology (Figure 3.4). In *cdc5-as1 cdc14-1 ndc10-1* cells, as the spindle is not connected to chromosomes, nuclei remained still and undivided. Unexpectedly, in *cdc5-as1 cdc14-1* cells nuclei were very dynamic and often appeared bilobated. As bilobated nuclei are generally indicative of

chromosome segregation, this finding seemed to question our hypothesis about the SCS defect of the *cdc5 cdc14* double mutant. More importantly, it was in contrast with what we observed in our previous IF analysis where bilobated nuclei were rarely observed (only in ~20% of cells) (Figure 3.2).

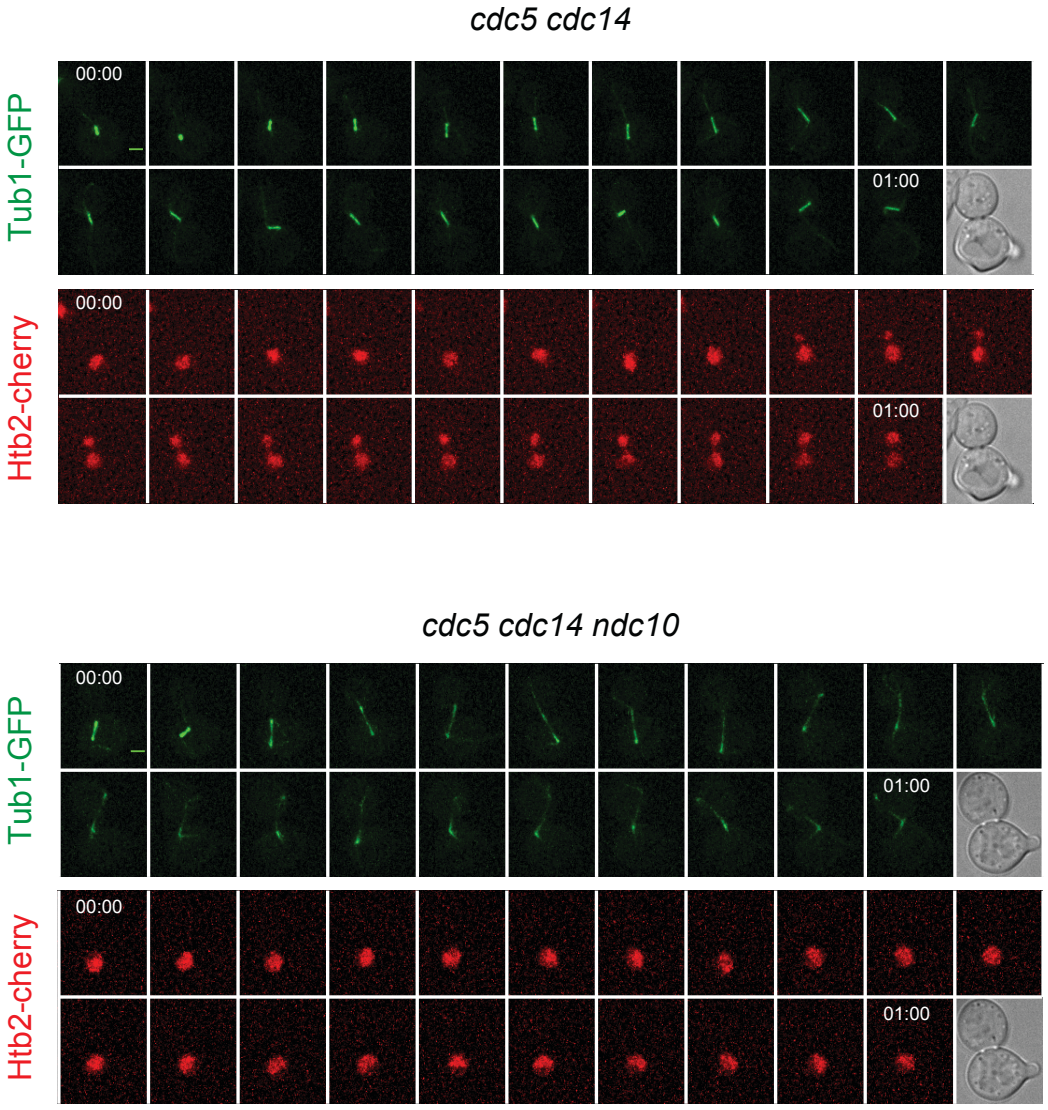

Figure 3. 4 *cdc5 cdc14* and *cdc5 cdc14 ndc10* representative cells.
Still images of representative cells (red: nucleus; green: spindle; scale bar: 2μm) from Figure 3.3 are shown.

3.1.3 Nuclei of *cdc5 cdc14* cells do not divide but move as a whole into the daughter cell

To explain the conflicting results about nuclei separation in *cdc5 cdc14* cells obtained by IF on fixed samples and by live imaging, we considered alternative possibilities that took into account the differences between the two techniques, more specifically population versus single cell analysis and DAPI staining versus Htb2-Cherry imaging. As live imaging provides a continuous probing, it is possible that it allowed for the visualization of a fast, transient and highly dynamic event gone unnoticed in population studies, where only a low percentage of the population might be captured at a transient step of the process. Thus, the bilobated morphology of nuclei could either indicate that nuclei started to separate when spindles attempted to elongate, but eventually rejoined as the spindle is defective in these cells, hence not able to pull nuclei apart; or it could reflect a transient state of nuclei being squeezed through the bud-neck while moving (or attempting to move) from the mother to the daughter cell. A passage of the nucleus from the mother to the daughter cell was a plausible explanation, as it is a phenotype shared both by DNA damage checkpoint mutants (*rad53* and *chk1* single mutants in which checkpoint activity is still sufficient to delay the cell cycle) when delayed in metaphase in presence of unrepairable DNA damage (Dotiwala *et al.*, 2007) and by different FEAR network component mutants in which cohesin cleavage was prevented (Ross and Cohen-Fix, 2004). Both possibilities could explain the observation that in our fixed cells experiments a "peak" (~20%) of bilobated nuclei appeared 120-150 min after G1 release and disappeared at later time points. Alternatively, the bilobated morphology observed in live imaging but not with IF might reflect intrinsic differences associated with the strategy of visualization of the nucleus, meaning that there might be something that can be detected with Htb2-Cherry but is not stained, or poorly stained, by DAPI. We reasoned that the nucleolus was a likely candidate. The nucleolus is a well-defined sub-nuclear compartment deputed to ribosome biogenesis. It contains several repetitions of the rRNA genes (rDNA) hosted on a single

chromosome (XII) and it divides after and independently from the rest of the genome (Granot and Snyder, 1991; D'Amours, Stegmeier and Amon, 2004; Sullivan *et al.*, 2004; Torres-Rosell *et al.*, 2004). While histone Htb2 is present on the rDNA, though at a lower level than the rest of DNA because chromatin is displaced from rRNA genes that are being actively transcribed (Merz *et al.*, 2008), DAPI intercalates rDNA very poorly and DAPI-stained nucleolus is often undistinguishable from background.

To discriminate among these possibilities, we probed nucleus and nucleolus in *cdc5-as1 cdc14-1* cells synchronously progressing trough the cell cycle after a G1 release both by IF and live imaging. Samples were analyzed through IF against spindle (anti-Tub1), nucleolus (anti-Nop1, a nucleolar protein) and nucleus (DAPI). Images were acquired and analyzed starting from 90 min after the G1 release, when cells entered mitosis. We found that while at 90 min after the release (corresponding to metaphase) nucleus and nucleolus were in close proximity, presumably in the mother cell, and the nucleus was undivided, at later time points a subset of cells appeared with the nucleus in one cell and the nucleolus in the other (Figure 3.5). At the terminal arrest the subset of cells with this configuration of nucleus and nucleolus accounted for 60% of the population. The combination of nucleus in one cell and nucleolus in the other might have contributed to shaping the bilobated morphology observed in living cells.

We next performed the same analysis in living cells. *cdc5-as1 cdc14-1* cells carrying Htb2-Cherry and Cfi1-GFP fusions were analyzed for nuclear (Htb2-Cherry) and nucleolar (Cfi1-GFP; Cfi1 always localizes in the nucleolus and can be used as nucleolar marker) morphologies and positions. We found that in 100% of the cells imaged (n=90) the nucleus progressively moved from the mother into the daughter cell while the nucleolus always remained in the mother. While passing through the bud-neck, the nucleus was squeezed and looked bilobated. Still images of representative cells are shown in Figure 3.6.

From this set of experiments, we concluded that the bilobated morphology of the nuclei visualized with Htb2-Cherry is both the result of nuclei passing in the daughter cell

and the combination of nucleus in the daughter and nucleolus in the mother. It does not reflect a process of chromosome segregation.

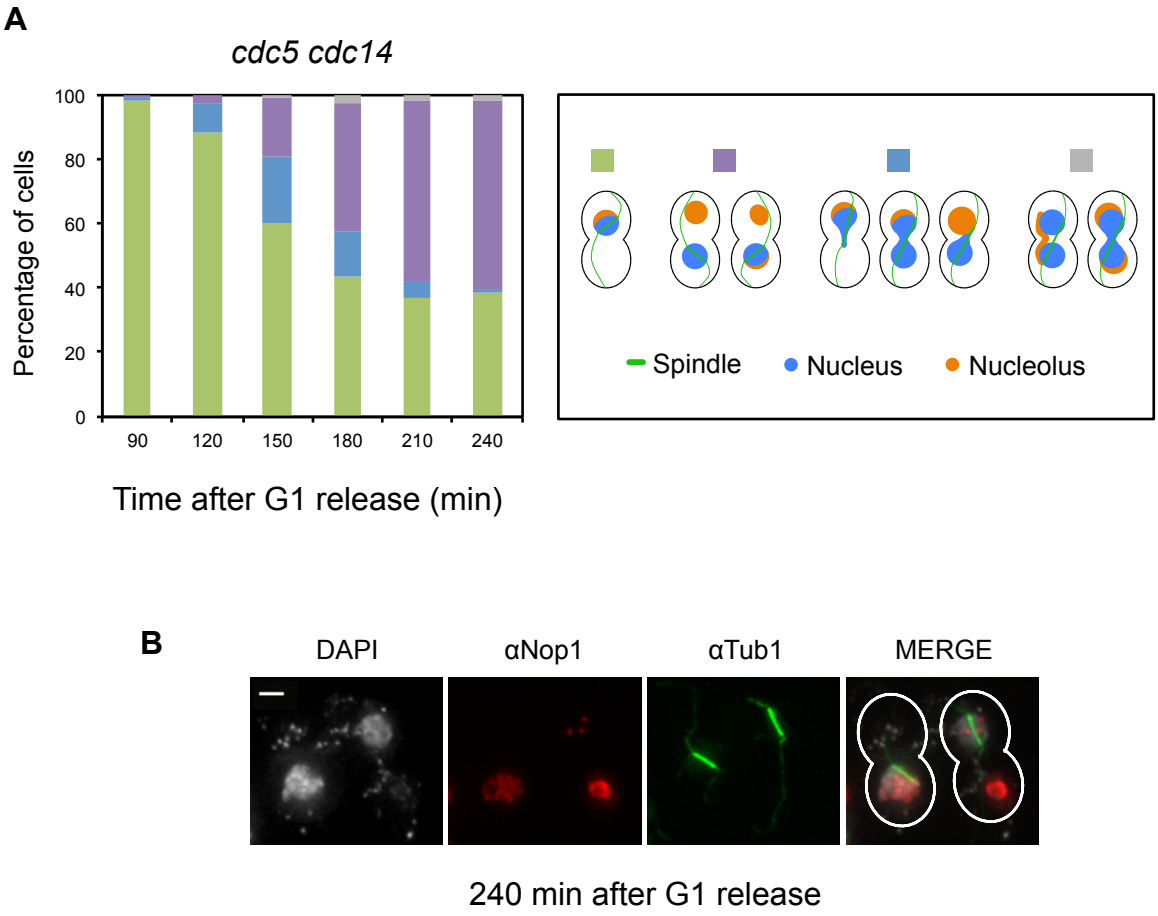

Figure 3. 5 Nuclear and nucleolar morphology of *cdc5 cdc14* cells.
cdc5-as1 cdc14-1 cells were arrested in G1 by addition of α-factor in YPD at 23°C and then synchronously released into the next cell cycle in new, prewarmed YPD medium supplemented with the CMK inhibitor at 37°C, to inactivate *cdc5-as1* and *cdc14-1*, respectively. Samples were collected every 30 min for 240 min and analyzed through IF (anti-Tub1, anti-Nop1, DAPI). **A.** Nuclear and nucleolar morphologies were analyzed starting from 90 min. Cells were classified in the shown categories (blue: nucleus, orange: nucleolus, green: spindle; n=200). **B.** Representative cells at 240 min are shown (scale bar: 2μm).

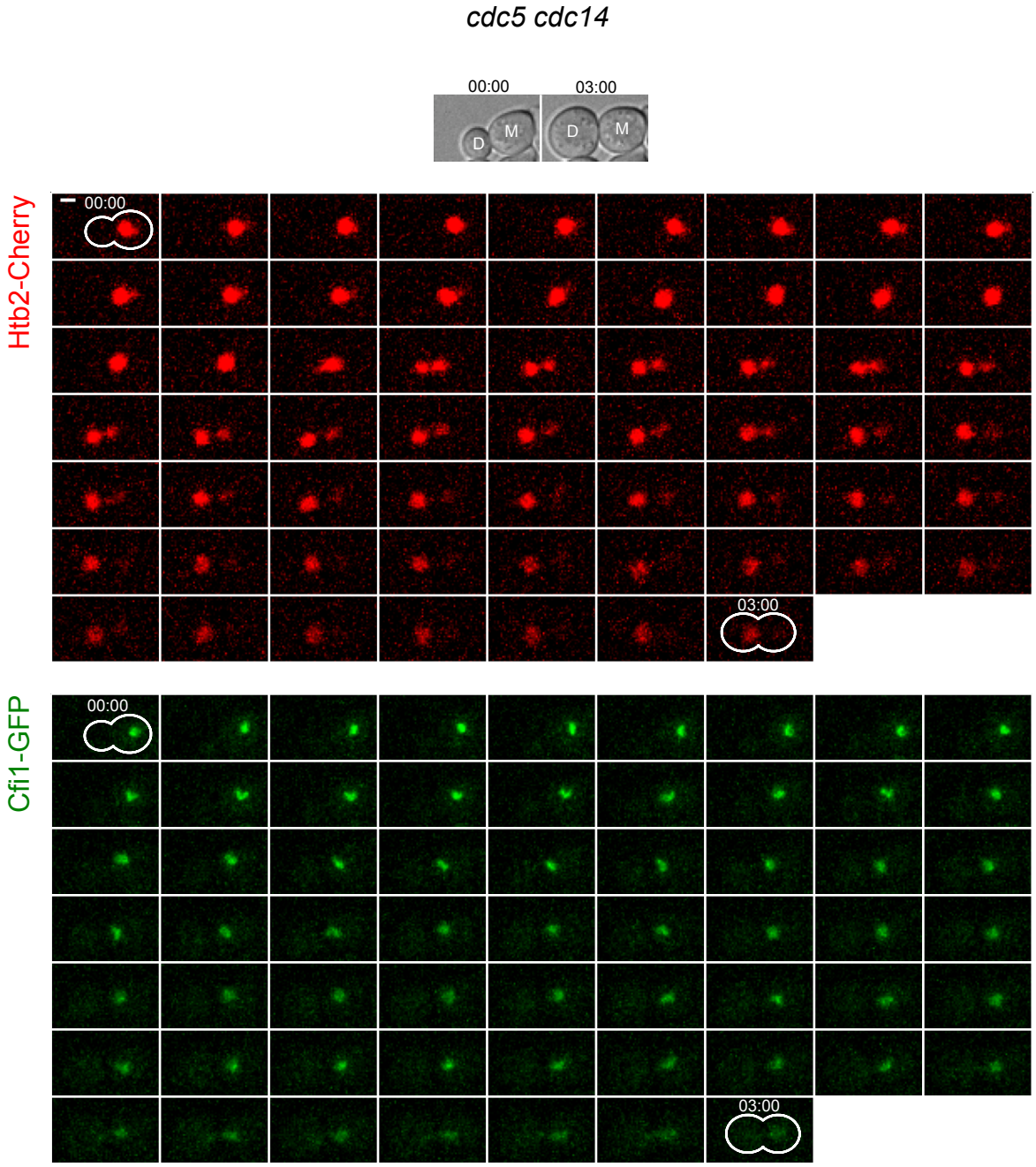

Figure 3. 6 *cdc5 cdc14* nuclei move as a whole into the daughter cells.
cdc5-as1 cdc14-1 HTB2-Cherry CFI1-GFP cells were arrested in G1 with α-factor in SCD medium at 23°C, loaded in the microfluidic plate and then released in SCD medium supplemented with CMK inhibitor at 37°C to inactivate *cdc5-as1* and *cdc14-1*, respectively. Cells were imaged starting from metaphase with a 3 min interval for 3 hours. A representative cell is shown (scale bar: 2μm). Grey: DIC; red: nucleus; green: nucleolus.

3.1.5 Searching for mutants arresting in mini-anaphase

Having established that *cdc5 cdc14* cells cannot segregate their genetic material and that they retain instead residual cohesion between chromatids at their terminal arrest raised the question as to whether the SCS defect identified in these cells is physiological for cells in mini-anaphase or a direct consequence of lacking Cdc5 and Cdc14 activities. In the first case, linkages removal would require only anaphase progression (for example, a decrease in Cdk activity or SE) and Cdc5 and Cdc14 would contribute only indirectly by promoting anaphase progression. In the second case, Cdc5 and Cdc14 would play a direct role in chromatid resolution. To discriminate between these possibilities, we searched for a control strain that would arrest in mini-anaphase independently from Cdc14 and Cdc5. To our knowledge, no other mutation or experimental condition leads to cells arresting in this cell cycle stage; yet, looking in the literature, we found a mutant that could serve our purpose. This mutant is the *cin8-3 dyn1Δ kip1Δ* triple mutant, in which the three motor proteins responsible for anaphase SE are either deleted (*dyn1Δ* and *kip1Δ*) or inactivated with a *ts* allele (*cin8-3*). This mutant was claimed to arrest in anaphase before SE from the observation that if shifted at the restrictive temperature for Cin8-3 after SPB separation (as either Cin8 or Kip1 are required for this (Roof, Meluh and Rose, 1992; Saunders and Hoyt, 1992)), these cells were able to assemble but not to elongate their spindles (Saunders *et al.*, 1995). Since the phenotype of this strain was never characterized (Saunders *et al.*, 1995) and since having a strain with an inactive spindle but active Cdc5 and Cdc14 would have been the perfect control for assessing Cdc5 and Cdc14 contribution to sister chromatid separation, we decided to characterize the terminal phenotype of *cin8-3 dyn1Δ kip1Δ* cells.

We first applied the experimental procedure described by Saunders and coworkers (Saunders *et al.*, 1995). *cin8-3 dyn1Δ kip1Δ* cells were arrested in S phase with hydroxyurea (HU) in permissive conditions, released from the arrest, and 60 min after the release shifted to 37°C (non-permissive condition for *cin8-3*). The delay between HU release and *cin8-3* inactivation is necessary to allow for SPB separation and bipolar spindle

assembly. In contrast with the literature, we found that 60 min after HU release these cells had not separated their SPBs nor assembled their spindles. We next tested several conditions in which we changed either the timing or the temperature for Cin8-3 inactivation. Unfortunately, in none of the conditions tested the spindles displayed the expected phenotype, not even when Cin8-3 was inactivated at the release from a metaphase arrest (Figure 3.7). Indeed, these cells depolymerized their spindles soon after Cin8-3 inactivation. We concluded that the *cin8-3 dyn1Δ kip1Δ* mutant did not arrest as *cdc5 cdc14* cells and could not be used as control for mini-anaphase.

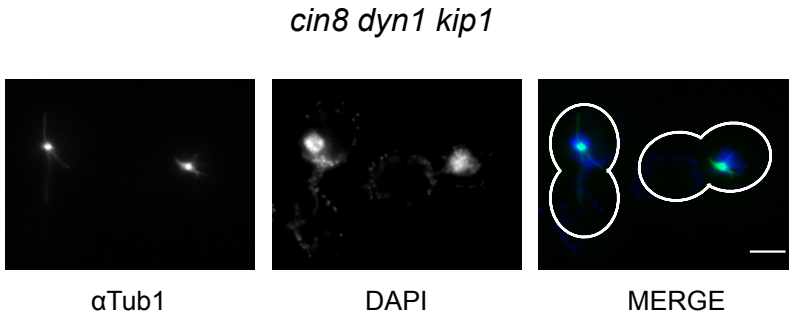

Figure 3. 7 *cin8 dyn1 kip1* cells do not arrest in mini-anaphase.
cin8-3 dyn1Δ kipΔ cdc20-AID cells were arrested in in G1 by addition of α-factor in YPD at 23°C and then synchronously released into the next cell cycle in new YPD medium supplemented with auxin to deplete Cdc20-AID and arrest cells in metaphase. At the metaphase arrest cells were released in auxin-free prewarmed YPD medium at 32°C. Representative images of cells collected 30' after metaphase release and analyzed through IF (anti-Tub1, DAPI) are shown.

3.1.4 Testing for the presence of residual cohesin complexes on chromatids

Even though we could not distinguish if the SCS defect of *cdc5 cdc14* cells is a physiological condition for mini-anaphase cells or a direct consequence of these cells lacking Cdc5 and Cdc14 activities, we considered this defect worth to be characterized nonetheless, as mini-anaphase cells have never been described. Aiming at identifying the nature of the residual cohesion causing the SCS defect, we first explored the possibility

that some cohesin complexes remain on chromatids, under the detection threshold of the techniques employed to assess their cleavage and displacement from chromatids (namely, western blotting and imaging) (Roccuzzo *et al.*, 2015). We decided to test this hypothesis by looking at specific loci on sister chromatids that are known to act differently whether they are held together by cohesin or not. To visualize chromosome loci, we took advantage of the *TetR-GFP/tetO* system in which an array of *tetO* operators is integrated in the locus of interest and is bound by the TetR repressor fused with GFP inserted into the genome, too (Michaelis, Ciosk and Nasmyth, 1997). We chose to analyze the behavior of a centromere (*CENXV*), a locus in the middle of chromosome arm (*HIS3*) and a telomere (*TELXV*), all located on the long arm of chromosome XV (Renshaw *et al.*, 2010). We choose chromosome XV because it does not carry any specialized sequence and, being one of the longest in yeast, it could exacerbate the SCS defect. In the presence of cohesin, sister chromatids are held closely together and GFP-marked sister loci are visualized as a single dot; when cohesin is lost, sisters separate originating two GFP dots (Michaelis, Ciosk and Nasmyth, 1997; Goshima and Yanagida, 2000; He, Asthana and Sorger, 2000; Tanaka *et al.*, 2000; Renshaw *et al.*, 2010). Exception to this are centromeres, where, as soon as bi-polar attachment is established, the tension exerted by the spindle manages to pull sister centromeres apart up to a distance of 1μm, despite the presence of cohesin. At this stage centromeres separate and rejoin continuously, a behavior known as "centromere breathing" that results from the counteracting forces of the spindle and the pericentromeric cohesin complexes (Goshima and Yanagida, 2000; He, Asthana and Sorger, 2000; Tanaka *et al.*, 2000). When cohesin is cleaved, centromeres stop breathing and separate farther apart. For our analyses, we compared sister loci dynamics of *cdc5 cdc14* cells with the ones of wild type cells arrested in metaphase, as spindle and nuclear morphologies are similar but cohesin is fully present only in the latter. To arrest cells in metaphase, we depleted the APC/C activating subunit Cdc20 with an auxin inducible degron (Nishimura *et al.*, 2009) (*cdc20-AID*). In the absence of Cdc20, the APC/C cannot be activated and cells remain

arrested in metaphase with uncleaved cohesin and high Cdk activity. When designing the experiment, we planned to visualize also the SPBs to monitor progression through mitosis and to use them as a reference for GFP-dots position. Unfortunately, we were unable to perform this analysis because introducing fluorescently tagged versions of SPB components in the *cdc5 cdc14* double mutant resulted in a synthetic interaction that altered the phenotype of *cdc5-as1 cdc14-1* double mutant cells. More specifically, *SPC42-eqFP cdc5-as1 cdc14-1* cells were not viable and *SPC110-mCherry cdc5-as1 cdc14-1* cells were defective in bipolar spindle formation and/or maintenance as suggested by the observation that SPBs rejoined after having separated.

cdc5-as1 cdc14-1 and *cdc20-AID* cells carrying either *CENXV-GFP*, *HIS3-GFP* or *TELXV-GFP* were arrested in G1 in the permissive conditions, released from the arrest in non-permissive conditions (37°C in presence of CMK inhibitor or auxin) and imaged for 3 hrs starting from metaphase. The distance between sister loci was measured on x, y, z in ~20 cells for each strain. In agreement with data in the literature, we observed that in metaphase-arrested wild type cells centromeres separated mostly up to 1μm (2μm in few cases) and the vast majority of the cells displayed centromere breathing (Figure 3.8A,B). In contrast, in the *cdc5 cdc14* mutant we observed that in 17 out of the 18 cells analyzed centromeres separated to greater distances (up to 4-5μm, with a mode around 2-3μm) and did not breathe (Figure 3.8A,C). This result indicated that, at least on centromeres, cohesin is completely removed. In respect to chromosome arms and telomeres, we observed that in metaphase-arrested wild type cells they did not separate, or did so very briefly, rarely and for a very short distance (Figure 3.9A,B and Figure 3.10A,B). In *cdc5 cdc14* cells instead both arms and telomeres separated in 19 out of the 20 cells analyzed and in most of them reached distances up to 3-4μm, indicating that cohesin is removed also from these regions (Figure 3.9A,C and Figure 3.10A,C). Interestingly, we noticed that in some cells arms and telomeres displayed a "breathing-like" behavior, meaning that they separated and rejoined continuously, but reaching distances much higher than 1μm. This "arm breathing"

phenomenon might be indicative of residual linkages, including cohesin, present on chromatids or just result from stochastic chromosome movements.

From this set of experiments, we concluded that: (1) the bulk of cohesin complexes has been cleaved and removed along the entire length of chromatids in *cdc5 cdc14* cells at their terminal arrest; (2) centromeres and pericentromeric regions are completely devoid of cohesin or any other type of linkage; (3) chromosome arms and telomeres likely maintain some type of linkage. As the breathing phenotype associated with cohesin observed on centromeres is determined by the spindle separating force and leads to distances up to 1μm, we favor the hypothesis that other types of linkages are responsible for the breathing-like phenomenon observed at these loci.

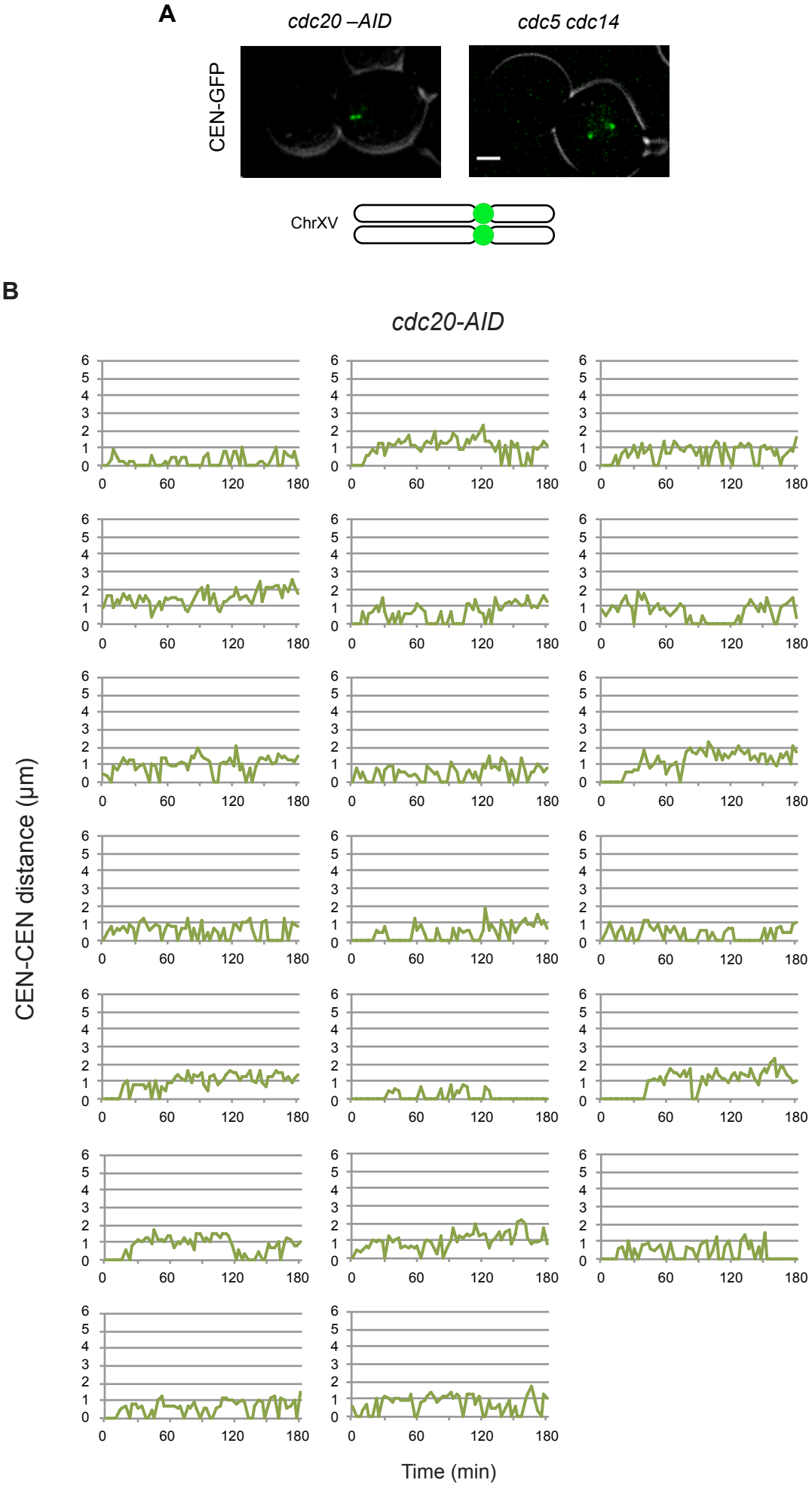
A
cdc20 –AID
cdc5 cdc14
CEN-GFP
ChrXV
B
cdc20-AID
CEN-CEN distance (μm)
Time (min)

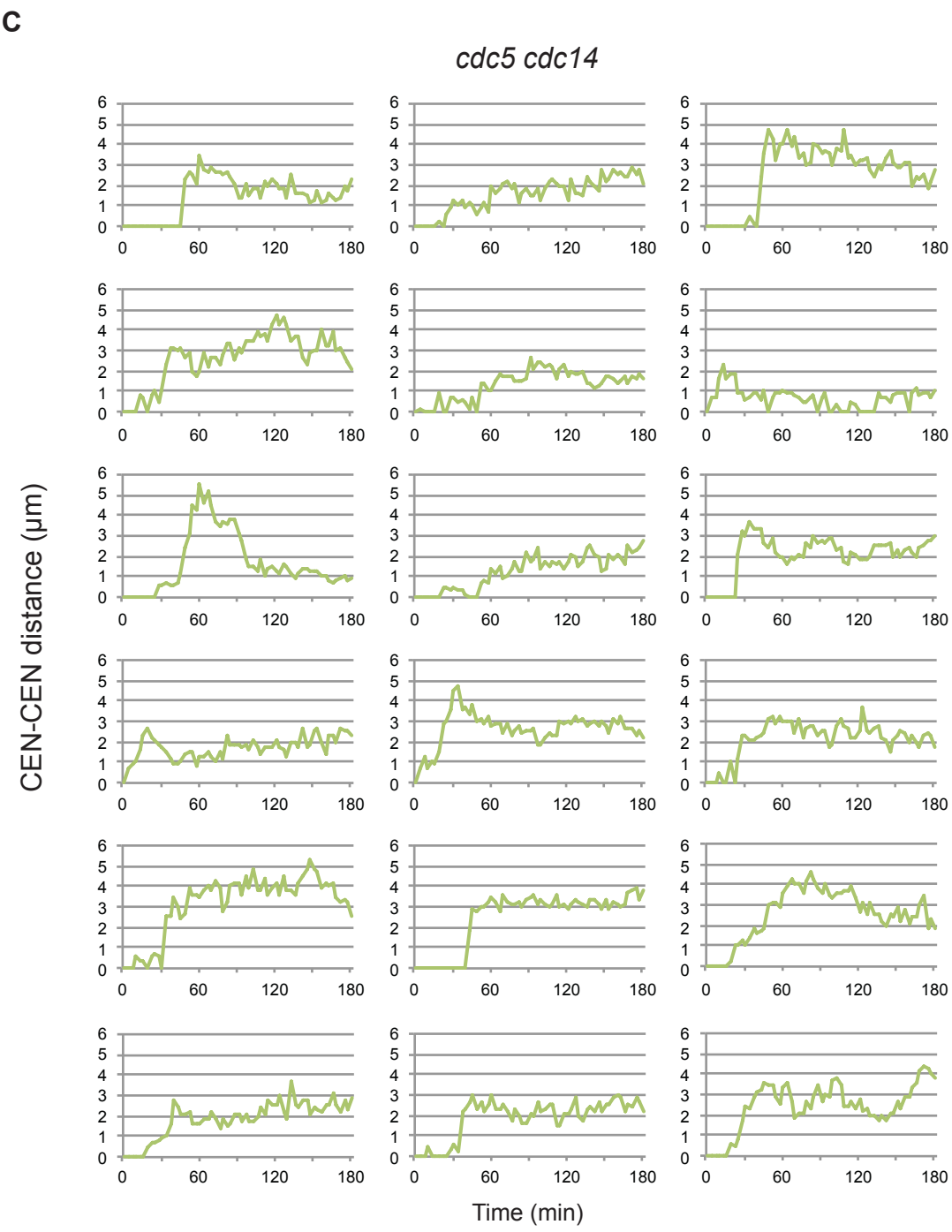

Figure 3. 8 Cohesin is lost at centromeres in *cdc5 cdc14* cells.
A. Representative *cdc20-AID* and *cdc5-as1 cdc14-1* cells carrying *CENXV-GFP* and GFP dot position on chromosome XV. **B.** *cdc20-AID CENXV-GFP* cells were arrested in G1 with α-factor in SCD medium at 23°C, loaded in the microfluidic plate and then released in SCD medium supplemented with auxin to deplete Cdc20-AID at 37°C. **C.** *cdc5-as1 cdc14-1 CENXV-GFP* cells were arrested in G1 with α-factor in SCD medium at 23°C, loaded in the microfluidic plate and then released in SCD medium supplemented with CMK inhibitor at 37°C to inactivate *cdc5-as1* and *cdc14-1*, respectively. Cells were imaged starting from metaphase with a 3 min interval for 3 hours. Distance between sister centromere GFP-dots was measured throughout the time-lapse on x,y,z.

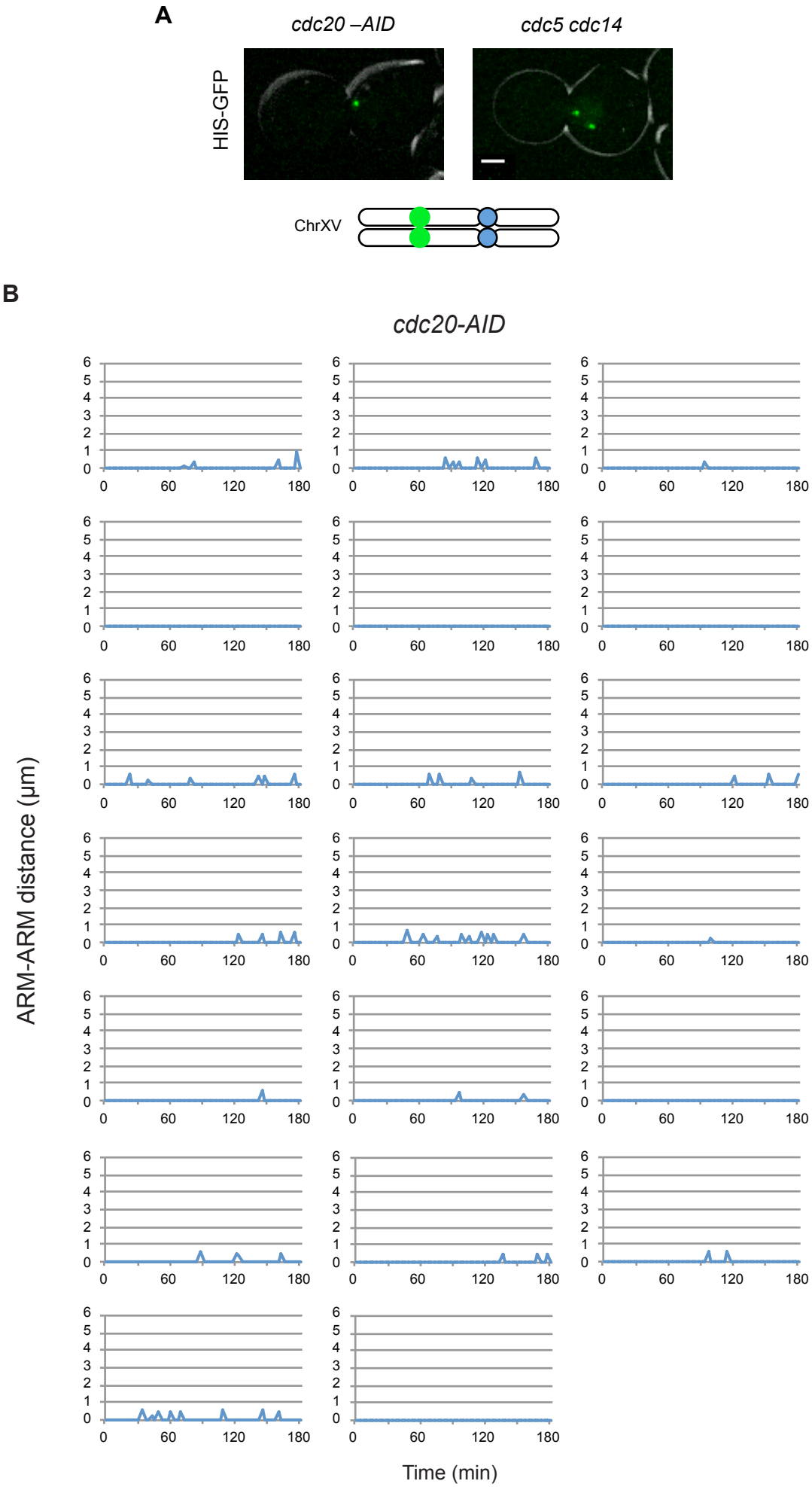
A
cdc20 –AID
cdc5 cdc14
HIS-GFP
ChrXV
B
cdc20-AID
ARM-ARM distance (µm)
Time (min)

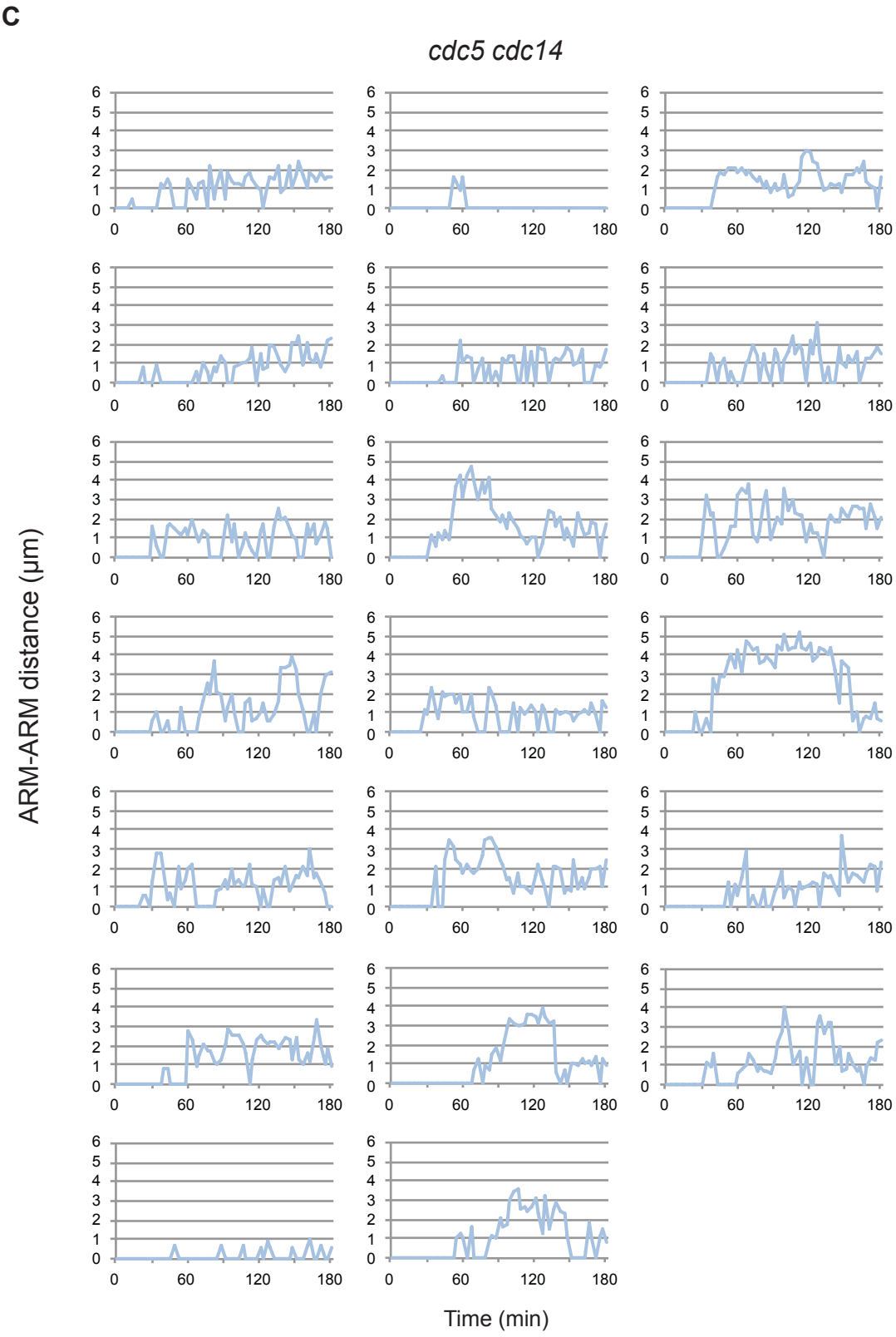

Figure 3. 9 Chromosome arm segregation in *cdc5 cdc14* cells.
A. Representative *cdc20-AID* and *cdc5-as1 cdc14-1* cells carrying *HIS3-GFP* and GFP dot position on chromosome XV. **B.** *cdc20-AID HIS3-GFP* cells were arrested in G1 with α-factor in SCD medium at 23°C, loaded in the microfluidic plate and then released in SCD medium supplemented with auxin to deplete Cdc20-AID at 37°C. **C.** *cdc5-as1 cdc14-1 HIS3-GFP* cells were arrested in G1 with α-factor in SCD medium at 23°C, loaded in the microfluidic plate and then released in SCD medium supplemented with CMK inhibitor at 37°C to inactivate cdc5-as1 and cdc14-1, respectively. Cells were imaged starting from metaphase with a 3min interval for 3 hours. Distance between sister arm GFP-dots was measured throughout the time-lapse on x,y,z.

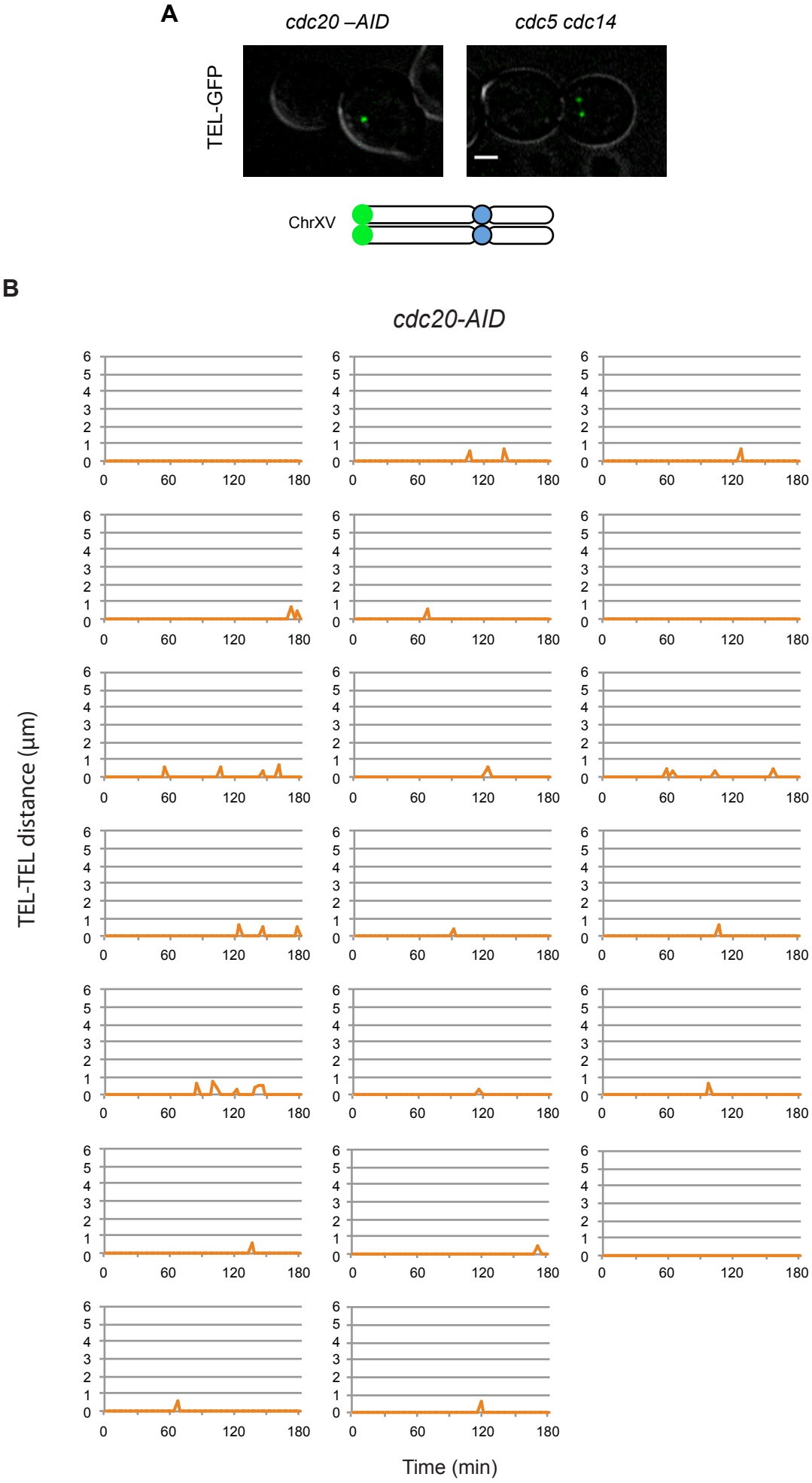
A
cdc20 –AID
cdc5 cdc14
TEL-GFP
ChrXV
B
cdc20-AID
TEL-TEL distance (µm)
Time (min)

C

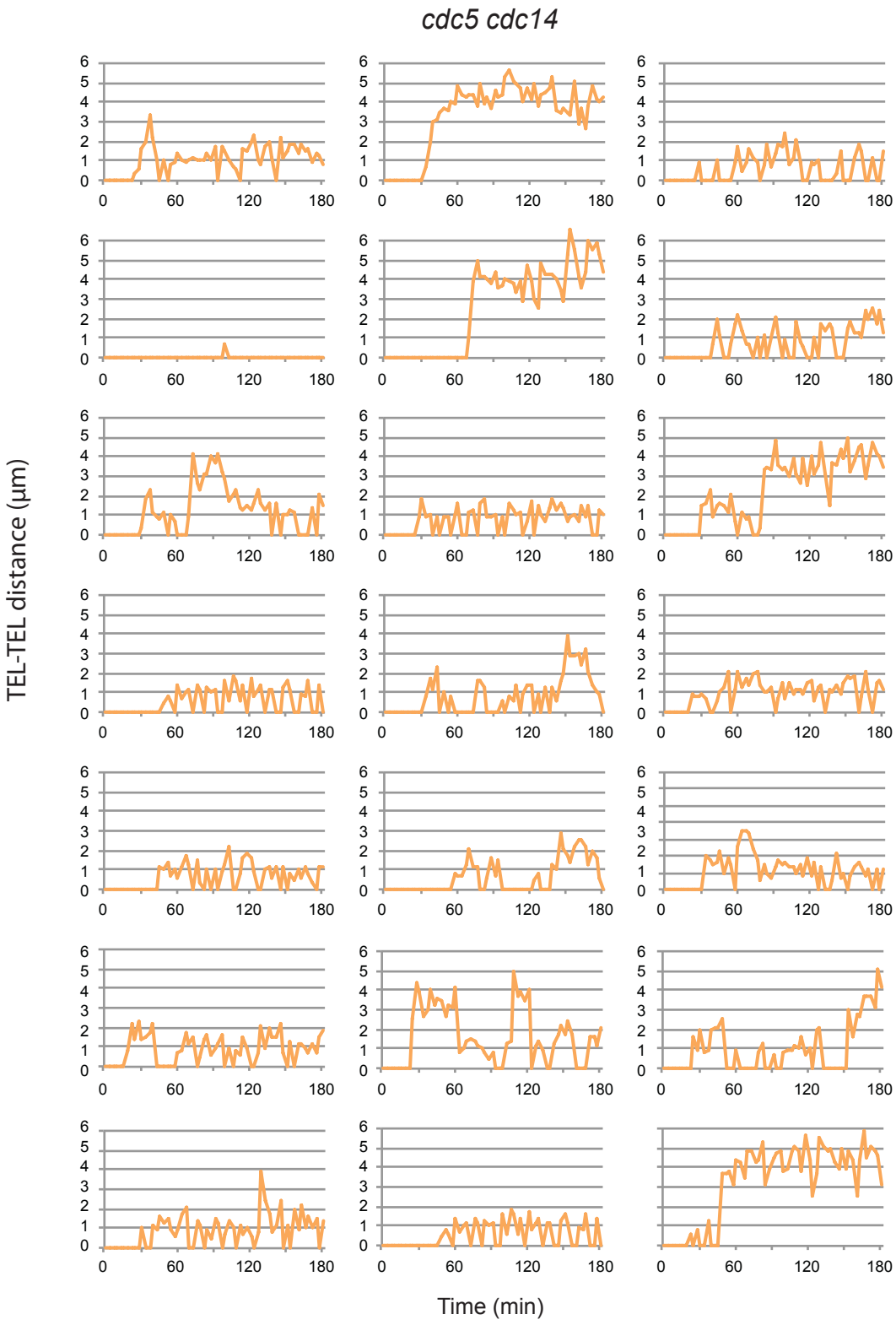

Figure 3. 10 Telomeres segregation in *cdc5 cdc14* cells.
A. Representative *cdc20-AID* and *cdc5-as1 cdc14-1* cells carrying *TELXV-GFP* and GFP dot position on chromosome XV. **B.** *cdc20-AID TELXV-GFP* cells were arrested in G1 with α-factor in SCD medium at 23°C, loaded in the microfluidic plate and then released in SCD medium supplemented with auxin to deplete Cdc20-AID at 37°C. **B.** *cdc5-as1 cdc14-1 TELXV*-GFP cells were arrested in G1 with α-factor in SCD medium at 23°C, loaded in the microfluidic plate and then released in SCD medium supplemented with CMK inhibitor at 37°C to inactivate cdc5-as1 and cdc14-1, respectively. Cells were imaged starting from metaphase with a 3min interval for 3 hours. Distance between sister telomere GFP-dots was measured throughout the time-lapse on x,y,z.

3.2 Forcing spindle elongation in *cdc5 cdc14* cells originates DNA anaphase bridges

3.2.1 DNA anaphase bridges form in *cdc5 cdc14* cells after forcing spindle elongation

Beyond cohesin, also linkages at the DNA level (named Sister Chromatid Intertwines, SCIs) can hold chromatids together. To test if the source of linkages between sister chromatids in *cdc5 cdc14* cells consisted of SCIs, we took advantage of the observation that cells that undergo anaphase with SCIs cannot fully separate their nuclei, that remain joined by DNA filaments, named DNA anaphase bridges. We reasoned that if we forced the spindle to elongate in *cdc5 cdc14* cells, then, by scoring for the presence of anaphase bridges we could obtain an indirect evidence for the presence or absence of SCIs. Knowing that combining the phospho-null, constitutively active allele *cin8-3A* (Avunie-Masala *et al.*, 2011) with the *cdc5 cdc14* double mutant rescues these cells ability to elongate their spindles (Roccuzzo *et al.*, 2015), we decided to force SE in *cdc5 cdc14* cells by overexpressing Cin8. Overexpression, differently from the *cin8-3A* allele, has the advantage of being an inducible system. To this purpose, we cloned *CIN8* under the *PGAL* promoter and integrated it into the genome without altering the endogenous *CIN8* gene. Leaving the endogenous *CIN8* unaltered was important to allow for physiological Cin8 levels and activity before *PGAL* induction. After checking the number of integrants by Southern blotting, we selected for our analysis two strains carrying either 1 or 2 copies of the construct. *cdc5-as1 cdc14-1*, *cdc5-as1 cdc14-1 PGAL-CIN8(x1)* and *cdc5-as1 cdc14-1 PGAL-CIN8(x2)* cells were grown in raffinose-containing medium, arrested in G1 in permissive conditions and synchronously released into the next cell cycle in non-permissive conditions. When cells had reached the *cdc5-as1 cdc14-1* terminal arrest (3.30 hrs after release), galactose was added to induce Cin8 overexpression.

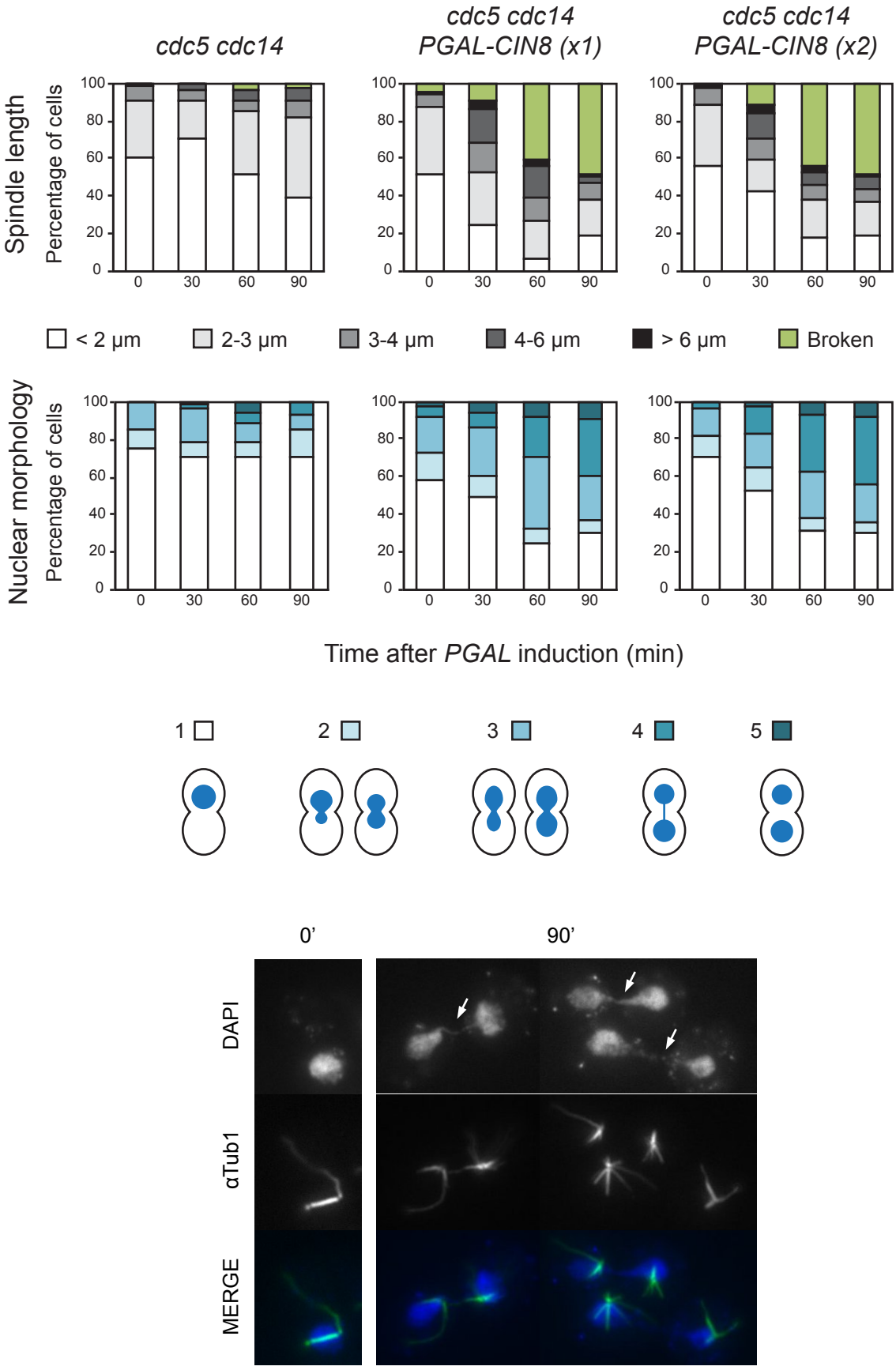

Figure 3. 11 Forcing spindle elongation in *cdc5 cdc14* cells is not sufficient to separate their nuclei.

cdc5-as1 cdc14-1, *cdc5-as1 cdc14-1 PGAL-CIN8 (x1)* and *cdc5-as1 cdc14-1 PGAL-CIN8 (x2)* cells were arrested in G1 by addition of α-factor in YPR at 23°C and then synchronously released into the next cell cycle in new, prewarmed YPR medium supplemented with the CMK inhibitor at 37°C, to inactivate *cdc5-as1* and *cdc14-1*, respectively. When cells had reached the

terminal arrest (3.30 hrs), 2% galactose was added to induce Cin8 overexpression. Samples were collected before galactose induction and 30, 60 and 90 min after and analyzed through IF (anti-Tub1, DAPI). Spindles were measured (upper graphs) and nuclear morphology was analyzed (lower graphs) (n=100). Cells were classified in the shown categories. Representative cells are shown (scale bar: 2μm)

Samples collected at 0 min, 30 min, 60 min and 90 min after induction were analyzed through IF for spindle length and nuclear morphology (anti-Tub1, DAPI) (Figure 3.11). We found that after galactose induction spindles remained unaffected in *cdc5-as1 cdc14-1* cells, but elongated and eventually broke in both *cdc5-as1 cdc14-1 PGAL-CIN8* strains. No clear difference was observed between cells carrying 1 or 2 copies of *PGAL-CIN8*. To score for anaphase bridges, cells were classified into 5 categories of nuclear morphologies as depicted in the legend of Figure 3.11. While no changes in nuclear morphology were observed in *cdc5-as1 cdc14-1* cells, in both *cdc5-as1 cdc14-1 PGAL-CIN8* strains, in parallel to spindle elongation, nuclei separated. Interestingly, even 90 min after induction only a low percentage (group 5, ~10%) of cells managed to completely separate their nuclei, while in ~60% of the cells (groups 3 and 4) the nuclei remained joined by anaphase bridges.

While this analysis clearly suggested that *cdc5 cdc14* cells retained SCIs at their terminal arrest, it carried few caveats: (1) as Cdc14 is required for nucleolar segregation, it is possible that the DNA bridges observed consisted of rDNA and did not represent a global defect in SCS; (2) as images were acquired with a single focal plane, the percentage of cells with DNA bridges might have been underestimated. To overcome these problems, we repeated our analysis in the same experimental setup, but with few improvements: (1) in addition to anti-Tub1 and DAPI, we stained our samples with an anti-Nop1 antibody to mark the nucleolus; (2) we acquired images as series of z-stacks and analyzed DAPI and anti-Nop1 signals as projections of a sum of intensities. As strains with 1 or 2 copies of *PGAL-CIN8* had the same phenotype, we analyzed only the one with 1 copy.

When scoring for anaphase bridges, we considered without bridges both cells

without DAPI staining between the two DNA masses and cells in which the DAPI signal completely overlapped with the Nop1 signal; instead, we considered with bridges both cells with only a DAPI signal between the segregated DNA masses and cells in which the DAPI and anti-Nop1 signals on the bridges did not co-localize (representative cells for each category are shown in Figure 3.12). This analysis was performed in cells collected 90 min after *PGAL-CIN8* induction and exclusively in those cells that had either elongated or broken spindles and that had started separating their nuclei (to compensate for this, we started with n~200). Hence, we did not score for bridges in *cdc5-as1 cdc14-1* control cells.

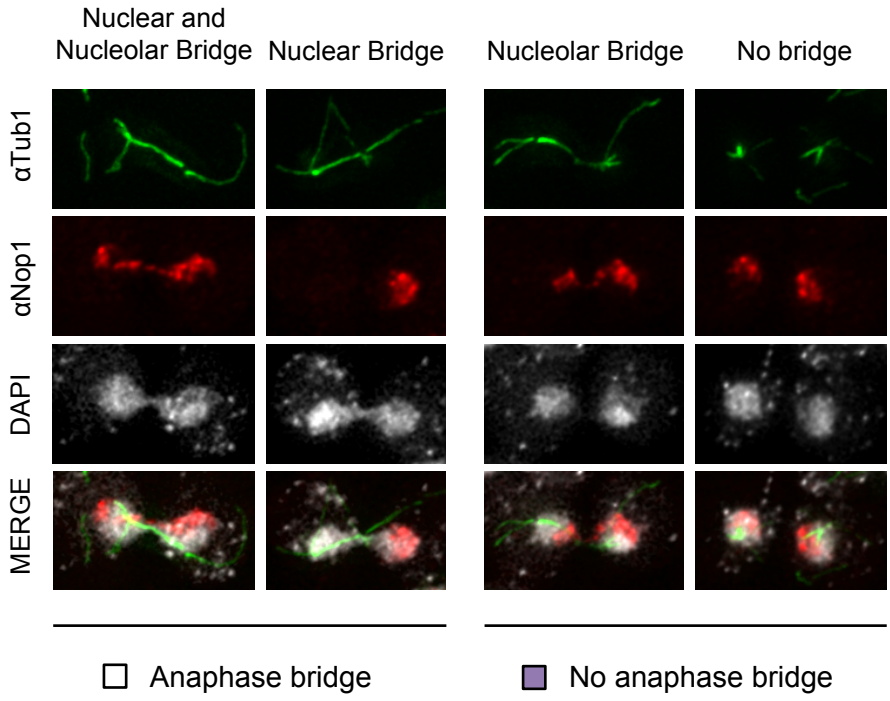

Figure 3. 12 Classification of DNA anaphase bridges.
Among those that had elongated or broken their spindle and started separating their nuclei, cells that have both nuclear and nucleolar bridges or a nuclear bridge were classified as having a DNA anaphase bridge while cells that have a nucleolar bridge or no bridge were classified as not having a DNA anaphase bridge. Representative cells from Figure 3.13 are shown.

With this analysis, we confirmed that Cin8 overexpression leads to spindle elongation and nuclei separation in *cdc5 cdc14* cells and found that forcing SE in this mutant originates anaphase bridges (Figure 3.13). Indeed, nuclear DNA bridges were present in almost 70% of the cells that had elongated their spindles and started separating

their nuclei, thus indicating that linkages, likely SCIs, are present in *cdc5 cdc14* cells at their terminal arrest. The contribution of the nucleolus in forming bridges instead was minimal as in most of the cells it remained undivided in the mother (not shown). This finding is in agreement with the knowledge that Cdc14 activity is required for nucleolar segregation and that SE is not sufficient (D'Amours, Stegmeier and Amon, 2004; Torres-Rosell *et al.*, 2004; Wang, Yong-Gonzalez and Strunnikov, 2004; Machín *et al.*, 2005).

The observation that SE is not sufficient to separate chromatids in *cdc5 cdc14* cells suggested that Cdc5 and/or Cdc14 play a direct role in this process.

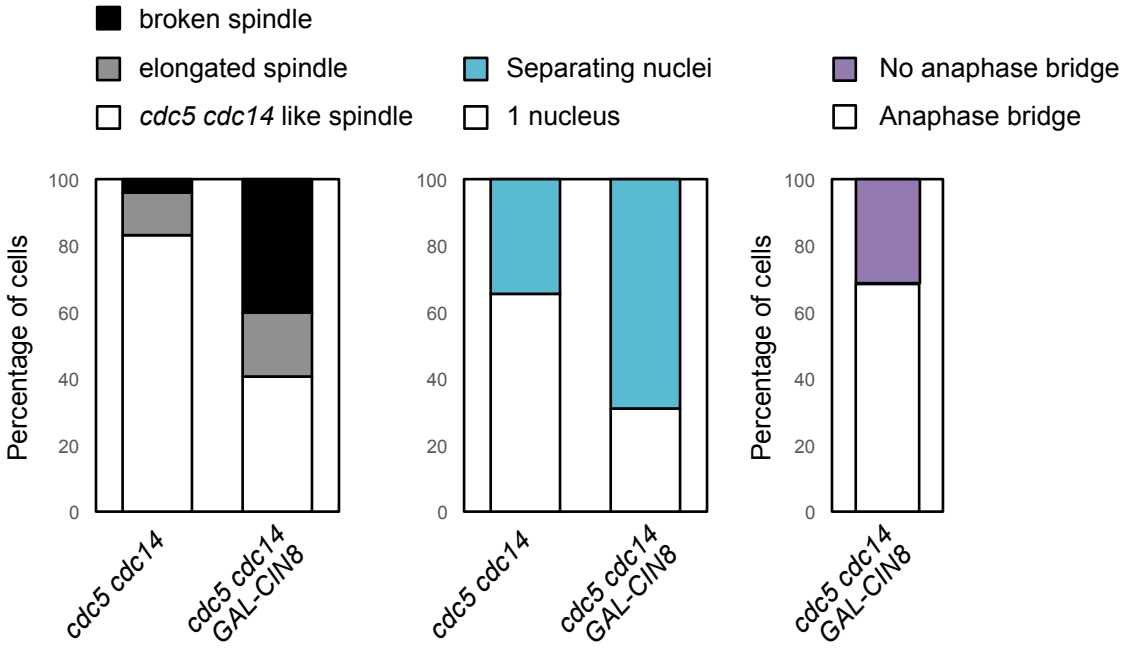

Figure 3. 13 Forcing spindle elongation in *cdc5 cdc14* cells originates DNA anaphase bridges.
cdc5-as1 cdc14-1 and *cdc5-as1 cdc14-1 PGAL-CIN8(x1)* cells were arrested in in G1 by addition of α-factor in YPR at 23°C and then synchronously released into the next cell cycle in new, prewarmed YPR medium supplemented with the CMK inhibitor at 37°C, to inactivate *cdc5-as1* and *cdc14-1*, respectively. When cells had reached the terminal arrest (3.30 hrs), 2% galactose was added to induce Cin8 overexpression. Samples were collected before (not shown) and 90 min after galactose induction and analyzed through IF (anti-Tub1, DAPI). Spindle (left graph) and nuclear (central graph) morphologies were analyzed (n~200). Among the cells with separating nuclei and elongated or broken spindle the presence of anaphase bridges was scored (right graph).

3.2.2 DNA anaphase bridge resolution requires Cdc5 and/or Cdc14

To assess whether the presence of SCIs is physiological for cells in mini-anaphase or a consequence of lacking a Cdc5 and/or Cdc14 activity required for their resolution, in the impossibility to test wild type cells arrested in mini-anaphase, we scored for the presence of anaphase bridges in wild type cells arrested in metaphase and forced to undergo SE via ectopic cohesin cleavage. Indeed, ectopically cleaving cohesin in cells arrested in metaphase was shown to be sufficient for SE and nuclei separation (Uhlmann *et al.*, 2000). We reasoned that, if in this experimental setup cells are able to fully separate their nuclei and do not retain DNA anaphase bridges, then bridges resolution specifically requires Cdc5 and/or Cdc14. To arrest cells in metaphase we depleted Cdc20 (*cdc20-AID* degron). To ectopically cleave cohesin we overexpressed the Tobacco Etch Virus (TEV) protease (Dougherty *et al.*, 1989) in cells carrying a modified allele of *SCC1* in which one of the two Esp1 cleaving sites was replaced with the TEV protease cleaving site ($scc1^{TEV268}$ allele) (Uhlmann *et al.*, 2000). *cdc20-AID PGAL-TEV* $scc1^{TEV268}$ cells were grown in raffinose-containing medium, first arrested in G1 and then released in fresh medium containing auxin to deplete Cdc20. When they reached metaphase (3 hrs after release), galactose was added to the culture to induce TEV protease expression and cohesin cleavage. Samples collected at the time of induction (not shown) and 90 min and 120 min after were analyzed through IF as described in Figure 3.13. We observed that after inducing cohesin cleavage most of the spindles elongated and then collapsed. In parallel, nuclei separated. Interestingly, 120 min after induction, when the ratio between cells with elongated and broken spindles was most similar to the one shown by *cdc5-as1 cdc14-1 PGAL-CIN8* cells (n.b. cells with mini-anaphase-like spindles were excluded from the analysis of bridges), only 37% of the cells maintained DNA bridges, in contrast to the 70% of *cdc5-as1 cdc14-1 PGAL-CIN8* cells. The observation that, in contrast to *cdc5 cdc14* arrested cells, forcing spindle elongation in metaphase-arrested wild type cells allows for the resolution of SCIs in the majority of cells, suggests that their resolution specifically

requires Cdc5 and/or Cdc14 activity.

A caveat with this comparison is that in both experiments SE was not physiological, with spindles appearing fragile and frequently collapsing. As such, it is possible that in either one or both experiments we overestimated the amount of leftover DNA bridges because a not fully functional spindle was inefficient in pulling chromatids apart.

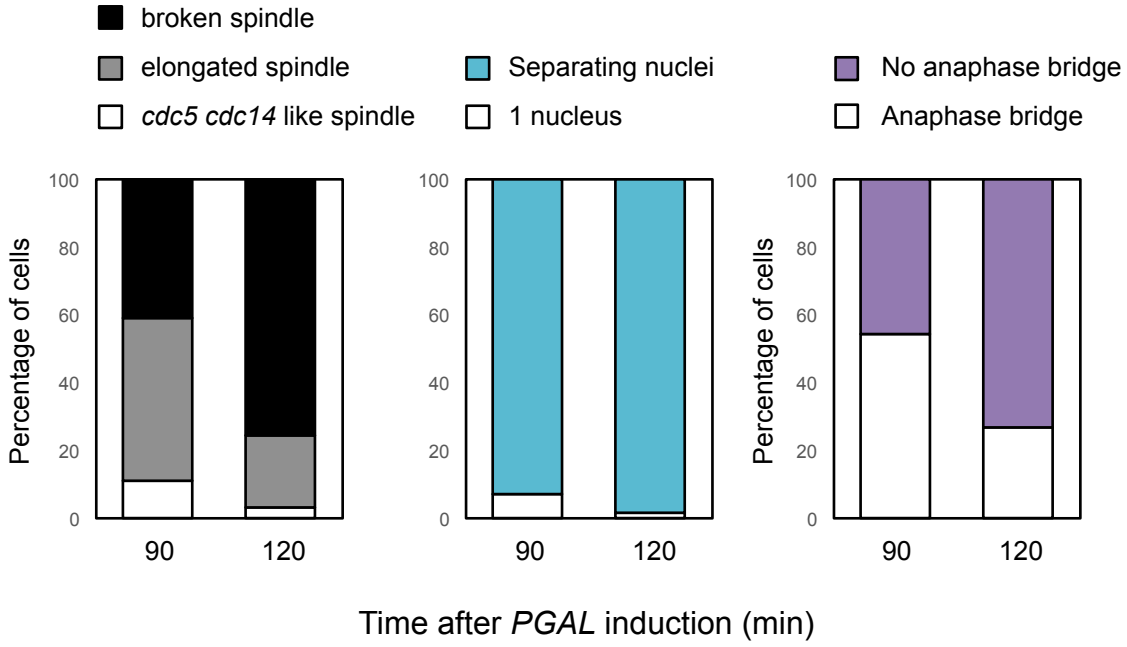

Figure 3. 14 Forcing spindle elongation in wild type cells does not originate DNA anaphase bridges.
cdc20-AID scc1^{TEV268} *PGAL-TEV* cells were arrested in in G1 by addition of α-factor in YPR at 23°C and then synchronously released into the next cell cycle in new, prewarmed YPR medium supplemented with auxin inhibitor to deplete Cdc20. When cells had reached the metaphase arrest (3 hrs), 2% galactose was added to induce TEV protease expression and Scc1^{TEV268} cleavage. Samples were collected before (not shown) and 90 and 60 min after galactose induction and analyzed through IF (anti-Tub1, DAPI). Spindle (left graph) and nuclear (central graph) morphologies were analyzed (n~200). Among the cells with separated or bilobated nuclei and elongated or broken spindle the presence of anaphase bridges was scored (right graph).

3.3 The presence of sister chromatid junctions is not responsible for the chromatid separation defect of *cdc5 cdc14* cells

Having assessed that *cdc5 cdc14* cells retained chromatid intertwines at their terminal arrest, we sought to identify the nature of these intertwines. Three types of DNA linkages have been described: sister chromatid junctions (SCJs) consisting of homologous recombination intermediates, regions of unreplicated DNA and DNA catenanes. The presence of SCJs seemed likely in *cdc5 cdc14* cells as Cdc5 and Cdc14 are required to activate two nucleases, Mus81-Mms4 and Yen1, respectively, that are active in mitosis to process SCJs that could not be dissolved earlier in S phase by the Sgs1-Top3-Rmi1 complex. Indeed, Mus81-Mms4 is activated by Cdc5 phosphorylation on the regulatory subunit Mms4 in G2/M (Matos *et al.*, 2011; Gallo-Fernández *et al.*, 2012; Schwartz *et al.*, 2012; Matos, Blanco and West, 2013; Szakal and Branzei, 2013; Princz *et al.*, 2017) and Yen1 by Cdc14 dephosphorylation in early anaphase (Blanco, Matos and West, 2014; Eissler *et al.*, 2014; García-Luis *et al.*, 2014). Also the presence of patches of unreplicated DNA seemed likely in the *cdc5 cdc14* double mutant, as they have been found in a *cdc14* single mutant (Dulev *et al.*, 2009).

To assess for the presence of SCJs, we tested whether a constitutively active allele of *YEN1* in which the 9 residues dephosphorylated by Cdc14 are mutated into the non-phosphorylatable amino acid alanine (*YEN1*^{ON}) (Blanco, Matos and West, 2014) was able to rescue the SCS defect of the *cdc5 cdc14* double mutant. Of note, it was reported that in addition to compensating for a lack of Cdc14 activation of Yen1, this allele can compensate also for a lack of Cdc5 activation of Mms4-Mus81, as it can rescue the DNA damage sensitivity of *mus81*Δ cells (Blanco, Matos and West, 2014). Interestingly, it was recently found that Yen1^{ON} is also able to resolve aberrant replication intermediates that accumulate in Dna2 helicase-defective cells (Ölmezer *et al.*, 2016). Thus, if SCJs or

intertwining between unreplicated parental DNA were the main source of the SCIs retained in the *cdc5 cdc14* double mutant, Yen1^{ON} should resolve them and *cdc5 cdc14 YEN1^{ON}* cells should display separating nuclei and slightly longer spindles than *cdc5 cdc14*. If this was the case, we expected *cdc5 cdc14 YEN1^{ON}* spindles to have a phenotype comparable to the one of *cdc5 cdc14 ndc10* cells, in which the defective spindle free of the restrain of chromatids can partially elongate. *cdc5-as1 cdc14-1* and in *cdc5-as1 cdc14-1 YEN1^{ON}* cells were synchronized in G1, released from the arrest and analyzed through IF. We found that constitutively active Yen1^{ON} had only a minor effect on both spindle length and nuclear division, thus indicating that recombination and replication intermediates are not the main source of linkages between sister chromatids in *cdc5-as1 cdc14-1* cells (Figure 3.14).

Although this result indicated that such DNA structures are not the major cause of the SCS defect of *cdc5 cdc14* cells, it did not rule out the possibility that they might contribute to it in a minor way. For this reason, we next asked whether Yen1^{ON} would decrease the percentage of cells with anaphase bridges after forcing SE. To this purpose, we scored for anaphase bridges in *cdc5-as1 cdc14-1 PGAL-CIN8* and *cdc5-as1 cdc14-1 YEN1^{ON} PGAL-CIN8* cells. Cells were grown in raffinose-containing medium, arrested in G1 and synchronously released into the next cell cycle in non-permissive conditions. When cells had reached the *cdc5-as1 cdc14-1* terminal arrest (3.30 hrs after release), galactose was added to induce Cin8 overexpression. Samples collected at induction (not shown) and 90 min after induction were analyzed through IF for spindle length, nuclear morphology and the presence of anaphase bridges (anti-Tub1, anti-Nop1, DAPI). Interestingly, we found that the presence of Yen1^{ON} allowed for a more efficient spindle elongation and for a higher percentage of cells with separating nuclei, thus suggesting that Yen1^{ON} removes linkages between sister chromatids capable of opposing resistance to spindle elongation (Figure 3.15). However, we found no difference in the occurrence of anaphase bridges between *cdc5-as1 cdc14-1 PGAL-CIN8* and *cdc5-as1 cdc14-1 YEN1^{ON} PGAL-CIN8* cells, indicating that linkages other than the ones resolved by Yen1 are the main source of SCIs

in *cdc5 cdc14* cells.

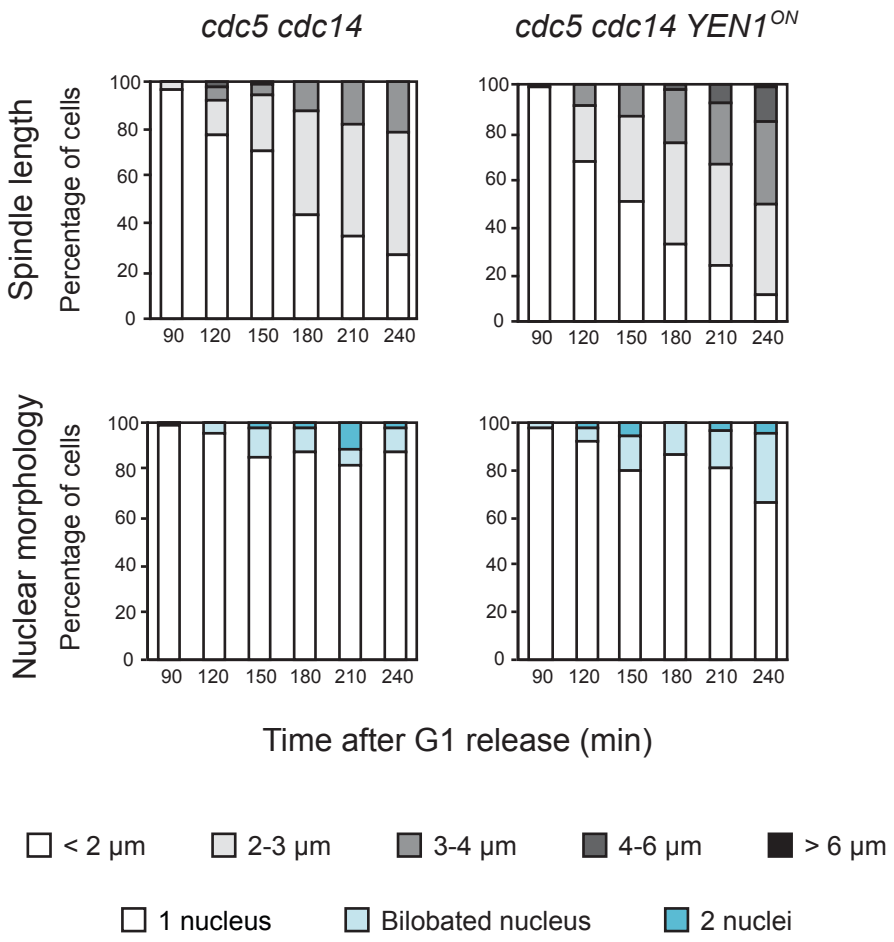

Figure 3. 15 Constitutively active Yen1 does not rescue the *cdc5 cdc14* mutant arrest.
cdc5-as1 cdc14-1 YEN1-MYC and *cdc5-as1 cdc14-1 YEN1^{ON}-MYC* cells were arrested in G1 by addition of α-factor in YPD at 23°C and then synchronously released into the next cell cycle in new, prewarmed YPD medium supplemented with the CMK inhibitor at 37°C, to inactivate *cdc5-as1* and *cdc14-1*, respectively. Samples were collected every 30 min for 240 min and analyzed through IF (anti-Tub1, DAPI). Starting from 90 min, when bipolar spindle formed, spindles were measured (left) and nuclei morphology was analyzed (right) (n=100).

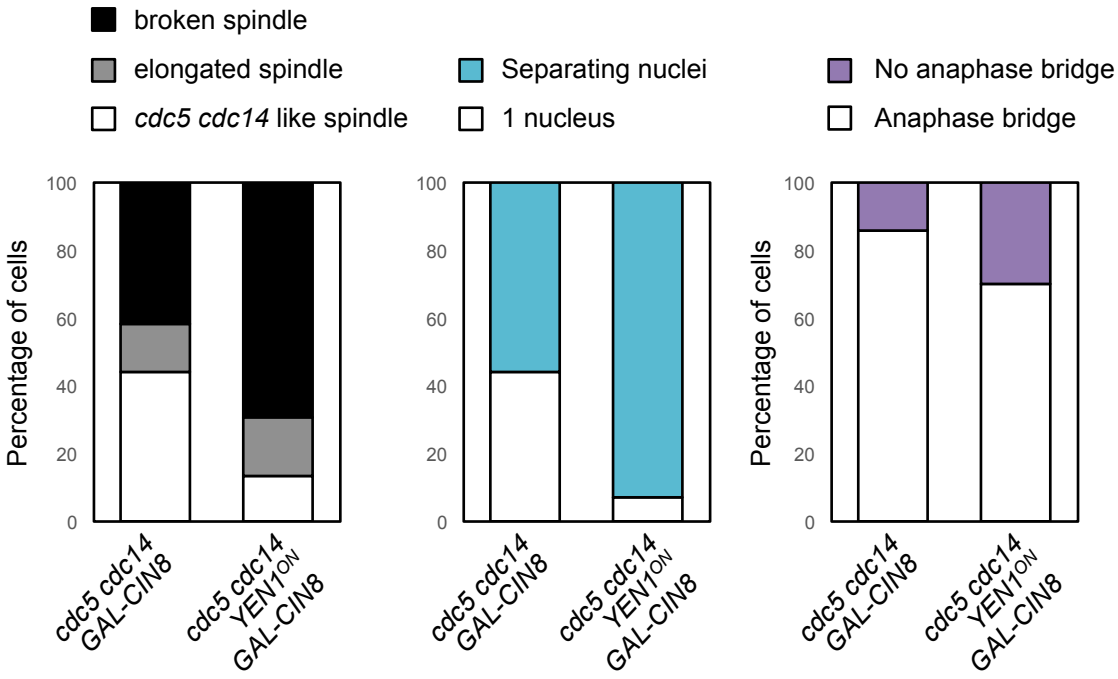

Figure 3. 16 Constitutively active Yen1 does not resolve anaphase bridges in *cdc5 cdc14* cells.

cdc5-as1 cdc14-1 PGAL-CIN8(x1) and *cdc5-as1 cdc14-1 YEN1^{ON} PGAL-CIN8(x1)* cells were arrested in G1 by addition of α-factor in YPR at 23°C and then synchronously released into the next cell cycle in new, prewarmed YPR medium supplemented with the CMK inhibitor at 37°C, to inactivate *cdc5-as1* and *cdc14-1*, respectively. When cells had reached the terminal arrest (3.30 hrs), 2% galactose was added to induce Cin8 overexpression. Samples were collected before (not shown) and 90 min after galactose induction and analyzed through IF (anti-Tub1, DAPI). Spindle (left graph) and nuclear (central graph) morphologies were analyzed (n~200). Among the cells with separated or bilobated nuclei and elongated or broken spindle the presence of anaphase bridges was scored (right graph).

3.4 The *cdc5 cdc14* double mutant is defective in DNA catenane resolution

3.4.1 Topo II overexpression rescues the *cdc5 cdc14* arrest

Forcing spindle elongation in *cdc5 cdc14* cells originates anaphase bridges that cannot be resolved by Yen1, indicating that intertwines other than Yen1 substrates are present. We thus decided to test for the presence of DNA catenanes. Catenanes are double-stranded DNA intertwines between sister chromatids that are generated by DNA replication and result from the turns of the helix of parental DNA (Sundin and Varshavsky, 1980, 1981). They are resolved by type II Topoisomerases (Top2 in *S. cerevisiae*) that are active throughout S phase to help progression of the replication fork (Bermejo *et al.*, 2007; Baxter and Diffley, 2008). Full resolution of catenanes however takes place in mitosis because it requires cohesin removal (Farcas *et al.*, 2011; Charbin, Bouchoux and Uhlmann, 2014; Sen *et al.*, 2016) and the combined actions of condensin and the mitotic spindle (Baxter *et al.*, 2011; Farcas *et al.*, 2011; Charbin, Bouchoux and Uhlmann, 2014; Leonard *et al.*, 2015; Sen *et al.*, 2016).

To test for the presence of residual catenanes, we decided to overexpress Topo II in *cdc5 cdc14* cells. We reasoned that if catenanes were the main source of linkages between sister chromatids, the overexpression of Topo II should mimic the phenotype of *cdc5 cdc14 ndc10* cells, with slightly elongated and fragile spindles but with separating nuclei. In parallel to yeast endogenous Top2, we also tested the consequences of overexpressing the smaller Topo II from the *Paramecium bursaria Chlorella* virus (cv-Topo II) (Lavrukhin *et al.*, 2000) that lacks the C-terminal regulatory domain characteristic of eukaryotic topoisomerases II. We reasoned that this enzyme could more likely overcome yeast regulation. Indeed, it was published that while overexpression of endogenous Top2 is

not able to promote nucleolar segregation in the absence of condensin, cv-Topo II is (D'Ambrosio, Kelly, *et al.*, 2008).

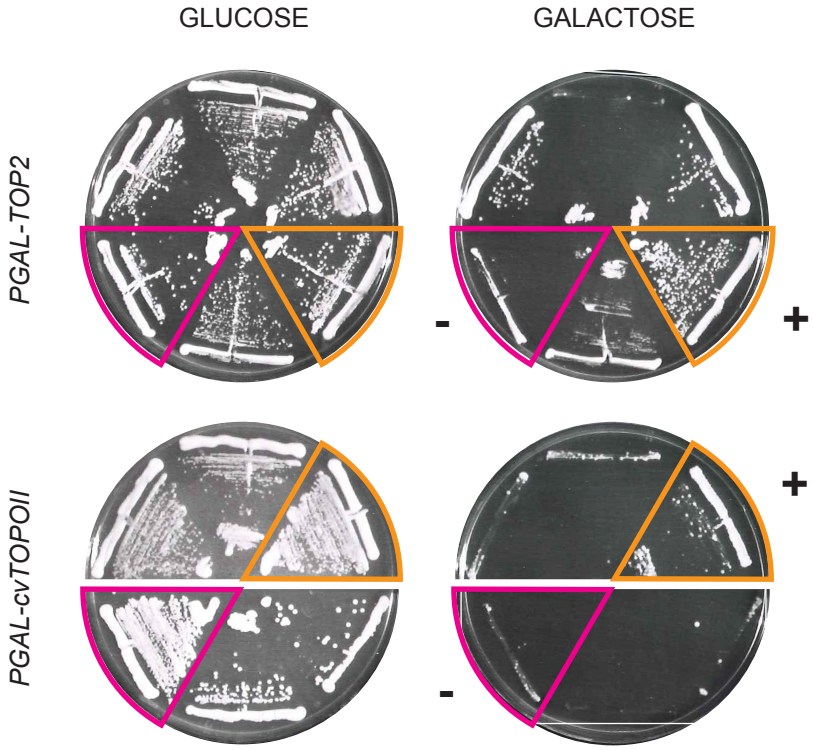

Figure 3. 17 Selection of cells transformed with *PGAL-cvTOPOII* or *PGAL-TOP2* constructs.
Colonies of wild type cells transformed with the *PGAL-cvTOPOII* (upper plates) or the *PGAL-TOP2* (lower plates) constructs were streaked on glucose containing (left) or galactose containing (right) plates. Transformants that grew on glucose and either grew (+) or not (-) on galactose were selected for subsequent experiments.

To overexpress Top2, we integrated into the genome of wild type yeasts a construct in which the *S. cerevisiae TOP2* gene was cloned under the control of the *PGAL* promoter (*PGAL-TOP2*). To overexpress cv-Topo II, we integrated into wild type yeast the *PGAL-cvTOPOII* construct created by Frank Uhlmann group (D'Ambrosio, Kelly, *et al.*, 2008). For both constructs, we streaked transformant colonies on galactose containing plates and selected a growing colony (likely carrying one/two integrants of the construct) and a non-growing one (likely carrying multiple integrants) assuming that different growth rates corresponded to different levels of protein expression. We next crossed the selected colonies with the *cdc5-as1 cdc14-1* mutant. As *cdc5-as1 cdc14-1* cells carrying likely

multiple copies of either *PGAL-scTOP2* or *PGAL-cvTOPOII* constructs were too sick and too slow-growing already in raffinose containing medium, before galactose induction, we analyzed only mutants that likely carried only 1 or 2 copies of the construct.

cdc5-as1 cdc14-1, *cdc5-as1 cdc14-1 PGAL-TOP2* and *cdc5-as1 cdc14-1 PGAL-cvTOPOII* cells were grown in raffinose containing medium, arrested in G1 in permissive conditions, and synchronously released into the following cell cycle in non-permissive conditions. When cells reached the *cdc5 cdc14* terminal arrest (3.30 hrs after release), galactose was added to induce Top2 and cv-Topo II overexpression. We found that while galactose addition had no effect on spindle length and nuclear morphology in *cdc5-as1 cdc14-1* cells, it had a striking effect in cells carrying the *PGAL-cvTOPOII* construct (Figure 3.18). Indeed, 30 min after cv-Topo-II expression approximately 60% of *cdc5-as1 cdc14-1 PGAL-cvTOPOII* cells had bilobated nuclei that became 90% by 90 min. On the contrary, the percentage of *cdc5-as1 cdc14-1* cells with bilobated nuclei remained around 20%. In parallel to nuclei separation, spindles became slightly longer, more fragile and unstable (Figure 3.18). This finding strongly suggested that *cdc5 cdc14* cells are defective in catenane resolution and that catenanes are sufficient to prevent chromatid separation and spindle elongation in these cells. However, the fact that nuclei did not separate completely indicated that cv-Topo II overexpression is sufficient to separate chromatids, but not to fully segregate them, which is consistent with *cdc5 cdc14* cells being defective also in SE.

In agreement with what was found for the rDNA region (D'Ambrosio, Kelly, *et al.*, 2008), overexpression of yeast endogenous Top2 had a minor effect than cv-Topo II. Indeed, after galactose induction *cdc5-as1 cdc14-1 PGAL-scTOP2* cells displayed only a minor increase in spindle length, while no clear effect was observed on nuclear morphology. Several reasons could account for this difference. First, it is possible that the two proteins are expressed at different levels, since we did not check the number of integrants, nor the expression levels of Top2 and cv-Topo II. Second, it is reported that cv-Topo II has a higher catalytic efficiency than eukaryotic Topo IIs (Fortune *et al.*, 2001).

Third, endogenous Top2 but not cv-Topo II might require an activating step that is not bypassed simply by its overexpression, suggesting that Top2 could be regulated by Cdc5 and/or Cdc14, directly or indirectly. Fourth, condensin might be defective in *cdc5 cdc14* cells: the observation that overexpression of cv-Topo II, but not of Top2, rescues nucleolar segregation in condensin mutants, allows to speculate that cv-Topo II might be able to promote decatenation with a lower condensin requirement.

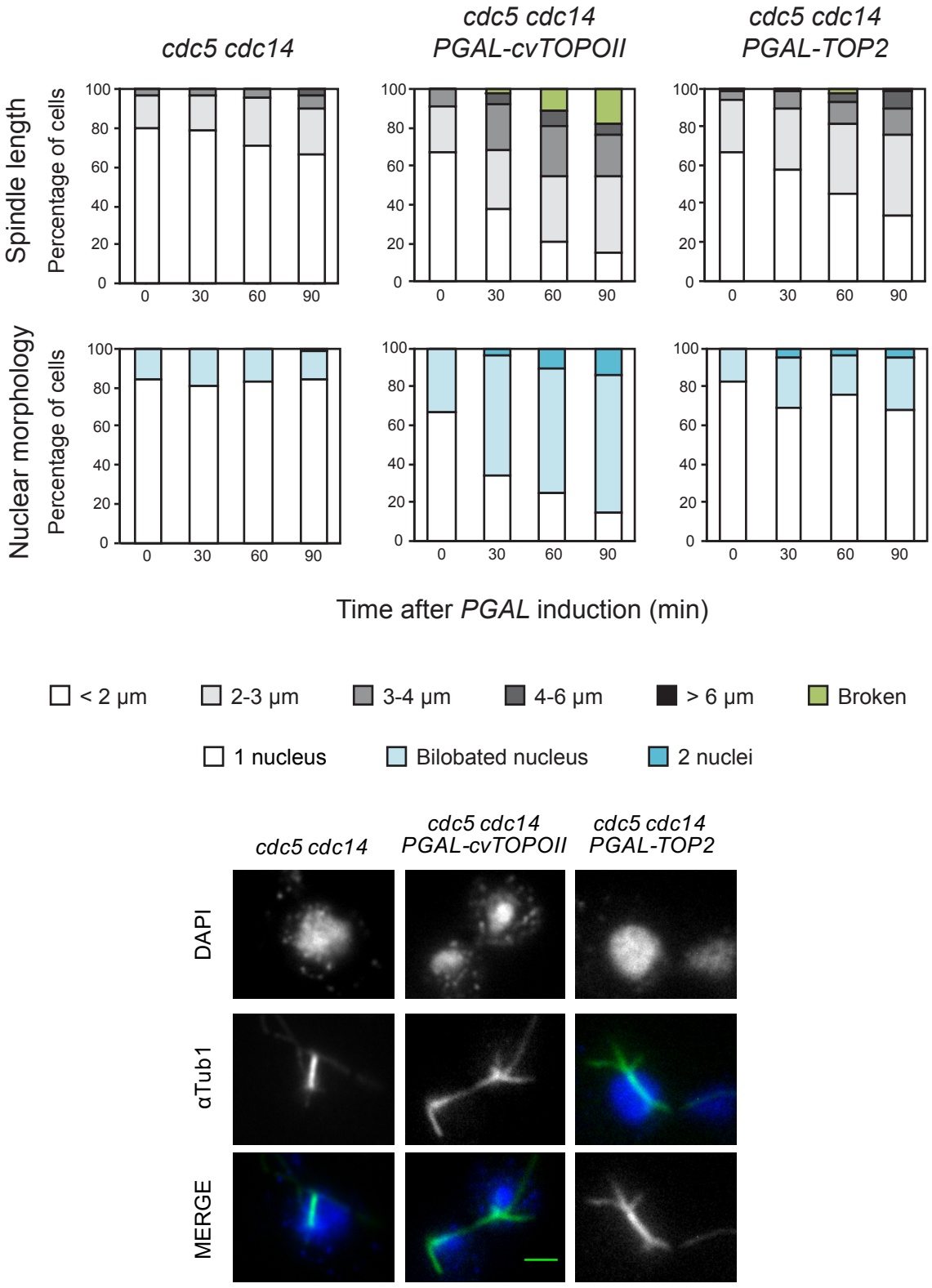

Figure 3. 18 Topo II overexpression rescues the *cdc5 cdc14* arrest
cdc5-as1 cdc14-1, *cdc5-as1 cdc14-1 PGAL-cvTOPOII* and *cdc5-as1 cdc14-1 PGAL-TOP2* cells were arrested in G1 by addition of α-factor in YPR at 23°C and then synchronously released into the next cell cycle in new, prewarmed YPR medium supplemented with the CMK inhibitor at 37°C, to inactivate *cdc5-as1* and *cdc14-1*, respectively. When cells had reached the terminal arrest (3.30 hrs), 2% galactose was added to induce Cin8 overexpression. Samples were collected before galactose induction and 30, 60 and 90 min after and analyzed through IF (anti-Tub1, DAPI). **A.** Spindles were measured (upper graphs) and nuclear morphology was analyzed (lower graphs) (n=100). **B.** Representative cells are shown (scale bar: 2µm)

3.4.2 Topo II overexpression resolves anaphase bridges in *cdc5 cdc14* cells

Our finding that cv-Topo II overexpression rescued nuclei separation and SE in *cdc5 cdc14* cells not only indicated that residual catenanes were still present at their terminal arrest, but also implied that catenanes were the main source of cohesion between sister chromatids in these cells. If this was indeed the case, then overexpression of cv-Topo II should also be able to resolve anaphase bridges originated by forcing spindle elongation. In other words, by restoring both spindle elongation and catenane resolution, the mini-anaphase arrest of the *cdc5 cdc14* mutant should be fully rescued.

To test this, we overexpressed cv-Topo II together with Cin8 in *cdc5 cdc14* cells at their terminal arrest. *cdc5-as1 cdc14-1*, *cdc5-as1 cdc14-1 PGAL-CIN8*, *cdc5-as1 cdc14-1 PGAL-cvTOPOII* and *cdc5-as1 cdc14-1 PGAL-CIN8 PGAL-cvTOPOII* cells were arrested in G1, synchronously released into the cell cycle in non-permissive conditions, and 3.30 hrs after release were added with galactose to induce both cv-Topo II and Cin8 overexpression. Samples were collected at induction (not shown) and 90 min after and analyzed through IF (anti-Tub1; anti-Nop1; DAPI) for spindle and nuclear morphology and for the presence of anaphase bridges. Consistently with our previous results, overexpression of either cv-Topo II or Cin8 or both led to nuclear division and spindle elongation or breakage (Figure 3.19). Their effect was additive at least in respect to spindle morphology. We next scored for the presence of anaphase bridges. Interestingly, while cells overexpressing only Cin8 retained anaphase bridges in approximately 80% of the cells, only 40% of the cells had bridges when also cv-Topo II was overexpressed. This result further indicated that linkages between sister chromatids in the *cdc5 cdc14* mutant mostly consisted of catenanes. However, cv-Topo II was not able to completely resolve all anaphase bridges. As our previous data suggested that also SCJs are present, we speculate that the remaining bridges likely consist of these types of SCIs.

While analyzing DNA bridges, we noticed a different phenotype in respect to the nucleolus following the overexpression of Top2 and Cin8. Indeed, nucleolar bridges were

present in ~30% of the cells after cv-Topo II overexpression, but only in 7% of cells after Cin8 overexpression. Moreover, in most of the cells the nucleolus was fully segregated after cv-Topo II overexpression, but still undivided after Cin8 overexpression. This finding is in agreement with the knowledge that the nucleolus is highly catenated and that cv-Topo II overexpression promotes its segregation (D'Ambrosio, Kelly, *et al.*, 2008). Moreover, as the highly catenated status of the nucleolus is a well-established phenotype (Sullivan *et al.*, 2004; D'Ambrosio, Kelly, *et al.*, 2008), it further supports our result that the *cdc5 cdc14* mutant is defective in mitotic catenane resolution and that SE *per se* is not sufficient to resolve catenanes in mitosis. However, as our main focus is not on this peculiar region, but aims at understanding a broader defect that involves the whole genome, we did not pursue this phenotype.

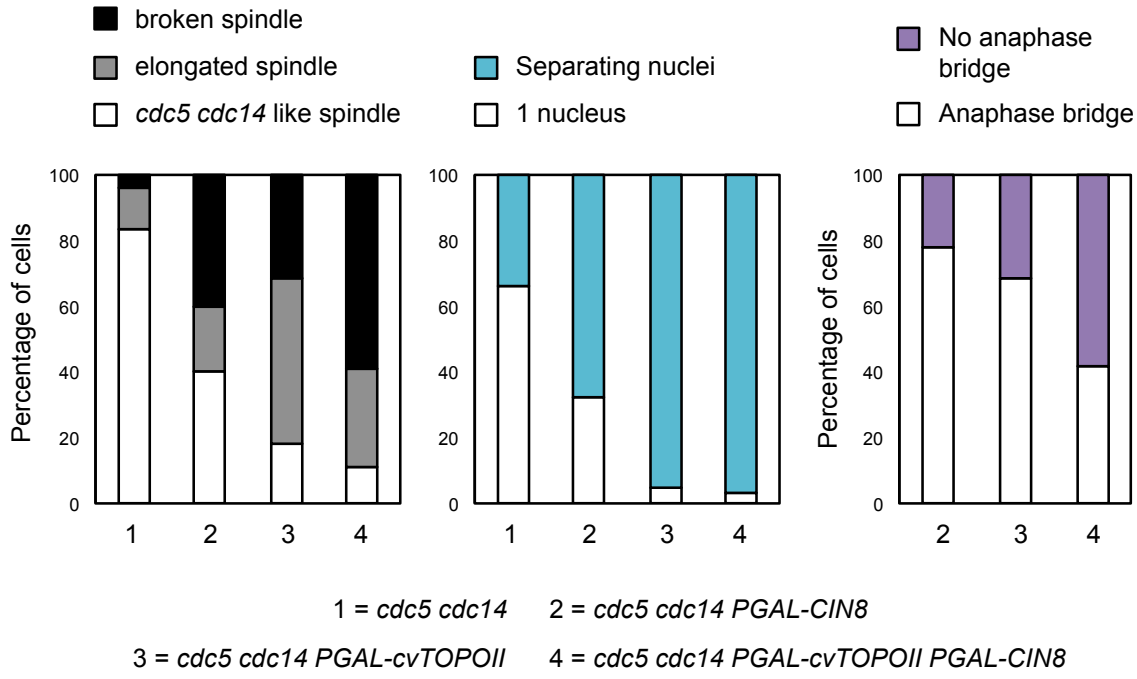

Figure 3. 19 Topo II overexpression resolves anaphase bridges in *cdc5 cdc14* cells.
cdc5-as1 cdc14-1, *cdc5-as1 cdc14-1 PGAL-CIN8(x1)*, *cdc5-as1 cdc14-1 PGAL-cvTOPOII* and *cdc5-as1 cdc14-1 PGAL-CIN8(x1) PGAL-cvTOPOII* cells were arrested in G1 by addition of α-factor in YPR at 23°C and then synchronously released into the next cell cycle in new, prewarmed YPR medium supplemented with the CMK inhibitor at 37°C, to inactivate *cdc5-as1* and *cdc14-1*, respectively. When cells had reached the terminal arrest (3.30 hrs), 2% galactose was added to induce Cin8 and Topo II overexpression. Samples were collected before (not shown) and 90 min after galactose induction and analyzed through IF (anti-Tub1, DAPI). Spindle (left graph) and nuclear (central graph) morphologies were analyzed (n~200). Among the cells with separated or bilobated nuclei and elongated or broken spindle the presence of anaphase bridges was scored (right graph).

3.4.3 Proceeding through S/M phase without cohesin ameliorates the *cdc5 cdc14* mutant phenotype.

Having found that cv-Topo II overexpression rescues nuclei separation in *cdc5 cdc14* cells, we sought to obtain additional evidence that catenanes persist in these cells causing their SCS defect. It was reported that the presence of cohesin on chromatids hinders catenane resolution (Farcas *et al.*, 2011; Charbin, Bouchoux and Uhlmann, 2014; Sen *et al.*, 2016), probably because keeping chromatids in close proximity, allows Topo II reaction to go toward catenation instead of decatenation (Sen *et al.*, 2016). Moreover, it was shown that in mutants in which cohesin was never loaded onto chromatids the accumulation of catenanes, detected as dimeric species of a circular mini-chromosome, was abolished (Farcas *et al.*, 2011; Charbin, Bouchoux and Uhlmann, 2014). Starting from these observations, we reasoned that if catenanes were indeed the main source of SCIs in the *cdc5 cdc14* double mutant, preventing cohesin loading would result in a milder SCS defect. To test for this, we employed the *mcd1-1* (Guacci, Koshland and Strunnikov, 1997) *ts* allele of Scc1 and inserted it in *cdc5-as1 cdc14-1* cells. To avoid cells from being delayed at the metaphase to anaphase transition because of spindle assembly checkpoint (SAC) activation (Stegmeier, Visintin and Amon, 2002), we also inactivated the SAC by deletion of *MAD1*. *cdc5-as1 cdc14-1*, *cdc5-as1 cdc14-1 mad1Δ* and *cdc5-as1 cdc14-1 mad1Δ mcd1-1* cells were arrested in G1 and released at 37°C to inactivate cohesin. We found that, while deleting *MAD1* alone in *cdc5 cdc14* cells had almost no effect on spindle length and nuclear morphology, when both SAC and cohesin were inactivated cells arrested with slightly longer spindles and a slightly higher percentage of bilobated nuclei (Figure 3.20). This result suggested that removing cohesin before metaphase allowed a more efficient pre-anaphase catenane resolution and implied that catenanes were present in *cdc5 cdc14* cells, counteracting both SE and nuclear segregation.

Of note, ectopically cleaving cohesin at the terminal arrest does not alter the *cdc5 cdc14* phenotype (Roccuzzo *et al.*, 2015), indicating that the differences noted in *cdc5*

cdc14 mad1 mcd1 cells are a consequence of a pre-anaphase effect caused by absence of cohesin.

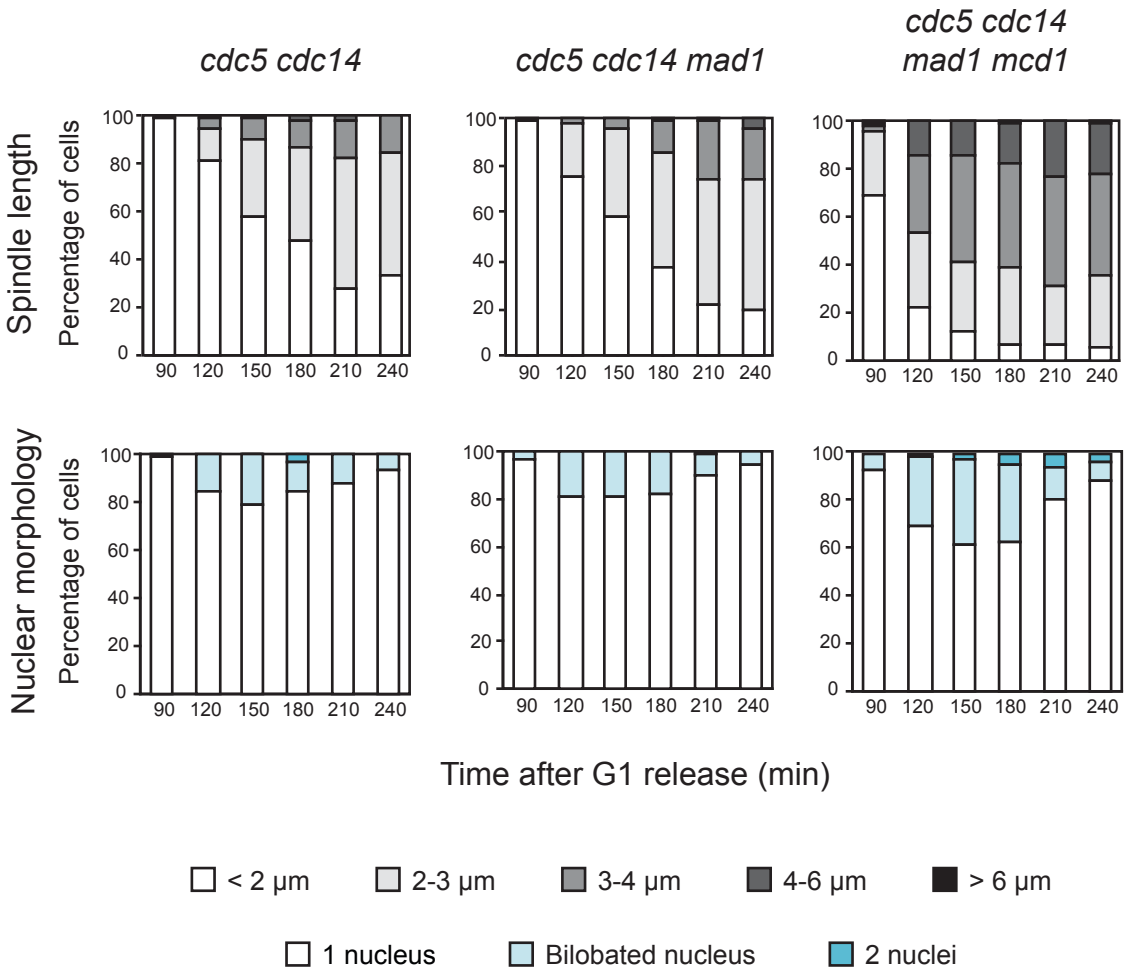

Figure 3. 20 Preventing cohesin loading ameliorates the *cdc5 cdc14* terminal arrest.
cdc5-as1 cdc14-1, *cdc5-as1 cdc14-1 mad1Δ* and *cdc5-as1 cdc14-1 mad1Δ mcd1-1* cells were arrested in G1 by addition of α-factor in YPD at 23°C and then synchronously released into the next cell cycle in new, prewarmed YPD medium supplemented with the CMK inhibitor at 37°C, to inactivate *cdc5-as1*, *cdc14-1* and *mcd1-1*. Samples were collected every 30 min for 240 min and analyzed through IF (anti-Tub1, DAPI). Starting from 90 min, when bipolar spindle formed, spindles were measured (left) and nuclei morphology was analyzed (right) (n=100).

3.4.4 DNA catenanes persist in mitosis in *cdc5 cdc14* cells

Although our finding that cv-Topo II overexpression rescues chromatid separation in *cdc5 cdc14* cells is a strong indication that these cells retain catenanes, it remained an indirect result. Therefore, we next moved on finding evidence for this defect through a more direct approach. The commonly used approaches to detect catenanes rely on the use of plasmids and techniques to separate their different topological isoforms (Baxter and Diffley, 2008;

Baxter *et al.*, 2011; Farcas *et al.*, 2011; Charbin, Bouchoux and Uhlmann, 2014; Leonard *et al.*, 2015; Sen *et al.*, 2016). Indeed, visualizing catenanes on chromatids is challenged by the fact that, being linear DNA molecules, they are able to disentangle from each other during the DNA isolation and separation steps, while plasmids, being circular, maintain their topology. When separated on native agarose gels, plasmids originate different bands whether they are monomeric or dimeric and whether they are supercoiled or relaxed. The use of plasmids is legitimized by the fact that large genomes are organized in domains with fixed ends that thereby behave like circular DNA. We chose to analyze a circular mini-chromosome rather than a small plasmid to be closer to "real" chromosomes; in particular we chose the previously described 21.2 Kbp mini-chromosome pS14-8 (Charbin, Bouchoux and Uhlmann, 2014) that is a good compromise between size and experimental feasibility. Moreover, this mini-chromosome was created with yeast endogenous sequences (fragments of yeast chromosomes XII and IV) and contains yeast centromere, replication origin and expressed genes (Charbin, Bouchoux and Uhlmann, 2014). Another advantage of using this mini-chromosome is that the band pattern originated by its different topological isoforms when run on native gel electrophoresis has been already fully characterized (Charbin, Bouchoux and Uhlmann, 2014).

We aimed at understanding whether the bands corresponding to the dimeric (i.e. catenated) mini-chromosome persisted in *cdc5 cdc14* cells at their terminal arrest. First, we performed a pilot experiment on wild type cells containing or not the pS14-8 mini-chromosome to test if we were able to reproduce the published electrophoretic pattern (Charbin, Bouchoux and Uhlmann, 2014) and to choose a suitable probe to detect it with Southern blotting. To enrich for the presence of the less abundant topological isoforms, we collected cells that were arrested in S phase by treatment with HU. We extracted DNA and ran it on gel electrophoresis with the protocol developed by Charbin and coworkers. To detect pS14-8, we designed probes recognizing the AmpR gene, that is present in the plasmid but not in wild type yeast strains. We prepared three different probes: AmpR-2 of

545bp, AmpR-3 of 527bp and AmpR-1 of 836bp. All three probes were specific for pS14-8 (no bands were detected on samples lacking the plasmid) and all three produced the same bands pattern (Figure 3.21).

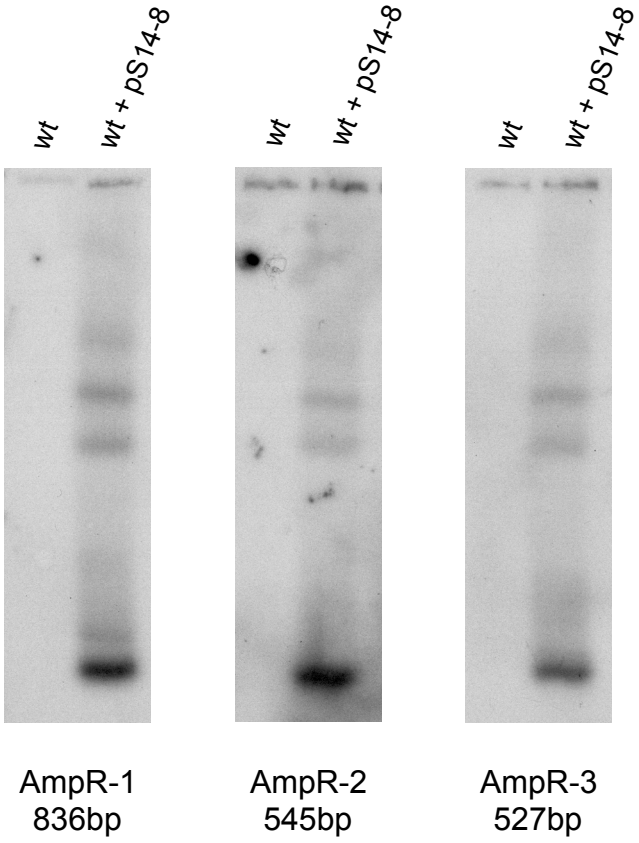

Figure 3. 21 Comparison of different AmpR probes.
Wild type cells and wild type cells carrying the pS14-8 mini-chromosome were grown in YPD and arrested in S phase with HU. DNA was extracted, run on gel electrophoresis, and hybridized with three different probes against the AmpR gene.

The only difference among them was the presence of an additional band with probe AmpR-1 and for this reason we discarded this probe. Among probe AmpR-2 and AmpR-3, we chose probe AmpR-3. Compared to published results (Charbin, Bouchoux and Uhlmann, 2014), in our blot two bands were missing. This could have depended on the fact that in our experiment cells were arrested in S phase by treatment with HU, while authors analyzed cells passing through S phase after a G1 release. To understand if this was indeed the case, rather than a technical issue, we next analyzed the electrophoretic pattern originated by the pS14-8 mini-chromosome visualized with probe AmpR-3, extracted from

wild type cells proceeding through the cell cycle after G1 release. Cell cycle progression was monitored through FACS analysis of DNA content and IF analysis of spindle and nuclear morphology (Figure 3.22). As this preliminary experiment aimed also at setting up the conditions for the analysis of *cdc5 cdc14* cells, cells were released from the G1 arrest at 37°C. We found that while at the beginning of the time course only the bands corresponding to monomeric species were present, all the other bands appeared during S phase, fully reproducing the pattern published by Charbin and coworkers and thereby validating our probe (Figure 3.22). As wild type cells grown at 37°C quickly entered a new cell cycle, in this experiment we were not able to observe dimeric species disappearing in mitosis. Despite several attempts, we never managed to fully re-arrest wild type cells in the next G1 and, since even a low percentage of cells in S phase resulted in the presence of dimeric mini-chromosome species, we decided to search for a negative control other than wild type cells.

Having validated the technique, we probed for the presence of catenanes in *cdc5 cdc14* double mutant cells throughout an entire cell cycle with the purpose of understanding whether the bands corresponding to catenated forms of the mini-chromosome persist in mitosis. Being unable to employ wild type cells as negative control, we chose the *cdc15* mutant that arrests in mitosis after complete chromosome segregation (Jaspersen *et al.*, 1998). As our previous experiments suggested that the presence of intertwines between sister chromatids in the *cdc5 cdc14* mutant directly depends on a lack of activity of either Cdc5 or Cdc14, we also analyzed *cdc5* and *cdc14* single mutants to assess for their individual contribution to the process. Since these experiments are quite laborious, we split the experiment in two: first we analyzed *cdc5-as1 cdc14-1* and *cdc5-as1* cells, then *cdc14-1* and *cdc15-2* cells. To avoid plasmid loss, cells were grown in a poor medium lacking leucine (for which pS14-8 carries the auxotrophic marker) and shifted to YPD for the G1 synchronization. Cells were then released from the arrest in YPD in non-permissive conditions. Cell cycle progression was monitored through DNA

content and spindle and nuclear morphology.

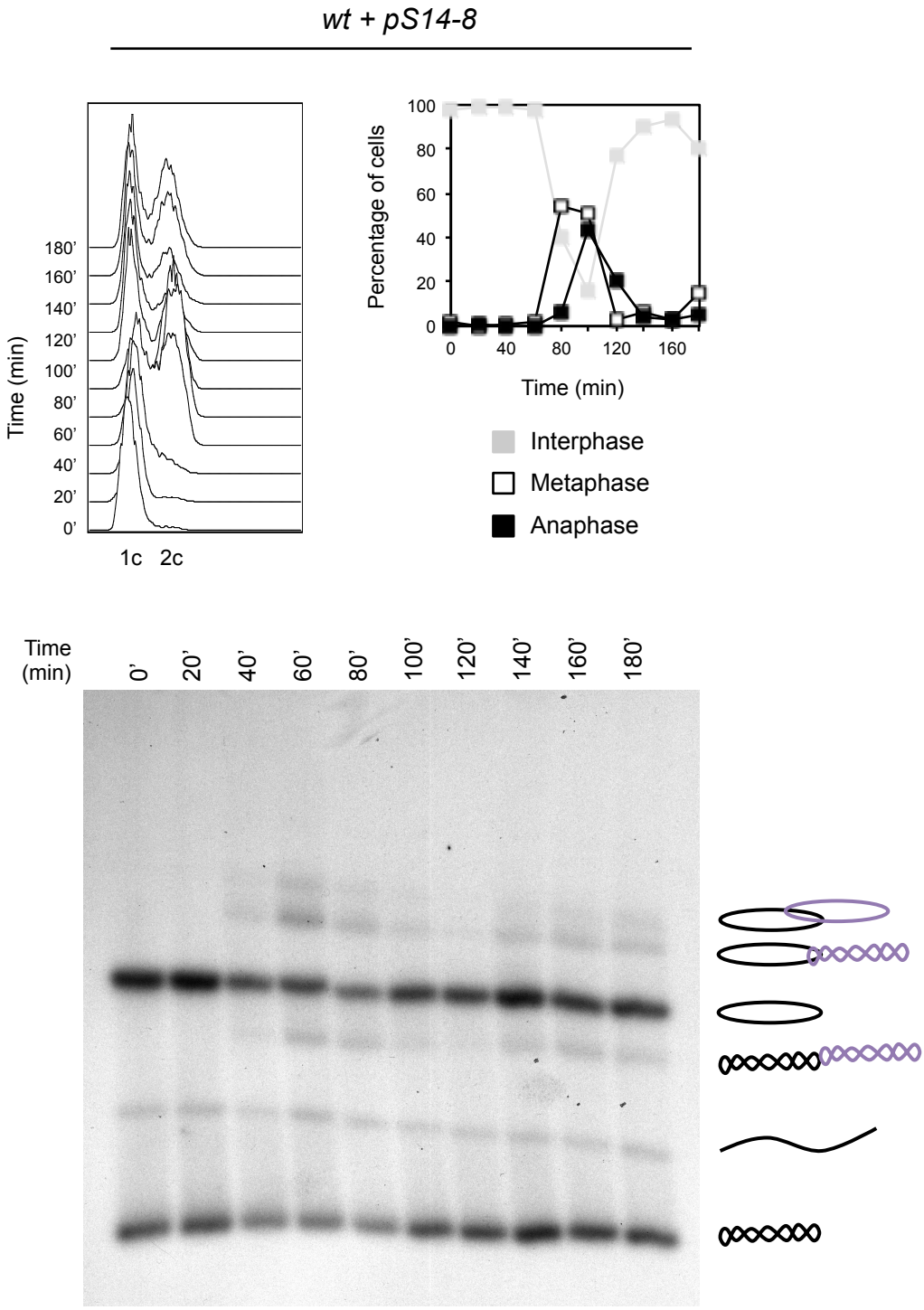

Figure 3. 22 Monitoring catenanes throughout the cell cycle
Wild type cells carrying the pS14-8 mini-chromosome were arrested in G1 by addition of α-factor in YPD at 23°C and then synchronously released into the next cell cycle in new, prewarmed YPD medium at 37°C. Samples were collected every 20 min for 3 hrs. Cell cycle progression was monitored by FACS analysis of DNA content to differentiate between G1, S and G2/M phases (left) and by IF (anti-Tub1, DAPI) to differentiate between interphase, metaphase and anaphase (right). pS14-8 forms were analyzed through gel electrophoresis and Southern blotting (probe AmpR-3; bottom). Plasmid isoforms, as identified by Charbin et al. 2014, are represented beside the corresponding bands.

We immediately noticed that *cdc5 cdc14* and *cdc5* cells entered faster into the cell cycle, as evidenced by the appearance of the 2C DNA peak on FACS analysis, if compared to *cdc14* and *cdc15* cells (Figure 3.23). As previous analyses did not detect such a difference (Roccuzzo *et al.*, 2015), we believe that this likely depended on the fact that these strains were analyzed separately, rather than being indicative of a real difference between the mutants. All strains arrested in mitosis with a 2C DNA content, with *cdc5 cdc14* cells in meta/mini-anaphase and the others in anaphase (Figure 3.23). We next probed for the presence of the catenated forms of the pS14-8 plasmid. In all strains they appeared at the beginning of S phase (at 20 min in *cdc5 cdc14* and *cdc5* cells, at 40 min in *cdc14* and *cdc15* cells) and decreased at mitotic entry. Interestingly, while these bands completely disappeared by the end of the time-course in *cdc15* cells, they still remained in the *cdc5 cdc14* double mutant at its terminal arrest, though at low levels (Figure 3.23A,B). As dimeric plasmids accumulation and initial decrease were not affected, we concluded that their persistence in mitosis was indicative of a mitosis-specific defect in catenane resolution.

In the *cdc14* single mutant, like in the *cdc15* mutant, bands corresponding to catenated plasmids completely disappeared at the terminal arrest. Instead, they persisted in the *cdc5* single mutant (Figure 3.23C,D). Though the difference is subtle, they seemed to be at a lower level than in the *cdc5 cdc14* double mutant. This result suggested that, between Cdc5 and Cdc14, Cdc5 promotes catenane resolution, while Cdc14 does not. However, as the *cdc5 cdc14* double mutant had a stronger phenotype than the *cdc5* single mutant, it is possible that Cdc14 has a minor function additive to Cdc5 in catenane resolution, detectable only if also Cdc5 is inactive.

Altogether, independently on whether Cdc5 and/or Cdc14 have a direct or indirect contribution, this experiment provides evidence that *cdc5 cdc14* cells are defective in catenane resolution.

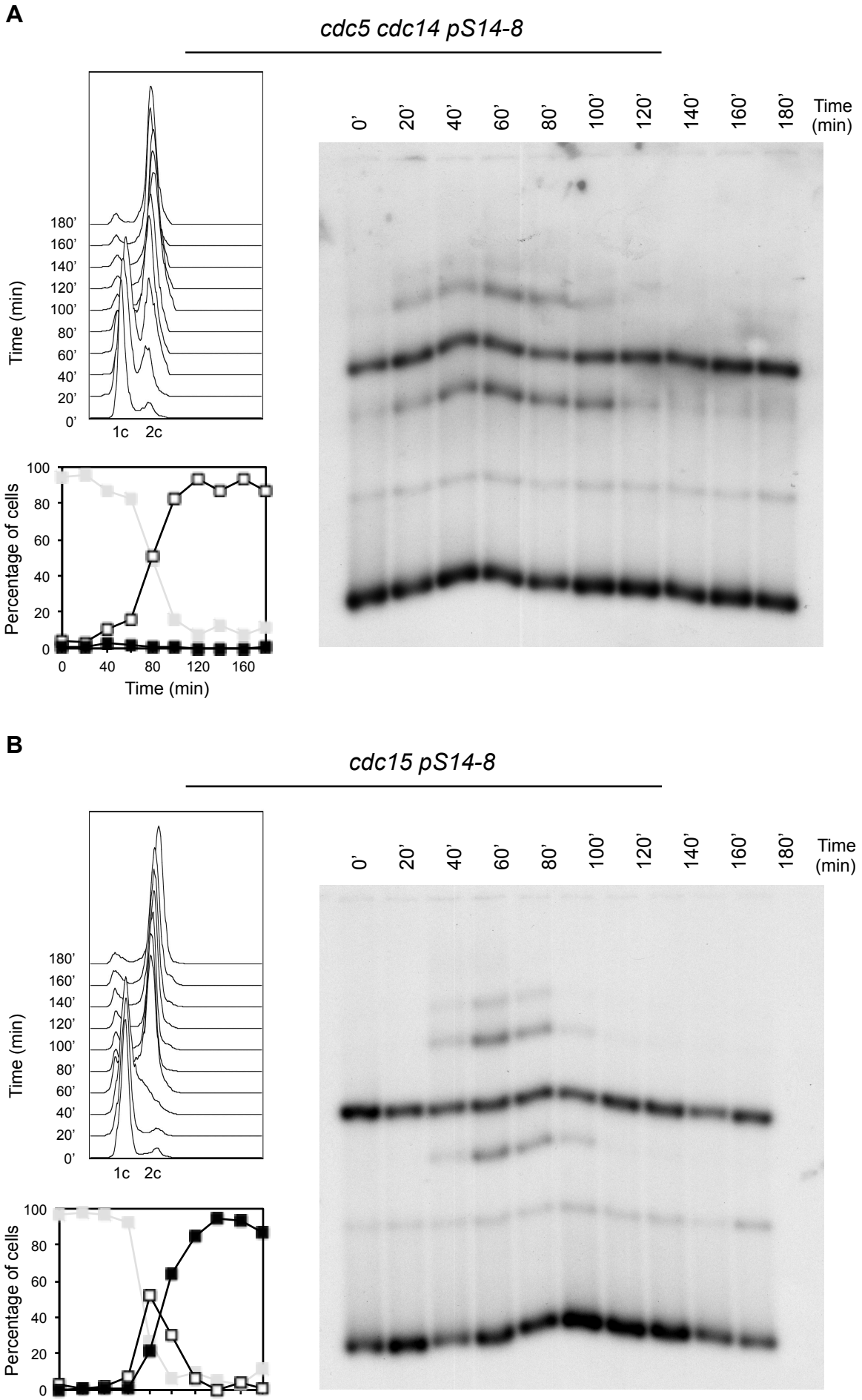
A
cdc5 cdc14 pS14-8
Time (min)
180'
160'
140'
120'
100'
80'
60'
40'
20'
0'
1c
2c
Percentage of cells
100
80
60
40
20
0
0
40
80
120
160
Time (min)
0'
20'
40'
60'
80'
100'
120'
140'
160'
180'
Time (min)
B
cdc15 pS14-8
Time (min)
180'
160'
140'
120'
100'
80'
60'
40'
20'
0'
1c
2c
Percentage of cells
100
80
60
40
20
0
0
40
80
120
160
Time (min)
0'
20'
40'
60'
80'
100'
120'
140'
160'
180'
Time (min)

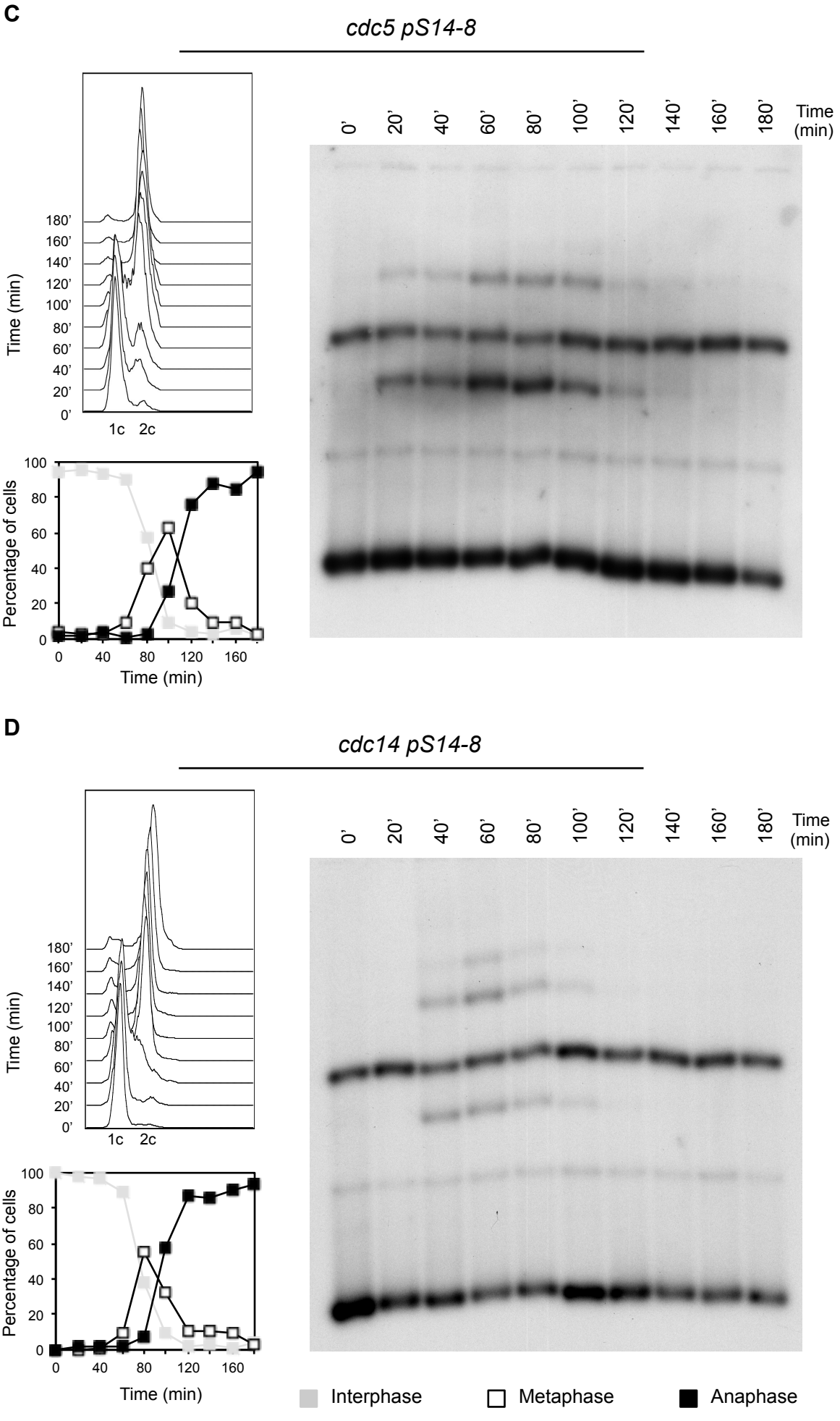
C
cdc5 pS14-8
Time (min)
180'
160'
140'
120'
100'
80'
60'
40'
20'
0'
1c 2c
Percentage of cells
100
80
60
40
20
0
0 40 80 120 160
Time (min)
0' 20' 40' 60' 80' 100' 120' 140' 160' 180'
Time (min)
D
cdc14 pS14-8
Time (min)
180'
160'
140'
120'
100'
80'
60'
40'
20'
0'
1c 2c
Percentage of cells
100
80
60
40
20
0
0 40 80 120 160
Time (min)
0' 20' 40' 60' 80' 100' 120' 140' 160' 180'
Time (min)
Interphase
Metaphase
Anaphase

Figure 3. 23 DNA catenanes persist in mitosis in *cdc5 cdc14* cells.
cdc5-as1 cdc14-1 (**A**), *cdc15-2* (**B**), *cdc5-as1* (**C**) and *cdc14-1* (**D**) cells carrying the pS14-8 mini-chromosome were grown overnight in SCD medium lacking leucine at 23°C, next shifted to YPD medium and arrested in G1 by addition of α-factor. Cells were then synchronously released into the next cell cycle in new, prewarmed YPD at 37°C to inactivate *cdc15-2* and *cdc14-1*; CMK inhibitor was added to *cdc5-as1 cdc14-1* and *cdc5-as1* cells to inactivate *cdc5-as1*. Samples were collected every 20 min for 3 hrs. Cell cycle progression was monitored by FACS analysis of DNA content to differentiate between G1, S and G2/M phases (upper left) and by IF (anti-Tub1, DAPI) to differentiate between interphase, metaphase and anaphase (lower left). pS14-8 forms were analyzed through gel electrophoresis and Southern blotting (probe AmpR-3; right).

3.5 Investigating the molecular mechanism underlying the catenane resolution defect of *cdc5 cdc14* cells

After obtaining evidence that catenanes persist in mitosis in *cdc5 cdc14* cells, we sought to understand the molecular origin of this defect. Different studies indicate that the full resolution of DNA catenanes in mitosis requires the combined action of Topo II, condensin and the mitotic spindle (Baxter *et al.*, 2011; Farcas *et al.*, 2011; Charbin, Bouchoux and Uhlmann, 2014; Leonard *et al.*, 2015; Sen *et al.*, 2016). Thus, in principle, any or all of the three could be responsible for this defect. Even though the spindle is defective in *cdc5 cdc14* cells, rescuing its elongation did not prove sufficient to rescue catenane resolution, indicating that some other enzymatic activity is required. The comparison between endogenous Top2 and ectopic cv-Topo II overexpression suggests that Top2 activity is impaired in *cdc5 cdc14* cells. Indeed, Top2 overexpression might not be sufficient to bypass a Top2 activation step, suggesting that either Top2 itself is impaired, or a factor required for Top2 activity (for example, to guide its localization) is impaired. Finally, a lack of condensin activity can account for the catenane resolution defect of the *cdc5 cdc14* mutant. We next performed a set of experiments aimed at addressing this possibility.

3.5.1 Assessing for condensin contribution

The possibility that condensin is impaired in *cdc5 cdc14* cells is suggested both by data in the literature and by one of our results. (1) Cdc5 phosphorylates the three non-SMC subunits of condensin in mitosis. This phosphorylation is required for rDNA segregation and leads to condensin hyperactivation *in vitro* (St-Pierre *et al.*, 2009). Recently, it was found that Cdc5 is required also for condensin relocalization from pericentromeres to

chromosome arms and it was suggested that Cdc5 promotes condensin supercoiling activity *in vivo* (Leonard *et al.*, 2015). (2) One of the possible interpretations of the different phenotypes obtained upon ectopic cv-Topo II and endogenous Top2 overexpression predicts a lower activity of condensin, that is still sufficient for cv-Topo II activity but not for the one of Top2 (D'Ambrosio, Kelly, *et al.*, 2008).

To assess for condensin contribution to the phenotype of *cdc5 cdc14* cells, we initially tested for genetic interactions of a condensin mutant with *cdc5-as1* and *cdc14-1* single and double mutants. To inactivate condensin we used the *smc2-8* allele of the Smc2 subunit of the complex (Freeman, Aragon-Alcaide and Strunnikov, 2000). When *smc2-8* cells are shifted at the restrictive temperature (37°C), the condensin complex disrupts and dissociates from chromatids becoming inactive (Lavoie, Hogan and Koshland, 2002). We searched for synthetic interactions by comparing the growth of cells carrying different combinations of *cdc5-as1*, *cdc14-1* and *smc2-8* alleles as serial dilutions on YPD plates incubated for 48 hrs at different temperatures (23°C, 26°C, 28°C, 30°C, 34°C and 37°C). While no synthetic interaction was observed between *cdc5-as1 cdc14-1* and *smc2-8* and between *cdc14-1* and *smc2-8*, we noticed that the *cdc5-as1* allele improved the viability of *smc2-8* cells at the semi-restrictive temperature of 30°C (Figure 3.24). A possible interpretation for this is that Cdc5-as1 is hypomorph at this temperature and slows down mitosis allowing chromosome segregation to take place even with partially active condensin.

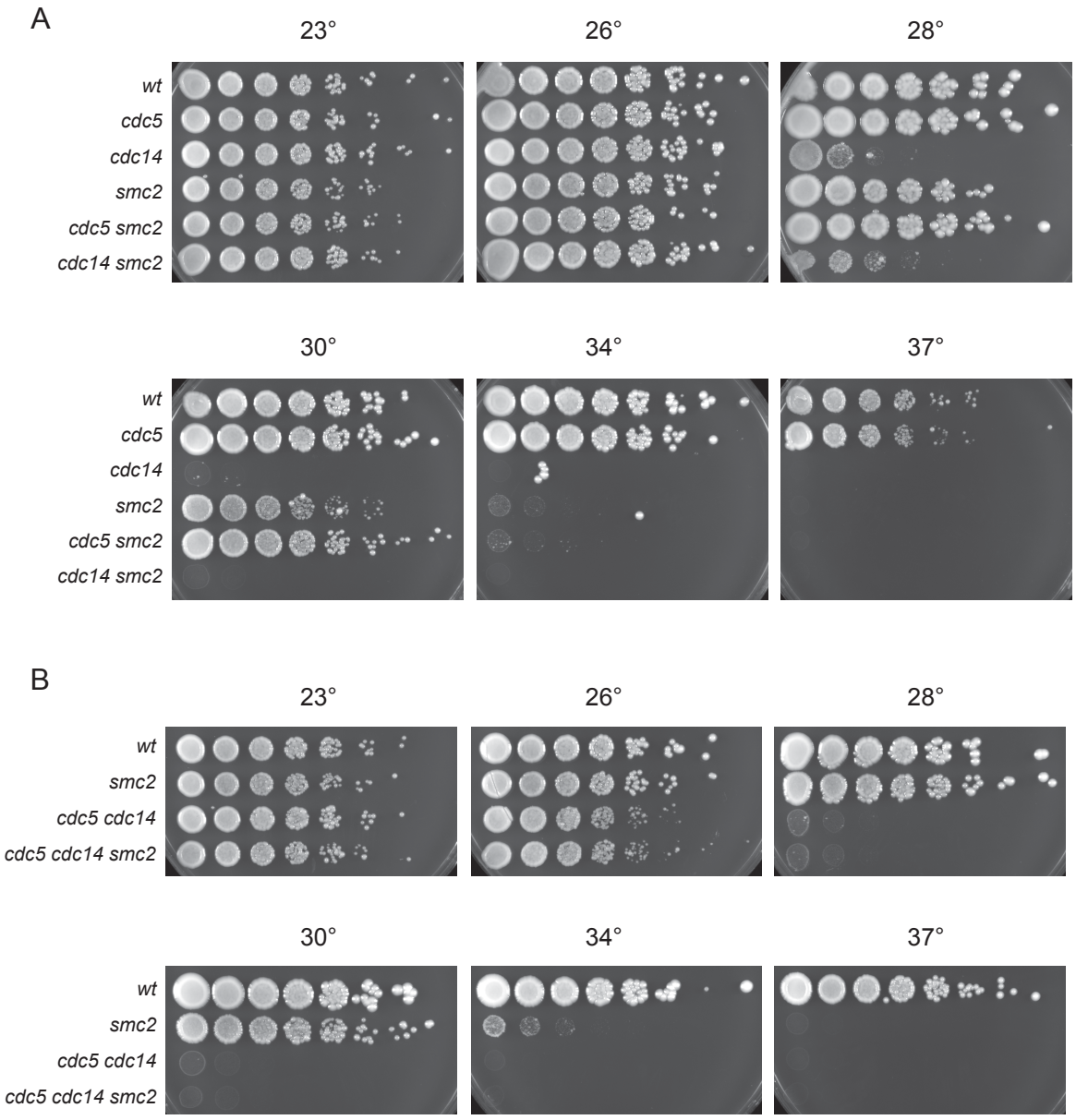

Figure 3. 24 Genetic interactions between *SMC2*, *CDC5* and *CDC14*.
Serial dilutions (1:5) of cells suspensions starting from OD_{600} = 1 were spotted onto YPD plates and incubated at 23°C, 26°C, 28°C, 34°C and 37°C for 48 hrs. **A.** Growth of serial dilutions of wild type, *cdc5-as1*, *cdc14-1*, *smc2-8*, *cdc14-1 smc2-8* and *cdc5-as1 smc2-8* cells. **B.** Growth of serial dilutions of wild type, *smc2-8*, *cdc5-as1 cdc14-1* and *cdc5-as1 cdc14-1 smc2-8* cells.

Next, we tested whether and how inactivating condensin would affect cell cycle progression of *cdc5-as1* and *cdc14-1* single and double mutants. We found that inactivation of *smc2-8* did not alter the phenotype of either *cdc5-as1* or *cdc14-1* single mutants, nor that of the *cdc5-as1 cdc14-1* double mutant (Figure 3.25).

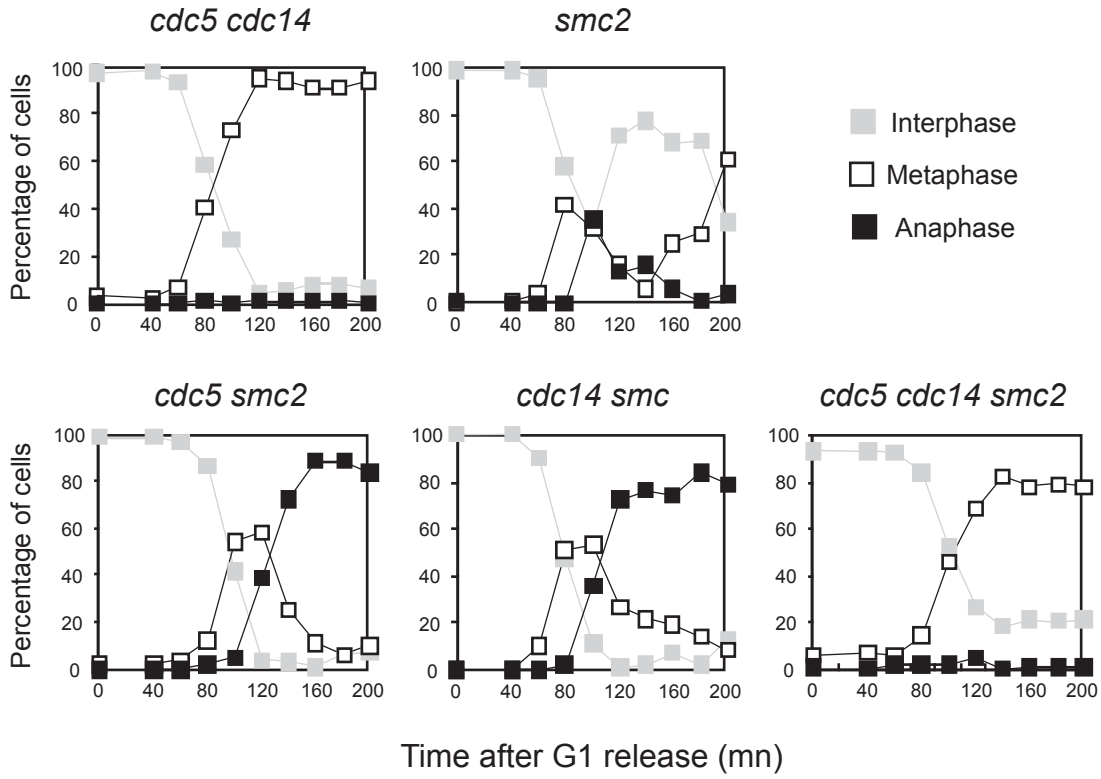

Figure 3. 25 Condensin inactivation in *cdc5* or *cdc14* mutants does not mimic the *cdc5 cdc14* mutant, nor affects the *cdc5 cdc14* mutant terminal arrest.
cdc5-as1 cdc14-1, *smc2-8*, *cdc5-as1 smc2-8*, *cdc14-1 smc2-8* and *cdc5-as1 cdc14-1 smc2-8* cells were arrested in G1 by addition of α-factor in YPD at 23°C and then synchronously released into the next cell cycle in new, prewarmed YPD medium supplemented with the CMK inhibitor at 37°C, to inactivate *cdc5-as1*, *cdc14-1* and *smc2-8*. Samples were collected every 20 min and analyzed through IF (anti-Tub1, DAPI) to differentiate between interphase, metaphase and anaphase (n=100).

After assessing that inactivating condensin does not alter the *cdc5 cdc14* mutant phenotype, we decided to test specifically whether condensin is active in its function of promoting Topo II activity and catenane resolution. To do so, we tested whether ectopic cv-Topo II overexpression is still able to rescue the *cdc5 cdc14* arrest if condensin was inactivated. We reasoned that, if condensin was already inactive, then cv-Topo II overexpression in *cdc5 cdc14* should have the same phenotype with and without the *smc2-8* mutation. *cdc5-as1 cdc14-1*, *cdc5-as1 cdc14-1 PGAL-cvTOPOII* and *cdc5-as1 cdc14-1 smc2-8 PGAL-cvTOPOII* cells were released from a G1 arrest in non-permissive conditions and galactose was added at the *cdc5 cdc14* terminal arrest to induce cv-Topo II overexpression. Samples were collected at the time of induction and 30 min, 60 min and 90 min after and were analyzed through IF for spindle length and nuclear morphology.

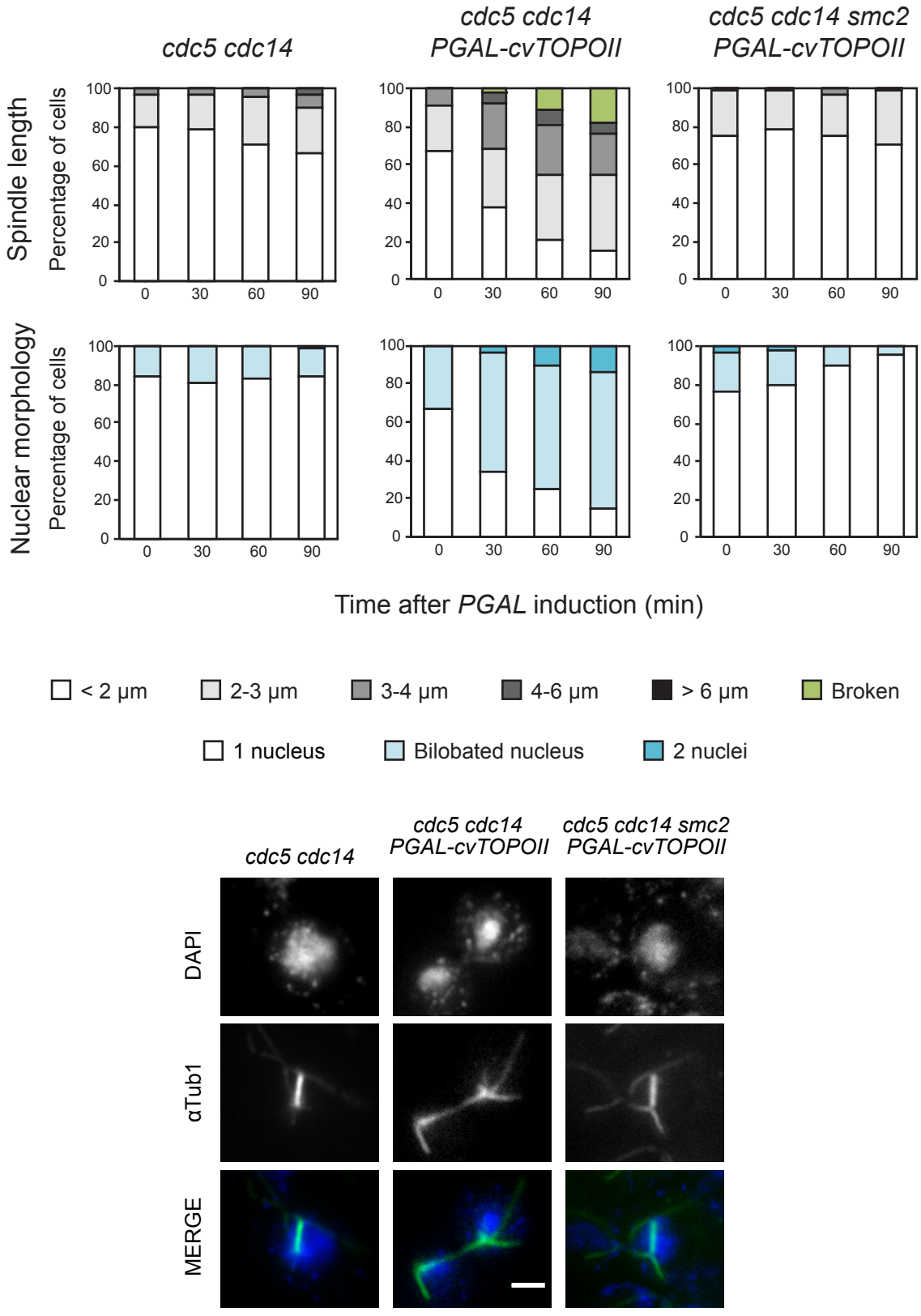

Figure 3. 26 Condensin inactivation prevents Topo II overexpression induced rescue of the *cdc5 cdc14* mutant arrest. *cdc5-as1 cdc14-1*, *cdc5-as1 cdc14-1 PGAL-cvTOPOII* and *cdc5-as1 cdc14-1 smc2-8 PGAL- cvTOPOII* cells were arrested in in G1 by addition of α-factor in YPR at 23°C and then synchronously released into the next cell cycle in new, prewarmed YPR medium supplemented with the CMK inhibitor at 37°C, to inactivate *cdc5-as1* and *cdc14-1*, respectively. When cells had reached the terminal arrest (3.30 hrs), 2% galactose was added to induce Cin8 overexpression. Samples were collected before galactose induction and 30, 60 and 90 min after and analyzed through IF (anti-Tub1, DAPI). **A.** Spindles were measured (upper graphs) and nuclear morphology was analyzed (lower graphs) (n=100). **B.** Representative cells are shown (scale bar: 2µm)

As expected, galactose addition had no effect on *cdc5-as1 cdc14-1* cells, but allowed nuclei separation and spindle elongation in *cdc5-as1 cdc14-1 PGAL-cvTOPOII* cells (Figure 3.26). Interestingly, in cells with inactive condensin cv-Topo II overexpression had no effect on both spindles, that did not elongate, and nuclei, that did not separate. Indeed, *cdc5-as1 cdc14-1 smc2-8 PGAL-cvTOPOII* cells were identical to *cdc5-as1 cdc14-1* cells (Figure 3.26). This result indicates that in the *cdc5 cdc14* mutant condensin is in part active, at least in its function to promote mitotic catenane resolution upon cv-Topo II overexpression.

Since this result does not rule out the possibility that condensin is partially inactive in *cdc5 cdc14* cells, we decided to overexpress the condensin complex in these cells. We reasoned that, if it was already active, its overexpression should have no effect, while if it was not fully active, then its overexpression should rescue the *cdc5 cdc14* arrest, resulting in a phenotype similar to the one obtained upon Topo II overexpression.

As condensin is composed by five subunits, all necessary for the activity of the complex, their overexpression is quite tricky. To this aim, we used constructs developed by D'Amours group where all subunits are under the control of *PGAL* promoters but three are hosted on a 2μ plasmid (*PGAL-SMC4-3StrepTagII PGAL-SMC2 PGAL-BRN1-3HA-12HIS*) and the other two on another (*PGAL-YCS4 PGAL-YCG1-3FLAG-9HIS*). A caveat with this setup is that, as the two plasmids can be present in the cell in different numbers, the subunits can be expressed not-stoichiometrically. To minimize for this, after transforming *cdc5 cdc14* cells with the two plasmids we screened several transformants by western blotting (anti-HA and anti-FLAG to recognize Brn1-HA and Ycg1-FLAG, carried on different plasmids) and by precipitation against the His tag, to select those that expressed Brn1 and Ycg1 at a similar level. We selected two clones and analyzed them in a preliminary experiment. *cdc5-as1 cdc14-1* cells and two strains of *cdc5-as1 cdc14-1* cells carrying *PGAL-SMC2, SMC4, BRN1, YCG1, YCS4* were released from a G1 arrest at non-permissive conditions and added with galactose at *cdc5 cdc14* terminal arrest. Samples

were taken at the time of induction and after 90 min and analyzed through western blotting (anti-HA; anti-FLAG; anti-Pgk1 as loading control) and IF (anti-Tub1; DAPI). Western blotting confirmed Brn1 and Ycg1 expression in both clones after galactose induction. A rough analysis of spindle and nuclear morphology showed that condensin overexpression does not alter the terminal phenotype of *cdc5 cdc14* cells, indicating that a lack of condensin activity does not underlie the chromatid separation defect of these cells. A more rigorous analysis will be necessary to confirm this observation. Though we checked that proteins from both plasmids were expressed, we did not check whether the five subunits had formed a complex. Thus, this experiment will be repeated in the future with the additional control of checking complex formation by analyzing the co-immunoprecipitation of the different subunits.

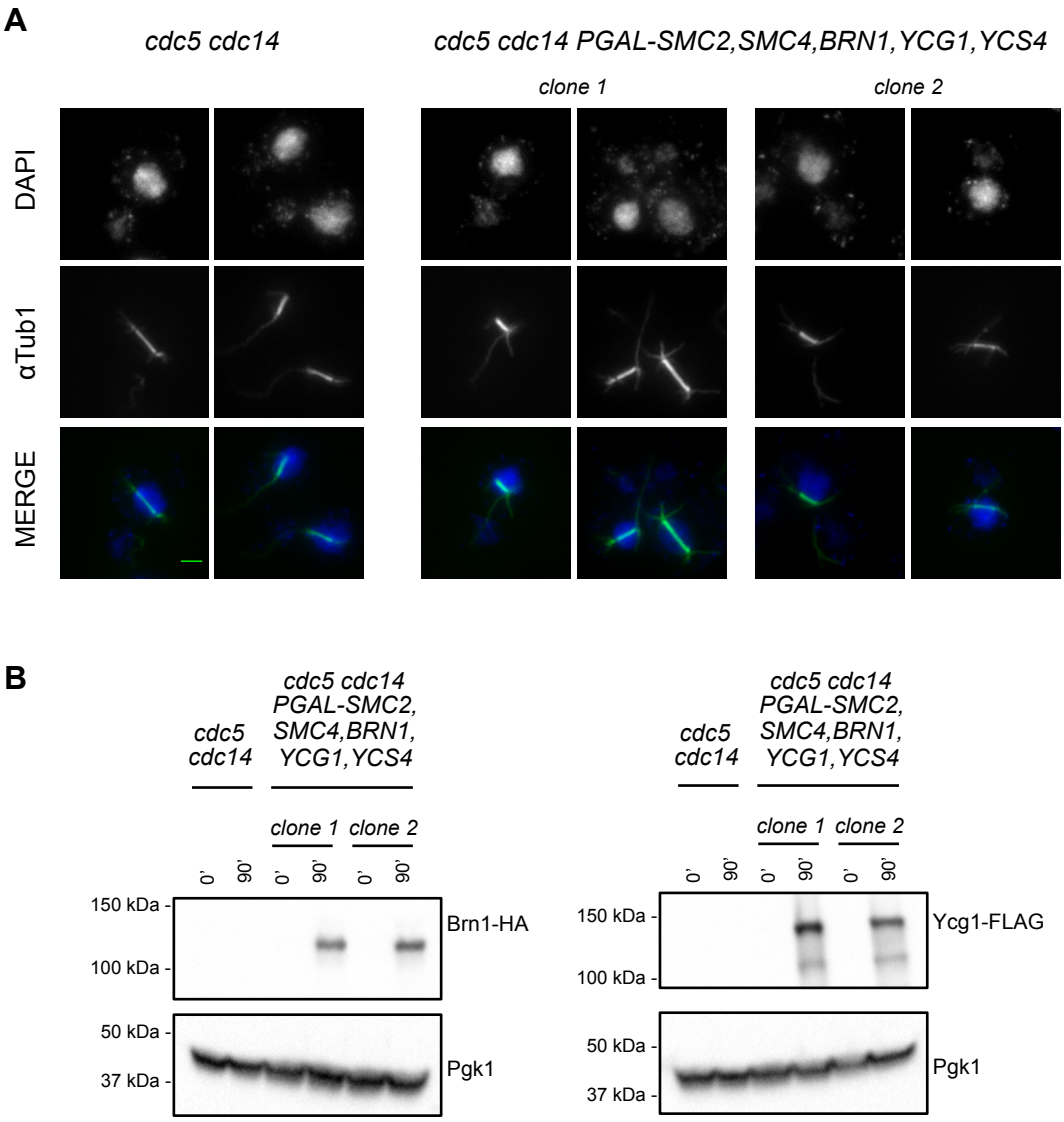

Figure 3. 27 Condensin overexpression does not rescue the *cdc5 cdc14* mutant arrest. *cdc5-as1 cdc14-1* and two clones of *cdc5-as1 cdc14-1 PGAL-SMC2, SMC4, BRN1, YCG1, YCS4* cells were arrested in G1 by addition of α-factor in YPR at 23°C and then synchronously released into the next cell cycle in new, prewarmed YPR medium supplemented with the CMK inhibitor at 37°C, to inactivate *cdc5-as1* and *cdc14-1*, respectively. When cells had reached the terminal arrest (3.30 hrs), 2% galactose was added to induce condensin subunits overexpression. Samples were collected at galactose induction and 90 min after. **A**. Representative cells collected 90 min after induction and analyzed through IF (anti-Tub1, DAPI) are shown. **B**. Condensin subunits overexpression was checked analyzing Brn1-HA (anti-HA) and Ycg1-FLAG (anti-FLAG) protein levels. Pgk1 protein was used as an internal loading control.

4. Discussion

The simultaneous inactivation of the Polo-like kinase Cdc5 and the phosphatase Cdc14 results in a synthetic interaction. While *cdc5* and *cdc14* single mutants arrest in late anaphase with elongated spindles and separated nuclei, the *cdc5 cdc14* double mutant arrests earlier in mitosis, with metaphase-like spindles and undivided nuclei, despite having cleaved cohesin. This stage was named mini-anaphase (Roccuzzo *et al.*, 2015).

The *cdc5 cdc14* mutant terminal arrest was quite unexpected, as cohesin cleavage was thought to be sufficient to trigger chromosome segregation (Uhlmann *et al.*, 2000). To our knowledge, no other mutant was ever described arresting at this stage. This finding provides a novel tool for studying the earlier steps of chromosome segregation. Indeed, the *cdc5 cdc14* synthetic interaction indicates that the two proteins redundantly control one or more processes in early anaphase that are necessary to start chromosome segregation. As both proteins regulate different aspects of chromosome segregation and mitotic exit, this synthetic interaction unveils the existence of a novel level of coordination of mitotic events that acts soon after cohesin cleavage.

While characterizing the *cdc5 cdc14* terminal phenotype, three defects in chromosome segregation were identified: the spindle fails to elongate (Roccuzzo *et al.*, 2015); the nucleus moves into the daughter cell and sister chromatids fail to separate.

The spindle elongation (SE) defect of *cdc5 cdc14* cells indicates that Cdc5 and Cdc14 are redundantly required to promote SE likely by stabilizing spindle dynamics. A role for Cdc14 in SE has already been proposed, but its essential function in the process was only evidenced in the absence of Cdc5 activity. Cdc14 is known to dephosphorylate several spindle midzone components among which the kinesin 5 motor protein Cin8

(Avunie-Masala *et al.*, 2011). Interestingly, among all Cdc14 substrates only Cin8 proved to be an essential target of the pathway redundantly controlled by Cdc14 and Cdc5 (Roccuzzo *et al.*, 2015) as evidenced by the observation that its overexpression rescues SE in *cdc5 cdc14* cells. Whether Cin8 is also a substrate of Cdc5 will be a matter of future investigation. One possible additional role for Cdc5 seems to be to contribute to decrease Clb2-Cdk activity in order to achieve the right kinase/phosphatase balance required for SE (Roccuzzo *et al.*, 2015). The role of Cdc5 in SE will be interesting to be elucidated in the future.

In the *cdc5 cdc14* mutant, the nucleus moves into the daughter cell during the arrest. This suggests that the two proteins are somehow involved in regulating nuclear positioning, maybe through regulation of astral microtubules dynamics. Such a phenotype was already observed in a series of other mutants, including a series of FEAR network mutants arrested in metaphase in the presence of uncleavable cohesin. Interestingly, in the case of the *slk19* mutant, this phenotype was rescued by the gain-of-function *TAB6* allele of *CDC14* (Ross and Cohen-Fix, 2004). This suggests a possible role for FEAR activated Cdc14 in controlling nuclear positioning. Interestingly, while the nucleus moves into the bud, the nucleolus remains in the mother. We speculate that this may result from two processes. (1) During anaphase, the nuclear envelope (NE) expands to allow chromosome segregation to take place without NE breakdown. This process is not inhibited in prolonged metaphase arrest, resulting in an increase of the nuclear surface (Witkin *et al.*, 2012). Thus, NE expansion could have allowed nucleus and nucleolus to move independently in *cdc5 cdc14* cells. (2) The rDNA, which constitutes the nucleolus, in budding yeast is entirely hosted on the long arm of chromosome XII, making it the longest in the genome. In unperturbed mitosis, the rDNA segregates after and independently from the rest of the genome (Granot and Snyder, 1991; Sullivan *et al.*, 2004; Torres-Rosell *et al.*, 2004; Machín *et al.*, 2005). Interestingly, both Cdc5 and Cdc14 promote anaphase rDNA condensation, which is required for its segregation (D'Amours, Stegmeier and

Amon, 2004; Sullivan *et al.*, 2004; Wang, Yong-Gonzalez and Strunnikov, 2004; St-Pierre *et al.*, 2009). We hypothesize that in *cdc5 cdc14* cells the longest, not properly condensed long arm of chromosome XII is not subjected to the same forces that pull the rest of the nucleus into the daughter cell and thereby remains in the mother. It would be interesting to test whether other late segregating regions, the telomeres (Clemente-Blanco et al., 2011), also remain in the mother cell.

4.1 The *cdc5 cdc14* mutant is defective in sister chromatid separation and in catenane resolution

The third defect of the *cdc5 cdc14* double mutant we identified is in sister chromatid separation (SCS). Indeed, rescuing SE in these cells does not fully rescue chromosome segregation but results in the accumulation of DNA anaphase bridges between the two separating DNA masses, that are indicative of linkages between sister chromatids. As removal of residual cohesin complexes that persist on chromatids in anaphase requires Esp1 (which is active in *cdc5 cdc14* cells), condensin (which is at least in part active in *cdc5 cdc14* cells) and SE (that we artificially rescued) (Renshaw *et al.*, 2010), these bridges are unlikely to be generated by cohesin but rather a consequence of persisting DNA linkages between sister chromatids. Supporting this is the finding that our analysis of sister chromatid loci dynamics in *cdc5 cdc14* cells completely excludes the presence of cohesin (or any other linkage) in the regions surrounding the centromeres and suggests that linkages present on arms and telomeres are of a less tight nature than cohesin. Thus, though it is possible that residual cohesin complexes are present on chromatids in *cdc5 cdc14* cells after bulk cohesin cleavage, also other types of linkages, namely DNA linkages, seem to be present.

A possible source of anaphase bridges are sister chromatid junctions (SCJs) generated by homologous recombination or by DNA damage tolerance mechanisms. Their

presence is likely in the *cdc5 cdc14* double mutant as such structures arise also in physiological conditions and their mitotic resolution requires specific nucleases, Mus81-Mms4 and Yen1, that are activated by Cdc5 and Cdc14, respectively (Blanco *et al.*, 2009; Matos *et al.*, 2011; Matos, Blanco and West, 2013; Szakal and Branzei, 2013; Blanco, Matos and West, 2014; Eissler *et al.*, 2014; García-Luis *et al.*, 2014). Moreover, as *cdc14* mutants were found to arrest with regions of unreplicated DNA (Dulev *et al.*, 2009), *cdc5 cdc14* cells might also retain junctions originated by intertwines between unreplicated parental DNA. When we probed for the presence of such structures in *cdc5 cdc14* cells, we found that they are likely present but they are not at the origin of the SCS defect of these cells. We found instead that this defect results from another type of linkages, DNA catenanes. Indeed, *cdc5 cdc14* cells retain DNA catenanes at their terminal arrest and their SCS defect is rescued after Topo II overexpression. As Topo II overexpression did not completely resolve *cdc5 cdc14* cells anaphase bridges, it would be interesting to test in the future if they consist of SCJs.

4.2 Relative contribution of Cdc5 and Cdc14 in catenane resolution

To our knowledge, the *cdc5 cdc14* arrest is not shared by other mutants. Having another mutant or experimental condition to compare the *cdc5 cdc14* mutant to would have been incredibly useful to discriminate between mini-anaphase specific phenotypes and phenotypes due to a lack of Cdc5 and Cd14 activity. In particular, in the characterization of the catenane resolution defect, having such a mutant would have allowed us to understand whether catenane resolution requires a direct function of Cdc5 and/or Cdc14 or whether they indirectly contribute to it by promoting other processes that would in turn result in catenane resolution. The second possibility was quite likely, since both proteins regulate SE and the spindle is involved in catenane resolution. Though our attempts to find a mutant arresting in mini-anaphase revealed unsuccessful, we managed to compare

anaphase bridges occurrence in *cdc5 cdc14* and metaphase-arrested wild type cells after ectopic SE and found that they are completely resolved in the latter. This indicates that Cdc5 and Cdc14 have a role in catenane resolution independent from SE and anaphase progression. It also indicates that a decrease in Cdk levels (that remain high in metaphase cells) is not required for catenane resolution, thus suggesting that Cdc5 and Cdc14 do not promote catenane resolution by driving Cdk inactivation.

As Cdc5 is already active in metaphase, while Cdc14 is not, we can speculate that, among the two, Cdc5 is the one that controls this process. However, some studies suggested a role for Cdc14 also in metaphase (Taxis *et al.*, 2009; Tomson *et al.*, 2009; Akiyoshi and Biggins, 2010). Moreover, as Cdc14 activation in early anaphase is still not fully understood, it is possible that cohesin cleavage and spindle elongation somehow contribute to its activation through a yet unknown mechanism. This possibility becomes relevant in late anaphase, when SPB passage into the daughter cell triggers MEN-dependent Cdc14 activation. Thus, a contribution of Cdc14 cannot be excluded. Supporting the idea that Cdc5, rather than Cdc14, promotes catenane resolution is our finding that residual catenanes persist in mitosis in a *cdc5* single mutant but not in a *cdc14* single mutant. However, as the *cdc5 cdc14* double mutant has a stronger phenotype than the *cdc5* single mutant, Cdc14 might have a minor function additive to Cdc5 in catenane resolution.

4.3 How does Cdc5 (and Cdc14) promote catenane resolution?

DNA catenanes are resolved by type II Topoisomerases. A complete chromosome segregation requires that every single catenane is resolved, but Topo II activity alone is not sufficient to do so. Indeed, in the crowded pre-mitotic nucleus, after having reached its reaction equilibrium, Topo II can both insert and remove catenanes. In mitosis, Topo II activity is guided by the individualization of sister chromatids that restrains chromatid

intertwines, including catenanes, only in specific areas where Topo II decatenation activity can prevail. Three factors, beside Topo II, have been shown to be necessary for catenane resolution in mitosis: a bipolar metaphase spindle, condensin and the absence of cohesin. As cohesin is already cleaved in *cdc5 cdc14* arrested cells, we reason that Cdc5 and/or Cdc14 function in mitotic catenane resolution could be in promoting the activity of anyone among spindle, condensin and Topo II.

4.3.1 By acting on the spindle

The knowledge that the spindle is required for catenane resolution derives from the comparison of cells arrested in metaphase by Cdc20 depletion treated or not with the MT depolymerizing drug nocodazole (Baxter *et al.*, 2011; Charbin, Bouchoux and Uhlmann, 2014). It has been suggested that the function of the spindle in promoting catenane resolution is indirect, as establishment of bipolar orientation is required for condensin relocalization from the pericentromere to chromosome arms where they fulfill their function for decatenation (Sen *et al.*, 2016). This suggests that a metaphase spindle is sufficient for catenane resolution. Another possibility is that the physical separation of chromatids driven by SE directs Topo II reaction towards decatenation. However, we have no indication on whether a full SE is necessary for catenane resolution, too. *cdc5 cdc14* cells arrest with a bipolar metaphase-like spindle but are defective in SE, which requires both Cdc5 and Cdc14 activity. Thus, both proteins could promote catenane resolution indirectly, by acting on the spindle. However, since rescuing SE in *cdc5 cdc14* cells originates anaphase bridges and since these bridges are at least in part resolved by Topo II, Cdc5 and/or Cdc14 likely act also independently of the spindle in catenane resolution.

4.3.2 By acting on condensin

Cdc5 and/or Cdc14 might act on condensin. Cdc5 has been shown to directly phosphorylate condensin non-SMC subunits, resulting in an increase in condensin

supercoiling activity *in vitro* and in their enrichment at the rDNA, necessary to promote its condensation (St-Pierre *et al.*, 2009). Recently, a role for Cdc5-dependent condensin activation has been suggested also outside the rDNA, as Cdc5 is required for condensin activation and relocalization from pericentromeres to chromosome arms (Leonard *et al.*, 2015). A role for Cdc14 in promoting condensin activity instead has been described only in the context of the rDNA and is likely to be indirect (D'Amours, Stegmeier and Amon, 2004; Sullivan *et al.*, 2004; Wang, Yong-Gonzalez and Strunnikov, 2004; Clemente-Blanco *et al.*, 2009). Thus, a lack of condensin activity in *cdc5 cdc14* seemed likely. However, our set of experiments aimed at understanding whether condensin is active in *cdc5 cdc14* cells suggests that condensin is at least partially active in these cells, and it is not at the basis of *cdc5 cdc14* cells SCS defect. Of note, none of our experiments rules out the possibility that condensin is partially inactive and not efficient in promoting full catenane resolution.

4.3.3 By acting on Topo II

Cdc5 and/or Cdc14 might directly or indirectly promote Topo II activity. Such possibility is supported by our observation that ectopic cv-Topo II overexpression but not endogenous Top2 overexpression rescues the *cdc5 cdc14* terminal arrest. A possible interpretation for this is that endogenous Top2, but not cv-Topo II, requires an activating step that is not bypassed simply by its overexpression. This result could suggest that Cdc5 and/or Cdc14 regulate Top2 activity. We can envision possible roles for Cdc5 in controlling Top2 activity in mitosis.

Human Plk1 (homolog of Cdc5) was found to phosphorylate Topo IIa in HeLa cells and this interaction was confirmed *in vitro* (Li, Wang and Liu, 2008). Such interaction might be conserved also in yeast. Indeed, when we scanned the Top2 CTD with Cdc5 consensus sequence, we found several putative sites for Cdc5 phosphorylation. If this is indeed the case, how does Cdc5-dependent Top2 phosphorylation promote its activity in

mitosis? Two recent studies in yeast and human cells found that the scaffold protein Dpb11/TOPB1 localizes to DNA anaphase bridges that at least in part consist of DNA catenanes (Germann *et al.*, 2014; Broderick *et al.*, 2015). In human cells TOPB1 is required to recruit Topo IIa to such structures (Broderick *et al.*, 2015). As this interaction requires TOPBP1 BRCT domains (Broderick *et al.*, 2015), that bind to phosphorylated substrates, it is likely to be regulated by phosphorylation events and possible candidates for this are mitotic kinases including Polo-like kinases (Broderick and Niedzwiedz, 2015). Thus, it is possible that Cdc5 directly phosphorylates Top2 and that this promotes its recruitment to sites of catenation through interaction with Dpb11. Alternatively, it might promote Top2 recruitment independently of Dpb11 or it might promote its activity independently from its localization.

It is also possible that Cdc5 contributes to Top2 activity indirectly. First, it may act through condensin. Indeed, it has been shown that Cdc5 is required for condensin relocalization from pericentromeres to chromosome arms and that this relocalization is required for Top2 relocalization, too (Leonard *et al.*, 2015). A lack of condensin-mediated Top2 recruitment could explain why overexpression of exogenous cv-Topo II but not of endogenous Top2 rescues SCS in *cdc5 cdc14* cells as the former, but not the latter, might be recruited independently of condensin. However, only condensin function in Top2 recruitment would be lacking, not other condensin functions that promote decatenation (i.e. shaping chromosome structure), as inactivating condensin prevents also ectopic cv-Topo II to rescue chromatid separation in *cdc5 cdc14* cells. As Cdc5-mediated phosphorylation promotes condensin activity and localization along chromosome arms, this would make sense only if Cdc5 promotes condensin recruitment of Top2 through an independent mechanism, for example by phosphorylating different residues.

A second possibility for an indirect function of Cdc5 in Top2 activation involves the SUMO protease Ulp2. Cdc5 is a negative regulator of Ulp2 (Baldwin *et al.*, 2009) and Top2 is one of the main targets of Ulp2 (Bachant *et al.*, 2002). Top2 sumoylation on its

CTD promotes its localization at centromeres where it collaborates to maintaining cohesion by recruiting Aurora B and thereby promoting its function in the SAC (Bachant *et al.*, 2002; Edgerton *et al.*, 2016). Likely, Ulp2-dependent Top2 desumoylation next allows loss of centromeric cohesion, which is necessary for chromosome segregation (Yoshida and Azuma, 2016). In *cdc5* mutants, Ulp2 is not inhibited and Top2 fails to accumulate in a sumoylated form (Baldwin *et al.*, 2009). Though Top2 sumoylation (at least in yeast) does not affect its catalytic activity but rather promotes its centromeric localization and Aurora B recruitment, it is possible that a lack of sumoylation affects Top2 activity also through other mechanisms, for example altering its localization. However, alterations of Top2 sumoylation are unlikely to explain the *cdc5 cdc14* defect since Top2 is likely to be desumoylated in these cells (in absence of *cdc5*) and since Top2 desumoylation seems to promote, rather than inhibit, Top2 anaphase functions, including loss of centromere cohesion and delocalization from centromeres to chromosome arms. Of note, centromeric cohesion is completely lost in *cdc5 cdc14* cells.

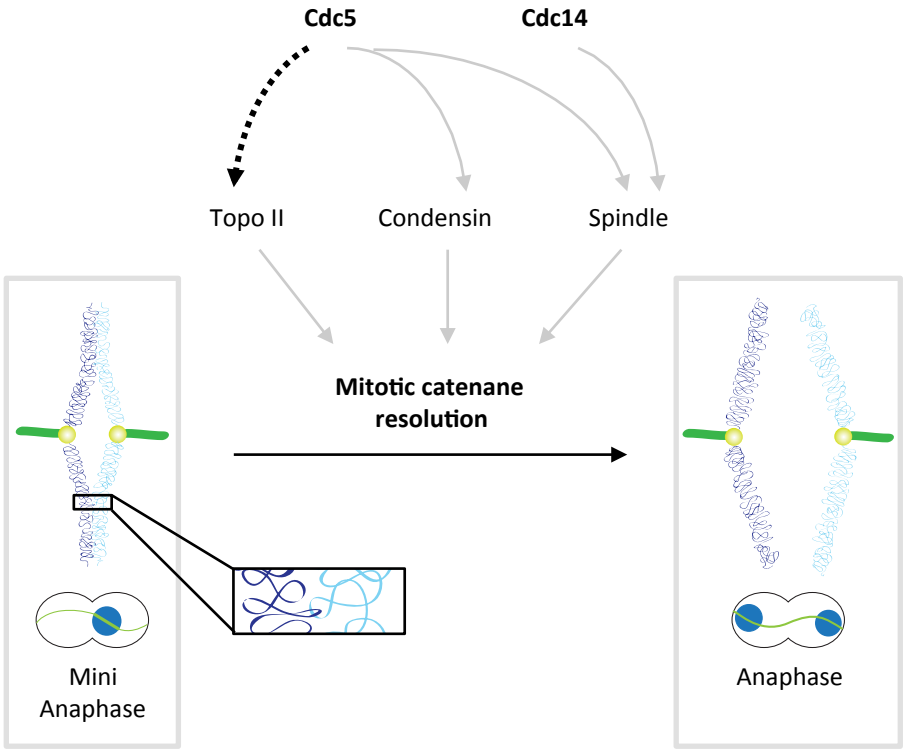

4.1 Model for Cdc5 and Cdc14 function in promoting catenane resolution.
Grey arrows indicate known function; black arrow indicates our speculation based on our results. The dotted line indicates that regulation might be either direct or indirect.

4.4 Cdc5 and Cdc14 as coordinators of early steps of chromosome segregation

The roles of Cdc5 and Cdc14 in promoting SCJ resolution and in promoting SE in early anaphase were already known and characterized. In this study, we identified an additional function of these two proteins in early anaphase, which is in promoting chromatid decatenation. Among the two, Cdc5 seems to play the major role in this function. Our results, together with data from the literature, suggest that Cdc5 does so by promoting Top2 activity, but future analyses will be necessary to explore this possibility.

Cdc5 is an essential mitotic kinase that plays several roles in promoting a correct chromosome segregation first and mitotic exit next. In chromosome segregation, Cdc5 promotes timely cohesin cleavage, condensin activity and SE. Our data now suggest that, in early anaphase, Cdc5 promotes also catenane resolution. As Cdc5 promotes Cdc14 activation both in early anaphase (FEAR network), when Cdc14 activity promotes correct chromosome segregation and SE, and in late anaphase (MEN), when Cdc14 activity promotes mitotic exit, it is tempting to speculate that Cdc5 and Cdc14 coordinate several aspects of chromosome segregation, among which catenane resolution and SE, with mitotic exit. We hypothesize that the two proteins do so as part of a broader control system that monitors chromosome segregation. Both Cdc5 and Cdc14 are components of the FEAR network. Though the exact organization of the network remains unclear, the most recent model organizes it in three parallel branches, represented by Cdc5, the separase Esp1 and the nucleolar protein Spo12 (Roccuzzo *et al.*, 2015). Interestingly, inactivation of the three branches results in cells arresting in mini-anaphase similarly to *cdc5 cdc14* cells, while interfering with one or two branches progressively slows down anaphase (Roccuzzo *et al.*, 2015). This finding allows us to speculate that each branch, in parallel to promoting Cdc14 activation, controls an aspect of chromosome separation and segregation and thus coordinates SE and mitotic exit with chromatid separation. As such, the FEAR network might work as a timer that slows down SE in response to defects in SCS. This hypothesis is supported by the fact that, beyond Cdc5, also Esp1 plays an essential role in

chromosome segregation, by cleaving cohesin. Thus, Esp1 coordinates cohesin cleavage with Cdc14-mediated SE. In addition, also Cdc14 itself, activated by the FEAR network, promotes both chromatid separation (SCJ resolution by dephosphorylating Yen1 and nucleolar segregation by shutting off rDNA transcription and promoting condensin recruitment) and SE.

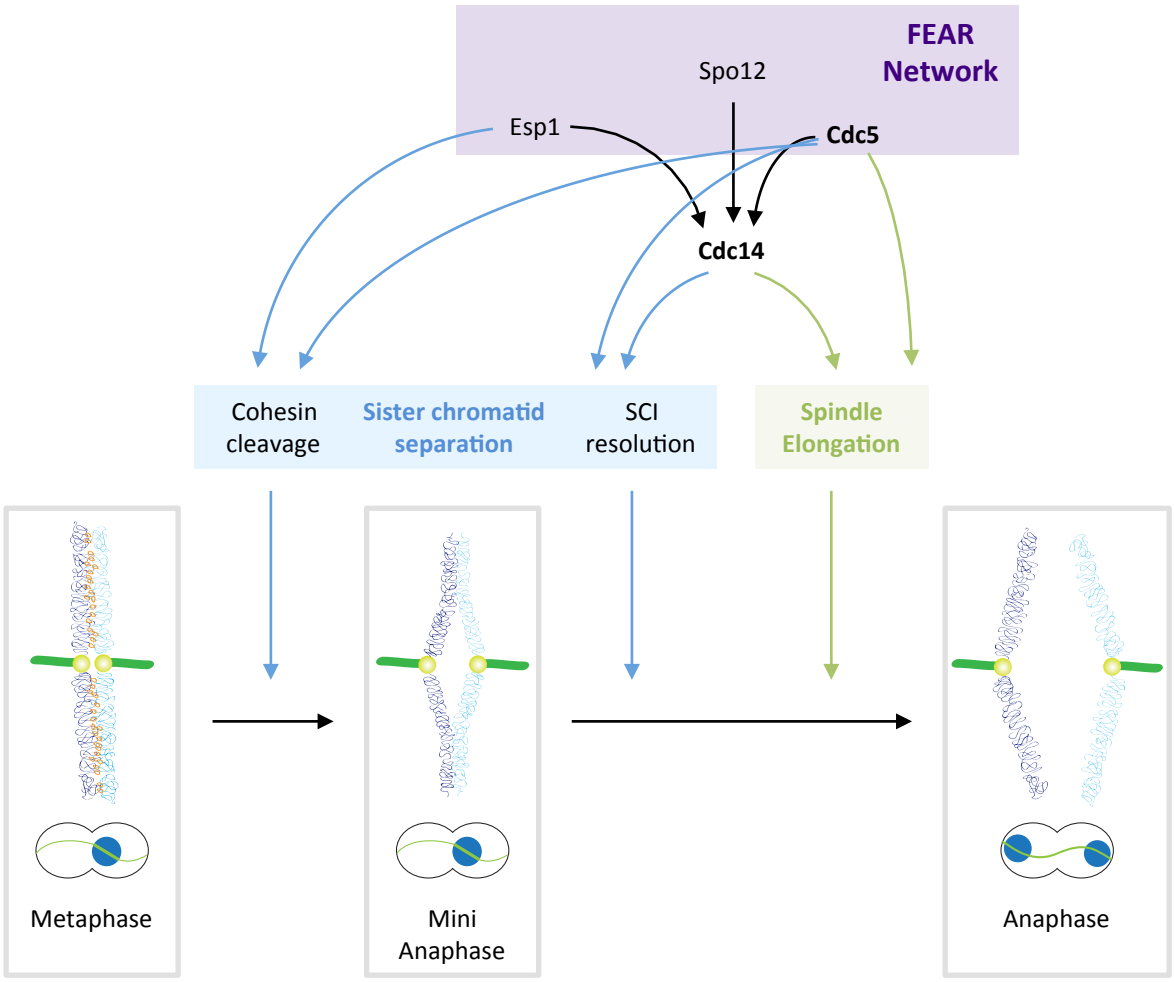

4.2 The FEAR network as a regulator for chromosome segregation.

As such, the three-branched organization of the FEAR network would create a highly controlled gradient of Cdc14 activation that would ensure the correct timing of anaphase events. The observation that Cdc14 has a higher affinity for its early substrates (Bouchoux and Uhlmann, 2011) is in agreement with this hypothesis. As control systems, or checkpoints, are present throughout the cell cycle to check that everything has been

correctly carried out before moving to the next stage, it is tempting to speculate that also chromosome segregation might be under such control to avoid that cells divide before segregation is complete. We propose that this role is played by the FEAR network.

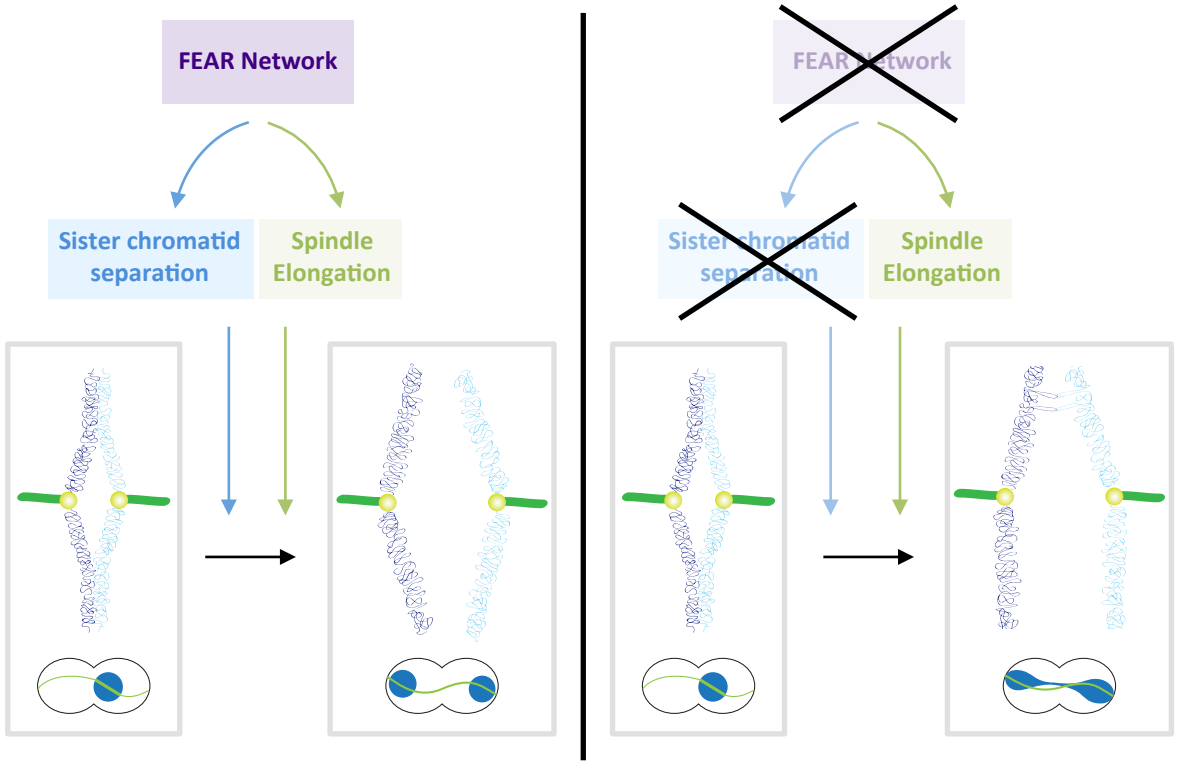

4.3 Model for coupling sister chromatids separation and spindle elongation by the FEAR network.
Left: coupling SCS and SE allows a correct chromosome segregation; right: SE uncoupled from SCS would originate anaphase bridges

5. Appendix

During the first year of my PhD training I worked on a project in collaboration with Dr. Peter De Wulf laboratory. The project dealt with understanding the role of the kinase Rio1 at the rDNA in *S. cerevisiae* and was published by Nature communication in 2015. The article is given in attachment to the thesis.

Iacovella, M. G., Golfieri, C., Massari, L. F., Busnelli, S., Pagliuca, C., Dal Maschio, M., Infantino, V., Visintin, R., Mechtler, K., Ferreira-Cerca, S., De Wulf, P. (2015). "Rio1 promotes rDNA stability and downregulates RNA polymerase I to ensure rDNA segregation". *Nature Communications*, *6*. doi: 10.1038/ncomms7643.

6. References

Akiyoshi, B. and Biggins, S. (2010) 'Cdc14-dependent dephosphorylation of a kinetochore protein prior to anaphase in Saccharomyces cerevisiae', *Genetics*, 186(4), pp. 1487–1491. doi: 10.1534/genetics.110.123653.

Alexandru, G. *et al.* (2001) 'Phosphorylation of the cohesin subunit Scc1 by Polo/Cdc5 kinase regulates sister chromatid separation in yeast', *Cell*, 105(4), pp. 459–472. doi: 10.1016/S0092-8674(01)00362-2.

Alfieri, C. *et al.* (2016) 'Molecular basis of APC/C regulation by the spindle assembly checkpoint', *Nature*, 536(7617), pp. 431–436. doi: 10.1038/nature19083.

Amaral, N. *et al.* (2016) 'The Aurora-B-dependent NoCut checkpoint prevents damage of anaphase bridges after DNA replication stress', *Nature Cell Biology*, 18(5), pp. 516–526. doi: 10.1038/ncb3343.

De Antoni, A. *et al.* (2005) 'The Mad1/Mad2 complex as a template for Mad2 activation in the spindle assembly checkpoint', *Current Biology*, 15(3), pp. 214–225. doi: 10.1016/j.cub.2005.01.038.

Arumugam, P. *et al.* (2003) 'ATP Hydrolysis Is Required for Cohesin's Association with Chromosomes', *Current Biology*, 13(22), pp. 1941–1953. doi: 10.1016/j.cub.2003.10.036.

Avunie-Masala, R. *et al.* (2011) 'Phospho-regulation of kinesin-5 during anaphase spindle elongation', *Journal of Cell Science*, 124(6), pp. 873–878. doi: 10.1242/jcs.077396.

Azzam, R. *et al.* (2004) 'Phosphorylation by cyclin B-Cdk underlies release of mitotic exit activator Cdc14 from the nucleolus', *Science*, 305(5683), pp. 516–519. doi: 10.1126/science.1099402.

Bachant, J. *et al.* (2002) 'The SUMO-1 isopeptidase Smt4 is linked to centromeric cohesion through SUMO-1 modification of DNA topoisomerase II', *Molecular Cell*, 9(6), pp. 1169–1182. doi: 10.1016/S1097-2765(02)00543-9.

Bachmair, A., Finley, D. and Varshavsky, A. (1986) 'In vivo half-life of a protein is a function of its amino-terminal residue', *Science*, 234(4773), pp. 179–186. doi: 10.1126/science.3018930.

Bakhoum, S. F. *et al.* (2014) 'The mitotic origin of chromosomal instability', *Current Biology*, pp. R148–R149. doi: 10.1016/j.cub.2014.01.019.

Baldwin, M. L. *et al.* (2009) 'The yeast SUMO isopeptidase Smt4/Ulp2 and the Polo Kinase Cdc5 act in an opposing fashion to regulate sumoylation in mitosis and cohesion at centromeres', *Cell Cycle*. doi: 9911 [pii].

Bardin, A. J., Boselli, M. G. and Amon, A. (2003) 'Mitotic exit regulation through distinct domains within the protein kinase Cdc15.', *Molecular and cellular biology*, 23(14), pp. 5018–30. doi: 10.1128/MCB.23.14.5018-5030.2003.

Bardin, A. J., Visintin, R. and Amon, A. (2000) 'A mechanism for coupling exit from mitosis to partitioning of the nucleus', *Cell*, 102(1), pp. 21–31. doi: 10.1016/S0092-8674(00)00007-6.

Bastians, H. (2015) 'Causes of chromosomal instability', in *Chromosomal Instability in Cancer Cells*, pp. 95–113. doi: 10.1007/978-3-319-20291-4_5.

Baxter, J. *et al.* (2011) 'Positive Supercoiling of Mitotic DNA Drives Decatenation by Topoisomerase II in Eukaryotes', *Science*, 331(6022), pp. 1328–1332. doi: 10.1126/science.1201538.

Baxter, J. (2015) '"Breaking up is hard to do": The formation and resolution of sister chromatid intertwines', *Journal of Molecular Biology*, pp. 590–607. doi: 10.1016/j.jmb.2014.08.022.

Baxter, J. and Diffley, J. F. X. (2008) 'Topoisomerase II Inactivation Prevents the Completion of DNA Replication in Budding Yeast', *Molecular Cell*, 30(6), pp. 790–802. doi: 10.1016/j.molcel.2008.04.019.

Beach, D. L. *et al.* (2000) 'The role of the proteins Kar9 and Myo2 in orienting the mitotic spindle of budding yeast', *Current Biology*, 10(23), pp. 1497–1506. doi: 10.1016/S0960-9822(00)00837-X.

Berger, J. M. *et al.* (1996) 'Structure and mechanism of DNA topoisomerase II', *Nature*, 379(6562), pp. 225–232. doi: 10.1038/379225a0.

Bermejo, R. *et al.* (2007) 'Top1- and Top2-mediated topological transitions at replication forks ensure fork progression and stability and prevent DNA damage checkpoint activation', *Genes and Development*, 21(15), pp. 1921–1936. doi: 10.1101/gad.432107.

Bhalla, N. (2002) 'Mutation of YCS4, a Budding Yeast Condensin Subunit, Affects Mitotic and Nonmitotic Chromosome Behavior', *Molecular Biology of the Cell*, 13(2), pp. 632–645. doi: 10.1091/mbc.01-05-0264.

Blanco, M. G. *et al.* (2009) 'Functional overlap between the structure-specific nucleases Yen1 and Mus81-Mms4 for DNA-damage repair in S. cerevisiae', *DNA Repair*, 9(4), pp. 394–402. doi: 10.1016/j.dnarep.2009.12.017.

Blanco, M. G., Matos, J. and West, S. C. (2014) 'Dual Control of Yen1 Nuclease Activity and Cellular Localization by Cdk and Cdc14 Prevents Genome Instability', *Molecular Cell*, 54(1), pp. 94–106. doi: 10.1016/j.molcel.2014.02.011.

Blat, Y. and Kleckner, N. (1999) 'Cohesins bind to preferential sites along yeast chromosome III, with differential regulation along arms versus the centric region', *Cell*, 98(2), pp. 249–259. doi: 10.1016/S0092-8674(00)81019-3.

Bloom, J. and Cross, F. R. (2007) 'Multiple levels of cyclin specificity in cell-cycle control', *Nature Reviews Molecular Cell Biology*. Nature Publishing Group, 8(2), pp. 149–160. doi: 10.1038/nrm2105.

Bouchoux, C. and Uhlmann, F. (2011) 'A quantitative model for ordered Cdk substrate dephosphorylation during mitotic exit', *Cell*, 147(4), pp. 803–814. doi: 10.1016/j.cell.2011.09.047.

Branzei, D. *et al.* (2006) 'Ubc9- and Mms21-Mediated Sumoylation Counteracts Recombinogenic Events at Damaged Replication Forks', *Cell*, 127(3), pp. 509–522. doi: 10.1016/j.cell.2006.08.050.

Branzei, D., Vanoli, F. and Foiani, M. (2008) 'SUMOylation regulates Rad18-mediated template switch', *Nature*, pp. 915–920. doi: 10.1038/nature07587.

Broderick, R. *et al.* (2015) 'TOPBP1 recruits TOP2A to ultra-fine anaphase bridges to aid in their resolution', *Nature Communications*, 6. doi: 10.1038/ncomms7572.

Broderick, R. and Niedzwiedz, W. (2015) 'Sister chromatid decatenation: bridging the gaps in our knowledge'. doi: 10.1080/15384101.2015.1078039.

Bush, N. G., Evans-Roberts, K. and Maxwell, A. (2015) 'DNA Topoisomerases', *EcoSalPlus*. doi: doi:10.1128/ ecosalplus.ESP-0010-2014.

Buvelot, S. *et al.* (2003) 'The budding yeast Ipl1/Aurora protein kinase regulates mitotic spindle disassembly', *Journal of Cell Biology*, 160(3), pp. 329–339. doi: 10.1083/jcb.200209018.

Carvalho, P. *et al.* (2004) 'Cell cycle control of kinesin-mediated transport of Bik1 (CLIP-170) regulates microtubule stability and dynein activation', *Developmental Cell*, pp. 815–829. doi: 10.1016/j.devcel.2004.05.001.

Champoux, J. J. and Been, M. D. (1980) 'Topoisomerases and the swivel problem', in *Mechanistic Studies of DNA Replication and Genetic Recombination: ICN-UCLA symposia on molecular and cellular biology*. Elsevier, pp. 809–815. doi: 10.1016/B978-0-12-048850-6.50072-7.

Chan, C. S. M. and Botstein, D. (1993) 'Isolation and characterization of chromosome-gain and increase-in-ploidy mutants in yeast', *Genetics*, 135(3), pp. 677–691.

Chan, K.-L. *et al.* (2013) 'Pds5 promotes and protects cohesin acetylation', *Proceedings of the National Academy of Sciences*. National Academy of Sciences, 110(32), pp. 13020–13025. doi: 10.1073/pnas.1306900110.

Chan, K. L. *et al.* (2012) 'Cohesin's DNA exit gate is distinct from its entrance gate and is regulated by acetylation', *Cell*, 150(5), pp. 961–974. doi: 10.1016/j.cell.2012.07.028.

Charbin, A., Bouchoux, C. and Uhlmann, F. (2014) 'Condensin aids sister chromatid decatenation by topoisomerase II', *Nucleic Acids Research*. Oxford University Press, 42(1), pp. 340–348. doi: 10.1093/nar/gkt882.

Chee, M. K. and Haase, S. B. (2010) 'B-Cyclin/CDKs regulate mitotic spindle assembly by phosphorylating kinesins-5 in budding yeast', *PLoS Genetics*. Edited by S. Biggins, 6(5), p. 35. doi: 10.1371/journal.pgen.1000935.

Cheng, T. M. K. *et al.* (2015) 'A simple biophysical model emulates budding yeast chromosome condensation', *eLife*, 2015(4), pp. 1–22. doi: 10.7554/eLife.05565.

Ciosk, R. *et al.* (1998) 'An ESP1/PDS1 complex regulates loss of sister chromatid cohesion at the metaphase to anaphase transition in yeast', *Cell*, 93(6), pp. 1067–1076. doi: 10.1016/S0092-8674(00)81211-8.

Ciosk, R. *et al.* (2000) 'Cohesin's binding to chromosomes depends on a separate complex consisting of Scc2 and Scc4 proteins', *Molecular Cell*, 5(2), pp. 243–254. doi: 10.1016/S1097-2765(00)80420-7.

Classen, S., Olland, S. and Berger, J. M. (2003) 'Structure of the topoisomerase II ATPase region and its mechanism of inhibition by the chemotherapeutic agent ICRF-187', *Proceedings of the National Academy of Sciences of the United States of America*, 100(19), pp. 10629–10634. doi: 10.1073/pnas.1934431100.

Clemente-Blanco, A. *et al.* (2009) 'Cdc14 inhibits transcription by RNA polymerase I during anaphase', *Nature*, 458(7235), pp. 219–222. doi: 10.1038/nature07652.

Clemente-Blanco, A. *et al.* (2011) 'Cdc14 phosphatase promotes segregation of telomeres through repression of RNA polymerase II transcription', *Nature Cell Biology*, 13(12), pp. 1450–1456. doi: 10.1038/ncb2365.

Cohen-Fix, O. *et al.* (1996) 'Anaphase initiation in saccharomyces cerevisiae is controlled by the APC-dependent degradation of the anaphase inhibitor Pds1p', *Genes and Development*, 10(24), pp. 3081–3093. doi: 10.1101/gad.10.24.3081.

Cohen-Fix, O. and Koshland, D. (1999) 'Pds1p of budding yeast has dual roles: Inhibition of anaphase initiation and regulation of mitotic exit', *Genes and Development*, 13(15), pp. 1950–1959. doi: 10.1101/gad.13.15.1950.

Corbett, K. D. (2017) *Molecular Mechanisms of Spindle Assembly Checkpoint Activation and Silencing*, *Progress in molecular and subcellular biology*. doi: 10.1007/978-3-319-58592-5_18.

Culotti, J. and Hartwell, L. H. (1971) 'Genetic control of the cell division cycle in yeast. 3. Seven genes controlling nuclear division', *Exp Cell Res*, 67(2), pp. 389–401. doi: 10.1016/0014-4827(71)90424-1.

Cuylen, S. *et al.* (2013) 'Entrapment of Chromosomes by Condensin Rings Prevents Their Breakage during Cytokinesis', *Developmental Cell*, 27(4), pp. 469–478. doi: 10.1016/j.devcel.2013.10.018.

Cuylen, S., Metz, J. and Haering, C. H. (2011) 'Condensin structures chromosomal DNA through topological links', *Nature Structural and Molecular Biology*, 18(8), pp. 894–901. doi: 10.1038/nsmb.2087.

D'Ambrosio, C., Kelly, G. P., *et al.* (2008) 'Condensin-Dependent rDNA Decatenation Introduces a Temporal Pattern to Chromosome Segregation', *Current Biology*, 18(14), pp. 1084–1089. doi: 10.1016/j.cub.2008.06.058.

D'Ambrosio, C., Schmidt, C. K., *et al.* (2008) 'Identification of cis-acting sites for condensin loading onto budding yeast chromosomes', *Genes and Development*, 22(16), pp. 2215–2227. doi: 10.1101/gad.1675708.

D'Amours, D., Stegmeier, F. and Amon, A. (2004) 'Cdc14 and condensin control the dissolution of cohesin-independent chromosome linkages at repeated DNA', *Cell*, 117(4), pp. 455–469. doi: 10.1016/S0092-8674(04)00413-1.

D'Aquino, K. E. *et al.* (2005) 'The protein kinase Kin4 inhibits exit from mitosis in response to spindle position defects', *Molecular Cell*, 19(2), pp. 223–234. doi: 10.1016/j.molcel.2005.06.005.

DiNardo, S., Voelkel, K. and Sternglanz, R. (1984) 'DNA topoisomerase II mutant of Saccharomyces cerevisiae: topoisomerase II is required for segregation of daughter molecules at the termination of DNA replication.', *Proceedings of the National Academy of Sciences of the United States of America*, 81(9), pp. 2616–20. doi: 10.1073/pnas.81.9.2616.

Dong, K. C. and Berger, J. M. (2007) 'Structural basis for gate-DNA recognition and bending by type IIA topoisomerases', *Nature*, pp. 1201–1205. doi: 10.1038/nature06396.

Dörter, I. and Momany, M. (2016) 'Fungal Cell Cycle: A Unicellular versus Multicellular Comparison', *Microbiology Spectrum*, 4(6). doi: 10.1128/microbiolspec.FUNK-0025-2016.

Dotiwala, F. *et al.* (2007) 'The yeast DNA damage checkpoint proteins control a cytoplasmic response to DNA damage.', *Proceedings of the National Academy of Sciences of the United States of America*, 104(27), pp. 11358–63. doi: 10.1073/pnas.0609636104.

Dougherty, W. G. *et al.* (1989) 'Characterization of the catalytic residues of the tobacco etch virus 49- kDa proteinase', *Virology*, 172(1), p. 302–10.

Dulev, S. *et al.* (2009) 'Essential global role of CDC14 in DNA synthesis revealed by chromosome underreplication unrecognized by checkpoints in cdc14 mutants.', *Proceedings of the National Academy of Sciences of the United States of America*, 106(34), pp. 14466–14471. doi: 10.1073/pnas.0900190106.

Earnshaw, W. C. *et al.* (1985) 'Topoisomerase II is a structural componenet of mitotic chromosome scaffolds', *Jcb*, 100(May), pp. 1706–1715.

Edgerton, H. *et al.* (2016) 'A noncatalytic function of the topoisomerase II CTD in Aurora B recruitment to inner centromeres during mitosis', *J. Cell Biol*, 213(6), pp. 651–664. doi: 10.1083/jcb.201511080.

Eissler, C. L. *et al.* (2014) 'The Cdk/Cdc14 Module Controls Activation of the Yen1 Holliday Junction Resolvase to Promote Genome Stability', *Molecular Cell*, 54(1), pp. 80–93. doi: 10.1016/j.molcel.2014.02.012.

Espert, A. *et al.* (2014) 'PP2A-B56 opposes Mps1 phosphorylation of Knl1 and thereby promotes spindle assembly checkpoint silencing', *Journal of Cell Biology*, 206(7), pp. 833–842. doi: 10.1083/jcb.201406109.

Fachinetti, D. *et al.* (2010) 'Replication Termination at Eukaryotic Chromosomes Is Mediated by Top2 and Occurs at Genomic Loci Containing Pausing Elements', *Molecular Cell*, 39(4), pp. 595–605. doi: 10.1016/j.molcel.2010.07.024.

Faesen, A. C. *et al.* (2017) 'Basis of catalytic assembly of the mitotic checkpoint complex', *Nature*, 542(7642), pp. 498–502. doi: 10.1038/nature21384.

Farcas, A. M. *et al.* (2011) 'Cohesin's Concatenation of Sister DNAs Maintains Their Intertwining', *Molecular Cell*, 44(1), pp. 97–107. doi: 10.1016/j.molcel.2011.07.034.

Flemming, W. (1882) *Zellsubstanz , Kern, und Zelltheilung (Cell substance, nucleus and cell division)*. Edited by F. C. W. Vogel. Leipzig.

Fortune, J. M. *et al.* (2001) 'Topoisomerase II from Chlorella Virus PBCV-1 Has an Exceptionally High DNA Cleavage Activity', *Journal of Biological Chemistry*. in Press, 276(26), pp. 24401–24408. doi: 10.1074/jbc.M101693200.

Fousteri, M. I. and Lehmann, A. R. (2000) 'A novel SMC protein complex in Schizosaccharomyces pombe contains the Rad18 DNA repair protein.', *The EMBO journal*, 19(7), pp. 1691–702. doi: 10.1093/emboj/19.7.1691.

Francisco, L., Wang, W. and Chan, C. S. (1994) 'Type 1 protein phosphatase acts in opposition to IpL1 protein kinase in regulating yeast chromosome segregation.', *Molecular and cellular biology*, 14(7), pp. 4731–40. doi: 10.1128/MCB.14.7.4731.Updated.

Fraschini, R. *et al.* (2006) 'Disappearance of the budding yeast Bub2-Bfa1 complex from the mother-bound spindle pole contributes to mitotic exit', *Journal of Cell Biology*, 172(3), pp. 335–346. doi: 10.1083/jcb.200507162.

Freeman, L., Aragon-Alcaide, L. and Strunnikov, A. (2000) 'The condensin complex governs chromosome condensation and mitotic transmission of rDNA', *Journal of Cell Biology*. Rockefeller University Press, 149(4), pp. 811–824. doi: 10.1083/jcb.149.4.811.

Fridman, V. *et al.* (2009) 'Midzone organization restricts interpolar microtubule plus-end dynamics during spindle elongation', *EMBO Reports*, 10(4), pp. 387–393. doi: 10.1038/embor.2009.7.

Fudenberg, G. *et al.* (2016) 'Formation of Chromosomal Domains by Loop Extrusion', *Cell Reports*, 15(9), pp. 2038–2049. doi: 10.1016/j.celrep.2016.04.085.

Gallo-Fernández, M. *et al.* (2012) 'Cell cycle-dependent regulation of the nuclease activity of Mus81-Eme1/Mms4', *Nucleic Acids Research*, 40(17), pp. 8325–8335. doi: 10.1093/nar/gks599.

Ganem, N. J. and Pellman, D. (2012) 'Linking abnormal mitosis to the acquisition of DNA damage', *Journal*

of Cell Biology, pp. 871–881. doi: 10.1083/jcb.201210040.

García-Luis, J. *et al.* (2014) 'Cdc14 targets the Holliday junction resolvase Yen1 to the nucleus in early anaphase', *Cell Cycle*. Taylor & Francis, 13(9), pp. 1392–1399. doi: 10.4161/cc.28370.

García-Luis, J. and Machín, F. (2014) 'Mus81-Mms4 and Yen1 resolve a novel anaphase bridge formed by noncanonical Holliday junctions', *Nature Communications*, 5. doi: 10.1038/ncomms6652.

Germann, S. M. *et al.* (2014) 'TopBP1/Dpb11 binds DNA anaphase bridges to prevent genome instability', *Journal of Cell Biology*, 204(1). doi: 10.1083/jcb.201305157.

Gerson-Gurwitz, A. *et al.* (2009) 'Mid-anaphase arrest in S. cerevisiae cells eliminated for the function of Cin8 and dynein', *Cellular and Molecular Life Sciences*, 66(2), pp. 301–313. doi: 10.1007/s00018-008-8479-2.

Gibcus, J. H. *et al.* (2017) 'Mitotic chromosomes fold by condensin-dependent helical winding of chromatin loop arrays', *BioRxiv*. Cold Spring Harbor Laboratory, p. 174649. doi: 10.1101/174649.

Goh, P. Y. and Kilmartin, J. V (1993) 'NDC10: A gene involved in chromosome segregation in Saccharomyces cerevisiae', *Journal of Cell Biology*, 121(3), pp. 503–512. doi: 10.1083/jcb.121.3.503.

Goloborodko, A. *et al.* (2016) 'Compaction and segregation of sister chromatids via active loop extrusion', *eLife*, 5(MAY2016). doi: 10.7554/eLife.14864.

Goshima, G. and Yanagida, M. (2000) 'Establishing Biorientation Occurs with Precocious Separation of the Sister Kinetochores, but Not the Arms, in the Early Spindle of Budding Yeast', *Cell*, 100(6), pp. 619–633. doi: 10.1016/S0092-8674(00)80699-6.

Goto, T. and Wang, J. C. (1982) 'Yeast DNA topoisomerase II. An ATP-dependent type II topoisomerase that catalyzes the catenation, decatenation, unknotting, and relaxation of double-stranded DNA rings.', *Journal of Biological Chemistry*, 257(10), pp. 5866–5872.

Goto, T. and Wang, J. C. (1984) 'Yeast DNA topoisomerase II is encoded by a single-copy, essential gene.', *Cell*, 36(4), pp. 1073–80. doi: 0092-8674(84)90057-6 [pii].

Granot, D. and Snyder, M. (1991) 'Segregation of the nucleolus during mitosis in budding and fission yeast', *Cell Motility and the Cytoskeleton*, 20(1), pp. 47–54. doi: 10.1002/cm.970200106.

Gruber, S. *et al.* (2006) 'Evidence that Loading of Cohesin Onto Chromosomes Involves Opening of Its SMC Hinge', *Cell*, 127(3), pp. 523–537. doi: 10.1016/j.cell.2006.08.048.

Gruber, S., Haering, C. H. and Nasmyth, K. (2003) 'Chromosomal cohesin forms a ring', *Cell*, 112(6), pp. 765–777. doi: 10.1016/S0092-8674(03)00162-4.

Guacci, V., Koshland, D. and Strunnikov, A. (1997) 'A direct link between sister chromatid cohesion and chromosome condensation revealed through the analysis of MCD1 in S. cerevisiae.', *Cell*. NIH Public Access, 91(1), pp. 47–57. doi: 10.1016/S0092-8674(01)80008-8.

Hadjur, S. *et al.* (2009) 'Cohesins form chromosomal cis-interactions at the developmentally regulated IFNG locus', *Nature*, 460(7253), pp. 410–413. doi: 10.1038/nature08079.

Haering, C. H. *et al.* (2002) 'Molecular architecture of SMC proteins and the yeast cohesin complex', *Molecular Cell*, 9(4), pp. 773–788. doi: 10.1016/S1097-2765(02)00515-4.

Haering, C. H. *et al.* (2008) 'The cohesin ring concatenates sister DNA molecules', *Nature*, 454(7202), pp. 297–301. doi: 10.1038/nature07098.

Harmon, F. G., DiGate, R. J. and Kowalczykowski, S. C. (1999) 'RecQ helicase and topoisomerase III comprise a novel DNA strand passage function: A conserved mechanism for control of DNA recombination', *Molecular Cell*, 3(5), pp. 611–620. doi: 10.1016/S1097-2765(00)80354-8.

Hartwell, L. H. *et al.* (1973) 'Genetic control of the cell division cycle in yeast: V. Genetic analysis of cdc mutants', *Genetics*, pp. 267–286. doi: 74(2): 267–286.

Hartwell, L. H. and Weinert, T. (1989) 'Checkpoints: controls that ensure the order of cell cycle events', *Science*, 246(4930), pp. 629–634. doi: 10.1126/science.2683079.

He, X., Asthana, S. and Sorger, P. K. (2000) 'Transient Sister Chromatid Separation and Elastic Deformation of Chromosomes during Mitosis in Budding Yeast', *Cell*, 101(7), pp. 763–775. doi: 10.1016/S0092-8674(00)80888-0.

Higuchi, T. and Uhlmann, F. (2005) 'Stabilization of microtubule dynamics at anaphase onset promotes chromosome segregation', *Nature*, 433(7022), pp. 171–176. doi: 10.1038/nature03240.

Hildebrandt, E. R. *et al.* (2006) 'Homotetrameric form of Cin8p, a Saccharomyces cerevisiae kinesin-5 motor, is essential for its in Vivo function', *Journal of Biological Chemistry*, 281(36), pp. 26004–26013. doi: 10.1074/jbc.M604817200.

Hildebrandt, E. R. and Hoyt, M. A. (2001) 'Cell cycle-dependent degradation of the Saccharomyces cerevisiae spindle motor Cin8p requires APC(Cdh1) and a bipartite destruction sequence.', *Molecular biology of the cell*, 12(11), pp. 3402–16. doi: 10.1091/mbc.12.11.3402.

Hirano, T. (2006) 'At the heart of the chromosome: SMC proteins in action', *Nature Reviews Molecular Cell Biology*, pp. 311–322. doi: 10.1038/nrm1909.

Holm, C. *et al.* (1985) 'DNA topoisomerase II is required at the time of mitosis in yeast', *Cell*, 41(2), pp. 553–563. doi: 10.1016/S0092-8674(85)80028-3.

Hornig, N. C. D. *et al.* (2002) 'The dual mechanism of separase regulation by securin', *Current Biology*, 12(12), pp. 973–982. doi: 10.1016/S0960-9822(02)00847-3.

Hu, F. *et al.* (2001) 'Regulation of the Bub2/Bfa1 GAP complex by Cdc5 and cell cycle checkpoints', *Cell*, 107(5), pp. 655–665. doi: 10.1016/S0092-8674(01)00580-3.

Indjeian, V. B. and Murray, A. W. (2007) 'Budding Yeast Mitotic Chromosomes Have an Intrinsic Bias to Biorient on the Spindle', *Current Biology*, 17(21), pp. 1837–1846. doi: 10.1016/j.cub.2007.09.056.

Ip, S. C. Y. *et al.* (2008) 'Identification of Holliday junction resolvases from humans and yeast', *Nature*. Nature Publishing Group, 456(7220), pp. 357–361. doi: 10.1038/nature07470.

Ira, G. *et al.* (2003) 'Srs2 and Sgs1-Top3 Suppress Crossovers during Double-Strand Break Repair in Yeast', *Cell*, 115(4), pp. 401–411. doi: 10.1016/S0092-8674(03)00886-9.

Ivanov, D. and Nasmyth, K. (2005) 'A topological interaction between cohesin rings and a circular minichromosome', *Cell*, 122(6), pp. 849–860. doi: 10.1016/j.cell.2005.07.018.

Ivanov, D. and Nasmyth, K. (2007) 'A Physical Assay for Sister Chromatid Cohesion In Vitro', *Molecular Cell*, 27(2), pp. 300–310. doi: 10.1016/j.molcel.2007.07.002.

Izawa, D. and Pines, J. (2015) 'The mitotic checkpoint complex binds a second CDC20 to inhibit active APC/C', *Nature*, 517(7536), pp. 631–634. doi: 10.1038/nature13911.

Jaspersen, S. L. *et al.* (1998) 'A late mitotic regulatory network controlling cyclin destruction in Saccharomyces cerevisiae.', *Molecular biology of the cell*. American Society for Cell Biology, 9(10), pp. 2803–2817. doi: 10.1091/mbc.9.10.2803.

Jaspersen, S. L., Charles, J. F. and Morgan, D. O. (1999) 'Inhibitory phosphorylation of the APC regulator Hct1 is controlled by the kinase Cdc28 and the phosphatase Cdc14', *Current Biology*, 9(5), pp. 227–236. doi: 10.1016/S0960-9822(99)80111-0.

Jensen, S. *et al.* (2001) 'A novel role of the budding yeast separin Esp1 in anaphase spindle elongation: Evidence that proper spindle association of Esp1 is regulated by Pds1', *Journal of Cell Biology*, 152(1), pp. 27–40. doi: 10.1083/jcb.152.1.27.

Johzuka, K. and Horiuchi, T. (2009) 'The cis Element and Factors Required for Condensin Recruitment to Chromosomes', *Molecular Cell*, 34(1), pp. 26–35. doi: 10.1016/j.molcel.2009.02.021.

Jorgensen, P. *et al.* (2007) 'The Size of the Nucleus Increases as Yeast Cells Grow', *Molecular biology of the cell*, 18(9), pp. 3523–32. doi: 10.1091/mbc.E06-10-0973.

Juang, Y. L. *et al.* (1997) 'APC-mediated proteolysis of Ase1 and the morphogenesis of the mitotic spindle', *Science*, 275(5304), pp. 1311–1314. doi: 10.1126/science.275.5304.1311.

Kakui, Y. *et al.* (2017) 'Condensin-mediated remodeling of the mitotic chromatin landscape in fission yeast',

Nature Genetics, 49(10), pp. 1553–1557. doi: 10.1038/ng.3938.

Kakui, Y. and Uhlmann, F. (2017a) 'Building chromosomes without bricks', *Science*, 356(6344). doi: 10.1126/science.aan8090.

Kakui, Y. and Uhlmann, F. (2017b) 'SMC complexes orchestrate the mitotic chromatin interaction landscape', *Current Genetics*, pp. 1–5. doi: 10.1007/s00294-017-0755-y.

Kaliraman, V. *et al.* (2001) 'Functional overlap between Sgs1-Top3 and the Mms4-Mus81 endonuclease', *Genes and Development*, 15(20), pp. 2730–2740. doi: 10.1101/gad.932201.

Kanno, T., Berta, D. G. and Sjögren, C. (2015) 'The Smc5/6 Complex Is an ATP-Dependent Intermolecular DNA Linker', *Cell Reports*, 12(9), pp. 1471–1482. doi: 10.1016/j.celrep.2015.07.048.

Keszthelyi, A., Minchell, N. E. and Baxter, J. (2016) 'The causes and consequences of topological stress during DNA replication', *Genes*, 7(12). doi: 10.3390/genes7120134.

Khmelinskii, A. *et al.* (2007) 'Cdc14-regulated midzone assembly controls anaphase B', *Journal of Cell Biology*, 177(6), pp. 981–993. doi: 10.1083/jcb.200702145.

Khmelinskii, A. *et al.* (2009) 'Phosphorylation-Dependent Protein Interactions at the Spindle Midzone Mediate Cell Cycle Regulation of Spindle Elongation', *Developmental Cell*, 17(2), pp. 244–256. doi: 10.1016/j.devcel.2009.06.011.

Kitada, K. *et al.* (1993) 'A multicopy suppressor gene of the Saccharomyces cerevisiae G1 cell cycle mutant gene dbf4 encodes a protein kinase and is identified as CDC5.', *Molecular and cellular biology*, 13(7), pp. 4445–4457. doi: 10.1128/MCB.13.7.4445.Updated.

Krenn, V. and Musacchio, A. (2015) 'The Aurora B Kinase in Chromosome Bi-Orientation and Spindle Checkpoint Signaling', *Frontiers in Oncology*, 5(October). doi: 10.3389/fonc.2015.00225.

Kschonsak, M. *et al.* (2017) 'Structural Basis for a Safety-Belt Mechanism That Anchors Condensin to Chromosomes', *Cell*, 171(3), p. 588–600.e24. doi: 10.1016/j.cell.2017.09.008.

Lavoie, B. D., Hogan, E. and Koshland, D. (2002) 'In vivo dissection of the chromosome condensation machinery: Reversibility of condensation distinguishes contributions of condensin and cohesin', *Journal of Cell Biology*. The Rockefeller University Press, 156(5), pp. 805–815. doi: 10.1083/jcb.200109056.

Lavoie, B. D., Hogan, E. and Koshland, D. (2004) 'In vivo requirements for rDNA chromosome condensation reveal two cell-cycle-regulated pathways for mitotic chromosome folding', *Genes and Development*. Cold Spring Harbor Laboratory Press, 18(1), pp. 76–87. doi: 10.1101/gad.1150404.

Lavrukhin, O. V *et al.* (2000) 'Topoisomerase II from Chlorella Virus PBCV-1 CHARACTERIZATION OF THE SMALLEST KNOWN TYPE II TOPOISOMERASE*'.

Lazar-Stefanita, L. *et al.* (2017) 'Cohesins and condensins orchestrate the 4D dynamics of yeast chromosomes during the cell cycle', *The EMBO Journal*, p. e201797342. doi: 10.15252/embj.201797342.

Lengronne, A. *et al.* (2004) 'Cohesin relocation from sites of chromosomal loading to places of convergent transcription', *Nature*, 430(6999), pp. 573–578. doi: 10.1038/nature02742.

Leonard, J. *et al.* (2015) 'Condensin Relocalization from Centromeres to Chromosome Arms Promotes Top2 Recruitment during Anaphase', *Cell Reports*, 13(11), pp. 2336–2344. doi: 10.1016/j.celrep.2015.11.041.

Li, H., Wang, Y. and Liu, X. (2008) 'Plk1-dependent phosphorylation regulates functions of DNA topoisomerase II?? in cell cycle progression', *Journal of Biological Chemistry*. in Press, 283(10), pp. 6209–6221. doi: 10.1074/jbc.M709007200.

Li, Y. *et al.* (2010) 'Escherichia coli condensin MukB stimulates topoisomerase IV activity by a direct physical interaction.', *Proceedings of the National Academy of Sciences of the United States of America*, 107(44), pp. 18832–18837. doi: 10.1073/pnas.1008678107.

Li, Y. and Elledge, S. J. (2003) 'The DASH complex component Ask1 is a cell cycle-regulated Cdk substrate in Saccharomyces cerevisiae.', *Cell cycle (Georgetown, Tex.)*, 2(2), pp. 143–148. doi: 10.4161/cc.2.2.336.

Li, Y. Y. *et al.* (1993) 'Disruption of mitotic spindle orientation in a yeast dynein mutant', *Proc Natl Acad Sci U S A*, 90(21), pp. 10096–10100. doi: 10.1073/pnas.90.21.10096.

Liberi, G. *et al.* (2005) 'Rad51-dependent DNA structures accumulate at damaged replication forks in sgs1 mutants defective in the yeast ortholog of BLM RecQ helicase', *Genes & Development*, 19(3), pp. 339–350. doi: 10.1101/gad.322605.

Lieberman-Aiden, E. *et al.* (2009) 'Comprehensive Mapping of Long-Range Interactions Reveals Folding Principles of the Human Genome', *Science*. American Association for the Advancement of Science, 326(5950), pp. 289–293. doi: 10.1126/science.1181369.

Litwin, I. and Wysocki, R. (2017) 'New insights into cohesin loading', *Current Genetics*, pp. 1–9. doi: 10.1007/s00294-017-0723-6.

Liu, D. *et al.* (2010) 'Regulated targeting of protein phosphatase 1 to the outer kinetochore by KNL1 opposes Aurora B kinase', *Journal of Cell Biology*, 188(6), pp. 809–820. doi: 10.1083/jcb.201001006.

London, N. *et al.* (2012) 'Phosphoregulation of Spc105 by Mps1 and PP1 regulates Bub1 localization to kinetochores', *Current Biology*, 22(10), pp. 900–906. doi: 10.1016/j.cub.2012.03.052.

London, N. and Biggins, S. (2014) 'Mad1 kinetochore recruitment by Mps1-mediated phosphorylation of Bub1 signals the spindle checkpoint', *Genes and Development*, 28(2), pp. 140–152. doi: 10.1101/gad.233700.113.

Longtine, M. S. *et al.* (1998) 'Additional modules for versatile and economical PCR-based gene deletion and modification in Saccharomyces cerevisiae', *Yeast*. John Wiley & Sons, Ltd., 14(10), pp. 953–961. doi: 10.1002/(SICI)1097-0061(199807)14:10<953::AID-YEA293>3.0.CO;2-U.

Losada, A., Hirano, M. and Hirano, T. (1998) 'Identification of Xenopus SMC protein complexes required for sister chromatid cohesion', *Genes and Development*. Cold Spring Harbor Laboratory Press, 12(13), pp. 1986–1997. doi: 10.1101/gad.12.13.1986.

Lu, Y. and Cross, F. R. (2010) 'Periodic cyclin-cdk activity entrains an autonomous cdc14 release oscillator', *Cell*, 141(2), pp. 268–279. doi: 10.1016/j.cell.2010.03.021.

Machín, F. *et al.* (2005) 'Spindle-independent condensation-mediated segregation of yeast ribosomal DNA in late anaphase', *Journal of Cell Biology*, 168(2), pp. 209–219. doi: 10.1083/jcb.200408087.

Mah, A. S., Jang, J. and Deshaies, R. J. (2001) 'Protein kinase Cdc15 activates the Dbf2-Mob1 kinase complex', *Proceedings of the National Academy of Sciences*, 98(13), pp. 7325–7330. doi: 10.1073/pnas.141098998.

Mankouri, H. W., Huttner, D. and Hickson, I. D. (2013) 'How unfinished business from S-phase affects mitosis and beyond', *EMBO Journal*, pp. 2661–2671. doi: 10.1038/emboj.2013.211.

Manzoni, R. *et al.* (2010) 'Oscillations in Cdc14 release and sequestration reveal a circuit underlying mitotic exit', *Journal of Cell Biology*, 190(2), pp. 209–222. doi: 10.1083/jcb.201002026.

Mapelli, M. and Musacchio, A. (2007) 'MAD contortions: conformational dimerization boosts spindle checkpoint signaling', *Current Opinion in Structural Biology*, pp. 716–725. doi: 10.1016/j.sbi.2007.08.011.

Marston, A. L. (2014) 'Chromosome segregation in budding yeast: Sister chromatid cohesion and related mechanisms', *Genetics*, 196(1), pp. 31–63. doi: 10.1534/genetics.112.145144.

Matos, J. *et al.* (2011) 'Regulatory control of the resolution of DNA recombination intermediates during meiosis and mitosis', *Cell*. Elsevier Inc., 147(1), pp. 158–172. doi: 10.1016/j.cell.2011.08.032.

Matos, J., Blanco, M. G. and West, S. C. (2013) 'Cell-Cycle Kinases Coordinate the Resolution of Recombination Intermediates with Chromosome Segregation', *Cell Reports*, 4(1), pp. 76–86. doi: 10.1016/j.celrep.2013.05.039.

Matos, J. and West, S. C. (2014) 'Holliday junction resolution: Regulation in space and time', *DNA Repair*. Elsevier, 19, pp. 176–181. doi: 10.1016/j.dnarep.2014.03.013.

Megee, P. C. *et al.* (1999) 'The centromeric sister chromatid cohesion site directs Mcd1p binding to adjacent sequences', *Molecular Cell*, 4(3), pp. 445–450. doi: 10.1016/S1097-2765(00)80347-0.

Mendoza, M. *et al.* (2009) 'A mechanism for chromosome segregation sensing by the NoCut checkpoint', *Nature Cell Biology*, 11(4), pp. 477–483. doi: 10.1038/ncb1855.

Merz, K. *et al.* (2008) 'Actively transcribed rRNA genes in S. cerevisiae are organized in a specialized chromatin associated with the high-mobility group protein Hmo1 and are largely devoid of histone molecules', *Genes and Development*, 22(9), pp. 1190–1204. doi: 10.1101/gad.466908.

Michaelis, C., Ciosk, R. and Nasmyth, K. (1997) 'Cohesins: Chromosomal proteins that prevent premature separation of sister chromatids', *Cell*, 91(1), pp. 35–45. doi: 10.1016/S0092-8674(01)80007-6.

Miller, R. K. and Rose, M. D. (1998) 'Kar9p is a novel cortical protein required for cytoplasmic microtubule orientation in yeast', *Journal of Cell Biology*, 140(2), pp. 377–390. doi: 10.1083/jcb.140.2.377.

Mohl, D. A. *et al.* (2009) 'Dbf2-Mob1 drives relocalization of protein phosphatase Cdc14 to the cytoplasm during exit from mitosis', *Journal of Cell Biology*, 184(4), pp. 527–539. doi: 10.1083/jcb.200812022.

Moore, J. K., Li, J. and Cooper, J. A. (2008) 'Dynactin function in mitotic spindle positioning', *Traffic*, 9(4), pp. 510–527. doi: 10.1111/j.1600-0854.2008.00710.x.

Morgan, D. O. (2007) *The cell cycle : principles of control*. New Science Press.

Movshovich, N. *et al.* (2008) 'Slk19-dependent mid-anaphase pause in kinesin-5-mutated cells', *Journal of Cell Science*, 121(15), pp. 2529–2539. doi: 10.1242/jcs.022996.

Murayama, Y. and Uhlmann, F. (2014) 'Biochemical reconstitution of topological DNA binding by the cohesin ring', *Nature*. Nature Publishing Group, 505(7483), pp. 367–371. doi: 10.1038/nature12867.

Murayama, Y. and Uhlmann, F. (2015) 'DNA Entry into and Exit out of the Cohesin Ring by an Interlocking Gate Mechanism', *Cell*, 163(7), pp. 1628–1640. doi: 10.1016/j.cell.2015.11.030.

Musacchio, A. (2015) 'The Molecular Biology of Spindle Assembly Checkpoint Signaling Dynamics', *Current Biology*, pp. R1002–R1018. doi: 10.1016/j.cub.2015.08.051.

Musacchio, A. and Salmon, E. D. (2007) 'The spindle-assembly checkpoint in space and time', *Nature Reviews Molecular Cell Biology*. Nature Publishing Group, pp. 379–393. doi: 10.1038/nrm2163.

Nasmyth, K. (2001) 'Disseminating the Genome: Joining, Resolving, and Separating Sister Chromatids During Mitosis and Meiosis', *Annual Review of Genetics*, 35(1), pp. 673–745. doi: 10.1146/annurev.genet.35.102401.091334.

Naumova, N. *et al.* (2013) 'Organization of the mitotic chromosome', *Science*, 342(6161), pp. 948–953. doi: 10.1126/science.1236083.

Neurohr, G. *et al.* (2011) 'A Midzone-Based Ruler Adjusts Chromosome Compaction to Anaphase Spindle Length', *Science*, 1037(April), pp. 465–468. doi: 10.1126/science.1201578.

Nezi, L. *et al.* (2006) 'Accumulation of Mad2-Cdc20 complex during spindle checkpoint activation requires binding of open and closed conformers of Mad2 in Saccharomyces cerevisiae', *Journal of Cell Biology*, 174(1), pp. 39–51. doi: 10.1083/jcb.200602109.

Ng, T. M. *et al.* (2009) 'Pericentromeric sister chromatid cohesion promotes kinetochore biorientation.', *Molecular biology of the cell*, 20(17), pp. 3818–27. doi: 10.1091/mbc.E09-04-0330.

Nishimura, K. *et al.* (2009) 'An auxin-based degron system for the rapid depletion of proteins in nonplant cells', *Nature Methods*, 6(12), pp. 917–922. doi: 10.1038/nmeth.1401.

Nitiss, J. L. (2009) 'DNA topoisomerase II and its growing repertoire of biological functions', *Nature Reviews Cancer*, pp. 327–337. doi: 10.1038/nrc2608.

Norden, C. *et al.* (2006) 'The NoCut Pathway Links Completion of Cytokinesis to Spindle Midzone Function to Prevent Chromosome Breakage', *Cell*, 125(1), pp. 85–98. doi: 10.1016/j.cell.2006.01.045.

Ocampo-Hafalla, M. T. *et al.* (2016) 'Evidence for cohesin sliding along budding yeast chromosomes', *Open Biology*, 6(6), p. 150178. doi: 10.1098/rsob.150178.

Ölmezer, G. *et al.* (2016) 'Replication intermediates that escape Dna2 activity are processed by Holliday junction resolvase Yen1', *Nature Communications*. Nature Publishing Group, 7, p. 13157. doi: 10.1038/ncomms13157.

Park, C. J. *et al.* (2003) 'Loss of CDC5 function in Saccharomyces cerevisiae leads to defects in Swe1p

regulation and Bfa1p/Bub2p-independent cytokinesis', *Genetics*, 163(1), pp. 21–33. doi: 10.1182/blood-2011-08-374363.

Paulson, J. R. and Laemmli, U. K. (1977) 'The structure of histone-depleted metaphase chromosomes', *Cell*, 12(3), pp. 817–828. doi: 10.1016/0092-8674(77)90280-X.

Paweletz, N. (2001) 'Walther Flemming: pioneer of mitosis research.', *Nature reviews. Molecular cell biology*, 2(1), pp. 72–75. doi: 10.1038/35048077.

Pearson, C. G. *et al.* (2001) 'Budding Yeast Chromosome Structure and Dynamics during Mitosis', *The Journal of Cell Biology*, 152(6), pp. 1255–1266.

Peeper, D. S. *et al.* (1993) 'A- and B-type cyclins differentially modulate substrate specificity of cyclin-cdk complexes.', *The EMBO journal*, 12(5), pp. 1947–1954.

Pereira, G. and Schiebel, E. (2003) 'Separase Regulates INCENP-Aurora B Anaphase Spindle Function Through Cdc14', *Science*, 302(5653), pp. 2120–2124. doi: 10.1126/science.1091936.

Piatti, S. *et al.* (2006) 'The spindle position checkpoint in budding yeast: The motherly care of MEN', *Cell Division*, p. 2. doi: 10.1186/1747-1028-1-2.

Piazza, I. *et al.* (2014) 'Association of condensin with chromosomes depends on DNA binding by its HEAT-repeat subunits', *Nature Structural and Molecular Biology*, 21(6), pp. 560–568. doi: 10.1038/nsmb.2831.

Piazza, I., Haering, C. H. and Rutkowska, A. (2013) 'Condensin: Crafting the chromosome landscape', *Chromosoma*, pp. 175–190. doi: 10.1007/s00412-013-0405-1.

Piskadlo, E., Tavares, A. and Oliveira, R. A. (2017) 'Metaphase chromosome structure is dynamically maintained by condensin I-directed DNA (de)catenation', *eLife*, 6. doi: 10.7554/eLife.26120.

Postow, L. *et al.* (2001) 'Topological challenges to DNA replication: Conformations at the fork', *Proceedings of the National Academy of Sciences*. National Academy of Sciences, 98(15), pp. 8219–8226. doi: 10.1073/pnas.111006998.

Princz, L. N. *et al.* (2017) 'Dbf4-dependent kinase and the Rtt107 scaffold promote Mus81-Mms4 resolvase activation during mitosis', *The EMBO Journal*, 36, p. e201694831. doi: 10.15252/embj.201694831.

Queralt, E. *et al.* (2006) 'Downregulation of PP2ACdc55 Phosphatase by Separase Initiates Mitotic Exit in Budding Yeast', *Cell*, 125(4), pp. 719–732. doi: 10.1016/j.cell.2006.03.038.

Queralt, E. and Uhlmann, F. (2008) 'Separase cooperates with Zds1 and Zds2 to activate Cdc14 phosphatase in early anaphase', *Journal of Cell Biology*, 182(5), pp. 873–883. doi: 10.1083/jcb.200801054.

Rahal, R. and Amon, A. (2008) 'The polo-like kinase Cdc5 interacts with FEAR network components and Cdc14', *Cell Cycle*, 7(20), pp. 3262–3272. doi: 6852 [pii].

Renshaw, M. J. *et al.* (2010) 'Condensins promote chromosome recoiling during early anaphase to complete sister chromatid separation', *Developmental Cell*, 19(2), pp. 232–244. doi: 10.1016/j.devcel.2010.07.013.

Rieder, C. L. *et al.* (1995) 'The checkpoint delaying anaphase in response to chromosome monoorientation is mediated by an inhibitory signal produced by unattached kinetochores', *Journal of Cell Biology*, 130(4), pp. 941–948. doi: 10.1083/jcb.130.4.941.

Robellet, X. *et al.* (2015) 'A high-sensitivity phospho-switch triggered by Cdk1 governs chromosome morphogenesis during cell division', *Genes and Development*, 29(4). doi: 10.1101/gad.253294.114.

Roca, J. *et al.* (1996) 'DNA transport by a type II topoisomerase: direct evidence for a two-gate mechanism.', *Proceedings of the National Academy of Sciences of the United States of America*, 93(9), pp. 4057–4062. doi: 10.1073/pnas.93.9.4057.

Roca, J. and Wang, J. C. (1992) 'The capture of a DNA double helix by an ATP-dependent protein clamp: A key step in DNA transport by type II DNA topoisomerases', *Cell*, 71(5), pp. 833–840. doi: 10.1016/0092-8674(92)90558-T.

Roca, J. and Wang, J. C. (1994) 'DNA transport by a type II DNA topoisomerase: Evidence in favor of a two-gate mechanism', *Cell*, 77(4), pp. 609–616. doi: 10.1016/0092-8674(94)90222-4.

Roccuzzo, M. (2013) *Regulation of chromosome segregation by conserved phosphatase Cdc14 and kinase Cdc5*.

Roccuzzo, M. *et al.* (2015) 'FEAR-mediated activation of Cdc14 is the limiting step for spindle elongation and anaphase progression', *Nature Cell Biology*, 17(3), pp. 251–261. doi: 10.1038/ncb3105.

Rock, J. M. and Amon, A. (2009) 'The FEAR network', *Current Biology*. doi: 10.1016/j.cub.2009.10.002.

Roof, D. M., Meluh, P. B. and Rose, M. D. (1992) 'Kinesin-related proteins required for assembly of the mitotic spindle.', *The Journal of cell biology*, 118(I), pp. 95–108. doi: 10.1083/jcb.118.1.95.

Roostalu, J. *et al.* (2011) 'Directional switching of the kinesin Cin8 through motor coupling', *Science*, 332(6025), pp. 94–99. doi: 10.1126/science.1199945.

Ross, K. E. and Cohen-Fix, O. (2004) 'A role for the FEAR pathway in nuclear positioning during anaphase', *Developmental Cell*, 6(5), pp. 729–735. doi: 10.1016/S1534-5807(04)00128-5.

Rowland, B. D. *et al.* (2009) 'Building Sister Chromatid Cohesion: Smc3 Acetylation Counteracts an Antiestablishment Activity', *Molecular Cell*, 33(6), pp. 763–774. doi: 10.1016/j.molcel.2009.02.028.

Ruchaud, S., Carmena, M. and Earnshaw, W. C. (2007) 'Chromosomal passengers: Conducting cell division', *Nature Reviews Molecular Cell Biology*, pp. 798–812. doi: 10.1038/nrm2257.

Rybenkov, V. V *et al.* (1997) 'Simplification of DNA topology below equilibrium values by type II topoisomerases', *Science*, 277(5326), pp. 690–693. doi: 10.1126/science.277.5326.690.

Sakai, A. *et al.* (2003) 'Condensin but not cohesin SMC heterodimer induces DNA reannealing through protein-protein assembly', *EMBO Journal*, 22(11), pp. 2764–2775. doi: 10.1093/emboj/cdg247.

Saunders, W. S. *et al.* (1995) 'Saccharomycescerevisiae kinesin- and dynein-related protein required for anaphase chromosome segregation', *J. Cell Biol.*, 128(4), pp. 617–624. doi: 10.1083/jcb.128.4.617.

Saunders, W. S. and Hoyt, M. A. (1992) 'Kinesin-Related Proteins Required for Structural Integrity of the Mitotic Spindle', *Cell*, 70(3), pp. 451–458. doi: 10.1016/0092-8674(92)90169-D.

Schalbetter, S. A. *et al.* (2015) 'Fork rotation and DNA precatenation are restricted during DNA replication to prevent chromosomal instability', *Proceedings of the National Academy of Sciences*, 112(33), pp. E4565–E4570. doi: 10.1073/pnas.1505356112.

Schalbetter, S. A. *et al.* (2017) 'SMC complexes differentially compact mitotic chromosomes according to genomic context', *Nature Cell Biology*, 19(9), pp. 1071–1080. doi: 10.1038/ncb3594.

Schmidt, B. H., Osheroff, N. and Berger, J. M. (2012) 'Structure of a topoisomerase II-DNA-nucleotide complex reveals a new control mechanism for ATPase activity', *Nat Struct Mol Biol*, 19(11), pp. 1147–1154. doi: 10.1038/nsmb.2388.

Schuyler, S. C., Liu, J. Y. and Pellman, D. (2003) 'The molecular function of Ase1p: Evidence for a MAP-dependent midzone-specific spindle matrix', *Journal of Cell Biology*, 160(4), pp. 517–528. doi: 10.1083/jcb.200210021.

Schwab, M., Lutum, A. S. and Seufert, W. (1997) 'Yeast Hct1 is a regulator of Cib2 cyclin proteolysis', *Cell*, 90(4), pp. 683–693. doi: 10.1016/S0092-8674(00)80529-2.

Schwartz, E. K. *et al.* (2012) 'Mus81-Mms4 Functions as a Single Heterodimer To Cleave Nicked Intermediates in Recombinational DNA Repair', *Molecular and Cellular Biology*, 32(15), pp. 3065–3080. doi: 10.1128/MCB.00547-12.

Sczaniecka, M. *et al.* (2008) 'The spindle checkpoint functions of Mad3 and Mad2 depend on a Mad3 KEN box-mediated interaction with Cdc20-anaphase-promoting complex (APC/C)', *Journal of Biological Chemistry*, 283(34), pp. 23039–23047. doi: 10.1074/jbc.M803594200.

Sen, N. *et al.* (2016) 'Physical Proximity of Sister Chromatids Promotes Top2-Dependent Intertwining', *Molecular Cell*, 64(1), pp. 134–147. doi: 10.1016/j.molcel.2016.09.007.

Shapira, O. *et al.* (2017) 'A potential physiological role for bi-directional motility and motor clustering of mitotic kinesin-5 Cin8 in yeast mitosis', *Journal of Cell Science*, 130(4), pp. 725–734. doi: 10.1242/jcs.195040.

Shaw, S. L. *et al.* (1997) 'Astral microtubule dynamics in yeast: A microtubule-based searching mechanism for spindle orientation and nuclear migration into the bud', *Journal of Cell Biology*, 139(4), pp. 985–994. doi: 10.1083/jcb.139.4.985.

Shintomi, K. *et al.* (2017) 'Mitotic chromosome assembly despite nucleosome depletion in Xenopus egg extracts', *Science*, 356(6344), pp. 1–5.

Shintomi, K., Takahashi, T. S. and Hirano, T. (2015) 'Reconstitution of mitotic chromatids with a minimum set of purified factors', *Nature Cell Biology*, 17(8), pp. 1014–1023. doi: 10.1038/ncb3187.

Shirayama, M. *et al.* (1999) 'APC(Cdc20) promotes exit from mitosis by destroying the anaphase inhibitor Pds1 and cyclin Clb5', *Nature*, 402(6758), pp. 203–207. doi: 10.1038/46080.

Shou, W. *et al.* (1999) 'Exit from mitosis is triggered by Tem1-dependent release of the protein phosphatase Cdc14 from nucleolar RENT complex', *Cell*, 97(2), pp. 233–244. doi: 10.1016/S0092-8674(00)80733-3.

Shou, W. *et al.* (2002) 'Cdc5 influences phosphorylation of Net1 and disassembly of the RENT complex', *BMC Molecular Biology*, 3, p. 3. doi: 10.1186/1471-2199-3-3.

Sjögren, C. and Nasmyth, K. (2001) 'Sister chromatid cohesion is required for postreplicative double-strand break repair in Saccharomyces cerevisiae', *Current Biology*, 11(12), pp. 991–995. doi: 10.1016/S0960-9822(01)00271-8.

Snead, J. L. *et al.* (2007) 'A Coupled Chemical-Genetic and Bioinformatic Approach to Polo-like Kinase Pathway Exploration'. doi: 10.1016/j.chembiol.2007.09.011.

St-Pierre, J. *et al.* (2009) 'Polo Kinase Regulates Mitotic Chromosome Condensation by Hyperactivation of Condensin DNA Supercoiling Activity', *Molecular Cell*, 34(4), pp. 416–426. doi: 10.1016/j.molcel.2009.04.013.

Stegmeier, F. *et al.* (2004) 'The replication fork block protein Fob1 functions as a negative regulator of the FEAR network', *Current Biology*, 14(6), pp. 467–480. doi: 10.1016/j.cub.2004.03.009.

Stegmeier, F. and Amon, A. (2004) 'Closing Mitosis: The Functions of the Cdc14 Phosphatase and Its Regulation', *Annual Review of Genetics*, 38(1), pp. 203–232. doi: 10.1146/annurev.genet.38.072902.093051.

Stegmeier, F., Visintin, R. and Amon, A. (2002) 'Separase, polo kinase, the kinetochore protein Slk19, and Spo12 function in a network that controls Cdc14 localization during early anaphase', *Cell*, 108(2), pp. 207–220. doi: 10.1016/S0092-8674(02)00618-9.

Steigemann, P. *et al.* (2009) 'Aurora B-Mediated Abscission Checkpoint Protects against Tetraploidization', *Cell*, 136(3), pp. 473–484. doi: 10.1016/j.cell.2008.12.020.

Straight, A. F., Sedat, J. W. and Murray, A. W. (1998) 'Time-lapse microscopy reveals unique roles for kinesins during anaphase in budding yeast', *Journal of Cell Biology*, 143(3), pp. 687–694. doi: 10.1083/jcb.143.3.687.

Stuchinskaya, T. *et al.* (2009) 'How Do Type II Topoisomerases Use ATP Hydrolysis to Simplify DNA Topology beyond Equilibrium? Investigating the Relaxation Reaction of Nonsupercoiling Type II Topoisomerases', *Journal of Molecular Biology*, 385(5), pp. 1397–1408. doi: 10.1016/j.jmb.2008.11.056.

Sudakin, V. *et al.* (1995) 'The Cyclosome, a Large Complex Containing Cyclin-Selective Ubiquitin Ligase Activity, Targets Cyclins for Destruction at the End of Mitosis', *Molecular Biology of the Cell*. American Society for Cell Biology, 6(2), pp. 185–197. doi: 10.1091/mbc.6.2.185.

Sullivan, M. *et al.* (2004) 'Cdc14 phosphatase induces rDNA condensation and resolves cohesin-independent cohesion during budding yeast anaphase', *Cell*, 117(4), pp. 471–482. doi: 10.1016/S0092-8674(04)00415-5.

Sullivan, M. and Morgan, D. O. (2007) 'Finishing mitosis, one step at a time', *Nature Reviews Molecular Cell Biology*, pp. 894–903. doi: 10.1038/nrm2276.

Sullivan, M. and Uhlmann, F. (2003) 'A non-proteolytic function of separase links the onset of anaphase to mitotic exit', *Nature Cell Biology*, 5(3), pp. 249–254. doi: 10.1038/ncb940.

Sundin, O. and Varshavsky, A. (1980) 'Terminal stages of SV40 DNA replication proceed via multiply intertwined catenated dimers', *Cell*, 21(1), pp. 103–114. doi: 10.1016/0092-8674(80)90118-X.

Sundin, O. and Varshavsky, A. (1981) 'Arrest of segregation leads to accumulation of highly intertwined catenated dimers: Dissection of the final stages of SV40 DNA replication', *Cell*, 25(3), pp. 659–669. doi: 10.1016/0092-8674(81)90173-2.

Sunkel, C. E. and Glover, D. M. (1988) 'polo, a mitotic mutant of Drosophila displaying abnormal spindle poles.', *Journal of cell science*, 89 (Pt 1), pp. 25–38. doi: 10.1016/j.

Suski, C. and Marians, K. J. (2008) 'Resolution of Converging Replication Forks by RecQ and Topoisomerase III', *Molecular Cell*, 30(6), pp. 779–789. doi: 10.1016/j.molcel.2008.04.020.

Szakal, B. and Branzei, D. (2013) 'Premature Cdk1/Cdc5/Mus81 pathway activation induces aberrant replication and deleterious crossover', *The EMBO Journal*, 32(8), pp. 1155–1167. doi: 10.1038/emboj.2013.67.

Talhaoui, I., Bernal, M. and Mazón, G. (2016) 'The nucleolytic resolution of recombination intermediates in yeast mitotic cells', *FEMS Yeast Research*. doi: 10.1093/femsyr/fow065.

Tanaka, T. *et al.* (1999) 'Identification of cohesin association sites at centromeres and along chromosome arms', *Cell*, 98(6), pp. 847–858. doi: 10.1016/S0092-8674(00)81518-4.

Tanaka, T. *et al.* (2000) 'Cohesin ensures bipolar attachment of microtubules to sister centromeres and resists their precocious separation.', *Nature Cell Biology*, 2(8), pp. 492–499. doi: 10.1038/35019529.

Taxis, C. *et al.* (2009) 'Efficient protein depletion by genetically controlled deprotection of a dormant N-degron', *Molecular Systems Biology*, 5. doi: 10.1038/msb.2009.25.

Terakawa, T. *et al.* (2017) 'The condensin complex is a mechanochemical motor that translocates along DNA', *Science*, p. eaan6516. doi: 10.1126/science.aan6516.

Tomson, B. N. *et al.* (2006) 'Ribosomal DNA Transcription-Dependent Processes Interfere with Chromosome Segregation', *Molecular and Cellular Biology*, 26(16), pp. 6239–6247. doi: 10.1128/MCB.00693-06.

Tomson, B. N. *et al.* (2009) 'Regulation of Spo12 Phosphorylation and Its Essential Role in the FEAR Network', *Current Biology*, 19(6), pp. 449–460. doi: 10.1016/j.cub.2009.02.024.

Torres-Rosell, J. *et al.* (2004) 'Nucleolar segregation lags behind the rest of the genome and requires Cdc14 phosphatase activation by the FEAR network', *Cell Cycle*, 3(4), pp. 496–502. doi: 10.4161/cc.3.4.802.

Toselli-Mollereau, E. *et al.* (2016) 'Nucleosome eviction in mitosis assists condensin loading and chromosome condensation', *The EMBO Journal*, 35(14), pp. 1565–1581. doi: 10.15252/embj.201592849.

Tóth, A. *et al.* (1999) 'Yeast cohesin complex requires a conserved protein, Eco1p(Ctf7), to establish cohesion between sister chromatids during DNA replication', *Genes and Development*, 13(3), pp. 320–333. doi: 10.1101/gad.13.3.320.

Traverso, E. E. *et al.* (2001) 'Characterization of the Net1 Cell Cycle-dependent Regulator of the Cdc14 Phosphatase from Budding Yeast', *Journal of Biological Chemistry*, 276(24), pp. 21924–21931. doi: 10.1074/jbc.M011689200.

Uemura, T. *et al.* (1987) 'DNA topoisomerase II is required for condensation and separation of mitotic chromosomes in S. pombe', *Cell*, 50(6), pp. 917–925. doi: 10.1016/0092-8674(87)90518-6.

Uhlmann, F. *et al.* (2000) 'Cleavage of cohesin by the CD clan protease separin triggers anaphase in yeast.', *Cell*, 103(3), pp. 375–386. doi: 10.1016/S0092-8674(00)00130-6.

Uhlmann, F. (2016) 'SMC complexes: From DNA to chromosomes', *Nature Reviews Molecular Cell Biology*, pp. 399–412. doi: 10.1038/nrm.2016.30.

Uhlmann, F., Lottspelch, F. and Nasmyth, K. (1999) 'Sister-chromatid separation at anaphase onset is promoted by cleavage of the cohesin subunit Scc1', *Nature*, 400(6739), pp. 37–42. doi: 10.1038/21831.

Uhlmann, F. and Nasmyth, K. (1998) 'Cohesion between sister chromatids must be established during DNA replication', *Current Biology*, 8(20), pp. 1095–1102. doi: 10.1016/S0960-9822(98)70463-4.

Varela, E. *et al.* (2009) 'lte1, Cdc14 and MEN-controlled Cdk inactivation in yeast coordinate rDNA decompaction with late telophase progression', *EMBO Journal*, 28(11), pp. 1562–1575. doi:

10.1038/emboj.2009.111.

Visintin, C. *et al.* (2008) 'APC/C-Cdh1-mediated degradation of the Polo kinase Cdc5 promotes the return of Cdc14 into the nucleolus', *Genes and Development*, 22(1), pp. 79–90. doi: 10.1101/gad.1601308.

Visintin, R. (1997) 'CDC20 and CDH1: A Family of Substrate-Specific Activators of APC-Dependent Proteolysis', *Science*, 278(5337), pp. 460–463. doi: 10.1126/science.278.5337.460.

Visintin, R. *et al.* (1998) 'The phosphatase Cdc14 triggers mitotic exit by reversal of Cdk-dependent phosphorylation', *Molecular Cell*, 2(6), pp. 709–718. doi: 10.1016/S1097-2765(00)80286-5.

Visintin, R. and Amon, A. (2001) 'Regulation of the mitotic exit protein kinases Cdc15 and Dbf2.', *Molecular biology of the cell*, 12(10), pp. 2961–2974. doi: 10.1091/mbc.12.10.2961.

Visintin, R., Hwang, E. S. and Amon, A. (1999) 'Cfi 1 prevents premature exit from mitosis by anchoring Cdc14 phosphatase in the nucleolus', *Nature*, 398(6730), pp. 818–823. doi: 10.1038/19775.

Visintin, R., Stegmeier, F. and Amon, A. (2003) 'The Role of the Polo Kinase Cdc5 in Controlling Cdc14 Localization', *Molecular Biology of the Cell*, 14(11), pp. 4486–4498. doi: 10.1091/mbc.E03-02-0095.

Vos, S. M. *et al.* (2011) 'All tangled up: How cells direct, manage and exploit topoisomerase function', *Nature Reviews Molecular Cell Biology*, pp. 827–841. doi: 10.1038/nrm3228.

Wagner, R. P. and Crow, J. F. (2001) 'Requirement for three novel protein complexes in the absence of the Sgs1 DNA helicase in Saccharomyces cerevisiae', *Genetics*, 157(1), pp. 103–118.

Walters, A. D. *et al.* (2014) 'The Yeast Polo Kinase Cdc5 Regulates the Shape of the Mitotic Nucleus', *Current Biology*, 24, pp. 2861–2867. doi: 10.1016/j.cub.2014.10.029.

Wan, J., Xu, H. and Grunstein, M. (1992) 'CDC14 of Saccharomyces cerevisiae. Cloning, sequence analysis, and transcription during the cell cycle.', *The Journal of biological chemistry*, 267(16), pp. 11274–11280. doi: 10.1074/jbc.273.3.1298.

Wang, B.-D. *et al.* (2005) 'Condensin binding at distinct and specific chromosomal sites in the Saccharomyces cerevisiae genome', *Mol Cell Biol*, 25(16), pp. 7216–7225. doi: 10.1128/MCB.25.16.7216-7225.2005.

Wang, B.-D., Yong-Gonzalez, V. and Strunnikov, A. (2004) 'Cdc14p/FEAR pathway controls segregation of nucleolus in S. cerevisiae by facilitating condensin targeting to rDNA chromatin in anaphase', *Cell Cycle*, 3(7), pp. 960–967. doi: 1003 [pii].

Wang, J. C. (2002) 'Cellular Roles Of DNA Topoisomerases: A Molecular Perspective', *Nature*, 3, pp. 430–440. doi: 10.1038/nrm831.

Wang, Y. and Ng, T.-Y. (2006) 'Phosphatase 2A negatively regulates mitotic exit in Saccharomyces cerevisiae.', *Mol Biol Cell*, 17(1), pp. 80–89. doi: 10.1091/mbc.E04-12-1109.

Watson, J. D. and Crick, F. H. C. (1953) 'Genetical implications of the structure of deoxyribonucleic acid.', *Nature*, pp. 964–967. doi: 10.1038/171964b0.

West, R. W. *et al.* (1987) 'GAL1-GAL10 divergent promoter region of Saccharomyces cerevisiae contains negative control elements in addition to functionally separate and possibly overlapping upstream activating sequences.', *Genes & development*, 1(10), pp. 1118–1131. doi: 10.1101/gad.1.10.1118.

Wigley, D. B. *et al.* (1991) 'Crystal structure of an N-terminal fragment of the DNA gyrase B protein.', *Nature*, 351(6328), pp. 624–629. doi: 10.1038/351624a0.

Wilhelm, L. *et al.* (2015) 'SMC condensin entraps chromosomal DNA by an ATP hydrolysis dependent loading mechanism in Bacillus subtilis', *eLife*, 4(MAY). doi: 10.7554/eLife.06659.

Wilkins, B. J. *et al.* (2014) 'A Cascade of Histone Modifications Induces Chromatin Condensation in Mitosis', *Science*, 343(6166), pp. 77–80. doi: 10.1126/science.1244508.

Witkin, K. L. *et al.* (2012) 'The budding yeast nuclear envelope adjacent to the nucleolus serves as a membrane sink during mitotic delay', *Current Biology*, 22(12), pp. 1128–1133. doi: 10.1016/j.cub.2012.04.022.

Woodbury, E. L. and Morgan, D. O. (2007) 'Cdk and APC activities limit the spindle-stabilizing function of Fin1 to anaphase', *Nature Cell Biology*, 9(1), pp. 106–112. doi: 10.1038/ncb1523.

Woodruff, J. B., Drubin, D. G. and Barnes, G. (2010) 'Mitotic spindle disassembly occurs via distinct subprocesses driven by the anaphase-promoting complex, Aurora B kinase, and kinesin-8', *Journal of Cell Biology*, 191(4), pp. 795–808. doi: 10.1083/jcb.201006028.

De Wulf, P., Montani, F. and Visintin, R. (2009) 'Protein phosphatases take the mitotic stage', *Current Opinion in Cell Biology*, pp. 806–815. doi: 10.1016/j.ceb.2009.08.003.

Xu, D. *et al.* (2008) 'RMI, a new OB-fold complex essential for Bloom syndrome protein to maintain genome stability', *Genes and Development*, 22(20), pp. 2843–2855. doi: 10.1101/gad.1708608.

Yamagishi, Y. *et al.* (2012) 'MPS1/Mph1 phosphorylates the kinetochore protein KNL1/Spc7 to recruit SAC components', *Nature Cell Biology*, 14(7), pp. 746–752. doi: 10.1038/ncb2515.

Yellman, C. M. and Burke, D. J. (2006) 'The role of Cdc55 in the spindle checkpoint is through regulation of mitotic exit in Saccharomyces cerevisiae.', *Molecular Biology of the Cell*, 17(2), pp. 658–666. doi: 10.1091/mbc.E05-04-0336.

Yoshida, M. M. and Azuma, Y. (2016) 'Mechanisms behind Topoisomerase II SUMOylation in chromosome segregation', *Cell Cycle*, pp. 3151–3152. doi: 10.1080/15384101.2016.1216928.

Yoshida, S. *et al.* (2006) 'Polo-like kinase Cdc5 controls the local activation of Rho1 to promote cytokinesis', *Science*, 313(5783), pp. 108–111. doi: 10.1126/science.1126747.

Yoshida, S., Asakawa, K. and Toh-e, A. (2002) 'Mitotic Exit Network controls the localization of Cdc14 to the Spindle Pole Body in Saccharomyces cerevisiae', *Current Biology*, 12(11), pp. 944–950. doi: 10.1016/S0960-9822(02)00870-9.

Zachariae, W. (1998) 'Control of Cyclin Ubiquitination by CDK-Regulated Binding of Hct1 to the Anaphase Promoting Complex', *Science*, 282(5394), pp. 1721–1724. doi: 10.1126/science.282.5394.1721.

Zhang, C. *et al.* (2005) 'A second-site suppressor strategy for chemical genetic analysis of diverse protein kinases', *Nature Methods*. Nature Publishing Group, 2(6), pp. 435–441. doi: 10.1038/nmeth764.

Zimniak, T. *et al.* (2009) 'Phosphoregulation of the budding yeast EB1 homologue Bim1p by Aurora/Ipl1p', *Journal of Cell Biology*, 186(3), pp. 379–391. doi: 10.1083/jcb.200901036.

nature COMMUNICATIONS

ARTICLE

Received 29 May 2014 | Accepted 13 Feb 2015 | Published 8 Apr 2015

DOI: 10.1038/ncomms7643

Rio1 promotes rDNA stability and downregulates RNA polymerase I to ensure rDNA segregation

Maria G. Iacovella[1,*], Cristina Golfieri[1,*,†], Lucia F. Massari[1], Sara Busnelli[1], Cinzia Pagliuca[1], Marianna Dal Maschio[1,†], Valentina Infantino[1,†], Rosella Visintin[1], Karl Mechtler[2,3], Sébastien Ferreira-Cerca[4] & Peter De Wulf[1]

The conserved protein kinase Rio1 localizes to the cytoplasm and nucleus of eukaryotic cells. While the roles of Rio1 in the cytoplasm are well characterized, its nuclear function remains unknown. Here we show that nuclear Rio1 promotes rDNA array stability and segregation in *Saccharomyces cerevisiae*. During rDNA replication in S phase, Rio1 downregulates RNA polymerase I (PolI) and recruits the histone deacetylase Sir2. Both interventions ensure rDNA copy-number homeostasis and prevent the formation of extrachromosomal rDNA circles, which are linked to accelerated ageing in yeast. During anaphase, Rio1 downregulates PolI by targeting its subunit Rpa43, causing PolI to dissociate from the rDNA. By stimulating the processing of PolI-generated transcripts at the rDNA, Rio1 allows for rDNA condensation and segregation in late anaphase. These events finalize the genome transmission process. We identify Rio1 as an essential nucleolar housekeeper that integrates rDNA replication and segregation with ribosome biogenesis.

[1] Department of Experimental Oncology, European Institute of Oncology, via Adamello 16, Milan 20139, Italy. [2] The Research Institute of Molecular Pathology, Dr Bohr-Gasse 7, Vienna 1030, Austria. [3] The IMBA Institute of Molecular Biotechnology of the Austrian Academy of Sciences, Dr Bohr-Gasse 3, Vienna 1030, Austria. [4] Lehrstuhl für Biochemie III, Universität Regensburg, Universitätsstraβe 31, 93053 Regensburg, Germany. * These authors contributed equally to this work. † Present addresses: German Center for Neurodegenerative Diseases (DZNE), Arnoldstraβe 18/18b, 01307 Dresden, Germany (C.G.); Università degli Studi di Brescia, Sede di Medicina e Chirugia, Viale Europa 11, 25123 Brescia, Italy (M.D.M.); Department of Cell Biology, University of Geneva, 30 Quai Ernest-Ansermet CH-1211, Geneva 4, Switzerland (V.I.). Correspondence and requests for materials should be addressed to P.D.W. (email: peter.dewulf@ieo.eu).

At anaphase onset, the replicated chromosomes separate and then segregate along the mitotic spindle into the daughter cells. In the budding yeast *Saccharomyces cerevisiae*, the locus containing the genes that encode the ribosomal RNAs (rDNA) segregates after the rest of the genome, in late anaphase[1–4]. The rDNA locus exists as a tandem-repeat array comprising ~150 rDNA units containing the 35S and 5S genes, which are transcribed by RNA polymerase I (PolI) and PolIII, respectively. Processing of the 35S pre-rRNA generates 5.8S, 18S and 25S rRNA that, together with the 5S rRNA, become the catalytic backbones of each ribosome[5,6]. Only in anaphase does yeast repress rDNA transcription[4], which allows the sister rDNA loci to condensate and segregate. PolI downregulation in anaphase is mediated by the Cdc14 phosphatase acting on PolI subunit Rpa43 (ref. 4), resulting in PolI dissociating from the 35S rDNA. The removal of PolI and the local resolution of its transcripts allow the condensin complex to bind. The latter compacts the rDNA array and recruits the DNA decatenating enzyme topoisomerase II (refs 1,3,4,7) resulting in the physical separation and subsequent segregation of the sister rDNA loci.

S. cerevisiae Rio1 belongs to the atypical RIO protein kinase family whose members lack the activation loop and substrate recognition domain present in canonical eukaryotic protein kinases[8–11]. Noteworthy, the RIO kinases may act especially as ATPases as they exhibit <0.1% kinase activity *in vitro*[12–14]. Cytoplasmic Rio1 contributes to pre-40S ribosome biogenesis by promoting 20S pre-rRNA maturation and by stimulating the recycling of trans-acting factors at the pre-40S subunit, both in yeast[12,15–18] and human cells[19,20]. Roles in the nucleus are unknown for any RIO member, either in yeast or eukaryotes beyond. Using *S. cerevisiae*, we now describe the first activities of Rio1 in the nucleus. Foremost, Rio1 downregulates PolI transcription through the cell cycle. In G1, Rio1 additionally promotes pre-rRNA processing to ensure a timely commencement of the cell cycle. In S phase, besides downregulating PolI, Rio1 also recruits the histone deacetylase Sir2 to ensure rDNA repeat-number stability. In anaphase, the downregulation of PolI by Rio1 and its activation of pre-rRNA processing drive rDNA condensation and segregation. Cells lacking nuclear Rio1 activity suffer from a delayed cell cycle entry, fragmented nucleolus, an expanded rDNA array, extrachromosomal rDNA circles (ERCs) and an inability to segregate rDNA. We identify Rio1 as an essential nucleolar housekeeper of rDNA integrity and transmission, and as an upstream regulator of ribosome biogenesis.

Results

Rio1 localizes dynamically to rDNA during the cell cycle. Previous work showed that substituting conserved catalytic residue D244E in the Rio1 kinase domain provoked plasmid loss in *S. cerevisiae*[21], suggesting an involvement of Rio1 in DNA replication and/or segregation. To examine this possibility, we imaged Rio1, labeled with green fluorescent protein (Rio1-GFP), in exponentially growing *S. cerevisiae* cells. We identified the protein both in the cytoplasm (consistent with its documented involvement in 20S pre-rRNA maturation[15] and pre-40S ribosome trans-factor recycling[12,17,18]), and in the nucleus (Fig. 1a). As the intranuclear localization of Rio1 could not be easily determined, we isolated the nuclei from exponentially grown yeast, crosslinked and then spread them on glass slides. Immunofluorescence (IF) microscopy with an anti-Rio1 antibody revealed that Rio1 was highly enriched at the nucleolus (co-localized with nucleolar marker Nop1; Fig. 1b), the subnuclear compartment that is organized around the rDNA array (Supplementary Fig. 1). However, Rio1 signal intensities were heterogeneous across the nuclei suggesting a cell cycle-dependent localization. To probe this observation further, 6myc-Rio1 cells were arrested in G1 with α-factor and then synchronously released into the cell cycle. Samples were taken during cell cycle progression, the nuclei were isolated, spread and analysed by anti-myc IF imaging (Fig. 1c,d). We observed that Rio1 was highly enriched at the nucleolus in G1. Rio1 signals then decreased by half through S phase. In metaphase, the nucleoli contained very low amounts of Rio1, whereas at anaphase onset Rio1 became actively re-recruited to the nucleolus, reaching levels similar to those measured in G1 (Fig. 1c,d and Supplementary Fig. 2a). Low amounts of Rio1 were detectable in the nucleus (beyond the nucleolus), especially in S phase (Fig. 1d). Using chromatin immunoprecipitation (ChIP) analysis, we next probed to which sites Rio1 localized at the rDNA. 6myc-Rio1 cells were arrested in G1, S phase, metaphase and anaphase (via use of α-factor, hydroxyurea, nocodazole and the *cdc15-2* allele, respectively). The rDNA sequences that were enriched with immunoprecipitated Rio1 were identified by real-time quantitative PCR (RT–qPCR) analysis using probes covering the rDNA unit. While the 6myc-Rio1 signals were distributed homogeneously across the rDNA in G1 and metaphase cells, we found the kinase to be enriched at the 35S rDNA promoter and gene sequence (probes 4 and 5) in S phase and anaphase (coloured lines in Fig. 1e). However, the averaged values obtained with the five probes (black bars in Fig. 1e) confirmed the Rio1 localization dynamics observed by imaging of the spread nuclei.

A previous report indicated that Rio1, overexpressed from the P_{GAL10} promoter, becomes degraded in S phase, suggesting Rio1 stability is cell cycle regulated[22]. However, our western blot analyses of yeast endogenously expressing Rio1 showed that its protein levels do not change through the cell cycle (Fig. 1f). Hence, the observed dynamic localization of Rio1 may reflect changes in its affinity for nucleolar factors and/or its active import–export from the nucleus. Rio1 shuttling between the nucleus and cytoplasm was evidenced previously by its intranuclear accumulation in an exportin mutant[16].

Besides its localization, a role for Rio1 at the rDNA was indicated by its recent co-purification with the phosphatase Cdc14 and its inhibitor Cfi1 (ref. 23), which together with the histone deacetylase Sir2 form the rDNA-silencing complex RENT[24] (Fig. 1g). Our own yeast two-hybrid screens that used Rio1 as the bait (Supplementary Fig. 2b) identified as interactors the rDNA helicase Sgs1 (confirmed by co-immunoprecipitation from yeast whole-cell extract; Supplementary Fig. 2c), the rDNA-silencing protein Tof2 and Rio1 itself (Supplementary Fig. 2b). These findings extend the current Rio1 protein-interaction map that mostly comprises ribosome biogenesis factors[25] (Fig. 1g).

Distinct sets of nucleolar proteins recruit Rio1. While the 150-unit repeat nature of the rDNA array satisfies yeast's huge demand for ribosomes[26], its configuration makes rDNA highly vulnerable to genetic instability during rDNA replication[27,28]. Although the replication fork moves bi-directionally from the rARS, the leftward-moving replisome is halted at the replication fork barrier site (RFB) to prevent it from colliding with PolI, transcribing the 35S rDNA sequence in rightward direction. Such a collision would generate incomplete 35S rRNA transcripts and produce double-strand breaks in the 35S unit. However, the replisome held at the RFB may collapse, resulting in the exposure of single-strand rDNA, progressing into a double-strand break. Double-strand DNA breaks are repaired by homologous recombination. For a correct repair to occur, the sister rDNA loci must be aligned. If not, homologous recombination will result in an expansion or contraction of the rDNA array and in the formation of ERCs[27,28], anomalies that have been linked to a

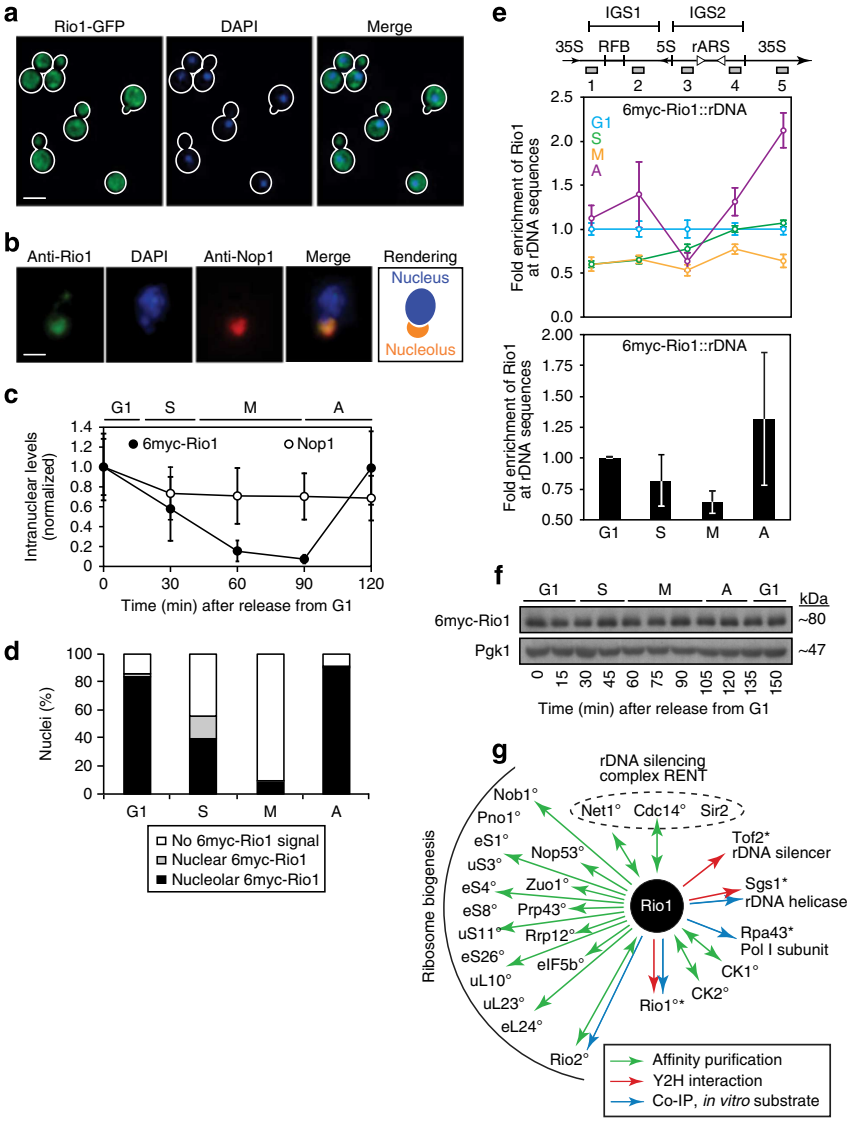

Figure 1 | Rio1 localizes to the rDNA in a dynamic, cell cycle stage-dependent manner. (**a**) Fluorescence microscopy image of DAPI-stained exponentially growing yeast cells endogenously expressing Rio1-GFP. Scale bar, 5 µm. (**b**) Indirect IF image of Rio1 (anti-Rio1) and nucleolar marker Nop1 (anti-Nop1) in a spread nucleus isolated from a G1 cell. Scale bar, 5 µm. (**c**) Nuclear 6myc-Rio1 and Nop1 levels (normalized to Nop1 concentrations in G1) measured from IF images (anti-myc, anti-Nop1) of spread nuclei isolated from cells progressing through the cell cycle. Error bars, s.d.'s, $n = 50$ per time point. (**d**) Intranuclear distribution of 6myc-Rio1 established from IF images of spread nuclei isolated from cells synchronously progressing through the cell cycle (from the experiment depicted in **c**). $n = 50$ Per time point. (**e**) 6myc-Rio1 protein levels at the rDNA as quantified by ChIP–qPCR analysis of cells arrested in G1, S phase, metaphase (M) or anaphase (A). Positions of the real-time qPCR probes along the rDNA unit are indicated (1–5). IGS, intergenic spacer region; RFB, replication fork barrier; rARS, origin of replication; 5S and 35S, genes encoding 5S and 35S rRNA, respectively. The upper plot shows the data obtained with each probe per cell cycle stage (each data point corresponds to the probe indicated above). Error bars, s.d.'s. $n = 3$. The lower plot shows the averages of the values obtained with the five probes. (**f**) Western blot of endogenous 6myc-Rio1 protein levels (anti-myc) through the cell cycle (Pgk1 = loading control). (**g**) The Rio1 interactome. Rio1 interactors reported in the literature [°][25] and identified in this study [*]).

shortened lifespan in yeast[29,30]. Various proteins contribute to sister rDNA alignment and faithful recombination, as described in Supplementary Fig. 1. They include Fob1, Tof2, RENT (Cfi1, Cdc14, Sir2), Sgs1, and the monopolin, cohesin and condensin complexes.

To determine the basis for the cell cycle-stage-dependent localization of Rio1 to the rDNA, we probed Rio1 recruitment by IF analysis of spread nuclei isolated from mutants lacking one of the above rDNA factors. Cells were released from G1 or S phase (a *sir2Δ* mutant does not respond to α-factor) and then tracked through the cell cycle by analysis of spindle morphology (anti-Tub1 IF) and DNA content (fluorescence-activated cell sorting, FACS) (Supplementary Fig. 3). In short, we found that Rio1 localization to rDNA in interphase depended on Fob1, Sgs1, Sir2 and Cdc14, while its anaphase recruitment required Fob1, Sgs1, monopolin and condensin (Fig. 2a,b and Supplementary Fig. 4a). Rio1 thus localizes to the rDNA at different cell cycle stages via distinct rDNA factors (summarized in Fig. 2c). The observed changes in Rio1 recruitment in the mutant backgrounds were not due to alterations in Rio1 expression or stability, as western blot analyses showed that Rio1 protein levels remained constant through the cell cycle in all of the mutants tested (Supplementary Fig. 4b). Noteworthy, the phosphatase Cdc14 is kept inactive in the nucleolus from G1 through metaphase by its inhibitor Cfi1 (ref. 31) and becomes released (activated) at anaphase entry. However, when we inactivated and delocalized Cdc14 in G1

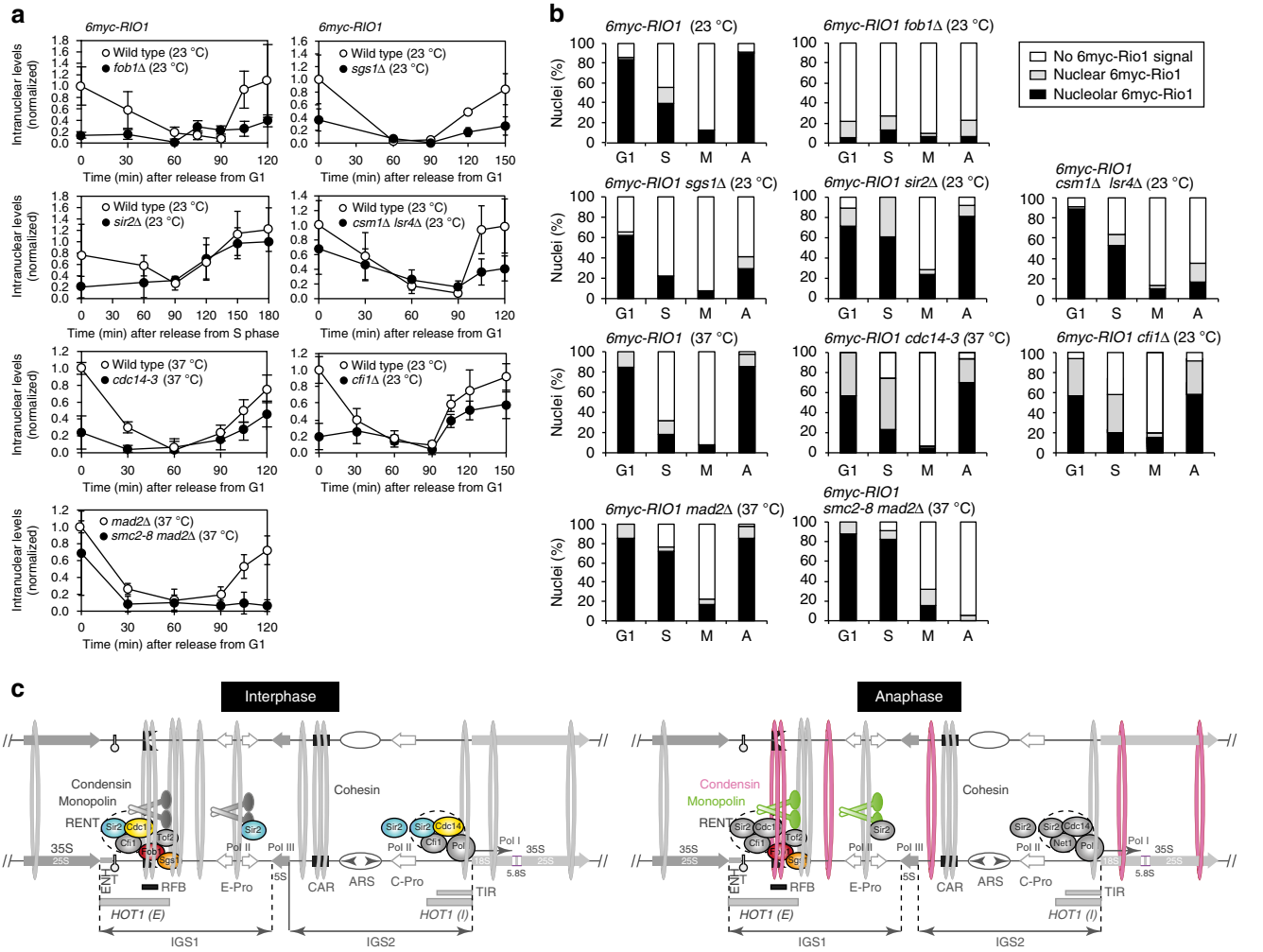

Figure 2 | Distinct sets of nucleolar proteins recruit Rio1 to interphase and anaphase rDNA. (**a**) Nuclear levels of 6myc-Rio1 through the cell cycle of strains mutated in a single rDNA regulator as determined by quantitative IF imaging (anti-myc) of spread nuclei. Signals are normalized to the 6myc-Rio1 levels measured in the wild-type control strains in G1. Error bars, s.d.'s. $n = 50$ Per time point. (**b**) Intranuclear distribution of 6myc-Rio1 in specific cell cycle stages ($n = 50$) as probed by IF imaging of spread nuclei isolated from the cells in **a**. (**c**) Graphic representation of the rDNA factors (coloured) that recruit Rio1 to rDNA in interphase (left) and anaphase (right).

(*cdc14-3* mutant at the non-permissive temperature), we observed a marked reduction in Rio1 levels at interphase nucleoli and, in parallel, a distribution of the kinase throughout the nucleus (Fig. 2b). A constitutive release of Cdc14 instigated by removing Cfi1 (*cfi1Δ*) confirmed this observation. Hence, albeit anchored in the nucleolus, Cdc14 serves at least to recruit Rio1 to interphase rDNA.

Characterization of a Rio1 nuclear depletion mutant. To study Rio1 activity at the rDNA, we wished to inducibly remove the kinase from the nucleus only. Based on the observation that Rio1 shuttles between the nucleus and the cytoplasm[16], we figured that conditionally removing its C-terminal tail containing a putative nuclear localization signal (NLS; Supplementary Fig. 5a) would prevent truncated Rio1 from entering the nucleus. Rio1 present in the nucleus at the moment of truncation should still be able to exit from the nucleus as its putative nuclear exit signal localizes at the outer edge of the RIO domain (Fig. 3a and Supplementary Fig. 5b). To allow for conditional truncation, we cloned the Tobacco Etch Virus (TEV) Protease with a C-terminal NLS under control of the galactose-inducible P_{GAL10} promoter on a high-copy plasmid (next named pP_{GAL10}-*TEV Protease*; Supplementary Fig. 5c). Next, we introduced a TEV Protease cleavage site just upstream of the NLS in 6myc-Rio1 (next referred to as 6myc-Rio1^{TEV}; Fig. 3a). To confirm the TEV Protease-induced cleavage of 6myc-Rio1^{TEV}, we grew the *6myc-rio1^{TEV}* strains carrying pP_{GAL10}-*TEV Protease* or the empty pP_{GAL10} vector (negative control) in 2% raffinose medium and then treated the cells for 1 h with 2% galactose. TEV Protease expression led to the removal of 6myc-Rio1's C-terminal 78 residues (Fig. 3b), as indicated by anti-myc western blot analysis. Within the hour, truncated 6myc-Rio1^{TEV} had also become depleted from the nucleus as shown by IF microscopy of spread nuclei (Fig. 3c) and whole cells (Fig. 3d). Whereas 6myc-Rio1^{TEV} was no longer detected in the nucleus, its signals could still be observed and quantified in the cytoplasm (Fig. 3d). When plated on 2% galactose medium, the mutant strain died, indicating that the C-terminal region of Rio1 is essential for viability, in agreement with previous observations[12]. Importantly, overexpressing the TEV Protease in wild-type yeast did not affect viability (Fig. 4a).

To determine whether truncated Rio1 remains a functioning kinase, we measured the kinase activity of full-length and cleaved 6myc-Rio1^{TEV}. We synchronized the *6myc-rio1^{TEV}* pP_{GAL10}-*TEV Protease* and *6myc-rio1^{TEV}* pP_{GAL10} strains in G1 and induced TEV Protease expression with 2% galactose (1 h) while keeping

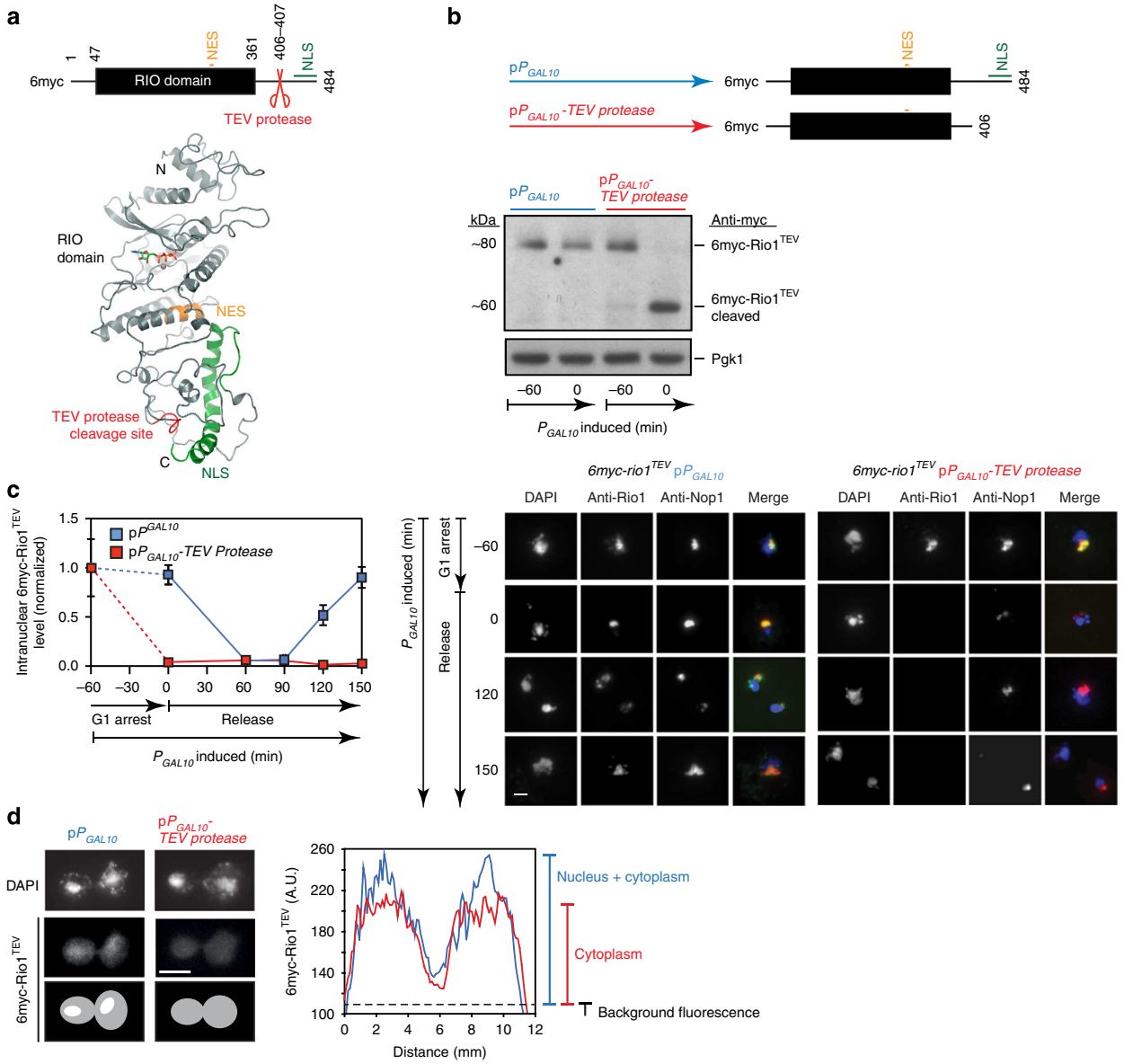

Figure 3 | Depletion of Rio1 from the nucleus. (**a**) The Rio1 nuclear depletion construct. To-scale representation and computational model of the 6myc-Rio1^{TEV} protein. The RIO domain, the putative nuclear export signal (NES), the putative NLS and the TEV Protease cleavage site (introduced between E406 and E407) are indicated. The model of full-length 6myc-Rio1^{TEV} bound to ATP and manganese was generated with Phyre2 (http://www.sbg.bio.ic.ac.uk/phyre2) based on the structure of *A. fulgidus* Rio1 (PDB 1ZTH)[45]. (**b**) Ectopic expression of the TEV Protease truncates the 6myc-Rio1^{TEV} protein at its C-terminus. Top: To-scale representation and western blot (anti-myc) of full-length and truncated 6myc-Rio1^{TEV} proteins in *6myc-rio1^{TEV}* pP_{GAL10} (blue) and *6myc-rio1^{TEV}* pP_{GAL10}*-TEV Protease* (red) cells before and after P_{GAL10} induction with 2% galactose (Pgk1, loading control). (**c**) Intranuclear 6myc-Rio1^{TEV} levels in cells lacking (blue) or expressing (red) TEV Protease, quantified from IF images (anti-myc) of spread nuclei. Both strains were grown in 2% raffinose medium and arrested in G1. P_{GAL10} was induced (1 h, 2% galactose), and the cells then released into the cell cycle (2% galactose medium, 150 min). $n = 50$ Per time point. Error bars, s.d.'s. Representative images are shown on the right. Scale bar, 5 μm. (**d**) IF images of 6myc-Rio1^{TEV} (anti-myc) in anaphase-arrested *cdc15-2* yeast cells that lack (left, blue) or express (right, red) TEV Protease (DAPI = DNA). Scale bar, 5 μm. Fluorescence levels were quantified along the horizontal axes.

the cells arrested in G1. Next, we released the cells in 2% galactose medium and took samples 1 h before, upon and 3 h after the release. Western blot analysis confirmed the C-terminal truncation of 6myc-Rio1^{TEV} in the strain expressing TEV Protease (Fig. 4b). Full-length and truncated 6myc-Rio1^{TEV} were then immunopurified (anti-myc beads) and their activity assayed on dephosphorylated casein[21]. The measured kinase activities were identical (Fig. 4b), confirming an earlier report that recombinant Rio1 lacking a similar C-terminal region is still active as a kinase *in vitro*[22]. To exclude a possible contribution from casein kinases CK1 and CK2, shown to co-purify with full-length Rio1 (refs 12,22) and with Rio1 lacking its C-terminal 46 residues[9], the assay was repeated in the presence of CK1 and CK2 inhibitors. While the overall kinase activity decreased, we measured no differences between the kinase activities of full-length and truncated 6myc-Rio1^{TEV} (Supplementary Fig. 6a).

The C terminus of Rio1 was previously shown to be necessary for cytoplasmic Rio1 to bind to the pre-40S ribosome and for promoting 20S pre-rRNA maturation[12]. As such, we examined whether truncated 6myc-Rio1^{TEV} could still mediate these functions within the 3-h time frame during which we phenotype the mutant cells (see further down). Specifically, we

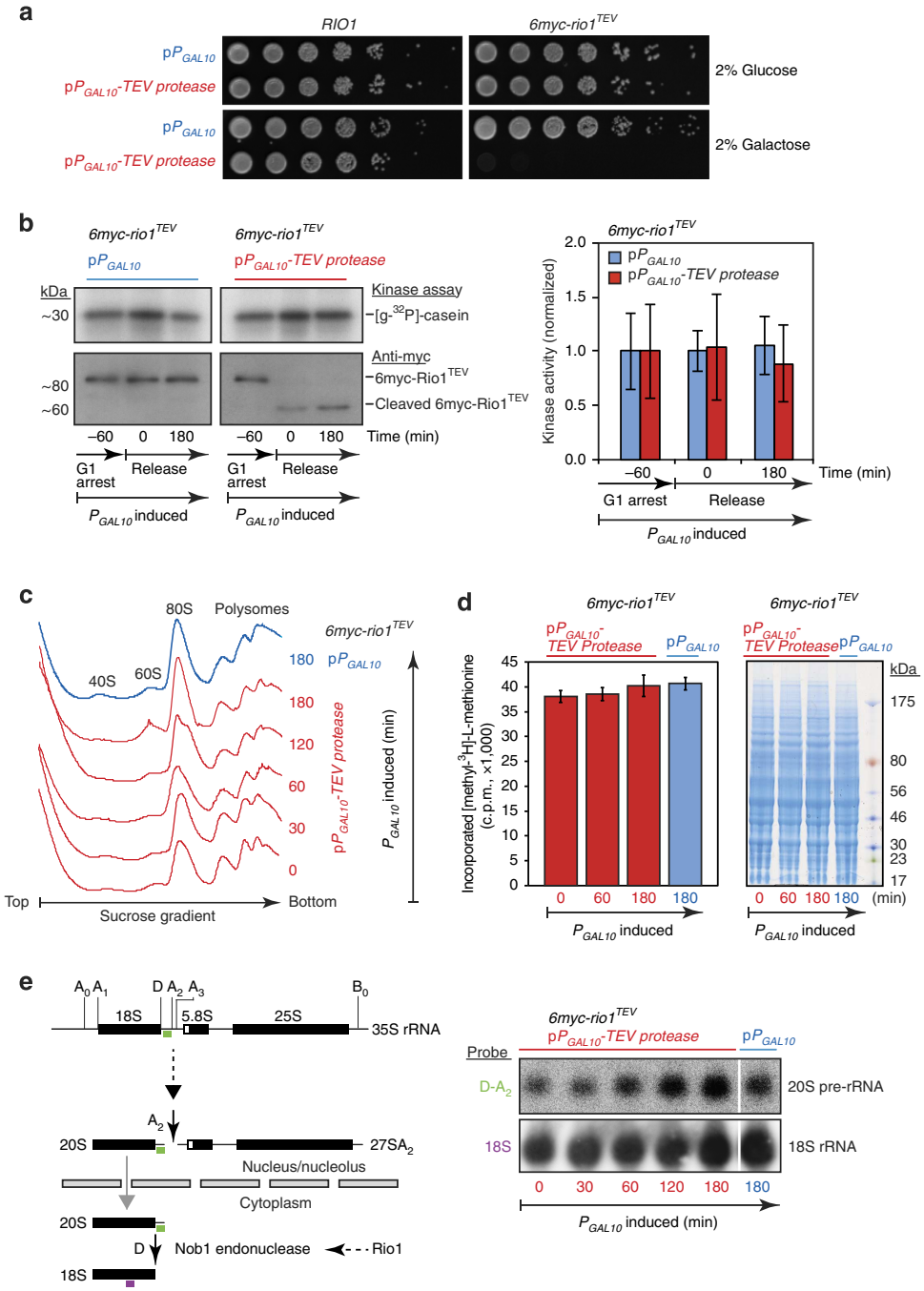

Figure 4 | Functional characterization of the Rio1 nuclear depletion mutant. (**a**) Growth of the *RIO1* and *6myc-rio1*^{TEV} strains carrying pP_{GAL10} (blue) or pP_{GAL10}-*TEV Protease* (red) on glucose and galactose media (23 °C). (**b**) *In vitro* kinase activity analysis of full-length or truncated 6myc-Rio1^{TEV} isolated from yeast lacking or expressing TEV Protease, respectively. The reaction contained [γ-^{32}P]ATP and dephosphorylated casein, as the substrate. Left; top: [γ-^{32}P]-phosphorylated casein visualized radiographically; bottom: western blots (anti-myc) of full-length or truncated 6myc-Rio1^{TEV}. The indicated times (min) are relative to the release from G1. Right: 6myc-Rio1^{TEV} kinase activity normalized to the activity measured 1 h before P_{GAL10} induction. $n = 3$. Error bars, s.d.'s. (**c**) Ribosome profiles of *6myc-rio1*^{TEV} pP_{GAL10} (blue) and *6myc-rio1*^{TEV} pP_{GAL10}-*TEV Protease* (red) strains. Samples were taken at the indicated time points and the cell extracts fractionated by 5–45% sucrose gradient ultracentrifugation. The 254-nm absorption profiles measured along the gradients are shown. (**d**) Cells depleted of nuclear Rio1 activity are not affected in protein neo-synthesis. *6myc-rio1*^{TEV} pP_{GAL10} (blue) and *6myc-rio1*^{TEV} pP_{GAL10}-*TEV Protease* cells (red) were grown in 2% raffinose medium and then treated with 2% galactose. The cells were provided (20 min) with [methyl-^{3}H]-L-methionine and its incorporation in nascent proteins quantified (scintillation counts) at the indicated time points. The numbers represent average values. $n = 3$. Error bars = s.d's. The extracted proteins were run in parallel on a Nu-PAGE gradient gel and then Coomassie stained, confirming that equal protein amounts were analysed for [methyl-^{3}H]-L-methionine incorporation. (**e**) Northern blots of total RNA isolated from *6myc-rio1*^{TEV} pP_{GAL10} (blue) and *6myc-rio1*^{TEV} pP_{GAL10}-*TEV Protease* cells (red) (from experiment in **d**). Positions of the D-A_2 (green) and 18S (purple) northern probes hybridizing with 20S pre-rRNA and 18S rRNA are indicated in the sketch on the left.

probed ribosome biogenesis, protein translation and 20S pre-rRNA to 18S rRNA maturation. Whole-cell extracts from exponentially grown *6myc-rio1*^{TEV} pP_{GAL10}-*TEV Protease* and 6myc-*rio1*^{TEV} pP_{GAL10} strains were collected at different time points (0–3 h) after P_{GAL10} induction. The extracts were fractionated by 5–45% sucrose gradient ultracentrifugation and their nucleic acid profiles were recorded at 254 nm. We observed a subtle decrease in 40S subunits levels (and concomitant increase in 60S levels) at the latest time points in the cells depleted of nuclear Rio1 (Fig. 4c). The ribosome (80S) and polysome profiles of both strains were basically identical suggesting similar mRNA translation capacities. We confirmed this conclusion as pulse labelling of the mutant and control cultures with [methyl-^{3}H]-L-methionine revealed no difference in the amount of radiolabelled methionine that was incorporated in the neo-synthesized proteins (Fig. 4d). Next, we probed cytoplasmic 20S pre-rRNA maturation at pre-40S particles via northern blot analysis. In good agreement with our slight decrease in 40S levels, we observed a mild 20S pre-rRNA to 18S rRNA processing defect (Fig. 4e). Because our data show that during the short time frame of one cell cycle (3 h), the cytoplasmic activity of truncated 6myc-Rio1^{TEV} is not markedly affected, we used this mutant to study how activities at the rDNA are affected in yeast depleted of nuclear Rio1.

Rio1 promotes rDNA stability and segregation. To phenotype the Rio1 nuclear exclusion mutant, we first analysed its progression through the cell cycle. Compared with the control cells, yeast depleted of nuclear Rio1 consistently showed a 15–20-min delay in cell cycle commencement at START (G1/S transition; orange triangles in Fig. 5a), whereas progression through the subsequent cell cycle stages was not affected. Importantly, overproduction of the TEV Protease in a wild-type strain did not delay cell cycle initiation (Supplementary Fig. 6b). IF microscopy of spread nuclei revealed nucleolar fragmentation in the absence of Rio1 (Fig. 5b), an anomaly that is indicative of rDNA instability. To probe this phenotype further, we grew the 6myc-*rio1*^{TEV} pP_{GAL10}-*TEV Protease* and 6myc-*rio1*^{TEV} pP_{GAL10} strains for eight divisions in 2% galactose medium. Electrophoretic analysis of their DNA content followed by Southern blot analysis with a 25S rDNA probe[32] revealed ERCs and an expanded rDNA array, as in a *sir2Δ* mutant (positive control; Fig. 5c), known to contain 200–300 rDNA units[33]. Homologous recombinations underlaid these rDNA-instability phenotypes as GFP-labelled recombination mediator Rad52 formed fluorescent foci at the nucleolar periphery, the area where rDNA recombination takes place[34] (Fig. 5d). Despite the rDNA hyper-recombination events, progression through S phase was not delayed (Fig. 5a) and the DNA damage checkpoint kinase Rad53 not activated/phosphorylated[35] (Fig. 5e). Importantly, the cells depleted of nuclear Rio1 were DNA checkpoint proficient as they arrested in S phase with phosphorylated Rad53 upon treatment with hydroxyurea (Fig. 5f and Supplementary Fig. 6c).

Through IF microscopy analysis of isolated nuclei, we next probed which rDNA regulators required nuclear Rio1 activity for their localization through the cell cycle. In short, cells lacking nuclear Rio1 had reduced levels of Sir2 at rDNA in interphase and metaphase, and of condensin in anaphase. The inability of these proteins to localize to the nucleolus led to their diffusion throughout the nucleus (Fig. 5g, and Supplementary Figs 7 and 8). Reduced Sir2-mediated silencing of rDNA transcription[36,37], required for sister rDNA alignment, may explain the observed rDNA-instability and array-expansion phenotype in yeast lacking nuclear Rio1 activity. As for condensin, this complex becomes highly enriched at anaphase rDNA to compact the array. Indeed, the large rDNA locus must be condensed before chromosome XII can move through the bud neck into the daughter cell[2]. In addition, condensin recruits topoisomerase II that resolves the remnant catenates lingering between the sister rDNA loci[2–4,7]. Both condensin-driven activities promote rDNA segregation in late anaphase. Indeed, live-cell microscopy revealed that yeast depleted of nuclear Rio1 was severely affected in its ability to segregate its GFP-marked rDNA loci (Fig. 6a). In contrast, centromere segregation was not affected (Supplementary Fig. 9a). Noteworthy, in cells lacking nuclear Rio1, the anaphase spindle (identified by mCherry-Tub1) extended till 11 μm (versus 7 μm in the control strain; Fig. 6a), likely to try and segregate the rDNA loci. This phenotype is consistent with a defect in rDNA condensation[3].

Rio1 downregulates PolI and stimulates pre-rRNA processing. For rDNA to condensate and segregate, yeast must turn down PolI activity and locally resolve its transcripts before condensin can be loaded[1,4]. The Cdc14 phosphatase was previously shown to downregulate PolI in anaphase[4]. We wondered whether also Rio1 reduces PolI activity since our ChIP–qPCR analyses had identified high levels of 6myc-Rio1 at the 35S promoter and gene sequence in anaphase cells (*cdc15-2*) (probes 4 and 5; Fig. 1e). As such, we arrested the 6myc-Rio1^{TEV} cells in anaphase (*cdc15-2*) following depletion of nuclear Rio1 activity at the metaphase–anaphase transition. RT–qPCR analysis of cDNA with a 5′-external transcribed spacer (5′ETS) probe (probe 4 in Fig. 6b) revealed a threefold increase in 35S rRNA levels, as compared with the control anaphase cells. This result was confirmed by northern blot hybridization with a $+1$-A_0 probe showing a 2.5-fold increase in 35S rRNA concentrations (Fig. 6b), suggesting that Rio1 downregulates PolI activity in anaphase. To corroborate this conclusion, we localized PolI by ChIP–qPCR analysis of its subunit Rpa43 in anaphase-arrested *cdc15-2* cells (37 °C) lacking or containing nuclear Rio1 activity. In the anaphase control cells, Rpa43 levels at the 35S promoter and gene sequence were low but increased by five- and eightfold, respectively, in the absence of nuclear Rio1 activity (red bars, Fig. 6c). Combined, our PolI transcription and localization data indicate that Rio1 downregulates PolI activity in anaphase. The Cdc14 phosphatase reduces PolI activity by dissociating PolI from the anaphase rDNA[4]. Our Rpa43 ChIP data show an accumulation of PolI at the 35S unit in the absence of nuclear Rio1 activity, suggesting that Rio1 represses PolI transcription in a similar fashion.

Since both the Cdc14 phosphatase[4] and Rio1 kinase downregulate PolI in anaphase, we next probed their relative contributions to this process. Whereas anaphase-arrested cells lacking Rio1 activity were characterized by a threefold increase in 35S rRNA concentrations (Fig. 5b, probe 4), anaphase cells lacking Cdc14 activity (*cdc14-3*) harboured only a 1.5-fold increase in 35S transcript levels as compared with *cdc15-2* control cells (Fig. 6d), confirming previous findings[4]. Removing both Cdc14 and Rio1 activities led to a fourfold increase, indicating that both enzymes repress in parallel PolI transcription in anaphase.

As Rio1 localizes to rDNA also before anaphase (Fig. 1c–e) and as PolI transcribes rDNA from G1 through metaphase[4], we wondered whether Rio1 also modulates PolI transcription before anaphase. To answer this question, we arrested 6myc-*rio1*^{TEV} pP_{GAL10}-*TEV Protease* and 6myc-*rio1*^{TEV} pP_{GAL10} control cells in G1, depleted the cells of nuclear Rio1 activity and synchronously released them into the cell cycle. Variations in 35S transcript levels measured with the 5′ETS RT–qPCR probe were rather small in the control cells (low in S phase, slight increase in metaphase and slight decrease in anaphase; Fig. 7a and Supplementary Fig. 9b). In

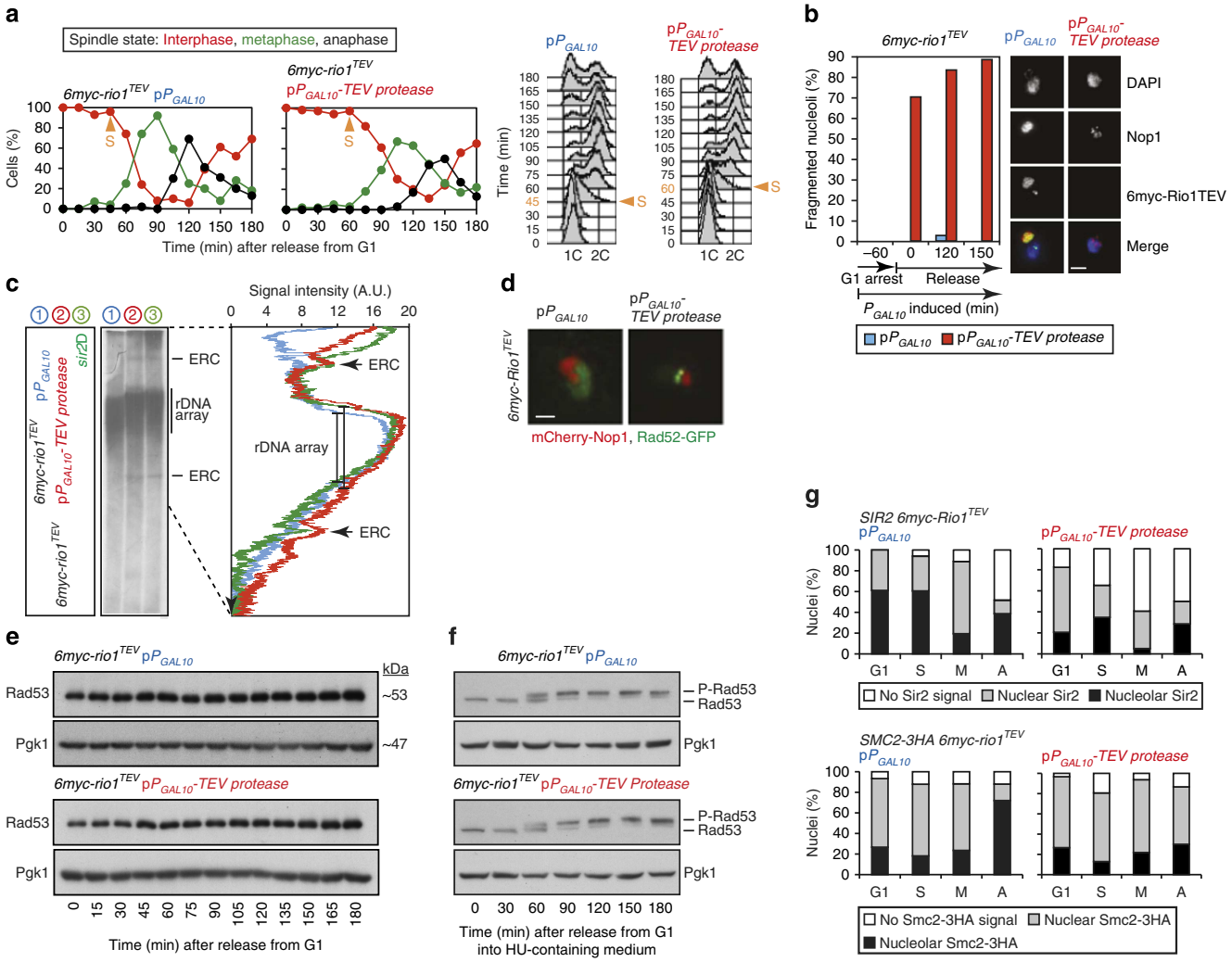

Figure 5 | Rio1 promotes timely cell cycle commencement and rDNA stability. (**a**) *6myc-rio1*^{TEV} pP_{GAL10} (blue) and *6myc-rio1*^{TEV} pP_{GAL10}*-TEV Protease* (red) cells were arrested in G1 (2% raffinose). P_{GAL10} was then induced (1 h, 2% galactose) and the cells released into the cell cycle (2% galactose medium). Cells were tracked by analysis of spindle morphology (anti-Tub1 IF; $n = 200$ cells per time point) and DNA content (FACS). The orange arrows indicate S phase. (**b**) Percentage of *6myc-rio1*^{TEV} pP_{GAL10} (blue) and *6myc-rio1*^{TEV} pP_{GAL10}*-TEV Protease* (red) cells, released from G1, with fragmented nucleoli (Nop1 = nucleolar marker), as established by IF imaging analysis of spread nuclei (anti-myc, anti-Nop1). $n = 50$ Per time point. Representative IF images are shown on the right. Scale bar, 5 μm. (**c**) Left: Southern blot (anti-*25S*) of total DNA isolated from *6myc-rio1*^{TEV} pP_{GAL10} (blue), *6myc-rio1*^{TEV} pP_{GAL10}*-TEV Protease* (red) and *sir2Δ* cells (green) grown for eight divisions in 2% galactose medium. The rDNA array and ERCs are indicated. Right: quantified hybridization signals. (**d**) Fluorescence microscopy image of *6myc-rio1*^{TEV} pP_{GAL10} (left) and *6myc-rio1*^{TEV} pP_{GAL10}*-TEV Protease* (right) cells expressing Rad52-GFP and mCherry-Nop1. Scale bar, 5 μm. (**e**) Western blots of DNA checkpoint kinase Rad53 (anti-Rad53; anti-Pgk1 = loading control) in *6myc-rio1*^{TEV} pP_{GAL10} (blue) and *6myc-rio1*^{TEV} pP_{GAL10}*-TEV Protease* (red) cells released from G1 in 2% galactose medium. (**f**) Western blots of Rad53 (anti-Rad53, anti-Pgk1 = loading control) in *6myc-rio1*^{TEV} pP_{GAL10} (blue) and *6myc-rio1*^{TEV} pP_{GAL10}*-TEV Protease* (red) cells released from G1 in 2% galactose medium containing hydroxyurea. (**g**) Intranuclear distribution of Sir2 and condensin (subunit Smc2-3HA) as determined by IF imaging of spread nuclei (anti-Sir2 and anti-HA, respectively) isolated from of *6myc-rio1*^{TEV} pP_{GAL10} and *6myc-rio1*^{TEV} pP_{GAL10}*-TEV Protease* cells released from G1 into the cell cycle (2% galactose medium). $n = 50$ Per analysis.

contrast, marked changes were observed in the cells depleted of nuclear Rio1. Primary transcript levels were sevenfold elevated in G1, then decreased through S phase (still 3.5-fold above the levels measured in the S phase control cells) and increased threefold in anaphase. This transcript–concentration profile is consistent with Rio1 localizing to the rDNA (Fig. 1c–e) to reduce PolI activity through the cell cycle.

To ensure rDNA segregation, yeast must not only reduce PolI activity but also locally resolve the PolI-generated transcripts. During our earlier northern blot analysis of 20S pre-rRNA processing in exponential cells depleted for 3 h of nuclear Rio1 activity (D-A_2 probe in Fig. 4e), we had noticed that the cells accumulated 32S rRNA transcripts (Supplementary Fig. 9d), indicating a defect in 32S cleavage at A_2 by the nucleolar SSU processome and associated factors[5,38–40]. As such, we probed rRNA transcript processing in our anaphase-arrested cells (*cdc15-2*) depleted of Rio1 activity. Northern hybridization of total rRNA with an A_2-A_3 probe revealed a 2.5-fold increase in 35S and 32S pre-RNA levels (Fig. 7b), indicating a derepressed PolI activity and a defect in nascent transcript processing at A_2. To determine whether the accumulation of pre-rRNA impaired rDNA segregation in yeast depleted of nuclear Rio1, we tracked rDNA-GFP through anaphase in *6myc-rio1*^{TEV} pP_{GAL10} and *6myc-rio1*^{TEV} pP_{GAL10}*-TEV Protease* cells that

inducibly expressed the *Aspergillus oryzae* ribonuclease RntA[4,41] from P_{GAL1} (Fig. 7c). We observed that the RntA-mediated degradation of the accumulated rRNA transcripts (Supplementary Fig. 9e) promoted rDNA segregation in yeast depleted of nuclear Rio1 (Fig. 7c). As such, rDNA transmission occurs only when Rio1, together with Cdc14, downregulates PolI activity and then stimulates the co-transcriptional processing of nascent transcripts in the nucleolus.

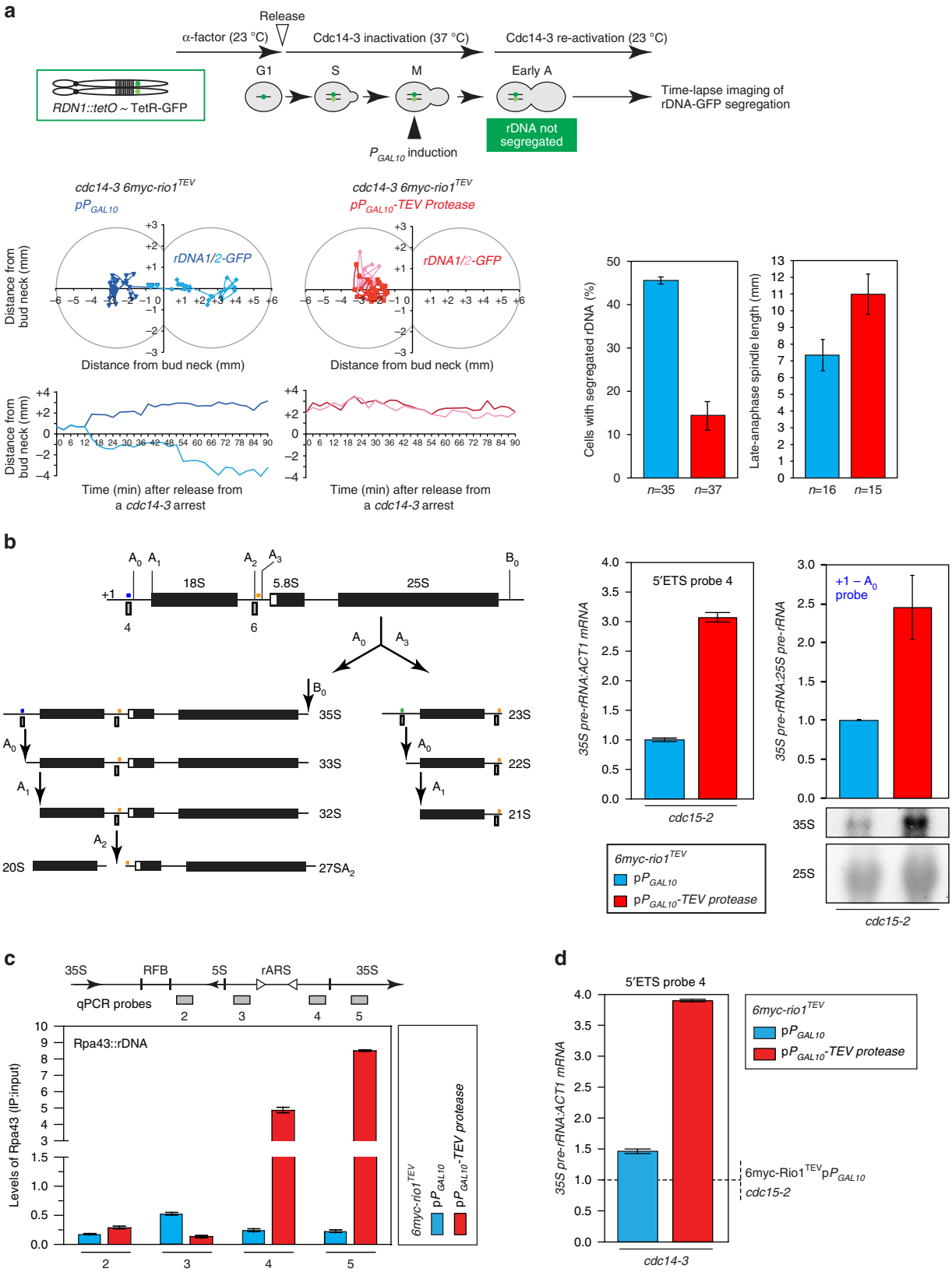

Rio1 reduces PolI activity by targeting subunit Rpa43. Transcription factor Rrn3 recruits PolI to the 35S promoter via PolI subunit Rpa43, an event that converts inactive PolI into an initiation-competent PolI (ref 42,43). In anaphase, the Cdc14 phosphatase downregulates PolI by dephosphorylating Rpa43, resulting in PolI dissociating from the anaphase rDNA[4]. To examine whether Rio1 also dislodges PolI by targeting Rpa43, we first probed their physical interaction and found that 6myc-Rio1 and Rpa43-3HA efficiently co-immunoprecipitated from exponentially growing cells (Fig. 8a). Next, PhosTag western blot analysis of Rpa43-3HA in *6myc-rio1^{TEV}* pP_{GAL10}-*TEV Protease* and *6myc-rio1^{TEV}* pP_{GAL10} cells identified a slow-migrating, anaphase-specific Rpa43-3HA phospho species that was absent in the cells lacking nuclear Rio1 activity (Fig. 8b). To further associate this anaphase-specific Rpa43 phospho species with Rio1 kinase activity, we analysed Rpa43 phosphorylation in cells expressing either a dominant-negative kinase-dead *rio1* allele (P_{GAL1}-*rio1^{D244A}*) or wild-type *RIO1* (P_{GAL1}-*RIO1*) (ref. 12). PhosTag western blot analysis showed that the cells expressing *rio1^{D244A}* lacked the slow-migrating Rpa43-3HA phospho species in anaphase (Fig. 8c). To examine whether Rio1 directly phosphorylates Rpa43, we performed an *in vitro* kinase assay with recombinant His6-Rio1 and Rpa43-His6-HA purified from *Escherichia coli* (Supplementary Fig. 9f) and found that Rpa43 was phosphorylated only in the presence of Rio1 (Fig. 8d). Interestingly, Rio1 autophosphorylation[12,22] was threefold (3.1 ± 0.6) higher in the presence of Rpa43, indicating that Rio1 binding to Rpa43 may have stimulated its own phosphorylation, which in turn may have promoted the phosphorylation of Rpa43 (the protein loading controls for the kinase assay are shown in Supplementary Fig. 9g). Finally, we sought to identify the Rpa43 residues targeted by Rio1 using mass spectrometry. After repeating the *in vitro* kinase assay in the presence and absence of unlabelled ATP, nanoLC-MS/MS analysis[44] (98.8% combined peptide coverage) found Rpa43 phospho-peptide QHLNPLV MKY73NNK to be threefold (3.2 ± 0.3) enriched over the negative-control peptide (unphosphorylated peptides were 1.1- to 1.3-fold upregulated versus their counterparts in the negative-control Rpa43 species; Fig. 8e). Tyrosine 73 was the sole Rpa43 residue found to be phosphorylated. Although no physiological substrates of Rio1 have yet been identified, Rio1 kinases are considered serine kinases as *Archeoglobus fulgidus* Rio1 phosphorylates itself at S108 (ref. 45) and because *S. cerevisiae* Rio1 phosphorylates serines in casein and in itself (residues not identified)[21]. However, recent studies suggested that RIO kinases can perform autophosphorylation at aspartate[12,13], within the RIO domain. Our findings further indicate that Rio1 phosphorylation activity is wide ranging and may harbour serine/tyrosine dual specificity, as observed for canonical kinases CK2 (refs 46,47), Hrr25 (ref. 48), Mps1 (ref. 49), Rad53 (ref. 50), Dusty[51] and Swe1 (ref. 52). Tyrosine 73 is one of the few evolutionary conserved residues present in Rpa43 (Fig. 8f and Supplementary Fig. 10) and resides–from a regulatory point of view—at a highly strategic position. Indeed, within Rpa43, Y73 lies in a short N-terminal β-strand proximal to six C-terminal β-strands and one α-helix that are enriched with phosphorylated residues, as identified by mass spectrometric analysis of Rpa43 isolated from yeast[53–55]. Y73 flanks K72 and lies near G78 and L87G88Y89, putative interaction points that may mediate Rpa43-Rpa14 heterodimer formation within PolI (refs 56,57). In addition, Y73 lies in close proximity to the negatively charged residues emanating from the C-terminus of Rpa135 (Fig. 5g). As such, Rio1 kinase activity could induce a charge-based repulsion and destablization of protein interactions within the polymerase complex. The N-terminal domain of Rpa43 that harbours Y73 also binds to the PolI-recruiting transcription factor Rrn3 (ref. 53). Taken together, our cell biological and biochemical data indicate that Rio1 phosphorylates Rpa43 in anaphase to remove PolI from the rDNA. Whether this clearance occurs via disruption of the Rpa43—Rrn3 interaction or via the dissolution of intra-PolI contacts will be determined in future research.

Discussion

We have identified Rio1 as a cell cycle-driven regulator of rDNA transcription, pre-rRNA processing, rDNA stability and segregation (Fig. 9). Yeast SSU processome mutants arrest at cell cycle entry (START) because pre-rRNA does not become processed and ribosomes are not being synthesized[58]. Our cell cycle experiments revealed that G1 cells lacking nuclear Rio1 activity accumulate primary 35S transcripts but also pre-rRNA species not yet processed at A_2 (RT–qPCR analysis with a probe covering the A_2 site; Supplementary Fig. 9c). These anomalies may help to explain the delay at START of our mutant.

In S phase, Rio1 acts at multiple levels. By tuning down transcription by PolI, Rio1 may reduce the frequency of collisions between the replisome and PolI within the 35S sequence, hence minimizing the production of double-strand breaks and incomplete transcripts[59]. Excessive PolI activity may also lead to extreme supercoiling and aberrant chromatin structures that stimulate DNA breakage and recombination. During rDNA replication, the RFB-bound proteins prevent the replisome from entering the 35S rDNA sequence and promote a correct alignment of the newly replicated sister rDNA arrays. Their recruitment of Rio1 indicates an involvement of the kinase in regulating these RFB activities. Rio1 also localizes the histone deacetylase Sir2 to rDNA chromatin. Sir2 promotes rDNA

Figure 6 | Rio1 promotes rDNA segregation by downregulating RNA PolI. (**a**) The *6myc-rio1^{TEV}* pP_{GAL10} and *6myc-rio1^{TEV}* pP_{GAL10}-*TEV Protease* strains, carrying the *cdc14-3* allele and marked with a 256x*tetO*∼TetR-GFP array flanking *RDN1* (rDNA-GFP) were arrested in G1 (2% raffinose medium, 23 °C). Cells were then released into the cell cycle (2% raffinose medium, 37 °C) and arrested in early anaphase by inactivation of Cdc14-3. 2% Galactose was then added to induce P_{GAL10} while the Cdc14-3 protein was re-activated in parallel (downshift to 23 °C). rDNA-GFP movement and segregation of the sister rDNA loci was tracked through anaphase by live-cell fluorescence microscopy. Left plots: single-cell rDNA segregation profiles. Projected movements of the sister rDNA arrays are shown in dark and light blue or in dark and light red colours. Right plots: percentage of cells with segregated sister rDNA-GFP loci, and the maximum length of their late-anaphase spindles. Error bars, s.d.'s. n = Indicated. (**b**) Sketch of 35S pre-RNA processing into 20S and $27SA_2$ pre-rRNA. The graphs show the quantification of primary 35S rRNA levels measured by RT–qPCR (5′ETS probe 4) or by northern blot analysis ($+1$-A_0 probe) of cDNA or total RNA, respectively. *6myc-rio1^{TEV} cdc15-2* cells carrying pP_{GAL10} (blue) or pP_{GAL10}-*TEV Protease* (red) were released from a metaphase arrest (nocodazole) under P_{GAL10}-inducing conditions (37 °C). Error bars, s.d.'s. $n = 2$. The northern blot with the $+1$-A_0 probe is shown underneath the graph. (**c**) ChIP–qPCR based measurement of Rpa43 levels at the rDNA of *cdc15-2 6myc-rio1^{TEV}* pP_{GAL10} (blue) and *cdc15-2 6myc-rio1^{TEV}* pP_{GAL10}-*TEV Protease* cells (red) arrested in anaphase following release from a metaphase arrest (37 °C, 2% galactose medium). Rpa43 levels across the rDNA unit were measured with probes 2–5. (**d**) RT–qPCR based quantification of primary 35S rRNA levels (5′ETS probe 4) in *6myc-rio1^{TEV} cdc14-3* carrying pP_{GAL10} (blue) or pP_{GAL10}-*TEV Protease* (red) arrested in anaphase (37 °C) after release from a metaphase arrest (nocodazole) under P_{GAL10}-inducing conditions. Reported values are normalized to the 35S levels measured for *cdc15-2 6myc-rio1^{TEV} pP$_{GAL10}$* cells, as indicated with a dashed line (Fig. 6b). Error bars, s.d.'s. $n = 3$.

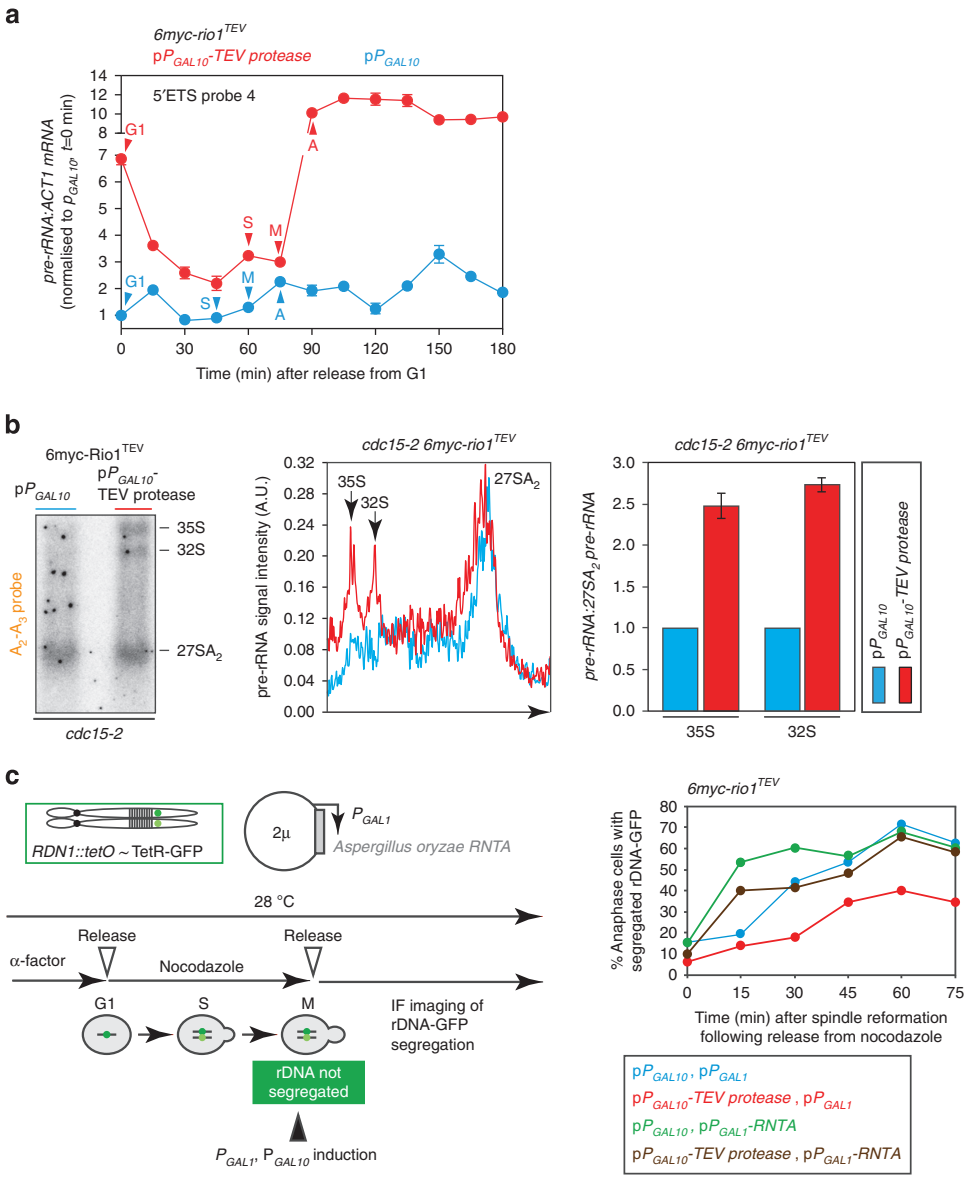

Figure 7 | Rio1 promotes rDNA segregation by removing RNA PolI and by stimulating the nucleolar processing of pre-rRNA transcripts. (**a**) RT–qPCR analysis of 35S cDNA (5′ETS probe 4) from *6myc-rio1*^{TEV} pP_{GAL10} (blue) and *6myc-rio1*^{TEV} pP_{GAL10}-*TEV Protease* (red) cells synchronously released from G1 into the cell cycle (2% galactose medium). P_{GAL10} was induced 1 h before releasing the G1 arrested cells. Error bars, s.d.'s. $n=3$. (**b**) Left: northern blot analysis with an A_2-A_3 probe of total RNA isolated from *6myc-rio1*^{TEV} *cdc14-3* cells carrying pP_{GAL10} (blue) or pP_{GAL10}-*TEV Protease* (red). The cells were arrested in anaphase after release from a metaphase arrest (nocodazole, 23 °C) under P_{GAL10}-inducing conditions (37 °C). Right: quantified northern blot signals, and 35S and 32S pre-rRNA levels relative to those of $27SA_2$ pre-rRNA. (**c**) *6myc-rio1*^{TEV} pP_{GAL10} and *6myc-rio1*^{TEV} pP_{GAL10}-*TEV Protease* cells marked with a 256x*tetO* ~ TetR-GFP array at *RDN1*, containing the pP_{GAL1}-*A. oryzae RNTA* or the pP_{GAL1} control vector. The strains were arrested in metaphase (nocodazole) and released into anaphase under P_{GAL1}- and P_{GAL10}-inducing conditions (2% galactose medium). rDNA-GFP segregation was tracked through anaphase by live-cell fluorescence microscopy ($n=30$ cells per time point).

stability by localizing both to the RFB and also to the cryptic E-Pro promoter. By repressing PolII-mediated transcription from E-Pro, Sir2 prevents the synthesis of non-coding E-Pro transcripts that displace the cohesin complexes and cause the sister arrays to misalign[36]. Double-strand rDNA breaks repaired by recombination between misaligned sister arrays results in rDNA repeat-number expansion or reduction, and in the formation of ERCs[27,28]. Both ERC accumulation and rDNA repeat-number instability have been linked to senescence (shortened lifespan)[29,30], suggesting that Rio1 may determine yeast life expectancy. When rDNA repeat numbers fall below wild-type level, reduced repression of E-Pro may promote unequal recombination and increase repeat numbers. As such, Rio1 could act as a monitor of rDNA copy number and as an array manager by dictating Sir2 levels and activity.

Once cells have endured rDNA replication, repression of PolI activity may no longer be necessary in metaphase. As such, Rio1 dissociating from the metaphase nucleolus may lead to a temporal increase in rDNA transcription before PolI becomes down-regulated in anaphase. Rio1, together with the conserved Cdc14 phosphatase, reduce PolI activity by targeting Rpa43, a subunit of the Rpa14-Rpa43 dimer, that lies at the outer edge of PolI and mediates PolI recruitment by Rrn3 (refs 42,43). The concurrent action by Rio1 and Cdc14 may establish a local phospho-threshold that commands the dissociation of PolI from 35S at anaphase entry.

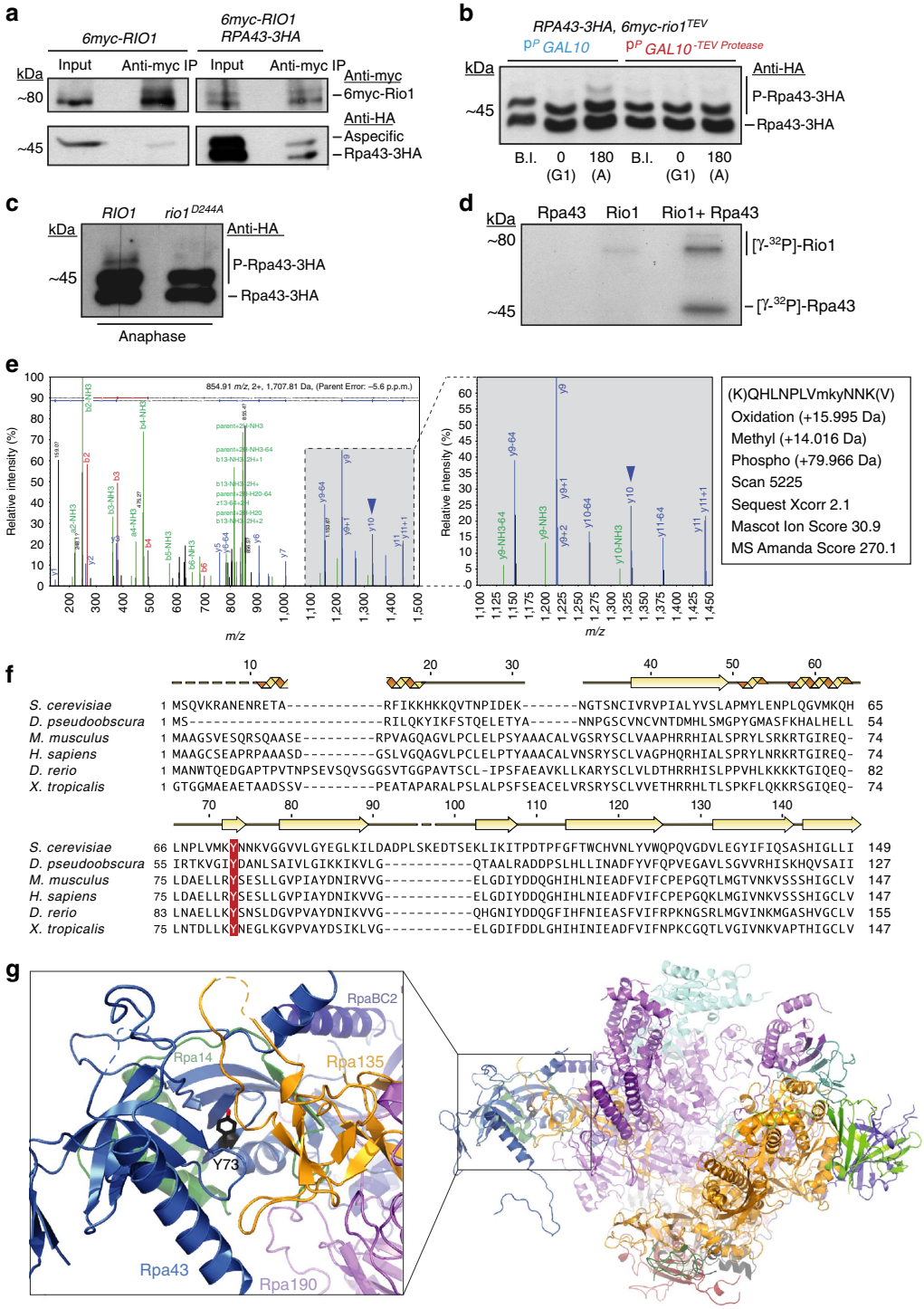

Figure 8 | Rio1 downregulates RNA PolI by targeting subunit Rpa43. (**a**) 6myc-Rio1 and Rpa43-3HA co-immunoprecipitate from whole-cell extract derived from exponentially growing *6myc-RIO1 RPA43-3HA* cells. (**b**) PhosTag western blot of Rpa43-3HA (anti-HA) in *6myc-rio1^{TEV}* pP_{GAL10} (blue) and *6myc-rio1^{TEV}* pP_{GAL10}-*TEV Protease* (red) cells. Cells were collected before P_{GAL10} induction (B.I.), after 1 h of induction during the G1 arrest (G1), and 3 h after the release from G1 (anaphase, A). (**c**) PhosTag western blot of Rpa43-3HA (anti-HA) in *RPA43-3HA* cells inducibly expressing wild-type *RIO1* or the dominant-negative kinase-dead *rio1^{D244A}* allele from P_{GAL1} on a 2 μ plasmid. The cells were collected in anaphase 3 h after release from G1 in 2% galactose medium. (**d**) *In vitro* kinase assay with recombinant His6-Rio1 (1 μg) and recombinant Rpa43-His6-HA (6 μg) in the presence of 0.05 μM [γ-^{32}P]ATP. The radiographs show phosphorylated His6-Rio1 and Rpa43-His6-HA. (**e**) NanoLC-MS/MS spectrum of the Rpa43 QHLNPVMKY73NNK phospho-peptide. The position of phospho-Y73 is indicated with an arrowhead. (**f**) Alignment of the Rpa43 proteins from *Saccharomyces cerevisiae*, *Drosophila pseudoobscura*, *Mus musculus*, *Homo sapiens*, *Dario rerio* and *Xenopus tropicalis* (UniProtKB database entries: A6ZPH0, Q29JY4, Q78WZ7, Q3B726, Q6PHG8 and F7BDD1, respectively) using Muscle (www.ebi.ac.uk/Tools/msa/muscle). The *S. cerevisiae* Y73 residue and its equivalents in the Rpa43 orthologues are indicated in white font on a red background. (**g**) Localization of Rpa43 Y73, indicated in black, within the 14-subunit RNA PolI enzyme complex[57] (top view rotated +90°; PDB 4C3J).

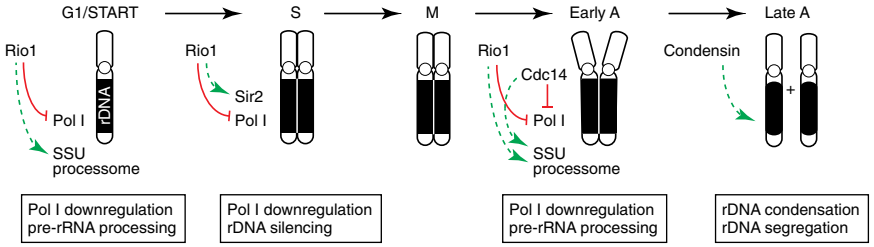

Figure 9 | Rio1 downregulates RNA PolI to promote rDNA stability and segregation. Working model of Rio1-mediated regulation of rDNA transcription, pre-rRNA processing, rDNA stability and segregation, as identified in this study. In G1, Rio1 downregulates 35S rDNA transcription by PolI and promotes pre-rRNA processing at A_2 by the SSU processome and associated factors, allowing for a timely commencement of the cell cycle at START. In S phase, the Rio1-mediated downregulation of PolI and recruitment of the histone deacetylase Sir2 to rDNA chromatin, promote rDNA stability. As rDNA replication progresses, Rio1 concentrations at S phase rDNA decrease, resulting in metaphase nuclei containing low levels of Rio1. At anaphase onset, Rio1 becomes re-recruited to the nucleolus to remove PolI from the rDNA by targeting PolI subunit Rpa43. PolI delocalization and promotion of pre-rRNA processing at the rDNA allow for condensin enrichment, resulting in rDNA compaction and segregation. Red lines: inhibitory activity, green lines: activating activity, solid lines: direct activity, dashed lines: direct or indirect activity.

By downregulating PolI and by stimulating PolI transcript processing at the A_2 site (as mediated by the SSU processome), Rio1 promotes condensin binding and rDNA transmission. Indeed, without Rio1 activity, the long right arm of chromosome XII harbouring the rDNA array does not segregate into the daughter cells, resulting in chromosome loss. We also observed that condensin itself recruits Rio1 to anaphase rDNA, suggesting that Rio1 might also promote condensin activity. The monopolin complex, which tethers the nucleolus to the nuclear membrane via the CLIP (Chromosome Linkage Inner nuclear membrane Protein) complex[48], also recruits Rio1 to anaphase rDNA. It is tempting to speculate that Rio1 targeting monopolin may facilitate rDNA segregation by inducing rDNA detachment from the nuclear envelope.

Rio1 and its human orthologue RIOK1 promote the endonucleolytic cleavage of 20S pre-rRNA at pre-40S ribosomes, and stimulate the recycling of trans-acting factors that catalyse 40S maturation[12,18–20]. While these events occur in the cytoplasm, a small pool of RIOK1 also localizes to the human nucleus[19,20]. Treating murine cells with toyocamycin, an inhibitor of Rio1 activity *in vitro*[61], impeded nucleolar pre-rRNA processing[62], indicating that RIOK1 might be involved in early pre-rRNA cleavage, as we observed for Rio1 in yeast.

In contrast to yeast, vertebrate cells contain five rDNA clusters on different chromosomes. In prophase, these nucleoli disassemble and their transcription becomes repressed to allow the stripped rDNA to segregate with the rest of the genome. Nucleolar transcription is downregulated by the CDK1-cyclin B kinase, whose phosphorylation of promoter selectivity factor SL1 prevents the formation of the PolI pre-initiation complex[63–65]. Similar to yeast Rio1, RIOK1 might just as well contribute to the transcriptional repression of PolI.

In conclusion, our study reveals the first nuclear functions of the Rio1 kinase. By downregulating PolI-mediated rDNA transcription and by promoting the processing of its transcripts, Rio1 ensures both a timely commencement and conclusion of the cell cycle (rDNA segregation permits exit from mitosis). Rio1 safeguards rDNA stability during DNA replication and integrates early nucleolar and late cytoplasmic events during ribosome biogenesis. As such, Rio1 activity allows yeast to actively grow and divide while ensuring the integrity and faithful transmission of its genome.

Methods

Yeast strains. Yeast strains (W303-1A background; Supplementary Table 1) were made by mating, tetrad dissection and spore selection, by introducing integrative or episomal plasmids or via transformation and homologous recombination of PCR-generated deletion or epitope cassettes. None of the epitopes affected yeast fitness or the activity of the tagged protein. The plasmids used in this study are listed in Supplementary Table 2.

To generate the *6myc-rio1*^{TEV} strain, 21 nucleotides (5′-GAAAACCTGTATT TTCAGGGC-3′) encoding the TEV Protease cleavage site (ENLYFQG) were introduced by PCR between the nucleotides encoding Rio1 residues E406 and E407 in an integrative *URA3*-based plasmid harbouring *6myc-RIO1* under control of its endogenous promoter, P_{RIO1}. After linearization in P_{RIO1} by the endonuclease SgraI, the plasmid was integrated at the endogenous P_{RIO1} in the genome of parent strain PDW001. Following incubation on complete minimal medium containing 1 g l^{-1} 5-fluoroorotic acid (Fluka), we PCR-identified the colonies in which wild-type *RIO1* had been recombined out, leaving the *6myc-rio1* allele expressed from P_{RIO1} and harbouring the TEV Protease cleavage site (named *6myc-rio1*^{TEV}) as the only source of Rio1. The episomal high-copy 2 μ pP_{GAL10}-*HA-TEV Protease-NLS* plasmid was made by subcloning the *HA-TEV Protease-NLS* sequence from pYeF1-TEV (ref. 66) into the *HIS3*-marked P_{GAL10} expression plasmid pYeHFc2H (pP_{GAL10}, gift from C. Cullin) as well as into pYeHFc2H provided with geneticin-resistance cassette *KanMX4*. After transforming the *6myc-rio1*^{TEV} strain, we obtained strain *6myc-rio1*^{TEV} pP_{GAL10}-*TEV Protease* and the *6myc-rio1*^{TEV} pP_{GAL10} control strains.

Cell cycle studies. Cells were grown at 23 °C in minimal synthetic drop-out media or in YEPA medium (1% yeast extract, 2% peptone and 0.3 mM adenine) containing 2% raffinose, 2% galactose or 2% glucose. To arrest yeast in G1, S phase or metaphase, cultures were treated (2.5–3 h) with 5 μg ml^{-1} α-factor (GeneScript), 10 μg ml^{-1} hydroxyurea (Sigma-Aldrich) or 15 μg ml^{-1} nocodazole (Sigma-Aldrich), respectively. To release the cells into the cell cycle, we filtered the yeast cultures, washed and then resuspended the cells in drug-free medium. To arrest the cells in anaphase, strains carrying either the temperature-sensitive *cdc15-2* or *cdc14-3* allele were first arrested in G1 or metaphase (23 °C) and then released at the non-permissive temperature (37 °C).

To deplete Rio1 activity from the nucleus, both the *6myc-rio1*^{TEV} pP_{GAL10}-*TEV Protease* strain and the *6myc-rio1*^{TEV} pP_{GAL10} negative-control strain were grown in 2% raffinose YEPA medium (raffinose does not affect P_{GAL10}) containing 220 μg ml^{-1} geneticin (G418, Life Technologies). While arrested or during exponential growth, the cells were treated with 2% galactose to induce P_{GAL10} (for 1 h during the arrest, for 3 h during exponential growth). Arrested cells were then released in medium containing 2% galactose, 2% raffinose and 220 μg ml^{-1} G418.

For rDNA and ERC analysis, total DNA was extracted from cells grown for 15 h (eight divisions) in 2% galactose medium, run on a 0.6% TBE-agarose gel, transferred for Southern blot analysis and hybridized with a 25S rDNA probe[32]. The oligomers used to produce the probe are listed in Supplementary Table 3.

Progression through the cell cycle was tracked by indirect IF microscopy analysis of spindle morphology (see further down) and by FACS analysis of DNA content. Regarding the latter, cells were fixed in 70% ethanol, incubated first with 1 mg ml^{-1} RNAse A (Sigma-Aldrich), then with 5 mg ml^{-1} pepsin (Sigma-Aldrich) and ultimately resuspended in 1 mg ml^{-1} propidium iodide (Sigma-Aldrich). After mild sonication, cell fluorescence was analysed with a FACScan (Becton Dickinson) sorter and DNA content profiles generated with CellQuest software.

IF imaging of yeast cells was performed with 1 ml of cell culture. The cells were centrifuged and crosslinked overnight in 1 ml of 3.7% formaldehyde. The cell walls were then digested (30 min) with zymolyase (100 μg ml^{-1}, Amsbio), washed with 1.2 M sorbitol and 100 mM phospho-citrate, pH 5.9, and bound to a multiwall poly-L-lysine-coated glass slide (Sigma-Aldrich). The slide was treated with DAPI and hybridized with rat monoclonal anti-Tub1 (YOL1/34, Adb Serotec MCA78G), rabbit polyclonal anti-GFP (Life Technologies,A-6455), goat polyclonal anti-Cdc14 (yE-17, Santa Cruz Biotech sc-12045) or mouse monoclonal anti-myc (9E10, Covance MMS-150R) primary antibodies. CY3 (715-165-151)- or fluorescein isothiocyanate (FITC; 111-095-144)-labelled secondary antibodies (Jackson Laboratory) were used to visualize the proteins.

IF imaging of rDNA or centromeres in fixed cell samples was done as described above and performed with strains whose *RDN1* or *CEN4* sequence was flanked with a 256x*tetO*∼TetR-GFP array. Images were acquired with a DeltaVision ELITE microscope (Applied Precision) carrying an Olympus IX71 UPlanSApo objective lens (numerical aperture 1.40) and a CoolSnap HQ2 CCD Camera (Photometrics). Fifteen Z-stacks were acquired every 0.4 µm, deconvoluted (SoftWoRx) and projected with maximum intensity.

IF imaging of spread nuclei was performed using 4 ml of cell culture. The cells were centrifuged and digested with zymolyase (30 µg ml^{-1}). The spheroblasts were then fixated on a glass slide with 4% paraformaldehyde and 3.4% sucrose, and spread with a glass rod. The slides were then hybridized with rabbit polyclonal anti-GFP (Life Technologies A-6455), mouse monoclonal anti-HA (16B12, Covance MMS-101P), mouse monoclonal anti-myc (9E10, Covance MMS-150R), mouse monoclonal anti-Nop1 (28F2, EnCore Biotech MCA28F2), rabbit polyclonal anti-Rio1 (gift from J.-P. Gelugne) or goat polyclonal anti-Sir2 (yN-19, Santa Cruz Biotech sc-6666) antibodies. CY3- or FITC-labelled secondary antibodies (Jackson Laboratory, see above) were used. Nuclei were imaged with a BX51 wide-field fluorescence microscope (Olympus).

Live-cell imaging of spindle (mCherry-Tub1) elongation and *RDN1*-GFP segregation was performed with microfluidic plates (CellASIC) and a DeltaVision microscope setup as described above via 15 Z-stacks (0.4 µm each). The images were deconvoluted (SoftWoRx), projected with maximum intensity and analysed with ImageJ1.43u (National Institutes of Health, N.I.H.).

Immunobloting. Cells were collected, treated with 5% trichloroacetic acid (TCA), resuspended in lysis buffer (50 mM Tris-Cl pH7.5, 1 mM EDTA.Na_2, 50 mM dithiothreitol, 60 mM β-glycerophosphate, 0.1 mM Na_3VO_4 and 5 mM NaF) containing protease inhibitors (Roche) and then disrupted with glass beads and a FastPrep-24 instrument (MP Biomedicals). Lysates were cleared by centrifugation, resuspended in sample loading buffer (8% SDS, 200 mM Tris-Cl, pH 6.8, 400 mM dithiothreitol, 0.4% bromophenol blue and 40% glycerol), heat-denatured and run on SDS polyacrylamide gels. To separate the phospho species of Rpa43-3HA, the SDS polyacrylamide gels were provided with 30 µM PhosTag (Manac Incorporated). Proteins were transferred onto Immobilon-P membranes (Millipore) and incubated with mouse monoclonal anti-Pgk1 antibody (1:5,000; Life Technologies 459250), mouse monoclonal anti-Rad53 EL7E1 (4 µg ml^{-1}, gift from M. Foiani), goat polyclonal anti-Cdc14 yE-17 (1:1,000; Santa Cruz sc-12045), mouse monoclonal anti-Flag M2 (1:4,000; Sigma-Aldrich A2220), mouse monoclonal anti-Myc 9E10 (1:1,000; Covance MMS-150R), mouse monoclonal anti-HA 16B12 (1:1,000; Covance MMS-101P) or mouse monoclonal anti-HIS H-3 (1:200, Santa Cruz sc-8036) antibodies. Horseradish peroxidase (HRP)-conjugated goat anti-mouse (1:10,000; Bio-Rad 170–6516) or goat anti-rabbit (1:10,000; Bio-Rad 170–6515) secondary antibodies were used to visualize the proteins with ECL chemiluminescence (GE Healthcare) and radiography film (GE Healthcare). Uncropped blots are shown in Supplementary Fig. 11.

To probe the interaction between 6myc-Rio1 and Rpa43-3HA or between 6myc-Rio1 and Sgs1-3FLAG, yeast whole-cell extract (3 µg of total protein) was incubated with anti-myc sepharose matrix (9E10, Covance AFC-150P) or anti-HA sepharose matrix (3F10, Roche 11815016001). Following four washes with high salt and detergent buffer (50 mM HEPES, pH 7.5, 500 mM NaCl, 2.5 mM $MgCl_2$, 0.5% Nonidet P (NP)-40 and 10% glycerol), Rpa43-3HA, 6myc-Rio1 or Sgs1-3Flag were visualized by western hybridization analysis.

Rio1 kinase activity measurements. To measure the kinase activity of full-length or truncated 6myc-Rio1^{TEV}, cells were grown in 2% raffinose medium, arrested in G1 and collected before, upon and after P_{GAL10} induction with 2% galactose. Cells were resuspended in lysis buffer (50 mM HEPES-KOH, pH 7.1, 50% glycerol, 300 mM NaCl, 1% NP-40, 1 mM Na3VO4, 1 mM NaF and 1 mM phenylmethylsulfonyl fluoride (PMSF)) and whole-cell extracts made with glass beads. Cleared extract (500 µg of protein) was then incubated (4 °C, overnight) with anti-myc sepharose beads (Covance). The beads were washed once with washing buffer (50 mM HEPES-KOH, pH 7.1, 300 mM NaCl, 1% NP-40, 1 mM Na_3VO_4, 1 mM NaF and 1 mM PMSF), and three times with kinase buffer (50 mM HEPES-KOH, pH 7.2, 5 mM $MgCl_2$ and 5 mM $MnCl_2$). Bead-bound 6myc-Rio1^{TEV} was incubated with 1.5 mg ml^{-1} of dephosphorylated casein (Sigma-Aldrich) and 0.03 µM [γ-32P]ATP (PerkinElmer) in kinase buffer. The assay (15 min, 24 °C) was performed in the presence or absence of CK1 and CK2 kinase inhibitors (5 µM each; CKI-7 dichlorhydrate and 4,5,6,7-tetrabromobenzotriazole (TBB), respectively; Sigma-Aldrich). The reactions were analysed on SDS polyacrylamide gels, which were then fixed in a 30% methanol + 10% acetic acid solution, and dried on a Gel Dryer (Bio-Rad). The phospholabelled proteins were visualized by autoradiography and quantified using ImageJ.

RT-qPCR analysis of rRNA. Total RNA was isolated[67] from cells collected through the cell cycle or enriched at a specific cell cycle stage. RNA (1 µg) was retrotranscribed into cDNA with Random Primers (Life Technologies) and ImProm-II Reverse Transcriptase (Promega). cDNA (5 ng) was analysed by RT–qPCR analysis (7500 Fast Real-Time PCR, Life Technologies) using TaqMan probes (Life Technologies; Supplementary Table 3) against the 5′ETS sequence of 35S pre-rRNA (probe 4 in the figures) or against the A_2-processing site of 35S, 33S and 32S pre-rRNA (probe 6). *ACT1* cDNA (housekeeping control) was used as the internal reference. Analyses were done in triplicate.

ChIP–qPCR analysis. For each analysis, 50 ml of cell culture were treated with 1% formaldehyde (2 h). Crosslinked cells were washed with Tris-buffered saline (50 mM Tris-Cl, pH 7.5, 150 mM NaCl) and resuspended in lysis buffer (50 mM HEPES, pH 7.5, 140 mM NaCl, 1 mM EDTA, 1% Triton X-100 and 0.1% sodium deoxycholate). The cells were broken with glass beads and the whole-cell extracts were sonicated on ice with a Branson Sonifier 250 (5 × 30 s, 2 min on ice) to reduce the genome in ∼500 bp fragments. Anti-myc sepharose beads and rabbit polyclonal anti-Rpa43 antibody (gift from M. Riva) conjugated to protein A-associated agarose beads (Pierce) were incubated (4 °C, overnight) with the extracts to isolate 6myc-Rio1 and Rpa43. The beads were then washed twice with lysis buffer, once with washing buffer (100 mM Tris-Cl, pH 8.0, 1 mM EDTA 1% Triton X-100, 0.1% sodium deoxycholate, 0.5% NP-40 and 250 mM LiCl) and once with TE buffer. The beads were resuspended (10 min, 65 °C) in elution buffer (1% SDS, 50 mM Tris-Cl, pH 8.0, 10 mM EDTA) and the eluted material then separated from the beads and heated (65 °C, overnight) to reverse the crosslinks. An amount of 25 µl of total chromatin solution were similarly heat treated (= Input). After treatment with 20 mg ml^{-1} proteinase K (Roche), the material was treated with 10 mg ml^{-1} RNase (Sigma-Aldrich) for 30 min at 37 °C, and the DNA was extracted with phenol and chloroform. Following precipitation, the DNA was resuspended in 40 µl water. Input and immunoprecipitated samples were analysed by RT–qPCR (probes are indicated in the Figures 1a, 6b and 6c and in Supplementary Table 3).

Yeast two-hybrid interaction screens. Yeast two-hybrid screens were performed by Hybrigenics Services (www.hybrigenics-services.com). The *RIO1* coding sequence (YOR119C) was cloned as a C-terminal fusion to *LEXA* or the *GAL4* encoding DNA-binding domain, or as an N-terminal fusion to *LEXA* or *GAL4*. The constructs were screened by mating and covered the complexity of the *S. cerevisiae* genomic library 5- to 14-fold. Prey fragments of positive clones were amplified by PCR, sequenced and the interacting sequences were identified in the GenBank database (NCBI).

Ribosome, protein translation and northern blot analysis. For ribosome profiling, *6myc-rio1^{TEV}* pP_{GAL10} and *6myc-rio1^{TEV}* pP_{GAL10}-*TEV Protease* cells were grown exponentially in 2% raffinose medium to an OD_{600} = 0.5. Galactose (2%) was added and samples were taken at the indicated time points and treated on ice (5 min) with 100 µg ml^{-1} cycloheximide to stabilize the polysomes. The cells were washed with extraction buffer (20 mM Tris-Cl, pH 7.5, 50 mM KCl, 10 mM $MgCl_2$ and 100 µg ml^{-1} cycloheximide). The cells were broken with glass beads and the cleared extract (OD_{254} = 5.0) was loaded on a 10.5 ml 5–45% sucrose gradient in extraction buffer lacking cycloheximide. Following centrifugation (16 h; 21,000 r.p.m.; SW41 Beckman rotor), gradients were collected at a 1 ml min^{-1} flow rate and the ultraviolet profile recorded at 254 nm by a ultraviolet detector (linked to BioLogic LB fractionator), visualized with LP Data View software (Bio-Rad) and exported to Excel (Microsoft Office).

For global translation analysis, cells were grown as described above. The cells were collected at an OD_{600} = 0.5 and washed with complete synthetic medium lacking methionine but containing 2% raffinose or 2% galactose. The cells were then resuspended in 1 ml of the corresponding medium and pulse-labelled with 100 µCi of 5′,6′ [^{3}H]-L-methionine for 20 min at 23 °C. Total proteins (TCA insoluble fraction) were extracted and washed twice with cold acetone before resolubilization. The amount of newly synthesized proteins was quantified using a scintillation counter. The solubilized proteins were also separated on a Nu-PAGE 4–10% gradient gel and Coomassie stained to evidence equal loading.

For northern hybridization analysis, total RNA was isolated from the whole-cell extracts submitted to ribosome profiling (see above). Denaturing agarose gel electrophoresis, transferring of the RNA onto a positive membrane and northern hybridization with ^{32}P-labelled oligomers (Supplementary Table 3) were performed as described[12].

***In vitro* phosphorylation of Rpa43 by Rio1.** Recombinant Rpa43-His6-HA was produced in *E. coli* Rosetta BL21(DE3) cells. Expression of Rpa43-His6-HA from plasmid pRSET-43A (gift from M. Riva) was induced at an OD_{600} = 0.5 with 150 mM IPTG (3.5 h, 24 °C). Cells were collected in lysis buffer (20 mM Tris-Cl, pH8.0, 300 mM NaCl, 10% glycerol, 20 mM imidazole, 1 mM PMSF and 1 mM Na_3VO_4) and lysed with a French press (15,000 p.s.i.; Microfluidics). The extract was incubated with Ni^{2+}-NTA beads (Qiagen). The beads were washed with 30 mM imidazole and Rpa43-His6-HA eluted with 200 mM imidazole before being submitted to size-exclusion chromatography (Superdex 200 HR 10/30, GE Healthcare). Recombinant His6-Rio1 was produced in *E. coli* BL21-RIL cells and expressed from plasmid pQE32-HIS6-RIO1 (gift from M. Angermayr)[21]. Expression was induced (3.5 h 30 °C) at an OD_{600} = 0.7 with 1 mM IPTG and the cells were collected in lysis buffer (50 mM NaH_2PO_4 pH8.0, 50% glycerol, 300 mM NaCl, 1 mM NaF, 1 mM PMSF, 1 mM Na_3VO_4, 1 µg ml^{-1} apoprotein and leupeptine, 1 mg ml^{-1} lysozyme, 5 µg ml^{-1} DNase and 100 µg ml^{-1} RNAse). The cell extract, obtained with a French press, was incubated with Ni^{2+}-NTA beads

(Qiagen), which were then washed with 20 mM imidazole. His6-Rio1 was eluted with 200 mM imidazole and the buffer was then exchanged into 50 mM HEPES, pH7.5, 5% glycerol, 1 μg ml^{-1} apoprotein and leupeptine using PD-10 columns (GE Healthcare). The purity of Rpa43-His6-HA and His6-Rio1 was confirmed via SDS–PAGE and GelCode Blue (Pierce) staining.

To examine phosphorylation of Rpa43-His6-HA by His6-Rio1, 1 μg of His6-Rio1, 6 μg of Rpa43-His6-HA and 0.05 μM (5 μCi) [γ-^{32}P]ATP (PerkinElmer) were incubated (2 h, 30 °C) in reaction buffer (50 mM HEPES-KOH, pH 7.2, 5 mM $MgCl_2$ and 5 mM $MnCl_2$). Phosphorylated Rpa43-His6-HA was visualized radiographically. In the control reactions, only His6-Rio1 or Rpa43-His6-HA was present. To produce phosphorylated Rpa43-His6-HA for mass spectrometric analysis, five kinase reactions were set up, pooled (giving 30 μg Rpa43-His6-HA) and separated by SDS–PAGE. Proteins were stained with GelCode Blue, Rpa43-His6-HA then excised from the gel, submitted to proteolytic cleavage and analysed by nanoLC-MS/MS (see below). In the negative-control assay, ATP was omitted from the kinase reaction.

NanoLC-MS/MS and data analysis. The nano HPLC system was comprised of an UltiMate 3000 HPLC RSLC nano system (Thermo Fisher Scientific) coupled to a Q Exactive mass spectrometer (Thermo Fisher Scientific), equipped with a Proxeon nanospray source (Thermo Fisher Scientific). Following proteolytic treatment of Rpa43-His6-HA, peptides were loaded onto a trap column (PepMap C18, 5 mm × 300 μm ID, 5 μm particles, 100 Å pores; Thermo Fisher Scientific) at a flow rate of 25 μl min^{-1} using 0.1% TFA as mobile phase. After 10 min, the trap column was switched in line with the analytical column (PepMap C18, 500 mm × 75 μm ID, 3 μm, 100 Å; Thermo Fisher Scientific). The peptides were eluted using a flow rate of 230 nl min^{-1}, and a binary 2-h gradient and a 165-min gradient. The gradient starts with the mobile phases: 98% A (water/formic acid, 99.9/0.1, v/v) and 2% B (water/acetonitrile/formic acid, 19.92/80/0.08, v/v/v) increases to 35% B over the next 120 min, followed by a gradient in 5 min to 90% B, stays there for 5 min and decreases in 5 min back to the gradient 98% A and 2% B for equilibration at 30 °C. The Q Exactive mass spectrometer was operated in data-dependent mode, using a full scan (*m/z* range 380–1,650, nominal resolution of 70,000; target value 3E6) followed by MS/MS scans of the 12 most abundant ions. MS/MS spectra were acquired using normalized collision energy 27%, isolation width of 2 and the target value was set to 1E5. Precursor ions selected for fragmentation (charge state 2 and higher) were put on a dynamic exclusion list for 10 s. In addition, the underfill ratio was set to 20% resulting in an intensity threshold of 4E4. The peptide match feature and the exclude isotopes feature were enabled.

For peptide identification, the RAW files were loaded into Proteome Discoverer (version 1.4.0.288, Thermo Scientific). The created MS/MS spectra were searched using Mascot 2.2.07 (Matrix Science, Sequest, Thermo Scientific)[68] and MSAmanda[69] against the *S. cerevisiae* genome database[25]. The following search parameters were used: β-methylthiolation on cysteine was set as a fixed modification, mono- and dioxidation on methionine, acetylation on lysine and protein-N terminus, deamidation on asparagine and glutamine, mono- and dimethylation on lysine, and arginine and phosphorylation on serine, threonine and tyrosine were set as variable modifications. Monoisotopic masses were searched within unrestricted protein masses for tryptic and chymotryptic peptides. The peptide mass tolerance was set to ±6 ppm and the fragment mass tolerance to ±30 mmu. The maximal number of missed cleavages was set to 2. The result was filtered to 1% false discovery rate using the Percolator algorithm integrated in Proteome Discoverer (Thermo Scientific). The localization of the phosphorylation sites within the peptides was performed with ptmRS, based on the algorithm of phosphoRS[70]. The ion series of the Rpa43 QHLNPLVMKYNNK phospho-peptide are shown in Supplementary Table 4.

References

1. Tomson, B. N., D'Amours, D., Adamson, B. S., Aragon, L. & Amon, A. Ribosomal DNA transcription-dependent processes interfere with chromosome segregation. *Mol. Cell. Biol.* **26,** 6239–6247 (2006).
2. Sullivan, M., Higuchi, T., Katis, V. L. & Uhlmann, F. Cdc14 phosphatase induces rDNA condensation and resolves cohesin-independent cohesion during budding yeast anaphase. *Cell* **117,** 471–482 (2004).
3. D'Ambrosio, C., Kelly, G., Shirahige, K. & Uhlmann, F. Condensin-dependent rDNA decatenation introduces a temporal pattern to chromosome segregation. *Curr. Biol.* **18,** 1084–1089 (2008).
4. Clemente-Blanco, A. *et al.* Cdc14 inhibits transcription by RNA polymerase I during anaphase. *Nature* **458,** 219–222 (2009).
5. Woolford, Jr J. L. & Baserga, S. J. Ribosome biogenesis in the yeast Saccharomyces cerevisiae. *Genetics* **195,** 643–681 (2013).
6. Thomson, E., Ferreira-Cerca, S. & Hurt, E. Eukaryotic ribosome biogenesis at a glance. *J. Cell. Sci.* **126,** 4815–4821 (2013).
7. D'Amours, D., Stegmeier, F. & Amon, A. Cdc14 and condensin control the dissolution of cohesin-independent chromosome linkages at repeated DNA. *Cell* **117,** 455–469 (2004).
8. Esser, D. & Siebers, B. Atypical protein kinases of the RIO family in archaea. *Biochem. Soc. Trans.* **41,** 399–404 (2013).
9. LaRonde-LeBlanc, N. & Wlodawer, A. A family portrait of the RIO kinases. *J. Biol. Chem.* **280,** 37297–37300 (2005).
10. LaRonde-LeBlanc, N. & Wlodawer, A. The RIO kinases: an atypical protein kinase family required for ribosome biogenesis and cell cycle progression. *Biochim. Biophys. Acta* **1754,** 14–24 (2005).
11. LaRonde, N. A. The ancient microbial RIO kinases. *J. Biol. Chem.* **289,** 9488–9492 (2014).
12. Ferreira-Cerca, S., Kiburu, I., Thomson, E., LaRonde, N. & Hurt, E. Dominant Rio1 kinase/ATPase catalytic mutant induces trapping of late pre-40S biogenesis factors in 80S-like ribosomes. *Nucleic Acids Res.* **42,** 8635–8647 (2014).
13. Ferreira-Cerca, S. *et al.* ATPase-dependent role of the atypical kinase Rio2 on the evolving pre-40S ribosomal subunit. *Nat. Struct. Mol. Biol.* **19,** 1316–1323 (2012).
14. Perrochia, L., Guetta, D., Hecker, A., Forterre, P. & Basta, T. Functional assignment of KEOPS/EKC complex subunits in the biosynthesis of the universal t6A tRNA modification. *Nucleic Acids Res.* **41,** 9484–9499 (2013).
15. Vanrobays, E. *et al.* Processing of 20S pre-rRNA to 18S ribosomal RNA in yeast requires Rrp10p, an essential non-ribosomal cytoplasmic protein. *EMBO J.* **20,** 4204–4213 (2001).
16. Vanrobays, E., Gelugne, J. P., Gleizes, P. E. & Caizergues-Ferrer, M. Late cytoplasmic maturation of the small ribosomal subunit requires RIO proteins in Saccharomyces cerevisiae. *Mol. Cell. Biol.* **23,** 2083–2095 (2003).
17. Hector, R. D. *et al.* Snapshots of pre-rRNA structural flexibility reveal eukaryotic 40S assembly dynamics at nucleotide resolution. *Nucleic Acids Res.* **42,** 12138–12154 (2014).
18. Turowski, T. W. *et al.* Rio1 mediates ATP-dependent final maturation of 40S ribosomal subunits. *Nucleic Acids Res.* **42,** 12189–12199 (2014).
19. Baumas, K. *et al.* Human RioK3 is a novel component of cytoplasmic pre-40S pre-ribosomal particles. *RNA Biol.* **9,** 162–174 (2012).
20. Widmann, B. *et al.* The kinase activity of human Rio1 is required for final steps of cytoplasmic maturation of 40S subunits. *Mol. Biol. Cell* **23,** 22–35 (2012).
21. Angermayr, M., Roidl, A. & Bandlow, W. Yeast Rio1p is the founding member of a novel subfamily of protein serine kinases involved in the control of cell cycle progression. *Mol. Microbiol.* **44,** 309–324 (2002).
22. Angermayr, M., Hochleitner, E., Lottspeich, F. & Bandlow, W. Protein kinase CK2 activates the atypical Rio1p kinase and promotes its cell-cycle phase-dependent degradation in yeast. *FEBS J.* **274,** 4654–4667 (2007).
23. Breitkreutz, A. *et al.* A global protein kinase and phosphatase interaction network in yeast. *Science* **328,** 1043–1046 (2010).
24. Huang, J. & Moazed, D. Association of the RENT complex with nontranscribed and coding regions of rDNA and a regional requirement for the replication fork block protein Fob1 in rDNA silencing. *Genes Dev.* **17,** 2162–2176 (2003).
25. Cherry, J. M. *et al.* Saccharomyces Genome Database: the genomics resource of budding yeast. *Nucleic Acids Res.* **40,** D700–D705 (2012).
26. Lempiainen, H. & Shore, D. Growth control and ribosome biogenesis. *Curr. Opin. Cell. Biol.* **21,** 855–863 (2009).
27. Kobayashi, T. Ribosomal RNA gene repeats, their stability and cellular senescence. *Proc. Jpn Acad. Ser. B Phys. Biol. Sci.* **90,** 119–129 (2014).
28. Tsang, E. & Carr, A. M. Replication fork arrest, recombination and the maintenance of ribosomal DNA stability. *DNA. Repair (Amst).* **7,** 1613–1623 (2008).
29. Ganley, A. R., Ide, S., Saka, K. & Kobayashi, T. The effect of replication initiation on gene amplification in the rDNA and its relationship to aging. *Mol. Cell* **35,** 683–693 (2009).
30. Saka, K., Ide, S., Ganley, A. R. & Kobayashi, T. Cellular senescence in yeast is regulated by rDNA noncoding transcription. *Curr. Biol.* **23,** 1794–1798 (2013).
31. Visintin, R., Hwang, E. S. & Amon, A. Cfi1 prevents premature exit from mitosis by anchoring Cdc14 phosphatase in the nucleolus. *Nature* **398,** 818–823 (1999).
32. Tsang, C. K., Li, H. & Zheng, X. S. Nutrient starvation promotes condensin loading to maintain rDNA stability. *EMBO J.* **26,** 448–458 (2007).
33. Kobayashi, T., Horiuchi, T., Tongaonkar, P., Vu, L. & Nomura, M. SIR2 regulates recombination between different rDNA repeats, but not recombination within individual rRNA genes in yeast. *Cell* **117,** 441–453 (2004).
34. Eckert-Boulet, N. & Lisby, M. Regulation of rDNA stability by sumoylation. *DNA. Repair (Amst).* **8,** 507–516 (2009).
35. Pellicioli, A. *et al.* Activation of Rad53 kinase in response to DNA damage and its effect in modulating phosphorylation of the lagging strand DNA polymerase. *EMBO J.* **18,** 6561–6572 (1999).
36. Kobayashi, T. & Ganley, A. R. Recombination regulation by transcription-induced cohesin dissociation in rDNA repeats. *Science* **309,** 1581–1584 (2005).
37. Michel, A. H., Kornmann, B., Dubrana, K. & Shore, D. Spontaneous rDNA copy number variation modulates Sir2 levels and epigenetic gene silencing. *Genes Dev.* **19,** 1199–1210 (2005).
38. Dragon, F. *et al.* A large nucleolar U3 ribonucleoprotein required for 18S ribosomal RNA biogenesis. *Nature* **417,** 967–970 (2002).

39. Phipps, K. R., Charette, J. & Baserga, S. J. The small subunit processome in ribosome biogenesis-progress and prospects. *Wiley Interdiscip. Rev. RNA* **2,** 1–21 (2011).
40. Horn, D. M., Mason, S. L. & Karbstein, K. Rcl1 protein, a novel nuclease for 18S ribosomal RNA production. *J. Biol. Chem.* **286,** 34082–34087 (2011).
41. Fujii, T., Yamaoka, H., Gomi, K., Kitamoto, K. & Kumagai, C. Cloning and nucleotide sequence of the ribonuclease T1 gene (rntA) from Aspergillus oryzae and its expression in Saccharomyces cerevisiae and Aspergillus oryzae. *Biosci. Biotechnol. Biochem.* **59,** 1869–1874 (1995).
42. Blattner, C. *et al.* Molecular basis of Rrn3-regulated RNA polymerase I initiation and cell growth. *Genes Dev.* **25,** 2093–2105 (2011).
43. Stepanchick, A. *et al.* DNA binding by the ribosomal DNA transcription factor rrn3 is essential for ribosomal DNA transcription. *J. Biol. Chem.* **288,** 9135–9144 (2013).
44. Kocher, T., Pichler, P., Swart, R. & Mechtler, K. Analysis of protein mixtures from whole-cell extracts by single-run nanoLC-MS/MS using ultralong gradients. *Nat. Protoc.* **7,** 882–890 (2012).
45. Laronde-Leblanc, N., Guszczynski, T., Copeland, T. & Wlodawer, A. Structure and activity of the atypical serine kinase Rio1. *FEBS J.* **272,** 3698–3713 (2005).
46. Marin, O. *et al.* Tyrosine versus serine/threonine phosphorylation by protein kinase casein kinase-2. A study with peptide substrates derived from immunophilin Fpr3. *J. Biol. Chem.* **274,** 29260–29265 (1999).
47. Wilson, L. K., Dhillon, N., Thorner, J. & Martin, G. S. Casein kinase II catalyzes tyrosine phosphorylation of the yeast nucleolar immunophilin Fpr3. *J. Biol. Chem.* **272,** 12961–12967 (1997).
48. Mekhail, K., Seebacher, J., Gygi, S. P. & Moazed, D. Role for perinuclear chromosome tethering in maintenance of genome stability. *Nature* **456,** 667–670 (2008).
49. He, X., Jones, M. H., Winey, M. & Sazer, S. Mph1, a member of the Mps1-like family of dual specificity protein kinases, is required for the spindle checkpoint in S. pombe. *J. Cell. Sci.* **111,** 1635–1647 (1998).
50. Wang, P. *et al.* II. Structure and specificity of the interaction between the FHA2 domain of Rad53 and phosphotyrosyl peptides. *J. Mol. Biol.* **302,** 927–940 (2000).
51. Peng, J. *et al.* Dusty protein kinases: primary structure, gene evolution, tissue specific expression and unique features of the catalytic domain. *Biochim. Biophys. Acta* **1759,** 562–572 (2006).
52. McMillan, J. N., Sia, R. A. & Lew, D. J. A morphogenesis checkpoint monitors the actin cytoskeleton in yeast. *J. Cell. Biol.* **142,** 1487–1499 (1998).
53. Gerber, J. *et al.* Site specific phosphorylation of yeast RNA polymerase I. *Nucleic Acids Res.* **36,** 793–802 (2008).
54. Albuquerque, C. P. *et al.* A multidimensional chromatography technology for in-depth phosphoproteome analysis. *Mol. Cell. Proteom.* **7,** 1389–1396 (2008).
55. Holt, L. J. *et al.* Global analysis of Cdk1 substrate phosphorylation sites provides insights into evolution. *Science* **325,** 1682–1686 (2009).
56. Kuhn, C. D. *et al.* Functional architecture of RNA polymerase I. *Cell* **131,** 1260–1272 (2007).
57. Fernandez-Tornero, C. *et al.* Crystal structure of the 14-subunit RNA polymerase I. *Nature* **502,** 644–649 (2013).
58. Bernstein, K. A. & Baserga, S. J. The small subunit processome is required for cell cycle progression at G1. *Mol. Biol. Cell* **15,** 5038–5046 (2004).
59. Takeuchi, Y., Horiuchi, T. & Kobayashi, T. Transcription-dependent recombination and the role of fork collision in yeast rDNA. *Genes Dev.* **17,** 1497–1506 (2003).
60. Christman, M. F., Dietrich, F. S., Levin, N. A., Sadoff, B. U. & Fink, G. R. The rRNA-encoding DNA array has an altered structure in topoisomerase I mutants of Saccharomyces cerevisiae. *Proc. Natl Acad. Sci. USA* **90,** 7637–7641 (1993).
61. Kiburu, I. N. & LaRonde-LeBlanc, N. Interaction of Rio1 kinase with toyocamycin reveals a conformational switch that controls oligomeric state and catalytic activity. *PLoS ONE* **7,** e37371 (2012).
62. Auger-Buendia, M. A., Hamelin, R. & Tavitian, A. Influence of toyocamycin on the assembly and processing of preribosomal ribonucleoproteins in the nucleolus of mammalian cells. *Biochim. Biophys. Acta.* **521,** 241–250 (1978).
63. Heix, J. *et al.* Mitotic silencing of human rRNA synthesis: inactivation of the promoter selectivity factor SL1 by cdc2/cyclin B-mediated phosphorylation. *EMBO J.* **17,** 7373–7381 (1998).
64. Sirri, V., Hernandez-Verdun, D. & Roussel, P. Cyclin-dependent kinases govern formation and maintenance of the nucleolus. *J. Cell Biol.* **156,** 969–981 (2002).
65. Leung, A. K. *et al.* Quantitative kinetic analysis of nucleolar breakdown and reassembly during mitosis in live human cells. *J. Cell Biol.* **166,** 787–800 (2004).
66. Sagot, I., Bonneu, M., Balguerie, A. & Aigle, M. Imaging fluorescence resonance energy transfer between two green fluorescent proteins in living yeast. *FEBS Lett.* **447,** 53–57 (1999).
67. De Sanctis, V. *et al.* In vivo topography of Rap1p-DNA complex at Saccharomyces cerevisiae TEF2 UAS(RPG) during transcriptional regulation. *J. Mol. Biol.* **318,** 333–349 (2002).
68. Eng, J. K., McCormack, A. L. & Yates, J. R. An approach to correlate tandem mass spectral data of peptides with amino acid sequences in a protein database. *J. Am. Soc. Mass Spect.* **5,** 976–989 (1994).
69. Dorfer, V. *et al. J. Proteome Res.* **13,** 3679–3684 (2014).
70. Sievers, F. *et al.* Fast, scalable generation of high-quality protein multiple sequence alignments using Clustal Omega. *Mol. Syst. Biol.* **7,** 539 (2011).

Acknowledgements

We thank A. Amon, M. Angermayr, L. Aragón, C. Cullin, D. D'Amours, M. Foiani, J.-P. Gelugne, K. Mekhail, M. Riva, E. Schiebel, T.U. Tanaka and F. Uhlmann for strains and reagents. We thank S. Pasqualato for help with the alignments and structure images, and D. Straußβ, J. Griesenbeck, H. Tschochner, P. Milkereit and J. Perez-Fernandez for discussions. This research was supported by a Howard Hughes Medical Institute International Early Career Scientist Grant and Investigator Grant 12878 from the Italian Association for Cancer Research to R.V., Investigator Grant 13243 from the Italian Association for Cancer Research to P.D.W., Austrian Science Fund FWF grants SFB F3402-B03, P2465-B24, TRP 308-N15, E.C. Seventh Framework Programme grant FP7/2007–2013, projects MEIOsys (222883-2) and PRIME-XS (262067) to K.M.

Author contributions

C.G., M.D.M. and V.I. initiated the project and created the 6myc-*rio1*^{TEV} nuclear depletion strain. M.G.I. proceeded with the project, observed the Rio1 depletion phenotypes and performed most of the described experiments together with L.F.M.. C.P. produced recombinant Rio1 and Rpa43, and did the Rio1-Sgs1 co-IP experiments. S.B. performed the Rio1-Rpa43 *in vitro* kinase assay, which was supervised by R.V. K.M. performed the mass spectrometric analysis of Rio1-phosphorylated Rpa43. S.F.-C. performed the ribosome profiling experiments, the pulse-chase protein translation studies and pre-rRNA processing analyses by northern hybridization. P.D.W., M.G.I. and S.F.-C. conceived the experiments with the person(s) performing them. M.G.I., L.F.M., S.F.-C. and P.D.W. wrote the paper. All authors have approved of the manuscript.

Additional information

Supplementary Information accompanies this paper at http://www.nature.com/naturecommunications

Competing financial interests: The authors declare no competing financial interests.

Reprints and permission information is available online at http://npg.nature.com/reprintsandpermissions/

How to cite this article: Iacovella, M. G. *et al.* Rio1 promotes rDNA stability and downregulates RNA polymerase I to ensure rDNA segregation. *Nat. Commun.* 6:6643 doi: 10.1038/ncomms7643 (2015).